RCA Engineer

Vol 22 No 2
Aug Sept
1976

Automotive electronics

RCA Engineer

A technical journal published by
RCA Research and Engineering
Bldg. 204-2
Cherry Hill, N.J. 08101
Tel. PY-4254 (609-779-4254)
Indexed annually in the Apr/May issue.

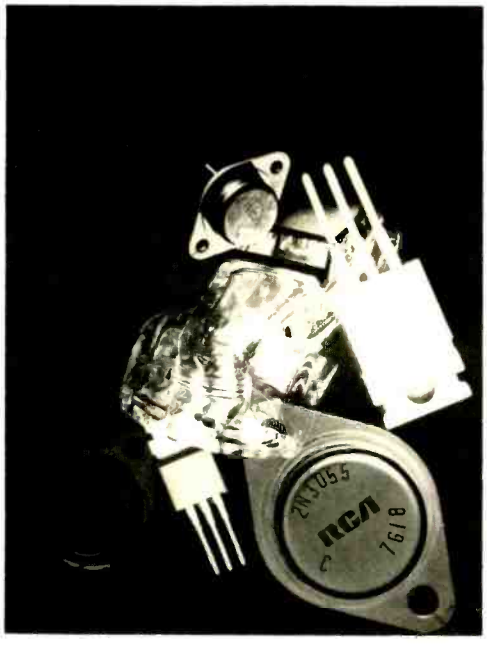

Our automotive issue cover superimposes multiple exposures of 2N3055 and 2N5298 power transistors over a glass car. The semiconductors are typical of the devices RCA supplies to the automotive industry.

Photo credit: Tom Cook, RCA Laboratories, Princeton, N.J.

- To disseminate to RCA engineers technical information of professional value
- To publish in an appropriate manner important technical developments at RCA, and the role of the engineer
- To serve as a medium of interchange of technical information between various groups at RCA
- To create a community of engineering interest within the company by stressing the interrelated nature of all technical contributions
- To help publicize engineering achievements in a manner that will promote the interests and reputation of RCA in the engineering field
- To provide a convenient means by which the RCA engineer may review his professional work before associates and engineering management
- To announce outstanding and unusual achievements of RCA engineers in a manner most likely to enhance their prestige and professional status.

The future for automotive electronics

Startling and unforeseen events have dramatically altered the future role of the automobile in American life in the three years since the *RCA Engineer* last covered automotive electronics (April/May 1973). The energy crisis and, specifically, the gasoline shortage of late 1973 and early 1974 painfully brought home to us the realities of an energy problem which should peak before the end of this century.

Suddenly, we realize that we do not control our own future—we are dependent to some extent upon the pleasures of the OPEC countries. And we will remain so dependent until the United States develops alternative sources of energy.

In the interim, public awareness and both current and potential government legislation will make it essential that automotive manufacturers use all technological advantages to maximize fuel efficiency, minimize pollution and optimize safety. Furthermore, the consumers' penchant for convenience features will place additional pressures on the manufacturers to fully use new technologies such as solid state.

The immediate implications for the semiconductor industry are reflected in some of the articles in this issue of the *Engineer*. The long-term implications, however, are less obvious. While the basic technologies are at hand, the applications and product engineering tasks, to a large extent, remain ahead. We know what can be done; we have yet to do it and find all the answers to the economic and reliability questions. The challenge, then, lies in creating an effective interface between the solid-state and automotive industries to quickly produce components and systems that are reliable and cost-effective.

Bernard V. Vonderschmitt

Bernard V. Vonderschmitt
Vice President and General Manager
Solid State Division
Somerville, N.J.

What's happening in automotive electronics

4 Fuel-economy thinking changes

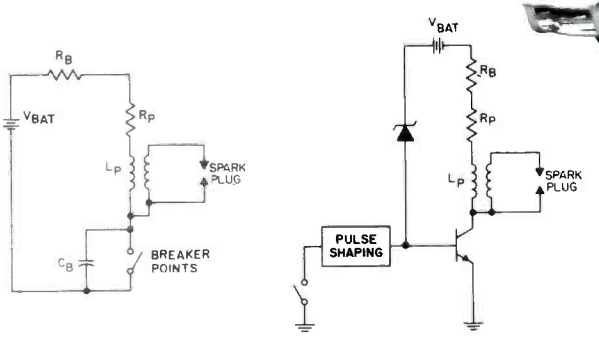

10 Ignition-system evolution

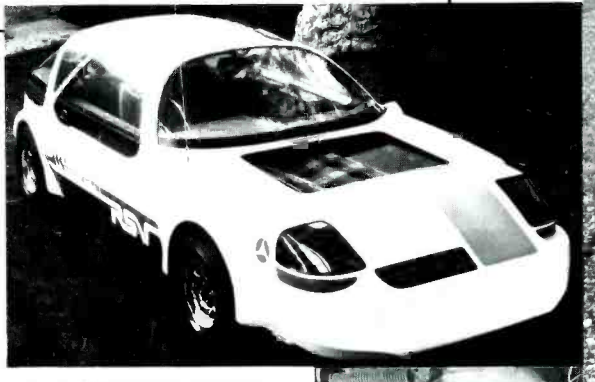

26 Automotive radar

50 Electronically controlled brakes

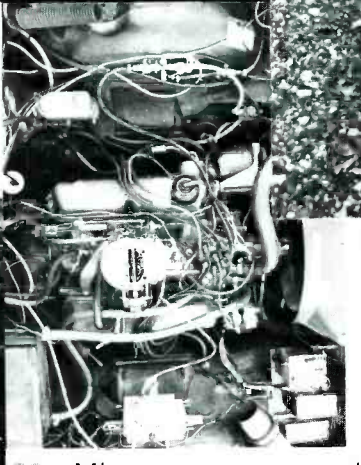

38 Microprocessor-controlled spark advance

74 Non-contact power testing

56 Learn digital electronics

RCA Engineer

overview

G.B. Herzog 4 The potential for electronic automobile controls

power switching

T. McNulty 10 Thyristors for automotive use

W.C. Simpson 14 High-voltage darlington for auto ignitions

J.E. Wojslawowicz 19 The GTO-SCR: solid-state's remote automotive power switch

M. Kalfus 24 Small-engine electronic ignition

microwave systems

Dr. F. Sterzer 26 Automotive radar development at the RCA Laboratories

G.S. Kaplan, A.D. Ritzie 29 Automatic vehicle tracking using microwave signpost reflectors

H.C. Johnson 34 Speed sensors for locomotives

computer control

A.D. Robbi, J.W. Tuska 38 A microcomputer-controlled spark advance system

S.E. Ozga 43 The B-12—an automotive microprocessor

48 The RCA Laboratories' 'electronic car'

W.R. Lile, J.W. Tuska 50 Electronic control of vehicle brakes

R.L. Pryor 53 An electronic timing reference with improved accuracy

special—short course

Dr. L. Shapiro 56 Digital electronics: Concepts and sampling theory

automated testing

R.T. Cowley 64 Engine test at the Automated Systems Division

R.F. Barry, J.M. Laskey 68 Application of automatic test equipment to bus maintenance

S.C. Hadden, L.R. Hulls, E.M. Sutphin 74 Non-contact instrumentation for engine testing and monitoring

G. Grube, D.J. Morand 80 Portable test equipment for army vehicles

on the job/off the job

R.L. Libbey 85 The ideal combo—a microprocessor and a music synthesizer

departments

89 pen and podium

91 dates and deadlines

92 patents

94 news and highlights

The potential for electronic automobile controls

G. B. Herzog

Electronic control can improve gas mileage and reduce pollution in a number of ways—it can cut idling and pumping losses, calculate and control spark timing and transmission shift points accurately, distribute fuel to all cylinders evenly, and possibly even prevent uneconomical driving habits. Taken individually, the mileage gains are not necessarily cost-effective, but the savings can be significant if a number of these concepts are combined into one overall electronic control system.

Gerald B. Herzog. Staff Vice President, Technology Centers, RCA Laboratories, Princeton, N.J., received the BSEE and MSEE from the University of Minnesota in 1950 and 1951, respectively. He joined RCA Laboratories in 1951 and in 1952 helped design and construct the first completely transistorized television receiver. Subsequently he worked on special color reproducer systems, video tape recording systems, ultra-high-speed logic including microwave and tunnel diode circuits, and large scale integrated circuits, including complementary MOS and silicon-on-sapphire devices. At the RCA Laboratories he has served as Director of the Process Research Laboratory, Director of Digital Systems Research Laboratory, and Director of the Solid State Technology Center (with locations in Princeton and Somerville, New Jersey). Mr. Herzog has presented and published many technical papers on advanced semiconductor device applications and holds 23 U.S. Patents. He is a member of Sigma Xi, Eta Kappa Nu, Fellow of the IEEE, and a past Chairman of the ISSCC. He has received two RCA Achievement Awards, two David Sarnoff Outstanding Team Awards in Science, and the University of Minnesota Outstanding Achievement Award in 1972.

Reprint RE-22-2-1 | Final manuscript received June 10, 1976.

FOR MANY years, there have been great expectations for the expansion of electronics' role in the automobile. At the 1967 IEEE Automotive Conference, a paper that was given stated "However, the 1975 model U.S. automobile will be loaded with electronic devices making life simpler and safer for its driver."[1] As with so many Utopian dreams, economics slowed down the realization of what was technologically feasible. Today, with the price of gasoline approximately twice what it was in 1967, some of these predictions have become more economically meaningful. If the price of gasoline goes to $1.00 per gallon, quite sophisticated electronic controls will become economically justifiable. Government regulations on fuel efficiency and pollution levels for cars are also hastening the advent of electronic controls. In the following material, I have cited various references to illustrate what is technologically possible. It remains to be seen what electronic control systems can be justified at any given point in time. This information has been gathered in the course of the RCA Laboratories project on microprocessor controls for automobiles, which started late in 1973.

Pollution misconceptions

During the course of this project I discovered that misunderstandings were prevalent among electrical engineers, including myself, about the operation of gasoline engines, their efficiencies, and pollution levels. It seemed to many people early in the fuel-crisis/air-pollution era that a properly operating, efficient engine should generate minimum pollution, or conversely that an engine adjusted for minimum pollution should be efficient, contrary to what seemed to happen to cars in the 1973-1974 period. The simple theory was that if all the fuel burned to carbon dioxide and water vapor, as we learned in elementary chemistry, there would be no pollution and all the energy would be available to drive the car. Unfortunately, there are secondary reactions, which the public has now learned about, that produce nitrogen oxides when the engine is running at its most efficient point. To minimize these reactions, EGR (Exhaust Gas Recirculation) was added to engines and the timing was changed to reduce the peak pressure and temperature during combustion. The efficiency went down as the timing was changed to a less optimum range.

Since not all the fuel was burning completely, some cars had air pumps added to the engines to force air into the hot exhaust manifold and encourage the complete combustion of the remaining hydrocarbons and convert the carbon monoxide to carbon dioxide. Unfortunately, some

This 1951 Lincoln got 25 miles per gallon and won its class in the Mobil Economy Run that year, despite the fact that it weighed 5200 lb. A comparable car today might get half its mileage.

people, even ones with years of engineering experience, were so cynical of our engineering brethren in Detroit that they thought the air pump merely diluted the mixture coming out of the car's tailpipe to comply with pollution testing standards. In fact, the federal standards specify that during an EPA test run, all the exhaust emissions must be captured and the pollutants of each class weighed. The acceptable levels for a given year are specified in grams per mile for a specific driving pattern. These standards are given in Table I, and apply regardless of the size of the car.

Table I — Federal pollution standards.

Model Year	Allowed Emissions (grams per mile) HC	CO	NO_x
1973	3.4	39.0	3.0
1975	1.5	15.0	3.1
1977	0.41	3.4	2.0
1978	0.41	3.4	0.4

These are the standards as originally set by the federal government. Because of the fuel crisis and difficulty of meeting the 1978 standards, the timetable has been extended repeatedly so that the most stringent requirements now fall in the 1980's. It is probable that the NO_x requirement of 0.4 gram per mile will be relaxed somewhat.

Fuel economy— past and present

A 1951 Lincoln weighing 5200 lb won that year's Mobile Economy Run (on a ton-mpg basis) with better than 25 mpg.[2] A comparable-sized car today might achieve 10 to 15 mpg or a little better than half the 1951 winning rate.

There are many things that can be done to increase fuel economy, and the mechanical engineers in Detroit and around the world are well aware of them. They have not suppressed these ideas as some would like us to believe, but have, in fact, made them available to the public on various occasions. Unfortunately, the public has not had the wisdom to accept fuel-economy devices at the necessary higher initial cost, or the economics has not truly been favorable. Overdrive is one such example. I had one on my 1951 Mercury, loved it, and got great gas mileage on the highway.[3] With gas at 25-30 cents per gallon, however, most people apparently did not want to pay extra for such a feature. It was also the beginning of the era of bigger and bigger engines, responding to customer demand for more performance and convenience. The stick-shift plus overdrive gave way to the automatic transmission, plus power steering, power brakes, air conditioning, etc. Hence, the 20-25 mile-per-gallon car of 1951 became the 10-13 mile-per-gallon car of today.

It is overly simplistic, however, to suggest that we can merely turn back the clock to achieve greater fuel economy. That great Model A Ford we keep hearing about had a low-compression engine and got rather poor mileage for such a light-weight car. Recently, as reported in the June 21, 1976 issue of *Automotive News*, Ford Motor Company ran the EPA mileage test on a 1936 Ford sedan that had spent the better part of its life in their museum. With 26,000 miles of use, it was in good condition, but gave only 15 mi/gal for city driving and 20 mi/gal highway, while generating 12.4 grams of hydrocarbons per mile and 86.8 grams of carbon monoxide per mile. Only the 2.8 grams of nitrogen oxides per mile came close to meeting today's pollution standards. For comparison, today's heavier Ford Granada, with similar size engine and three-speed transmission, gave 22 mi/gal city driving and 30 mi/gal highway. This indicates that good mechanical approaches can achieve significant results.

What further might be done? There are many possible improvements—some simple, some complex, and almost none economically justifiable by themselves. Taken together, however, several of them might be justified if the cost of fuel goes up and the cost of electronics continues to drop.

Idling waste

Idling is the most wasteful of all modes of operation, yet an engine may be idling as much as 10-60% of the time in city driving. We all recognize idling at stop signs as wasteful, but it accounts for perhaps only 10% of our city driving time. Other idling periods occur when we abruptly let up on the gas as we slow down for a corner, heavy traffic, or a

stop sign. In city driving we are almost always accelerating and then coasting. Besides wasting gas, this also increases pollution, because rapidly closing the throttle stops the air flow suddenly while the heavier fuel continues to flow for a moment, causing an overly rich mixture. A large V-8 engine burns nearly a gallon of gas per hour idling. If we spend 40% of the time with the engine doing no useful work, it is no wonder that a car gives poor gas mileage in city driving.

Two companies, one in Europe and one in Japan, have developed systems that shut off an engine at stop lights and restart it automatically to save gas. A hot restart of a V-8 engine takes less gas than idling for 24 seconds.[4] One wonders, however, how long the starter would last with such an attachment. A more practical approach might be an electronic idle speed controller. On large cars with power steering, power brakes, and air conditioning, the idle speed is set high to insure that the engine doesn't stall when the air conditioning load comes on or when parking maneuvers impose a heavy load on the power steering pump. In most cars one can easily detect the drop in engine speed as the air conditioner clutch engages, though some cars now have electromechanical devices to adjust the idle setting to compensate for the added load. The idle speed is often set so high that the car will travel at about 10 mi/h on a level road, and faster if the choke is closed. That means that our brakes are fighting the engine as we try to stop at each stop sign.

An electronic control could maintain engine rpm at the lowest level consistent with pollution standards and still assure power for the accessories. This would save considerable gas in cars used primarily for city driving. But would the cost be justified by the fuel savings? Probably not. But if that same idle control were part of a more extensive control system, however, it would certainly be beneficial. The Bosch fuel injection system used in the VW

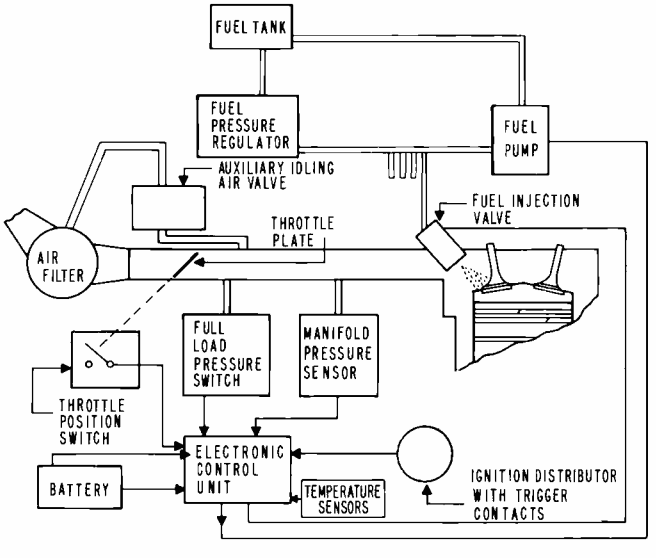

This early electronic fuel injection system was developed by Bosch and appeared on some Volkswagen engines in 1968. A set of contacts in the distributor triggered the injectors, and the control unit determined pulse duration after receiving information on engine speed, vacuum, and temperature. The control unit had 220 discrete components, but did not control spark advance.

Squareback and Fastback, circa 1968, shuts the fuel flow off when the throttle is closed and engine rpm exceeds the set idle speed, that is, when the car is pushing the engine. This not only saves fuel but gives improved engine braking, saving wear on the brakes.

Power loads and pumping losses

The most significant problem that the mechanical engineer in Detroit must face is that an automobile engine always operates in the dynamic mode, i.e., it is always changing its speed or power output. However, the testing facilities available to him are designed to test engines running at fixed loads and speeds. It is extremely difficult to measure the engine parameters during the transient as the throttle opens and closes, yet that is what is happening most in normal driving. We may think we drive at a constant speed on the highway, but we are a rather poor actuator in an elementary servo system and we are constantly speeding up or slowing down to hold an average speed. In addition, there is no such thing as a truly flat road, so the power output required is subject to changes even at a constant speed. It is claimed that the "cruise control" option available on some cars will save appreciable gas, especially in mountainous areas. Again, its cost cannot be defrayed by fuel savings, except perhaps for the traveling salesman or others doing a lot of highway driving. Such controls are purchased primarily because of their convenience value.

"A large car requires only about 20 hp to travel 60 mi/h on a level road."

A large car requires only about 20 hp to travel at 60 mi/h on a level road. Yet such cars are often equipped with 200-hp engines because the purchaser demands rapid acceleration and power-robbing accessories. One study estimated that the normal driver uses maximum power only 1% of the time and uses less than 10% of engine power 43% of the time. When such an engine is running at modest speeds, at low power output, much of the engine's power is used to overcome pumping losses, i.e., working to suck air through the closed throttle structure. Even at 50 mi/h, much of the fuel energy input to a 200-hp engine is used to overcome the engine's losses, since only 20 hp is actually required. One reason a diesel engine is more efficient than a spark-ignited gasoline engine is that it operates at nearly wide-open throttle all the time, eliminating much of the pumping losses. Power output is controlled by the amount of fuel injected into each cylinder.

Pontiac engineers did some interesting experiments with gasoline engines several years ago. They modified a V-8 engine so that it could run on only four of its cylinders while the other four were vented to reduce the pumping losses. During idle and cruise, only four cylinders were in use. During periods requiring more power, such as during rapid acceleration, steep hills, etc., the other four

cylinders were brought into service. A 15% increase in gasoline mileage was claimed. With only mechanical linkages and electromechanical control mechanisms available, such a system might be a costly nightmare. But if fuel reaches $1.00 per gallon and Federal legislation dictates a certain average gasoline mileage for all new cars, such a scheme might be revived for large cars. Hopefully, a microprocessor system will simplify its control. Alternatively, the diesel engine might make such complicated schemes unnecessary.

The electronic transmission

Since the spark-ignited gasoline engine is most efficient near wide-open throttle and at modest speeds, an infinitely variable gear ratio transmission is needed, but not available. The old stick-shift with three forward speeds plus overdrive has become the 4-speed and 5-speed transmission in today's small cars. The large-car purchaser still prefers the automatic transmission, however, even with the losses incurred in the torque converter. The point at which the automatic transmission shifts is a compromise based on fuel economy and performance. Performance takes priority because automotive magazines and the general public rate cars on the acceleration from 0-60 mi/h. When the shift points are controlled by mechanical governors, vacuum valves, and hydraulic pistons, the shift-point compromises made during design are literally "cast in iron". If electronic controls (which have been built and tested by the automotive industry) were used instead, the shift-point compromises could be selected by the driver. The driver could select an economy range for around-town shopping trips, modest performance for casual Sunday rides in the country, or super performance for the hot-rod set. Again, an electronic system just to control the transmission shifting would in itself probably not be justified by a 5-10% increase in gasoline mileage.[5] However, if it were part of a larger control system it could be achieved at practically no increase in cost over today's hydraulic systems.

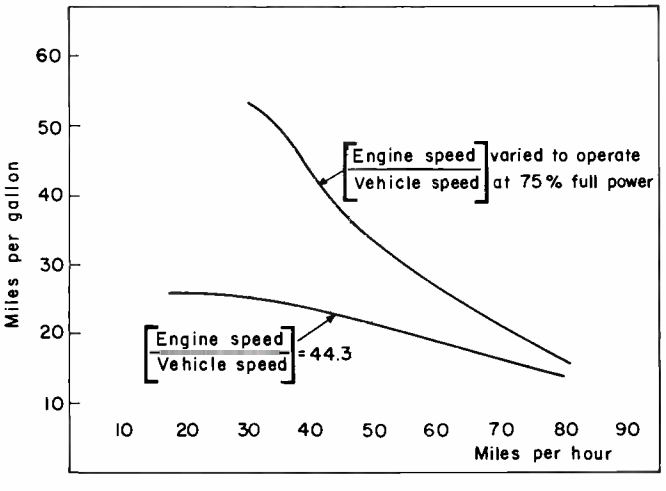

An ideal transmission could vary infinitely to operate an engine at the most efficient speed for each vehicle speed. This graph shows the difference such a transmission could make in mileage. The limitation of 400-rpm engine speed does not permit operation at 75% of full power below 30 mi/h. Taken from Kummer, *Technology Review*, Feb 1975. Source: Jandasek, *SAE Transactions*, 61, 95 (1953).

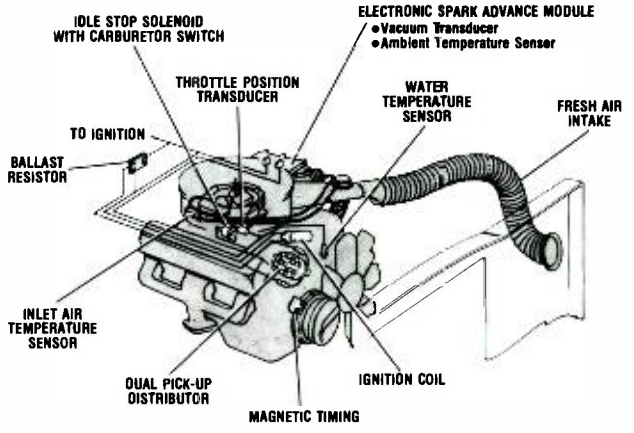

Chrysler Corporation's 'lean burn' ignition system can meet the 1976-1977 pollution standards without a catalytic converter or exhaust gas recirculation. It does this with a special carburetor designed for a lean 18:1 air/fuel ratio, magnetic timing, and electronic spark advance. The system is available only on Chrysler's 400-cubic-inch, four-barrel engine for 1976, but will be used on other engines in 1977.

Ignition 'kludges'

The gasoline engine operates most efficiently and develops maximum power when the combustion produces maximum pressure in the cylinder just after the piston reaches the top of its compression stroke. Because the combustion rate is controlled by the fuel-mixture density, which is proportional to manifold pressure as set by the throttle position, and because the amount of time available for burning varies with the speed of the engine, the ignition point must be a variable. In the past, a simple vacuum diaphragm and governor mechanism on the engine's distributor, monitoring manifold pressure and engine rpm, controlled the point of ignition. This control

"...if a lean air-fuel mixture is used in conjunction with electronic control of the spark advance, neither a catalytic converter nor EGR is necessary to meet the 1976-1977 federal pollution standards."

system provided an approximation to the advance that was necessary to give best performance. Unfortunately, the condition of best engine performance also corresponds to a condition of maximum nitrogen oxide production under certain driving conditions. Therefore, over the past several years the distributor mechanism has become more complicated. Additional vacuum diaphragms have been added along with electronic controls used to switch the vacuum from one diaphragm to another, depending upon engine temperature, driving speed, etc. While these mechanical-pneumatic kludges have been satisfactory to meet the pollution standards of the 1974-1976 time frame, they will become increasingly inadequate as the allowable emissions are reduced.

The poor fuel economy achieved on the 1974 cars was due to the retarding of the spark-advance curve to meet the

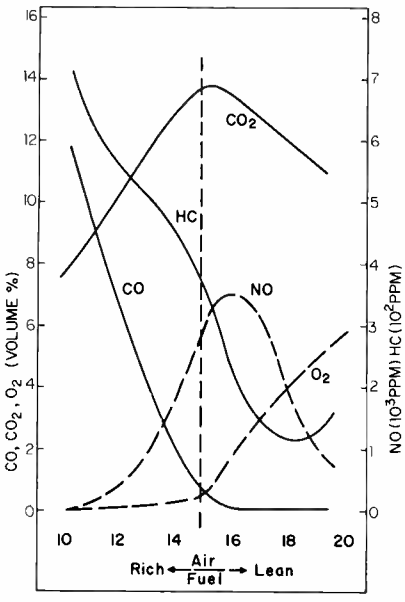

Varying the air-fuel ratio in an engine varies its exhaust constituents. The vertical line marks the "ideal" stoichiometric air-fuel proportions for combustion; the vertical scales are different for some constituents to make the curves comparable. Taken from Kummer, *Technology Review*, Feb 1975.

Table II.

How thermodynamics and friction reduce mileage in the real-life automobile—a 2000-cc (122 cu in.), 4-cylinder engine with automatic transmission

	Thermal efficiency (per cent)	*Miles per gallon*	*mpg reduction (per cent)*
All chemical energy converted into mechanical energy	100	194	
Theoretical Otto cycle (ideal gases, perfect heat release)	57	116	
Real Otto cycle (heat loss dissociation, non-ideal gases, indicated efficiency)	33	68	
After subtracting pumping losses at road load, 40 mi/h	23	44.6	34
Ater subtracting mechanical losses (engine friction) at road load, 40 mi/h	17	33	26
After subtracting carburetor metering, choke, accelerator pump, fan, manifold distribution, and distributor retard losses	15.5	30	9
After subtracting automatic transmission losses	11.9	23	23
After subtracting power steering and generator losses	10.3	20	14
After subtracting air-conditioning losses (1.5 hp continuous—air-conditioning requires higher idle speed and is used only at certain times)	8.5	16.4	18

(As taken from Kummer, *Technology Review*, Feb 1975)

pollution standards of that year. When the 1976 standards took effect, the engines needed catalytic converters to further reduce the excess hydrocarbons and convert carbon monoxide to carbon dioxide. This allowed the engine designers to readjust the spark advance toward the optimum condition, resulting in improved fuel economy for the 1976 cars versus the 1974 cars. Chrysler Corporation's 1976 400-cubic-inch "lean burn engine" demonstrates that if a lean air-fuel mixture is used in conjunction with electronic control of the spark advance, neither a catalytic converter nor EGR is necessary to meet 1976-1977 federal pollution standards. Also, in an experimental project with a Mark IV, Ford Motor Company reported a 10-20 percent increase in mileage through the use of electronic spark advance and EGR control.[6] This car did use a catalytic converter in addition, however.

Carburetion *vs* fuel injection

The gasoline engine operates best when the air-fuel mixture is near the stoichiometric ratio, that is, when there is just sufficient oxygen present to theoretically cause the fuel to burn completely. Unfortunately, this is also the condition that generates the most nitrogen oxides. A lean mixture of 16 to 18:1 versus the stoichiometric ratio of 15:1 gives greater efficiency and less pollution, but less than maximum power from the engine. It is also more difficult to ignite than a rich mixture. Recent cars use so-called high-energy electronic ignition systems to ensure ignition of the leaner mixtures being used in the 1976 cars and to prevent misfires that would put raw fuel into the catalytic converter and cause excessive heating.

"What once was a fairly simple device has become another electromechanical kludge."

Controlling the air-fuel ratio to the accuracy necessary to meet both pollution standards and fuel economy is quite difficult for the standard carburetor. What once was a fairly simple mechanical device has become another electromechanical-pneumatic kludge. The carburetor works on a fairly simple Venturi principle based on Bernoulli's laws of mass flow. Unfortunately, because of the wide dynamic range over which the engine operates, many approximations must be made. With the engine idling, the throttle is nearly fully closed, and very small amounts of air flow through the main body of the carburetor. Separate idle jets must be provided to supply the correct amount of fuel during this condition. During normal part-throttle operation, the flow of air through the carburetor body sucks fuel from the main jets, which are set to provide approximately the right fuel mixture during average driving conditions. Under wide-open throttle conditions, however, the engine must develop maximum power, and it is necessary to provide fuel enrichment. This is done by various means, including a piston to squirt additional fuel into the carburetor during acceleration, and so-called power valves, which open up additional passageways to allow additional fuel into the carburetor.

These relatively crude schemes have been the cause of excessive pollution in the past. One of the reasons that the 1974 cars had so many problems with hesitation and stumble was that these mechanical means had been refined to their practical limits. With the catalytic converter, though, somewhat larger amounts of excess fuel can be supplied to the engine at acceleration. The converter is then called upon to burn up the excess fuel to prevent it from being emitted as a pollutant. We are

"One of the reasons that the 1974 cars had so many problems with hesitation and stumble was that [with all the polution controls added] these mechanical [carburetion] means had been refined to their practical limits."

currently hearing, however, about the intense heat that the catalytic converter gives off when it burns excess fuel. It is claimed that this can be a fire hazard near locations where fuel has been spilled or in high-underbrush areas.

Another problem with existing carburetor systems has to do with the fuel-mixture distribution. On the way from the carburetor to the various cylinders in a large engine, the fuel-air mixture changes composition. As the fuel travels to the furthermost cylinders, some of the fuel droplets that are not fully vaporized strike the intake manifold walls and run along the walls as rivulets rather than as an air-fuel mixture. This causes some cylinders to run with a leaner mixture than others, so the carburetor must be set so that the cylinder with the leanest mixture still has a mixture rich enough for proper ignition.

An electronic fuel injection system can help overcome this problem by injecting fuel in the vicinity of the intake valve for each cylinder. This allows more precise control of the air-fuel ratio under all driving conditions, but not without a price penalty. The Cadillac Seville for 1976 has such a system. Fuel injection trades the problem of intake manifold design for the problem of exactly matching fuel injectors, which must be precisely made and are consequently expensive. In addition, some accurate way of measuring the air-mass flow must be devised to determine how much fuel to inject for a given operating condition. This has been a major problem in implementing fuel injection systems that must meet both performance requirements and pollution standards. As presently achieved with analog control circuitry, the cost is prohibitive for the mass-produced, standard-sized U.S. automobile. Using microprocessors in the next generation of fuel injection systems, however, promises to improve performance and reduce the cost of the electronics substantially. The cost of the fuel injectors can be reduced by mass production.

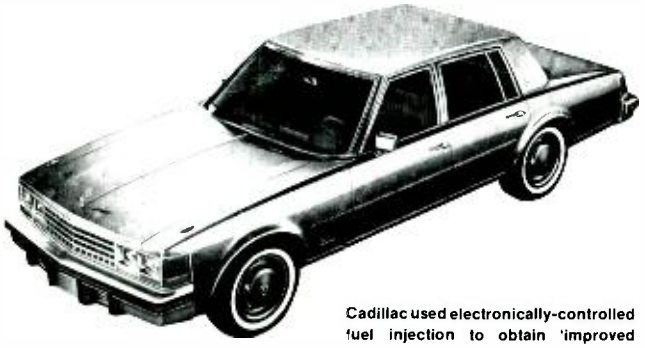

Cadillac used electronically-controlled fuel injection to obtain 'improved driveability' on the 1976 Seville's 350-cubic-inch engine. Electronic fuel injection systems will probably remain luxury items, however, until microprocessor control and mass production bring costs down.

Microprocessor control

Finally, there is one major element in the automobile that can play a significant role in reducing fuel consumption—the driver of the car. Unnecessarily rapid acceleration wastes an enormous amount of gas. Letting up on the accelerator suddenly also wastes gas and increases pollution. A slow, steady acceleration and a slow, steady deceleration is the best mode of operation. A microprocessor can be interposed between the driver and the engine to force better driving habits. By putting the microprocessor in the driving loop, the car can be inhibited from unnecessarily rapid accelerations, except in emergency situations where, as with the kickdown feature of an automatic transmission, more rapid acceleration could be achieved upon driver command. For average driving the operator could select a microprocessor control mode designed to maximize the automobiles' fuel economy. This efficiency mode would suffice for a high percentage of driving conditions, but a high-performance mode could be selected by the driver when desired.

"A microprocessor can be interposed between the driver and the engine to force better driving habits."

Conclusions

In summary, it seems certain that the microprocessor will play an important part in the car of our future; it is only a question of how far in the future. Other papers in this issue go into more detail on the contributions that RCA is making toward accomplishing that Utopian goal predicted in the 1967 paper referenced earlier. For those readers wishing more details on the what has been or could be tried to improve fuel economy, the February 1975 issue of the *MIT Technology Review* contains several papers that make extremely interesting reading.

References

1. Hugle, W.B., "How microcircuits will be used in cars," *IEEE Automotive Conf. Record*, (Sep 21-22, 1967) pp. 1-9.
2. Cohn, C.E.; "Improved fuel economy for automobiles," *MIT Technology Review*, (Feb 1975) p. 52.
3. Cohn, C.E.; "Improved fuel economy for automobiles," *MIT Technology Review* (Feb 1975) p. 49. ("Overdrive, which was quite popular twenty years ago... can yield a 15 per cent improvement in fuel economy").
4. Cohn, C.E.; "Improved fuel economy for automobiles," *MIT Technology Review*, (Feb 1975) p. 49. (The companies are Toyota in Japan and E. Jucker Relaisbau of Zurich, Switzerland).
5. Kummer, Joseph T., Chemistry Department, Ford Motor Co.; "The automobile as an energy converter," *MIT Technology Review*, (Feb 1975) p. 27. ("If the transmission were more efficient in urban driving and if it could provide a better match between the engine speed and vehicle speed, there would be a large gain in fuel economy, perhaps in the ideal case as much as 50% for a vehicle with a large engine in urban driving.")
6. Moyer, D.F.; and Mangrulkar, S.M.; "Engine control by an on-board computer," *SAE Convergence '75, Automotive Electronics II*, (Feb 1975) pp. 75-77.

Thyristors for automotive use

T. McNulty

SCR's, now used in capacitative-discharge ignition systems, may find broader automotive use with the development of the gate-turn-off SCR.

A THYRISTOR is a semiconductor device whose bistable action depends on the regenerative feedback associated with a pnpn structure. Its name derives from the fact that it combines the latching properties of the thyraton tube with the hole-electron movement of the transistor.

The SCR (Silicon-Controlled Rectifier) is probably the best known and certainly the oldest thyristor device. It is unidirectional (current flow is from anode to cathode), has three terminals, and is capable of two states, *on* or *off*. One can think of an SCR as a rectifier with a controlled gate, i.e., its rectifying action is controlled by injecting current into the gate.

From transistor to SCR

To better understand SCR regenerative feedback, let us start with the basic transistor structure of Fig. 1, which shows n-type conductivity, where the majority carriers are electrons. If a transistor is biased as in Fig. 2, then the base injects positive charge carriers (holes) that are collected in the emitter. The presence of holes in the n-type emitter dislodges electrons, which are attracted to the collector because of the positive bias from the external supplies. Current flow will continue as long as the base continues to inject positive charges to the emitter. The magnitude and duration of current flow is proportional to the number of base-injected positive carriers. In the absence of base current, there is no electron charge movement; therefore, current flow is zero.

SCR's differ from transistors in that they are four-layer devices. The fourth layer sustains regeneration once the SCR is triggered into the on-state. In Fig. 3, note that the two emitters are of different conductivity. The upper emitter (n) supplies electrons and the bottom emitter (p) supplies holes, giving the two necessary ingredients for current flow in a solid-state device. Let us analyze the SCR structure for the bias shown in Fig. 4. The base region is p-type, capable of injecting holes to the n-type emitter. A hole carrier arriving at the n emitter dislodges an electron, which is attracted to the p emitter by the external bias.

Reprint RE-22-2-2
Final manuscript received May 18, 1976.

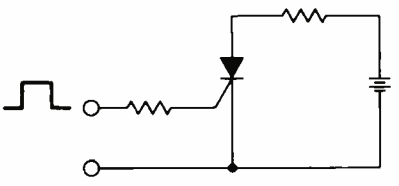

Fig. 4 — Simple SCR circuit.

So far, we have transistor action. However, the collector here is not n-type, as in a transistor, but p-type. Therefore, an electron arriving at the p emitter dislodges a hole that is then attracted to the n emitter. Now we have two sources of hole carriers: the base, which first initiated the hole carrier, and the p emitter. As more holes are injected into the n emitter, more electrons are attracted to the p emitter, which dislodges more holes to be attracted to the n emitter, and so on. Once a sufficient amount of holes and electrons is available from the p and n emitters, the device is in regeneration and no longer needs the base-injected holes. With the base signal removed, the SCR will remain in the low-impedance state.

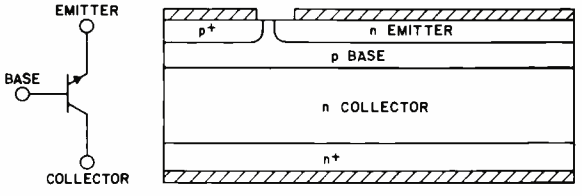

Fig. 1 — Basic transistor structure.

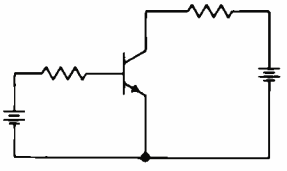

Fig. 2 — Simple transistor circuit.

Two-transistor analogy

One can make another interesting analysis of SCR structure by using the two-transistor analogy shown in Fig. 5. The pnpn SCR structure is analogous to a pair of complementary npn and pnp bipolar transistors. As shown in Fig. 5b, the base of the pnp is the collector of the npn, and the collector of the pnp is the base of the npn. By connecting discrete transistors as in Fig. 5c, SCR action can

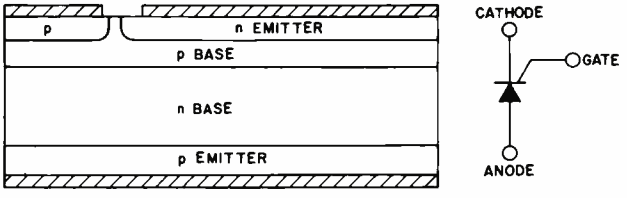

Fig. 3 — Basic SCR structure.

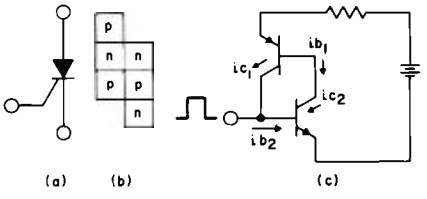

Fig. 5 — Two-transistor SCR analogy.

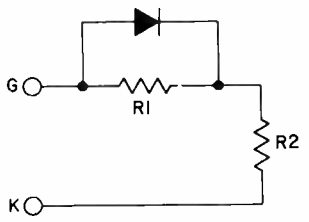

Fig. 6 — Internal gate impedance for SCR.

readily take place. When base current is injected into the lower npn transistor, collector current begins to flow as a function of the npn beta. Once npn collector current flows into the base of the pnp, the collector current of the pnp transistor begins to flow, now also a function of the pnp beta. The external battery supports the current flow of the two transistors, but once sufficient anode current is available, the original base current, which initiated regeneration, can be removed.

Although not evident from the models, turn-off of the discrete transistors or the SCR requires the main current to be reduced to zero or some negative value. Turn-off cannot be accomplished by simply grounding the gate or lowering the gate to some negative potential. Fig. 6, an illustration of the internal gate impedance, shows why. Grounding the gate cannot remove sufficient main gate current to cause turn-off, since R1 is much greater than R2. If R1 could be made much lower than R2, then turn-off could be accomplished at the gate electrode. Effects of gate turn-off will be discussed later in the paper.

SCR advantages and disadvantages

From the above analysis of SCR structures, some of the advantages of SCR's can be summarized as follows:

- only a small gate trigger current is required to initiate regeneration;
- power gain is in the thousands, e.g., milliwatts of gate power can control kilowatts of anode power;
- increases in anode current have little effect on SCR forward voltage drop because of regeneration properties;
- inrush surge-handling capability is approximately ten times the steady state current, e.g., a 7-A SCR can handle a 70-A single-cycle 60-Hz surge;
- gate trigger currents need not be steady state, but may be pulses;
- volt-ampere per area ratings are high when compared with an equivalent transistor.

Some of their disadvantages are:

- difficulty in obtaining reliable turn-off in dc circuits without outboard components;
- junction-temperature limitations associated with a four-layer regenerative structure;
- slightly higher forward voltage drop compared to a saturated transistor's.

The three ignition systems

Let us now explore the area of automotive uses for SCR's. One area in which the SCR has found widespread use is in capacitor discharge ignition systems, which have not been accepted as original equipment by the automotive manufacturers, but have found success in the after-market area. Before we analyze the SCR ignition system, let us briefly review the conventional point-type ignition system and an electronic transistor system to present an objective picture of the relative merits of the three systems.

The objective of any ignition system is to generate a high voltage capable of breaking down the gap between the sparkplug electrodes in order to ignite the combustible mixture in the cylinder. The spark must provide sufficient energy for adequate combustion, and the timing of the spark must occur at the precise moment and proper cylinder for maximum efficiency. The three systems meet the objective in providing proper spark, but differ in their operating efficiencies.

Standard breaker-point ignition

The basic breaker-point ignition system has served the automotive industry from its early beginning. It is an inductive storage system consisting of the induction coil, breaker points, capacitor, and power supply, as shown in Fig. 7. When the breaker points are closed, primary

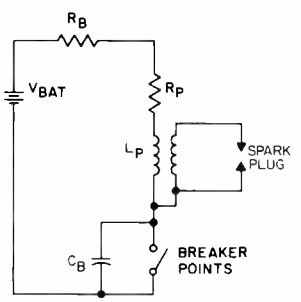

Fig. 7 — Breaker-point automotive ignition.

Tom McNulty, Engineering Leader, Power Applications Engineering, Solid State Division, Somerville, NJ received the BSEE in 1966 from Newark College of Engineering. Prior to joining RCA in 1966 he gained extensive experience in digital logic-system design at Burroughs Corporation. His first assignment with RCA was in Mountaintop as an Applications Engineer with Thyristor Rectifier Engineering. In 1967 he transferred to Somerville, where he is now engaged in the development of circuits for ac power-control. McNulty holds several patents and has written a number of papers on the use of SCR's and triacs in ac power-control and appliance-control applications.

current begins to flow at an exponential rate, which can be expressed as

$$i_p = [V_{bat}/(R_p+R_{bat})][1 - \exp(t/\tau)];$$

where

$$\tau = L_p/(R_p + R_{bat})$$

This expression is valid only when the points are closed. Therefore, the magnitude of the primary current is a function of the time constant and the dwell time of the points. For low rpm (under 1000), dwell time is long enough to allow steady-state levels to be reached. Above 1000 rpm, the primary current begins to fall off because of the shorter dwell times. The voltage developed at the sparkplug occurs when the points open and is expressed by $V_s = NL_p\, di_p/dt$. It is clear from the previous discussions that the secondary voltage, V_s, drops off at higher engine speeds because of the decrease in i_p. Fig. 8 is a performance curve of V_s and I_p as a function of engine rpm. Actually, the secondary voltage

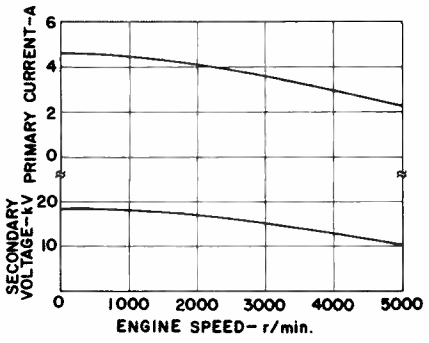

Fig. 8 — Performance curve for breaker-point ignition.

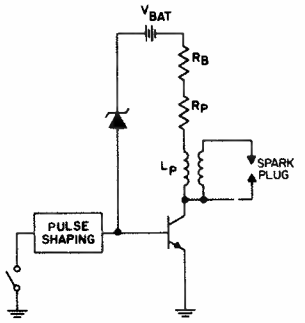

Fig. 9 — Electronic ignition; high-speed transistor replaces breaker points.

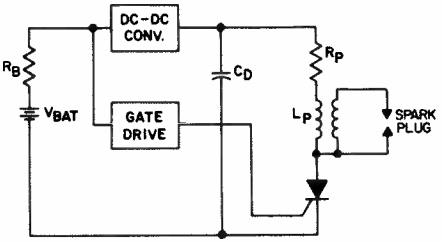

Fig. 10 — Capacitor discharge ignition.

shown in Fig. 8 is less than ideal, because of breaker-point losses at the low rpm levels.

Electronic ignition

The electronic ignition system employs a high-speed transistor in place of the breaker points. A simplified schematic is shown in Fig. 9. The power transistor is the important element in the solid-state ignition system—it performs the same function as the breaker points, but more efficiently. The primary current remains an exponential rise as a function of the time constant τ, so one can still expect a fall-out in secondary voltage at higher engine speeds. At lower speeds, however, the more efficient power transistor allows the secondary voltage to approach the ideal value.

Capacitor discharge ignition

The capacitor discharge (CD) system, differs vastly from the previous two systems because of its SCR requirements. If we were to substitute an SCR for the transistor switch, turn-on can be achieved, but some external means must be provided to shut the SCR off reliably. The new approach used is shown in Fig. 10. The basic difference in the CD system is the need for a dc-dc converter to boost the battery's 12V to approximately 350V. The induction coil need only be a pulse transformer, since the CD system is a resonant system comprising of C_D, R_p and L_p. Performance at high engine speeds is not restricted by an exponential time constant, but rather by the time required to charge capacitor C_D to the required voltage level. With C_D charged to 350V, closing the breaker points provides a gate signal which turns on the SCR. Capacitor C_D discharges through R_p, L_p and the power SCR, developing a pulse voltage at the secondary, V_s, and the stored energy is delivered to the spark plug as a pulse when the SCR is turned on. The diode in parallel with the SCR allows reverse energy to flow during the negative half-cycle of the resonant frequency. Without the diode, the spark duration is limited to approximately half the resonant LC frequency.

The capacitor discharge system has many advantages in that:

1) the coil transformer is less expensive than an ignition coil;
2) the input power increases with increased plug power at higher engine speeds; and
3) the fast rise times associated with SCR turn-on are far more efficient when firing fouled plugs.

However, the additional cost of the dc-dc converter used in the charging circuit of the storage capacitor is a disadvantage. Despite this additional cost, there are a number of CD systems available for the after-market.

Non-ignition power switching ...problem

The single most attractive feature of an SCR for automotive use is its current-handling capability. For example, consider the many lamp loads in today's automobile. The ratio of inrush to steady-state currents can easily be handled by SCR's with minimum power losses in the gate drive logic. The same is not true for transistors. Another example is in motor-drive requirements. Today's fast-turn-off SCR's can easily handle 40A rms at 20-kHz switching speeds. Again, a challenge for the transistor counterpart. But the SCR has not yet been accepted for automotive use, mainly because of its turn-off requirements when used in dc circuits. SCR's were used in windshield wiper pause controls, where the shorting switch of the motor was used to turn off the SCR. Sequential light systems use SCR's, but additional circuitry is always needed to insure reliable turn-off. This additional cost of outboard components needed for turn-off is reflected in the auto industry's limited use of SCR's.

...and solution

If we can combine the turn-on properties of SCR's with the turn-off properties of transistors, then truly we have a power switch for the automotive needs of today and the future. And, a recent development combining epitaxial transistor technology with SCR technology has produced a new power switch with both these properties. This device, commonly referred to as a gate turn off-SCR (GTO-SCR), can control automotive loads by applying appropriate gate signals to the gate terminal. A positive gate signal turns the device on, as with an SCR, and a negative gate signal turns off the power switch, similar to transistor action. This combination of transistor-SCR technology provides a power switch capable of meeting most, if not all, automotive load requirements and also provides the system designer the flexibility needed to control the various electrical loads through low-level logic sources. This new device brings the idea of multiplexed automotive electrical systems closer to reality. See Wojslawowicz's article in this issue, "The GTO-SCR—solid-state's remote automotive power switch," for a description of this system and actual GTO applications.

As mentioned earlier, conventional SCR's cannot be turned off at the controlled gate because of their internal gate impedance. However, the base spreading

resistance can be controlled in a GTO-SCR such that the lateral resistance under the cathode region is low enough for reliable gate turn-off. Fig. 11 depicts the vertical structure of a conventional SCR. The p area under gate and cathode is the lateral base resistance. For reliable turn-off, this resistance must: 1) be low enough to minimize the IR drop; and 2) maintain a high reverse-avalanche breakdown. Neither of these conditions are met with the conventional SCR. However, epitaxial technology can be used to grow two independent p areas under the cathode region and so meet both conditions. The control of the base spreading resistance is a contributing factor in the success of a GTO, but it is not the only one—the distance of the lateral resistance, and vertical and horizontal geometries are also important. By employing digitation between the cathode and base regions, low lateral distances are controlled. Meeting these conditions and using epitaxial technology for process control has now resulted in the birth of a new SCR family—the GTO-SCR's.

GTO applications

Now let us look at the many automotive applications where the GTO can play an important role as the main power switch. First, let us consider lamp applications. A high-beam headlamp with a steady state current of 4.5A has a peak inrush current of 26A, decaying to approximatley 25% in 10 ms. An active power switch must be capable of supporting the inrush currents as well as the steady state currents. Does this application require a 25-A transistor? How does one design the base drive requirements necessary to meet both inrush and steady-state currents? Doesn't this requirement sound like a nightmare for any circuit design engineer? Not so with a GTO, since it combines transistor and thyristor technology.

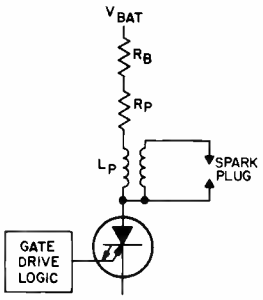

Fig. 13 — GTO can replace power transistor in ignition circuit.

Table I — GTO vs. transistors.

	GTO	*Epitaxial base transistor*	*High-voltage transistor*
Type	G550M	2N6486	2N6513
Pellet size	150 mils	150 mils	180 mils
Voltage	600V	50V	400 V
Current	10A	6A	3A
Peak current	60A	15A	7A
t_{on}*	1.5μs	0.5 μs (typ)	1.5μs
t_{off}*	1.0μs	0.8 μs (typ)	1.5μs

*T_j = 125°C for GTO; T_j = 25°C for transistors.

Looking at the inrush current of the lamp, a 26-A peak for 10ms is duck soup for any power SCR. Nominal gate trigger currents, which can be pulses, will turn the SCR on. When the lamp filaments are hot, steady-state currents are reached, and 4.5A turn-off is easy for a GTO-SCR. Consider the circuit shown in Fig. 12. With S1 in position 1, the GTO-SCR easily accepts the lamp inrush. For turn-off, S1 is moved to position 2, which grounds the gate of the GTO and in effect provides a reverse bias to the cathode (same as a negative voltage to the gate), and turns the GTO off. So, through the use of a GTO-SCR, circuit simplicity is easily achieved.

Next, let us look at inductive load applications—specifically a heater blower motor. Steady-state requirements for the motor are 10A, with a peak inrush of 50A. Again the challenge to the circuit designers is how to provide base drive for both inrush and steady-state conditions. But with the GTO-SCR, the inrush currents are handled by the SCR section and typical transistor drive circuits take care of turn-off. One might argue that the power darlington is a strong competitor to the GTO, but the darlington still suffers, as the transistor does, in accepting inrush currents. Both devices experience quasi-saturation at currents beyond a specified maximum value; the GTO does not, since it employs regeneration during the on state.

Finally, let us consider the GTO in an automotive ignition application. In Fig. 13, the GTO is used as the power switch with an anode load. In this application, we are only concerned with steady state currents, so how can a GTO compete with a transistor for this socket? The answer is in its volt-ampere capability. Because of the SCR structure, blocking voltages up to 800V have been achieved with 10-A switching capability. The high volt-ampere rating allows the circuit designer to operate the GTO power switch at high voltage without protective devices. For this application, the GTO offers the performance of a transistor with high SCR blocking capability. Table I compares GTO's and power transistors.

AC automotive power in the future?

Of course, since all automotive circuits are now dc-source supplied, the triac ac switch was not covered here. However, since all automobiles are now equipped with ac alternators that could be made into the power source, the triac could replace the dc power switches. The volt-ampere capability of a triac is equivalent to an SCR's. With an ac-source supply, triac turn-off will occur at the zero-current crossing after the gate drive had been removed. On-off lamp controls could be combined with simple lamp dimming circuits, motor speed control can be accomplished by simple RC phase controls, and the cost for logic control of ac devices would be considerably less than for dc devices. However, the trend to convert to ac power sources is not evident in Detroit.

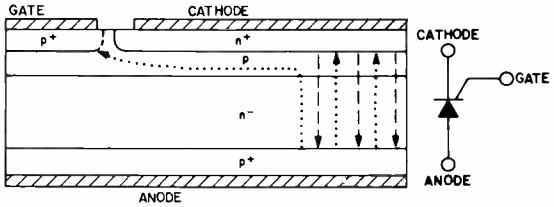

Fig. 11 — Vertical structure of conventional SCR. Resistance of p area under cathode and gate must be controlled for reliable dc turn-off. GTO-SCR does this by using epitaxial technology to grow two independent p areas under cathode.

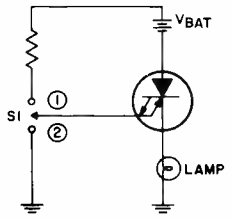

Fig. 12 — Lamp-control circuit using GTO-SCR handles inrush and steady-state currents.

High-voltage darlington for auto ignitions

W.C. Simpson

Electronic ignition has already progressed from the early discrete devices to more reliable monolithic IC's. The automotive environment produces difficult specifications and constraints; this article details the numerous optimizations and trade-offs the designer must make in developing a new monolithic device.

FIRST-GENERATION electronic ignition systems consisted of many discrete components built into modules with at least four discrete switching transistors in various configurations as primary components. While these modules offer high reliability and excellent performance, their energy capability is not sufficient to allow usage in the wide-spark-gap/lean-fuel-mixture/high-energy systems now being used to cope with increasingly strict pollution standards and economic considerations.

In designing the new high-energy systems, using monolithic darlingtons for both the low-voltage input and high-voltage output stages yields significant size and reliability advantages. The RCA TA8766 high-voltage darlington, used in the output stage, and the RCA 2N6385 low-voltage darlington, used in the input stage, are both simple monolithic circuits. They consist of bipolar transistor driver and output devices, two resistors, and a diode. Both are fabricated using standard monolithic techniques and interconnected as single high-gain transistors. Discrete, monolithic, and RCA power darlington circuits are shown in Fig. 1. shown in Fig. 1.

While this article deals specifically with the high-voltage darlington for automotive ignitions, RCA power darlingtons have many other potential applications including industrial switching, hammer drivers, voltage regulation, high-voltage inverters and audio amplification.

Device requirements

The device characteristics required for automotive ignition usage are quite specific though they vary with the design of the individual customer's module. There are a number of basic requirements, however, which they share.

First, they must be capable of withstanding high energy dissipation, 300 millijoules minimum. They must have high sustaining voltages in the reverse mode (e.g., $V_{cer(sus)} > 400V$). They must be capable of high gains at low supply voltages to accommodate the 12V auto battery, even when lower voltage is present in cold weather or when the battery has been partially drained by use. Saturation voltages must likewise be low, to avoid monopolizing too much of the battery voltage, since the darlington will be in series with a number other components, notably the IC driver. They must be capable of switching within the specific time windows required by the particular module; typical requirements are a $t_{storage}$ of approximately 59 to 25μs and a t_{fall} of under 20μs. They must also be capable of operating over a wide temperature range, usually specified as from −30 to 150°C. Specifically, they must maintain high gain and low leakage over this range, though the specifications do allow for some degradation from room temperatures. They are also required to withstand battery reversal for a finite period of time, typically 5 min. Table I lists typical performance specifications.

Design constraints

In designing an automotive-ignition darlington, there are a number of constraints which should be considered. The device design and processing must be compatible with present RCA power transistor technology for ready transfer to the factory. In the development time

RE-22-2-4
Final manuscript received May 6, 1976.

William Simpson, Power Transistor Design, Solid State Division, Somerville, N.J. received the BSEE from Newark College of Engineering in 1973. After graduation, he joined the Power Transistor Design Group working on the devleopment of the TA8766 high-voltage darlington. His responsibilities included model shop process development, modification of device design, and introduction of the TA8766 into the factory. He is currently working on new darlington designs.

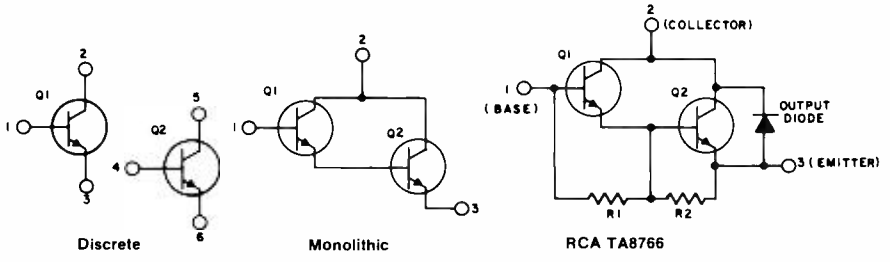

Fig. 1 — Progression of darlington switching transistors for automotive ignition. Future design may include built-in zener clamp to regulate darlington breakdown voltage.

cycle considered, Ni-Pb metalization and a non-passivated mesa structure with mechanized mounting in the standard TO-3 package were chosen to meet performance and high-reliability requirements. Perhaps most importantly, it should be capable of high volume production and relatively inexpensive manufacture in order to survive in the highly competitive automotive marketplace.

Design optimization

With these considerations in mind, the designer can address himself to these basic design questions:

1. What geometry, vertical structure, and technology is best capable of meeting all required specifications?
2. What compromises must be made in terms of geometry, structure, and technology to make the design cost-effective and insure compatibility with existing manufacturing technology?
3. Can new technologies or processes required be implemented, if necessary?

To an engineer involved in pure design or development, the last two questions may seem to go beyond basic design considerations, but for a designer in a close factory-related function, they are often more basic than the first.

Vertical structure

There are several device requirements that are directly related to vertical structure—energy dissipation, sustaining voltage, switching speed, and saturation voltages.

Energy dissipation

In order to withstand high energy dissipation, some form of collector ballasting is necessary. With a diffused collector structure, this ballasting is automatic, though difficult to control, resulting from the doping profile within the collector region. An epitaxial structure, however, is not normally graded, but abruptly layered. Experience on the 2N5840 and 2N6510 auto switching transistors has shown that the graded profile of a diffused collector can be approximated by using multiple epi layers[2] with decreasing resistivity. The vertical epi structure is shown in Fig. 2. The result is the controlled collector of the epi structure, while retaining and increasing the ballasting and energy capability of the diffused structure. Control of the epitaxial layers guarantees termination of the electric field within the device before it can reach the heavily doped substrate. This provides a region for additional field spread under base-widening conditions, thereby increasing the secondary-breakdown energy capability. The energy capability of the device can be increased by enlarging the thickness of the collector epi or modifying the grade to produce a smoother transition from the high-resistivity region to the substrate.

Fig. 2a — Starting wafer.

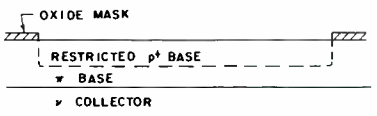

Fig. 2b — Oxidation; define, deposit and diffuse diborane-restricted P+ base.

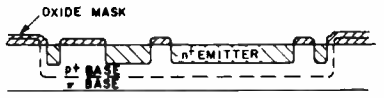

Fig. 2c — Define, deposit, and drive emitter.

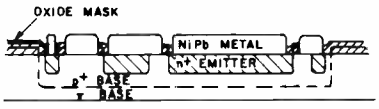

Fig. 2d — Define contacts and metalize.

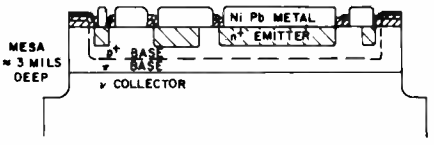

Fig. 2e — Define and etch mesa; test and separate pellets for assembly.

Fig. 2 — Process and vertical structure for high-voltage darlington.

Sustaining voltage

The sustaining voltage, or that V_{ce} which the device will sustain in breakdown from collector to emitter, is likewise dependent on the epi profile,[3] primarily the high-ρ collector (ν) and the epi base (π) layers, though the N^- buffer layer also contributes. The relative voltage support contributions of each layer are shown in Fig. 3. It is readily apparent that an increase in either the thickness (w) or resistivity (ρ) of these regions will produce higher sustaining voltages. This is done, however, at the expense of the saturation voltage and beta.

An increase in the thickness or conductivity of the π layer increases the effective base width of the transistor and thereby decreases beta. An increase in collector thickness or resistivity increases the collector resistance and thereby $V_{ce(sat)}$. It should be noted that while sustaining voltage and energy vary ±50% with changes in vertical structure, the saturation voltages vary only by about ±10 to 15%. Variations in beta likewise appear significant, though there are so

Table I — Typical test requirements for TA8766 monolithic IC.

Test	*Conditions*	*Specification*
V_{cer}	I_c = 0.25A, R_{bc} = 27 ohms	>400V
$V_{be\ (on)}$	I_c = 8A, V_{ce} = 1.5V	<2.1V
$V_{ce(sat)}$	I_c = 8A, I_b = 500mA	<1.4V
$I_{s/b}$	V_{ce} = 30V, I_c = 5A, t = 1s	Pass
I_{ceo}	V_{ce} = 400V, R_{bc} = 27 ohms	<4.5mA

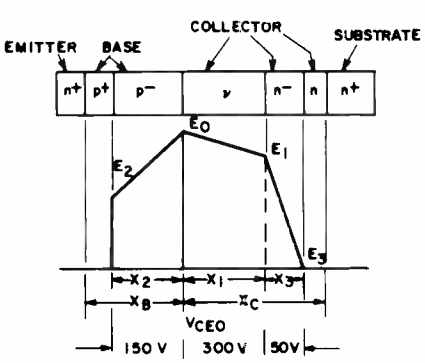

Fig. 3 — Field profile for TA8766. Area under curve gives breakdown voltage.

many factors affecting beta, (base width, surface effects, including leakage, and lifetime), that it is difficult to assess the actual contribution from each.

Switching speed

Another factor related to vertical structure is the switching speed, most notably storage time ($t_{storage}$). In trying to understand large-signal switching phenomenon, a good analogy is the stored-base-charge transistor analysis advanced by Beaufoy and Sparkes and used by Philips in "Transistor Engineering".[4] In this concept, collector current is related to base charge, with changes in collector current being the consequence of changes in base charge. Storage time is that time required to remove excess charge from the base (and high-resistivity collector regions) when turning the device from hard *on* to *off*.

The amount of charge stored depends in part on the ability of the structure to store charge and on the excess charge available for storage. Since excess charge is that charge which the circuit supplies beyond that which the device requires for saturation, a low saturation voltage makes more excess charge available for storage. The amount the device is capable of storing depends on the resistivity and thickness of the charge-storage regions, i.e., the base and low-ohmic collector region.

The overall result is that with ρ and w held constant, $t_{storage}$ varies inversely with $V_{(sat)}$. Likewise, with $V_{(sat)}$ held constant, $t_{storage}$ varies directly with the ρ and the w of the storage regions. This has been shown by experimental data gathered on the TA8766, though the results have been at times difficult to analyze properly. While the saturation voltage is readily measured, the thickness and resistivity of the various charge storage regions are difficult, requiring mazur probe analysis. While good correlation of $t_{storage}$ and $V_{(sat)}$ has been found on homogeneous epitaxial wafer lots, where the charge storage regions presumably are identical or nearly so, substantial additional work with carefully categorized epitaxial layers would be necessary to show clear correlation of $t_{storage}$ and $V_{(sat)}$ across the epi spectrum.

The vertical structure finally chosen for the monolithic darlington is shown in Fig. 4. It seems to offer the best compromise of characteristics from the available wafers. It is basically the same vertical structure as that used in the 2N6510 automotive switching transistor, except for increased layer thickness and minor differences in the base and emitter diffusion profiles.

Geometry decisions

There were a number of considerations affecting the physical layout or geometry of the device, though all were basic ones. The darlington was to include, in addition to the two transistors, both input and output resistors, and an output diode for reverse battery protection. This is shown in Fig. 1c.

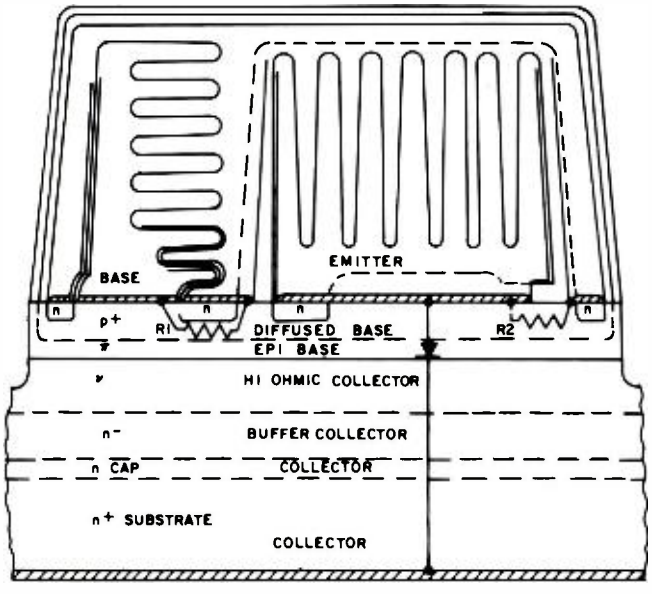

Fig. 4 — Vertical structure for monolithic darlington.

Resistors for leakage protection

The resistors were used to provide a measure of stability and improved voltage capability. Leakage is always a concern in high-voltage, high-power devices, and this is especially true of the high-voltage darlington. Because the darlington is a self-contained multistage amplifier, any leakage generated can be amplified within itself, resulting in the transistor's turning on and running away at elevated temperatures. By building shunt paths of sufficiently low resistance into the monolithic darlington, R1 and R2, leakage can be effectively controlled. Because leakage into the base of Q1 is amplified by the beta of Q1, and then fed into the base of Q2, Q2 is particularly susceptible to leakage turn-on. R2 is therefore designed to a relatively low value to give Q2 added leakage immunity at both room and elevated temperatures.

Sustaining voltage increase

The resistors also serve to increase the sustaining voltages. The maximum sustaining voltage for a given device occurs when the base is shorted to the emitter in the common-emitter configuration, V_{ces}. The minimum sustaining voltage occurs in the V_{ceo} condition, when the base is open-circuited. The V_{cer} condition, or voltage collector to emitter with base tied to the emitter by a resistor, gives some intermediate voltage depending on whether the resistance value approaches infinity (V_{ceo}) or zero (V_{ces}). The darlington, then, with built-in resistors, when measured in the V_{ceo} mode, is actually in the V_{cer} mode with a corresponding increase in voltage. Likewise, when measured in the V_{cer} mode, the external resistor is in parallel with the internal resistors, lowering the effective resistance value, which also gives a voltage increase although it is generally not significant.

Silicon minimization

Since silicon area is always at a premium, these resistors should be made using minimum device area. The output resistor should be sufficiently low in value to provide some leakage immunity at elevated temperatures, as previously noted. Experiments with a hybrid darlington analog indicated an optimum range from 20 to 100 ohms, and a nominal 50-ohm target value was es-

tablished. A typical base sheet resistance of 20 ohms/square made this value easily obtainable with little territorial loss. This is shown in Fig. 4.

The input resistor required a range of 250 to 1000 ohms, with a nominal 500-ohm target value. To form a surface resistor of this value at 20 ohms/square meant either considerable area loss or very fine lines with subsequent processing problems. An alternative solution was to use a pinch resistor, taking advantage of the common-base construction, as had been done on earlier low-power darlingtons.[1] R1 is therefore formed under the driver emitter with little loss in area. This is shown in the vertical profile, Fig. 4. The only drawback of this type of R1 formation is the dependence of R1 on emitter depth, though it has been demonstrated that this can be adequately controlled. In addition, R1 also varies with base doping and width, and is affected to a large extent by device temperature, though again the variation is considered to be within controllable limits.

Protective diode

An output or commutating diode was required as insurance against reverse battery failure by several customers. This diode is formed as a natural consequence of the formation of the R2 surface resistor. Using this diode for reverse battery protection required allowing it sufficient area to withstand the high forward current density imposed by the battery reversal. This was achieved by leaving a large (approximately 1000 square mil) gap in the output emitter area and shorting the emitter metalization over it. Since very little of the output current flows from the center of the emitter, using portions of this area as an output diode does not affect the device performance. The diode is capable of drawing more than 10A in the forward direction before overheating and destruction occur.

Geometry and production

The final geometry decision considered here, though in fact it is the first decision made in the design process, is by far the most important. What type of pattern and area distribution among the two transistors will yield the most efficient and reproducible device? Here again, major constraints come into play. High current-gain requirements require maximum-output emitter peripheries to reduce current crowding, hot-spotting, and high-current beta fall-off.

Interdigitated design

For these reasons an interdigitated design was chosen. With Ni-Pb, pattern geometry must be carefully optimized for lead coverage as well as theoretical performance. Optimized performance on the drawing board is totally negated if the device cannot be metalized properly. While using the Ni-Pb system places limits on the fingers' widths and lengths, and therefore the potential periphery-to-area ratios, reasonable compromises are possible.

Though lead-dipping is both effective and inexpensive, the resultant lead coverage varies in thickness across the pattern, depending as it does on the surface tension of the molten lead. The result is varying metalization resistance and voltage drop along the lengths of the fingers; the thinner the lead, the greater the drop, and vice versa. This then tends to "turn off" certain segments of the pattern by limiting the current flow in these regions. This can be observed clearly during an infrared scan of an operating device. Those areas which are turned on hard glow brightly, while those areas with high resistance, where current flow is limited, appear much fainter. Fig. 5 is an example of this phenomenon. The uneven current flow causes hot spots and diminished efficiencies.

Ballasting

One solution to this problem is ballasting the pattern, or adding selective local resistances, in such a way as to equalize the voltage drops to all pattern areas. This is done by building resistances or voltage drops into normally low-voltage-drop areas and bringing their values up to those of the high-drop areas. This increases saturation voltages, but the improvement in efficiency often more than compensates.

Fig. 5 — Infrared scan of operating "snowflake" darlington. High-resistance areas limit current flow, appear much fainter than hard-turned-on areas.

Because of the tight $V_{ce(sat)}$ and $V_{be(sat)}$ specifications, it was necessary to limit ballasting. The pattern finally chosen is a basic straight-finger interdigitated design, with low-level ballasting achieved by tapering the fingers and pulling back the metalization from the junction in high-current-density regions. Other designs using the intedigitated snowflake geometry are also being studied with very encouraging results. Assuming that improved processing can lower our susceptibility to $V_{(sat)}$ problems, a design of this type can readily take advantage of its improved current distribution. Both patterns are shown in Fig. 6.

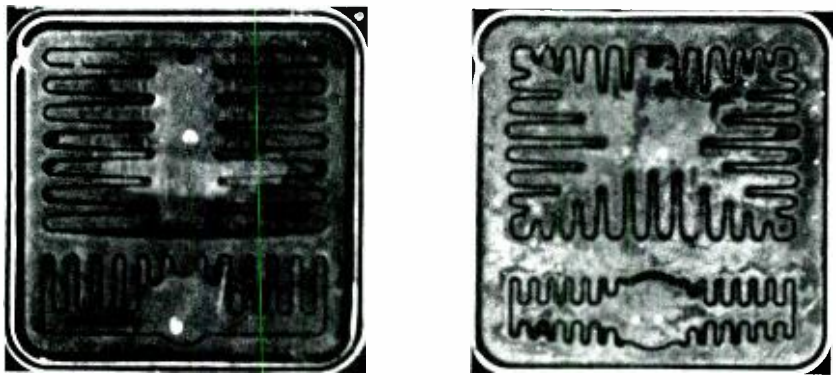

Fig. 6 — Current distribution for straight-finger-interdigitated (left) and interdigitated-snowflake (right) designs.

Current distribution

One of the prime reasons for using the monolithic darlington is the excellent high-current beta it achieves through multi-stage amplification. Because the driver operates at far lower current levels than the output device, it is reasonable to allocate less area for the transistor driver than the output device. This increases area utilization for the output transistor, which operates at far greater current densities, resulting in improved efficiency through better current distribution. Considerable work was done by W.G. Einthoven and C.F. Wheatley[5] to derive the optimized relationships between the two devices. In summary, peak high current is achieved by making the driver size approximately half that of the output, though the exact dimensions are not critical. This relationship has been followed in all recent design efforts.

Mesa structure

An additional geometry consideration is the choice between the standard grid mesa and the uni-moat mesa. (Both are shown in Fig. 7.) The standard mesa results from etching an interconnected grid across the entire wafer between adjacent pellets. The pellets are then separated by laser-scribing down the center of the grid lines and breaking the pellets apart. While this process, with variations, has been used for most of the years mesa devices have been manufactured, it has drawbacks. First, damage may be introduced while scribing through the grid. Because sustaining voltage and leakage are both extremely sensitive to mesa conditions (both are important power-device characteristics), either can be adversely affected by mesa damage should it extend into or near the base-collector junction. A wide grid can help keep the damage from reaching the junction, though losing any silicon real estate is undesirable from a cost standpoint.

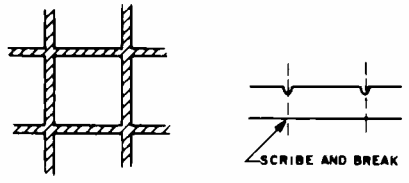

(a) STANDARD GRID MESA

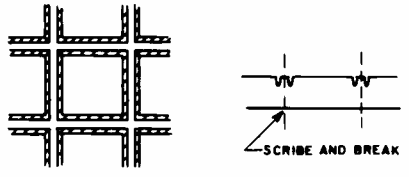

(b) UNI-MOAT MESA

Fig. 7 — Mesa types.

Secondly, mesa devices should be encapsulated in some type of dielectric to insure maximum voltage capability. This reduces the possibility that air-dielectric breakdown can occur across the base-collector junction. It also helps keep the mesa uncontaminated during subsequent processing and sealing, and complete coverage of the mesa with encapsulant is important.

An alternative to the grid mesa is etching a single non-connected moat (or uni-moat) around each individual pellet. The scribing can then be done in an area outside the moat, eliminating possible damage to the mesa during scribing. The moat can also act as a trap for the encapsulation, channeling it around the pellet and ensuring more complete mesa coverage. The uni-moat is, however, more difficult to etch and control. For this reason, the darlington is manufactured with the standard grid mesa, though the uni-moat is under study, and could be adapted in the future.

The darlington was likewise designed for mechanized mounting and the tooling required for this is presently being readied. This has several advantages including rapid assembly, lower cost, and slightly higher yields.

Process considerations

The darlington process is compatible with the factory high-voltage power line. The basic process is outlined in Fig. 2 and includes several features which may or may not be used on various transistor types, but which are felt to be necessary to meet the stringent darlington specifications. A restricted P^+ base is used to obtain maximum field spread at the mesa and subsequent maximum voltage in the sustaining mode. Slow cooling is used on all furnace steps above 1100°C, and slow push/pull boat insertion and removal on all steps above 1000°C, to obtain maximum lifetime and increased beta. The lean emitter ($Nd<10^{20}$) process is used to flatten the beta curve and improve reproducibility.

Where to from here

This device, the TA8766, is presently being manufactured at the Mountaintop facility at low volumes, although the marketplace could easily demand in excess of half a million devices per month in the foreseeable future if the automotive industry undergoes a 100%-turnover from discrete to darlington ignitions, as predicted.

The darlington described offers many potential areas for improvement. The main problem areas are high-temperature stability in terms of leakage, marginal $V_{(sat)}$ performance, and ballasting requirements for maximum energy capability through more uniform current distribution. All three areas will respond to design modification. High-temperature leakage may be minimized through passivation of the base-collector junction. The goal is to produce a darlington capable of operating at junction temperatures of 200°C. The present product is capable of 175°C.

More in the package

Cost effectiveness is always a continuing struggle, as we are forced to frequently revise prices downward in an attempt to maintain our share of the market against stiff competition. One way to gain a competitive advantage while actually increasing or maintaining present prices is to offer the customer more in terms of device performance or capability. An example of this is the elimination of the zener clamp built into ignition modules to regulate the darlington breakdown voltage. By integrating this clamp into the monolithic darlington package, we could eliminate the need for a discrete zener in the module. This offers overall size, price, and reliability advantages to the customer, which could be used to justify a slight price increase for the darlington package with virtually no penalty in terms of manufacture. This is a distinct improvement in cost effectiveness, and a design of this type is under development.

References

1. "RCA power transistors", SSD204C, 1975.
2. "RCA solid-state power circuits", SP-52, 1971.
3. Denning, R., and Moe, D.: "Epitaxial pi-nu n-p-n high voltage power transistors," ST-4287, 1970.
4. Phillips, Alvin B., "Transistor Engineering," McGraw-Hill, 1972.
5. Einthoven, W.G.; and Wheatley, C.F., Jr.: "On the proportioning of chip area for multi-stage darlington power transistors," ST-6405, 1975.

The GTO-SCR: solid-state's remote automotive power switch

J.E. Wojslawowicz

This recent solid-state device development has brought semiconductor control of automotive loads, and even multiplexed electrical systems, closer to reality.

THE COMPLEXITY of today's wiring harness has outdistanced the control concepts of the system of which it is a part. The necessity of selecting wire sizes and switches capable of controlling the full-load current in an automobile has resulted in a wiring system that is not only expensive to manufacture, but also has a higher potential for failures. The number of wires in the harness has increased beyond the optimum as car buyers have demanded more convenience features. Power windows, power door locks, power seat controls, the power antenna, and similar items have resulted in a bundle of wires that is awkard in size and hard to handle.

The problem is compounded by the fact that most of these items must be controlled from the driver's seat. The "brute force" method of distributing electrical power throughout the automobile has created this problem. The horn relay and the starter relay represent exceptions to this method; but although relays could possibly be used as for remote power switching, the problems of chatter, corroding contacts, and mechanical failure have not made them attractive for general-purpose use in the automotive electrical environment.

Using solid-state devices as the remote power switches has always had appeal because of their noiseless operation and long-term reliability, but the severe automotive electrical environment has been a strong constraint against their use. Voltage transients, inrush-current surges, low on-state voltage drops, and low battery drain during off times all present unique requirements for the solid-state device.

However, all of these requirements are met by the GTO-SCR (gate-turn-off silicon-controlled rectifier).It needs only small signals to control taillamps, blowers and other automotive loads, so its use can reduce wiring and switch sizes significantly. The device has the usual solid-state reliability advantages, and is also logic-compatible.

GTO's are being proposed for the multiplexed distribution system, which would consist of a single heavy-duty power bus running around the perimeter of the car and light-duty wiring running from the dashboard switches or logic to the GTO's, which would tap off power for the individual components. Not only would this system save on wiring and interconnections, it would increase reliability and simplify troubleshooting and repair procedures.

Basic GTO operating characteristics

The GTO, a member of the thyristor family, is a four-layer, three-junction semiconductor device. These layers of opposite-impurity doping give it a bistable switching characteristic; that is, the device remains stable in either the *off* (high-impedance) or *on* (low-impedance) state until a control signal is applied to the control electrode, or gate. Applying a positive current to the device switches it from the high-impedance *off* state to the *on* state. Once the device has achieved turn-on (is in the regenerative state), the gate drive can be removed. This feature makes the GTO capable of being turned on by only a pulse of current. However, because it operates using an internal regenerative feedback mechanism, the main-terminal current flow must be limited by the external circuit.

The GTO's ability to drive itself into saturation enables it to sustain surges of main-terminal current flow of short duration, allowing the device to handle cold-filament lamp inrush currents and motor startup currents quite readily. Once the device is stable in the *on* state, it maintains itself there until something is done to curtail the internal regenerative feedback mechanism. In the GTO, this feedback is interrupted by applying a short pulse of current to the gate. The polarity of the current must be opposite to that required for turn-on and can last only until the device regains its high-impedance or *off* state. The low average drive-power requirement of the GTO is a result of the fact that only short current pulses are necessary to achieve the transitions between states. This advantage, along with the capability of the GTO to withstand surges of current in excess of its steady-state rating, makes it a viable remote power switch for automotive electrical loads.

Jack Wojslawowicz, Applications Engineer, Solid State Div., Somerville, N.J., received his BSEE *cum laude* from Newark College of Engineering in 1970 and joined the RCA Solid State Div. that year. He became active in the characterization and application of thyristor products, and was assigned application responsibility for the gate-turn-off SCR during the early development of the RCA Solid State Technology Center. Mr. Wojslawowicz's duties also include overseeing the development of an automated testing system for RCA's thyristor products. This project has encompassed the development of new operating software for computerized test systems and new testing networks for device characterization. He has authored or co-authored several papers, holds one patent, and has another pending. He serves as an alternate member for RCA on the EIA Committee on Thyristors and Rectifiers JC-22, and is a member of Phi Eta Sigma, Eta Kappa Nu, Tau Beta Pi, and the IEEE.

Reprint RE-22-2-3
Final manuscript received April 19, 1976.

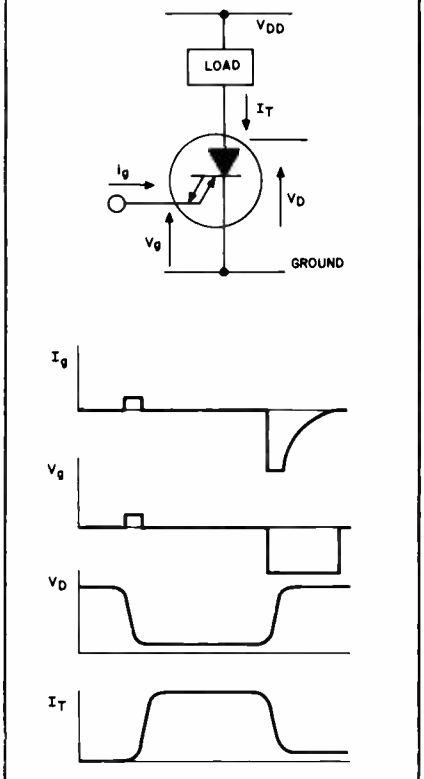

Fig. 1 — Basic anode-load configuration.

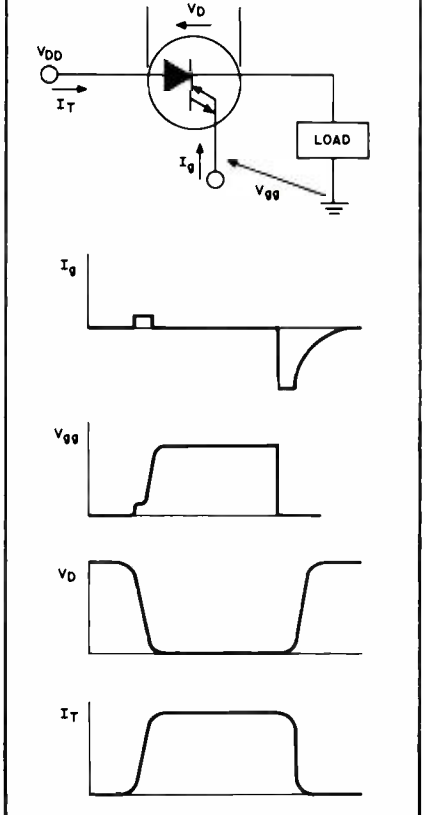

Fig. 2 — Basic cathode-load configuration.

Basic circuit configurations

With the unique ability of the GTO to act as a switch in a dc circuit, its potential for use in an automobile becomes almost limitless. There are two basic circuit configurations that can be used to control a load by means of a GTO (Figs. 1 and 2). A circuit designer can choose either the anode-load or cathode-load configuration. The most obvious difference between the circuits is in the placement of the load, but there are more subtle differences in the techniques that must be employed to drive the GTO.

In the anode-load configuration, Fig. 1, the gate can be biased with a positive current to initiate turn-on by connecting it through a resistor to the supply potential, V_{DD}. However, to achieve turn-off in this configuration, the gate must be biased with a potential that is negative with respect to the cathode or ground. This biasing can be accomplished using a supply that has dual polarity with respect to ground. Then the device is turned off by bringing the gate to the negative potential. Circuits employing inductors and capacitors can also be used to generate the negative voltages needed; but these circuits add complexity, which need not be tolerated if other circuit configurations are available. Moreover, a floating load in an automobile may present additional problems.

The cathode-load configuration shown in Fig. 2 uses a grounded-load concept similar to the load-control methods presently found in automobiles. The device still requires a pulse of positive current to turn it on; the pulse can be provided by terminating the gate through a resistor to the supply, V_{DD}. The load then acts as the return path to ground. The gate potential with respect to ground, V_{gg}, of Fig. 2b, then becomes equal to the load potential plus the gate voltage developed while the device is in the *on* state. To achieve turn-off, current must be extracted from the gate by a source of potential that is negative with respect to the cathode. In the configuration shown in Fig. 2, the cathode is at the positive potential of the load, and the GTO can be turned off simply by bringing the gate to ground; the load will act as the source of negative potential necessary for turn-off.

The photographs in Fig. 3 show the progress of this method of turn-off. The

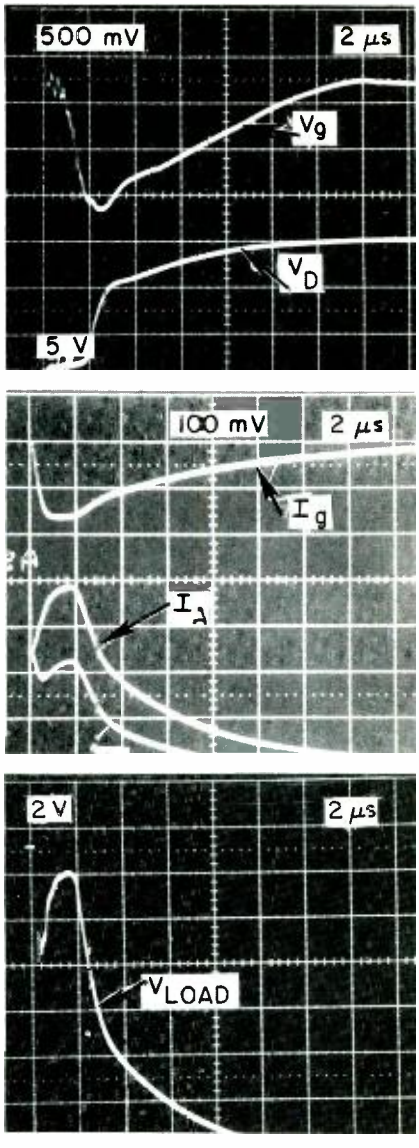

Fig. 3 — Progress of cathode-load turn-off.

device was turned on with a load current of 5A from a 15-V supply. At time t=0, the gate was brought to ground potential through a saturated transistor. The traces in the upper photos show the negative gate voltage and the anode voltage. The second photo shows the gate, anode, and cathode currents during the turn-off process. As the pictures show, turn-off is initiated by the extraction of current from the cathode flow, indicated by the drop in the magnitude of the current, while the remainder of the turn-off current comes from an increase in the anode flow. As the load current starts to decrease, the bias on the gate decreases simultaneously. Eventually a time is reached when the anode current has decayed below the device's holding current, the minimum current necessary to support internal regeneration. After this point the device cannot

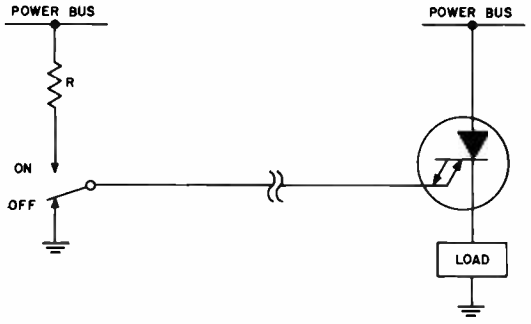

Fig. 4 — Basic cathode-load GTO operating circuit.

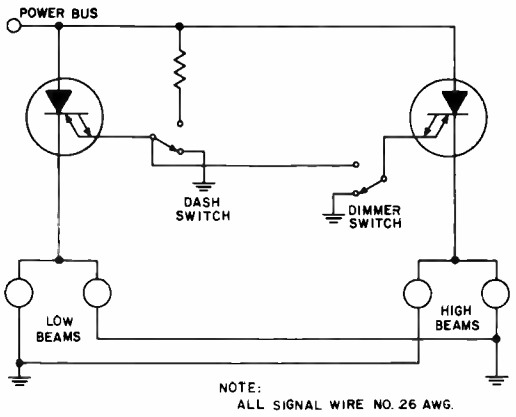

Fig. 5 — Headlamp circuit.

sustain the regeneration mechanism, and it reverts to the *off* state. Because this method of turn-off is compatible with present automotive circuits, it is the best way to use the GTO as a remote automotive power switch.

Using the GTO in the automotive environment then becomes a question of which basic load configuration to use. The cathode load configuration is shown in Fig. 4. A simple single-pole, double-throw (SPDT) switch provides the gate termination needed for turn-on and turn-off. This control technique serves as the basis for several circuits showing the GTO's automotive potential.

Headlamp circuits

The circuit in Fig. 5 employs low-signal switches and GTO's to control the low and high beams of a headlamp system. The GTO's, located at the headlamps, are fed from two switches that provide the dash- and dimmer-switch functions. Operation is straightforward, with the dash switch controlling the low and high beams in conjunction with the dimmer switch. With both switches in the *off* position, neither GTO can be turned on, since both gates are at ground potential. Should the dimmer switch be moved to the *on* position, the high-beam GTO cannot receive gate drive for turn-on, because that path is still held at ground by the dash switch. The high beams can be actuated by that path only when the dash switch is *on*. The dash switch, then, retains control of both sets of lamps as in the present system. Moving the dash switch to the *on* position turns the GTO's on by providing gate drive through the resistor. The dimmer switch can then activate or deactivate the high beams, and turn-off of both sets of beams is possible with the dash switch. The result is a system that operationally duplicates the present set-up without the need for wires or switches capable of controlling the full headlamp load. In fact, using GTO's drops the wire size from AWG 14 all the way down to AWG 26.

Turn/brake/hazard circuit

An all-solid-state approach to replacing complex automotive switching is possible for controlling the lamps for turn, brake, and hazard signalling. The present circuitry uses mechanical switches to provide the logic and load-current handling. The scheme outlined here replaces the load-current-handling contacts with GTO's and the switching logic with an SSI (small scale integration) integrated circuit driven by simple small switches. Shown in Fig. 6, the system would use a logic module to decode the information from the switches and then provide command signals to the individual interface circuits for each GTO-controlled lamp in the automobile. Figs. 7 and 8 show a realization of this scheme, with Fig. 7 showing the logic necessary to decode the information from the very simple turn, brake, and hazard switches. The module also includes an astable multivibrator that provides a modulated output when necessary. Fig. 8 is a schematic diagram of the interface circuit used to drive the GTO's. This circuit has a totem-pole output similar to those used in TTL logic circuits. When the output is high, the circuit turns on the upper output transistor and allows it to supply drive to turn on the GTO, and hence the load. With a low input the lower darlington part is turned on, shutting the GTO off. When the systems of Figs. 7 and 8 are combined, they provide the same kind of operational control presently available for automobile lamps.

Auxiliary lighting controls

Occasionally it is necessary to operate standard automotive lights at higher voltages. The techniques used to ac-

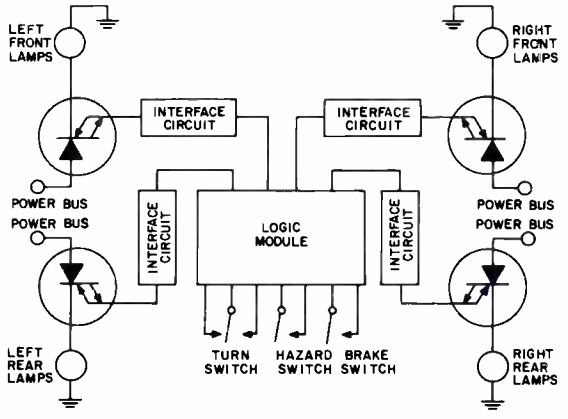

Fig. 6 — Turn/brake/hazard circuit using logic and GTO's.

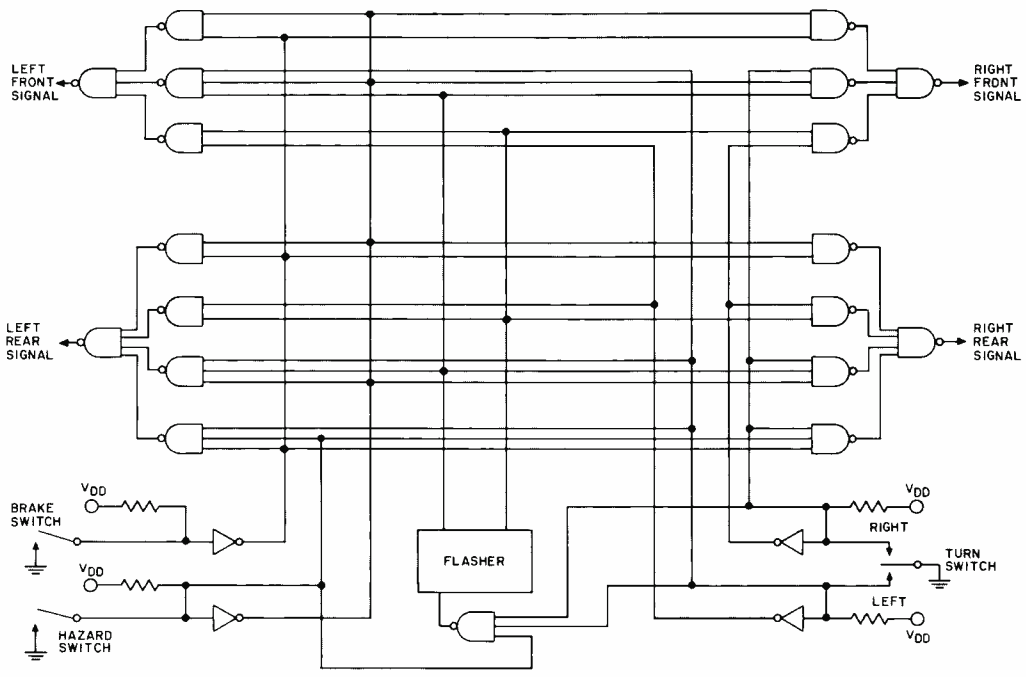

Fig. 7 — Logic for turn/brake/hazard lamp control system.

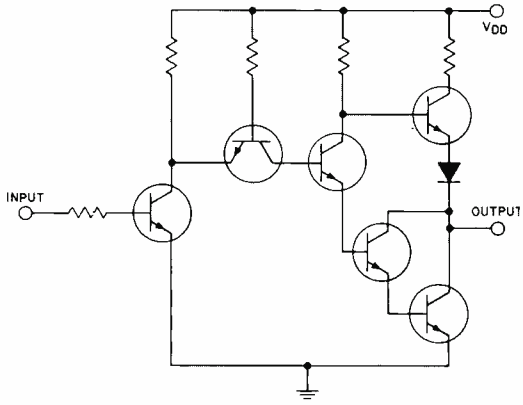

Fig. 8 — Interface for controlling cathode-load GTO with logic signals.

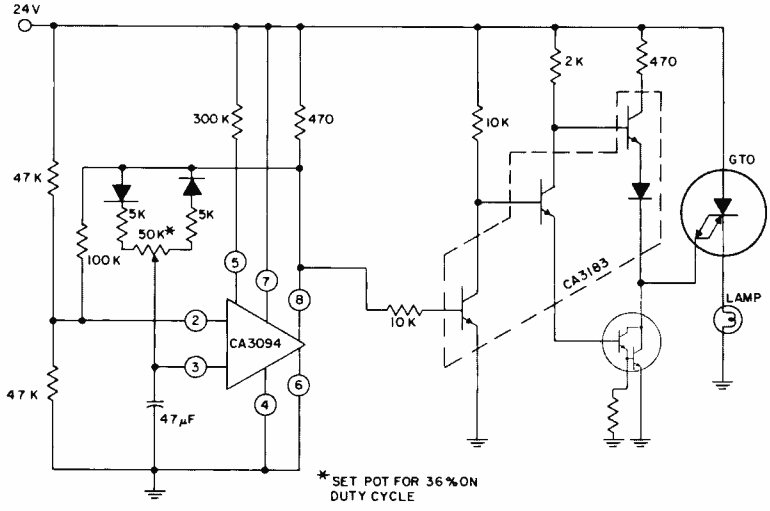

Fig. 9 — 24V-to-12V headlamp system using pulse-width-modulated GTO circuit.

complish this generally have consisted of using series dropping resistors. The GTO, when operated in a pulse-width-modulated scheme, can perform the same function at much higher efficiency. The circuit in Fig. 9 has been used to operate 12-volt headlamps off a 24-volt supply. The CA3094 is set up as a constant-frequency, constant-duty-cycle oscillator driving an interface circuit consisting of a CA3183 and a darlington. The GTO turns on for 36% of the cycle, giving lamp brillance equivalent to operation at a constant 12 volts.

Lamp control by another lamp

As the number of lamps in a circuit increases, as it has in the flasher circuit, loading problems are produced. The GTO, with its ability to be turned off through a low-resistance path from the gate to ground, can alleviate this problem with the arrangement shown in Fig. 10. In this method of control, the auxiliary load is connected in the normal cathode-load configuration. The gate, however, is connected to a conventional lamp circuit. The lamp then provides the GTO with a low-impedance path to ground for turn-off. The closed switch provides turn-on drive to the GTO and simultaneously routes current to the lamp acting as the gate shunt path. The gate current drawn by the GTO then represents a minimal load on the circuit while the GTO is controlling the auxiliary load on its cathode. This arrangement provides a very convenient means of adding auxiliary loads to a circuit without loading it down or requiring extensive wiring modifications.

Motor controls

The GTO is well-suited for the job of motor control. Since it can withstand inrush currents, a GTO can replace many of the present-day mechanical switches used to control seat motors, electric-window lift motors and blower motors. The following are examples of these applications.

Electric window control circuit

In the circuit of Fig. 11, two GTO's in cathode-load configurations each control a separate field of a split-wound-field motor. The windings are wound to produce opposite motor rotations when energized. The logic decodes the input from two switches—a master representing the driver's control switch, and a slave representing the passenger's switch. The decoding network, implemented with the CD4041, the CD4012's and the CD4023, signals the appropriate gate driver circuits for the various switch inputs. The interface provides a pulse of positive drive to the GTO on the positive transition of the output from the decoder, and it shunts the gate of the GTO to ground for a short time on the negative transition.

Blower motor speed control

The circuit shown in Fig. 12 is used to control the speed of a PM blower motor by means of pulse-width modulation. The GTO, with the motor connected in a cathode load configuration, is turned on and off by the interface circuit (a TA6805 integrated circuit). The constant-frequency oscillator (CA3094 op-amp) has a variable duty-cycle controlled by a potentiometer; this switching action varies the average dc level supplied to the motor, and hence its speed. This solid-state control circuit has energy conservation advantages, since eliminating the series dropping resistors presently used raises system efficiency.

Conclusions

As can be seen from the circuits presented, the GTO can be used as a replacement for many of the mechanical switches presently used in today's automobiles. Since it needs only a low-power control signal, using the GTO can produce a significant reduction in the amount of copper wire in the harness. The low-power control signals also permit the use of smaller, more functionally-designed switches. Also, the switches can be placed in areas more accessible and convenient to the driver. The GTO's ability to be controlled by an integrated circuit makes it a viable candidate as the remote power switch in the multiplex electrical system envisioned for future automobiles. With it, convenience items can be added at minimal cost in the multiplex system because each additional control circuit becomes just a different integrated circuit.

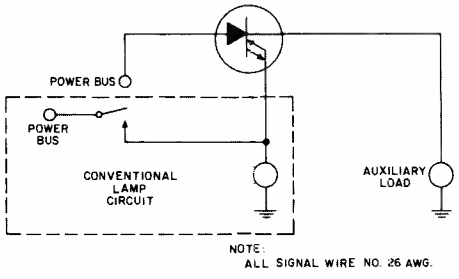

Fig. 10 — GTO circuit controls one lamp by another.

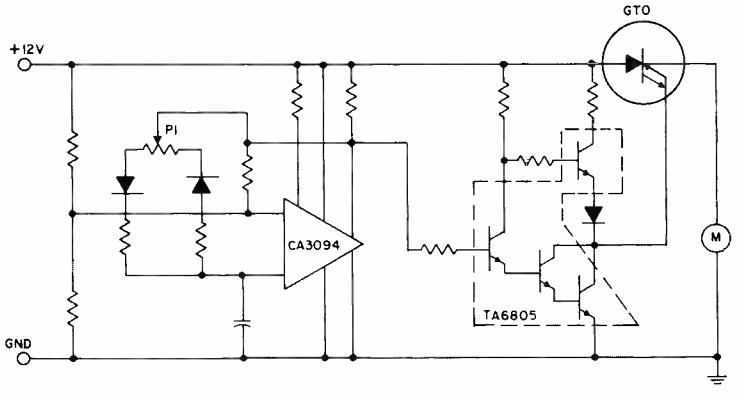

Fig. 12 — GTO speed control for blower motor.

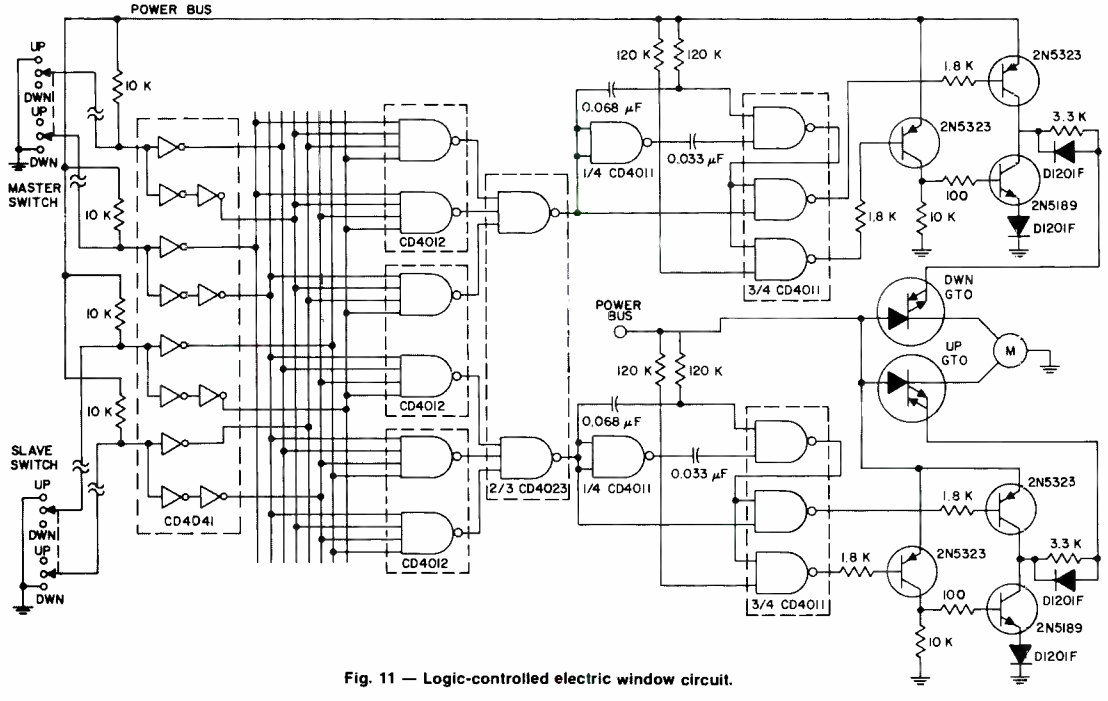

Fig. 11 — Logic-controlled electric window circuit.

Small-engine electronic ignition

M. Kalfus

SCR capacitive-discharge ignition systems perform well in two-cycle engines because of their ability to ignite fouled spark plugs; they also have minimal maintenance requirements. These advantages and declining prices are forming an expanding market.

LONG BEFORE solid-state ignition became a standard automotive item, electronic components were in use as original equipment in many small engines—chain saws, lawnmowers, marine outboards and off-road recreational vehicles such as tractors, snowmobiles, and motorcycles. Small-engine electronic-ignition systems are usually associated with capacitive-discharge circuits.

Simplicity and independence

Small-engine electrical systems are unique in that a magneto flywheel is used to generate ignition and accessory power, thus making the engines completely independent of external power, such as a battery. The flywheel contains one or more permanent magnets, which pass by fixed stator windings and so generate an ac voltage for ignition or accessories. The magneto flywheel feature lends itself to simple capacitive-discharge ignition-circuit design, as it easily realizes 200- to 400-volt charging potentials. Ignition timing is also conveniently accomplished by pick-up coils located around the flywheel.

The advantages of solid-state ignition in small engines are: a faster rise time; higher ignition voltage during starting; variable retarded timing to facilitate starting; and better ignition under the fouled-plug conditions encountered in two-cycle engines, which burn a mixture of gasoline and oil. Of course, the magneto capacitive-discharge ignition has no rotor or points, a feature that virtually eliminates ignition maintenance, except for spark plug replacements.

The capacitive-discharge ignition stores energy in a capacitor charged to 200 to 600 volts, depending on the system. At the proper time, the magneto system generates a trigger signal, an SCR is gated on, and the capacitor discharges rapidly through the primary winding of a step-up transformer (ignition coil). The coil's secondary winding generates a rapidly rising voltage that fires the spark plug. After ignition, the flywheel magneto recharges the capacitor in preparation for the next ignition cycle (Fig. 1).

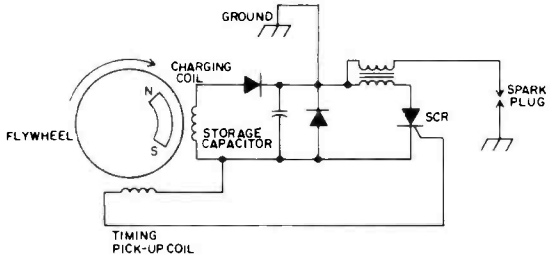

Fig. 1 — Basic flywheel-charged, capacitive-discharge ignition system.

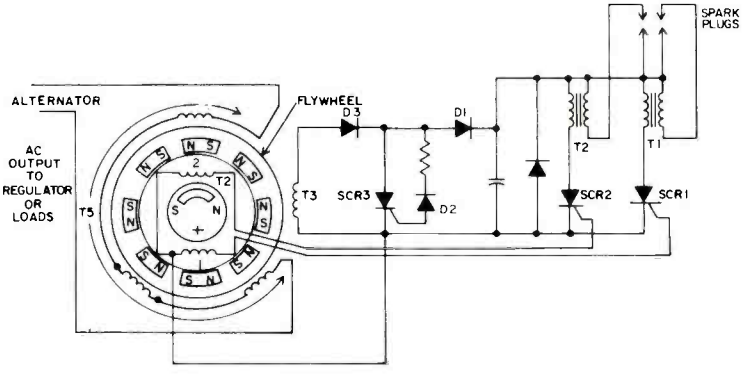

Fig. 2 — Typical capacitive ignition system for a two-cylinder, two-cycle engine.

The initial use of factory-installed capacitive-discharge ignition systems began in the outboard market for two-, three-, four-, and six-cylinder, two-cycle engines. Problems with oil-fouled spark plugs in two-cycle engines were a factor in directing this industry toward capacitive ignition systms. Arcless distribution of ignition energy was readily accomplished using the existing magneto system; i.e., no rotor or distributor was needed to steer the high voltage to each spark plug because a separate ignition coil fired each spark plug.

A typical capacitive-discharge ignition system for a two-cylinder, two-cycle engine is shown in Fig. 2, which also includes the alternator accessory windings, T5, and the circuitry required for regulating the capacitor charging voltage. The ac voltage generated for capacitor-charging by T3 in Fig. 2 is rectified by D3 and clamped by the regulator, SCR3, D2, and D1 to limit the peak capacitor voltage. Timing for gating is established by the relationship between the flywheel and trigger coil T2. The same flywheel magnets that produce the capacitor charging voltage also provide the magnetic flux for the alternator windings, T5 that provide electrical power for accessories.

Automatic timing advance

Since ignition timing depends on the gate current provided to the SCR, and since gate current is a function of the rate of change of flux through the pick-up coil (and thus rpm), specifying gate current requirements within narrow minimum and maximum limits can automatically advance the timing as rpm increases. This feature makes easier starts possible with retarded-spark ignition and produces higher power output at higher engine rpm when the timing is advanced.

The automatic timing advance works in the following manner. The magnetic coupling between the pick-up coil and the flywheel magnets is varied by shaping the coil core so that the size of air gap changes with the angular position of the flywheel, as shown in Fig. 3. At low starting rpm, loose coupling of the large air gap does not provide adequate gate current to trigger the SCR. However, as the flywheel continues rotating, the small air gap's tight coupling generates enough

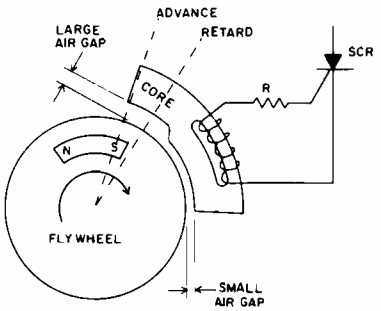

Fig. 3 — Automatic timing advance is possible using this variable-air-gap coil configuration. At low rpm, magnetic coupling can only fire the SCR when the magnet on the the flywheel is at the small-air-gap (retarded ignition) position. At high rpm, voltage increases, and the SCR can be fired through the large-air-gap portion of the coil (advanced ignition).

gate current to fire the SCR. The small gap is located so that firing is retarded for an easy start. As rpm increases, the voltage generated by the large air gap's coupling increases to a level sufficient to trigger the SCR. When this occurs, the timing has been advanced sufficiently (dashed line) to allow greater engine output power.

Fig. 4 is an illustration of the functional characteristics of the automatic timing advance. At low rpm, the portion of the waveform denoted *A* is not adequate to gate the SCR, which must wait until the curve has progressed through *B* before ignition can occur. Increasing the rpm, though, increases the pick-up coil voltage sufficiently to fire the SCR earlier.

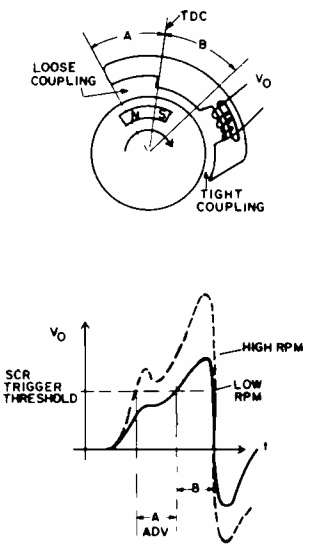

Fig. 4 — Automatic timing advance uses variable magnetic coupling. Voltage initially reaches SCR trigger threshold at B for low rpm, but reaches it earlier (at A) at high rpm.

Martin R. Kalfus, Technical Staff, Solid State Div., Somerville, N.J., received his BSEE from Newark College of Engineering in 1967. He joined RCA in 1970, working in thyristor applications, with responsibilities for high-current triacs and SCR's. The customer interfaces there dealt with industrial and capacitive-discharge-ignition applications, requiring domestic and far-east travel. Since late 1975, when he joined the Automotive Power Applications group, his responsibilities have been inductive ignition, CD ignition, and GTO (gate-turn-off) SCR automotive market introduction.

Reprint RE-22-2-5
Final manuscript received June 24, 1976.

The market

More than three million RCA SCR's per year go into the small engine markets, with the major portion going to marine applications. Because of dropping costs and minimal maintenance requirements, nearly all new lawnmowers will have solid-state ignition systems within the next few years. This will mean a great expansion in the volume of SCR's manufactured.

Today, the most widely used capacitive-discharge-ignition device is the RCA S2600, a seven-ampere TO-5 device. Some of the major features of the S2600 family of SCR's that make them well suited to this application are: high di/dt capability (200 A/μs); sensitive gate trigger current (typically 7 to 10 mA); high static dV/dt capability; and stable low leakage current at up to 600 volts and 125°C. However, new applications and older cost-reduced applications will be incorporating plastic-packaged SCR's, such as the RCA S106, S206 and S280 types.

Automotive radar development at RCA Laboratories

Dr. F. Sterzer

"...the simultaneous maturing of three technologies—microwave solid-state sources, microwave hybrid integrated circuits, and microcomputers built around microprocessors—makes it likely that radars will become useful automobile accessories within the next few years."

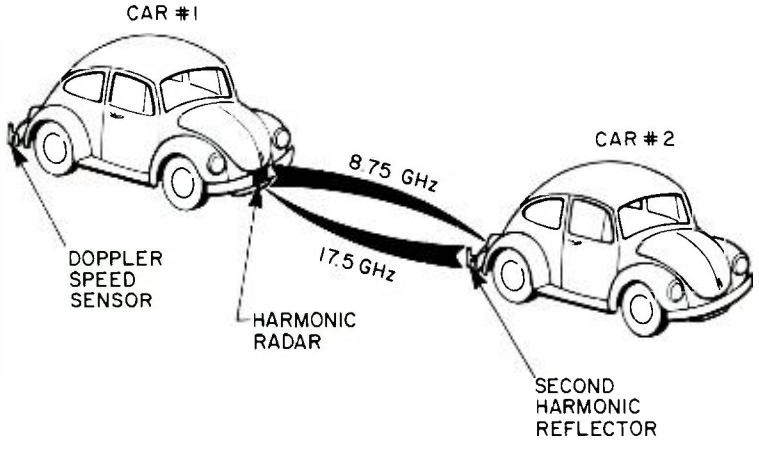

Fig. 1 — Harmonic radar principles.

DESIGNING a practical automotive radar is a formidable task. The radar must be compact, reliable, inexpensive, and consume little dc power. The antenna of the radar must be small enough to fit unobtrusively on the outside of an automobile, and the maximum rf power density radiated by the antenna must conform to strict radiation hazard standards. The radar must have a low false alarm rate, and the probability of the radar's being blinded by similar radars in other automobiles must be very small. Finally, the radar must, of course, offer significant benefits in either driver convenience or safety.

While substantial amounts of research and development have been devoted to automotive radars in Europe, Japan, and in the United States, no automotive radars have to date been widely marketed, although a small number of radars designed for trucks have been sold. However, the simultaneous maturing of three technologies—microwave solid-state sources, microwave hybrid integrated circuits, and microcomputers built around microprocessors—makes it likely that radars will become useful automobile accessories within the next few years.

Harmonic radar system

RCA's work on automotive radars started in 1971 with the development of a cooperative harmonic radar system by a team of RCA Laboratory researchers headed by Dr. H. Staras. The team included H.C. Johnson, G.S. Kaplan, R.J. Klensch, and Dr. J. Shefer.[1,2] In the harmonic radar system, the radar transmitters are tuned to a center frequency f_0, while the radar receivers are tuned to a center frequency $2f_0$. All highway vehicles carry second-harmonic reflectors mounted on their backs. When a harmonic reflector is illuminated by a radar signal of frequency f_0, the reflector automatically returns a signal at frequency $2f_0$. (See Fig. 1.) Since no natural objects return detectable second-harmonic signals when illuminated by a radar transmitter, the harmonic radar "sees" only vehicles or other designated traffic hazards equipped with second-harmonic reflectors: clutter returns from roadways, highway signs, overpasses, trees, etc., as well as signals emitted from other automobile radars are automatically rejected.

The harmonic radar built at RCA Laboratories was a cw-fm radar using a transferred electron oscillator as the transmitter power source (see Fig. 2). The center transmitter frequency was 8.75 GHz and the center receiver frequency 17.5 GHz. The harmonic reflector consisted of a passive Schottky barrier diode frequency doubler connected between an 8.75-GHz receiving antenna and a 17.5-GHz transmitting antenna. Both antennas were in printed-circuit form,[3] and the entire harmonic reflector was only slightly larger than a typical license plate. The cw-fm radar measured range and range-rate to the harmonic reflector carried on the vehicle in front of it, the maximum range being about 100 meters. A separate cw doppler radar measured ground speed. (This cw doppler radar has since

Author Sterzer with model of 'electronic license plate.'

Fred Sterzer, Director, Microwave Technology Center, Princeton, N.J., received his PhD in Physics from New York University in 1955. He joined RCA in 1954, and has worked in the fields of microwave spectroscopy, microwave tubes, light modulators and demodulators, and microwave solid state devices. Dr. Sterzer is the author of over 55 technical papers. He is a member of Phi Beta Kappa, Sigma Xi, the American Physical Society, and is a Fellow of the IEEE. He holds 26 patents in the microwave field.

Fig. 2 — Harmonic radar built at RCA Laboratories around 1971.

Reprint RE-22-2-10
Final manuscript received June 14, 1976.

been redesigned for use on locomotives. See H.C. Johnson, "Speed Sensors for Locomotives," this issue.) The information from the two radars was fed into a simple computing circuit that sounded an alarm and actuated the brakes whenever the combination of range, range-rate, and vehicle velocity were computed to be unsafe.

Electronic license plate

The harmonic radar system was extended in 1974 by the present author with the introduction of the electronic license plate.[4] This concept is based on the use of compact, inexpensive electronic license plates mounted on the rear of every motorized highway vehicle. Each license plate provides the following three functions: 1) when electronically interrogated, the license plate responds with a code representing an identifying number assigned to the vehicle to which the plate is attached; 2) the plate is the receiver and transmitter for messages to and from the vehicle; and 3) the plate serves as a harmonic reflector in the harmonic radar system.

A block diagram of the license plate is shown in Fig. 3. The plate consists of the following major components: a printed-circuit antenna covered by a visual display of the license number of the vehicle, a frequency doubler, a modulator, and an rf detector. The antenna and the frequency doubler are similar to the ones used in the harmonic reflector of the harmonic radar system. The modulator is based on a concept developed in 1973 by R.J. Klensch of the RCA Laboratories for automatic vehicle identification.[5] A COS/MOS circuit generates a binary code representing the identifying number assigned to the vehicle to which the plate is attached, as well as special coded messages. The output of the modulator is

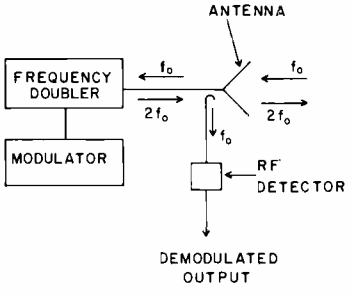

Fig. 3 — Original electronic license plate concept.

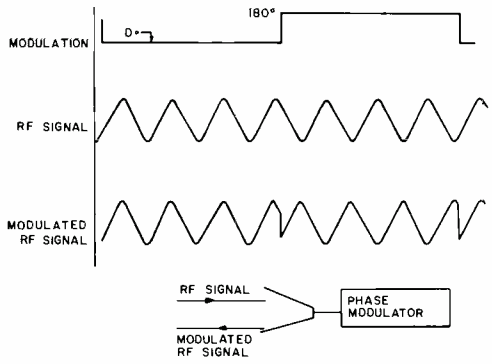

Fig. 4 — Waveforms of modulation and incident and reflected signals for modulated-fundamental-frequency reflector.

An experimental fundamental frequency reflector built by Kaplan operates at an rf frequency of 10 GHz with a reflection loss of less than 2 dB. This compares to a typical loss of about 20 dB in the harmonic reflector. A COS/MOS code generator is used to impress a 10-bit code on the biphase modulator. Coding is FSK with tones at 50 and 60 kHz. The bit rate is 400 bits per second, but both the bit rate and the number of bits can easily be made much larger.

an on-off keyed voltage that modulates the bias on the multiplier diode in the second-harmonic generator. Thus, when the license plate is interrogated with a cw signal at 8.75 GHz, the plate responds with a 17.5-GHz signal that is on-off modulated with codes representing the identifying number of the vehicle and the special message.

The rf detector consists of a Schottky barrier silicon diode embedded in a circuit that is printed on the same dielectric board as the antenna. Part of the 8.75-GHz radiation received by the antenna is sampled by a printed-circuit directional coupler and demodulated in the detector.

Application of the license plate

The identifying number of any vehicle carrying the electronic license plate, as well as additional special codes, can be read electronically by interrogators that can be mounted on automobiles, on the side of roads, buried in roadways, etc. A suitable interrogator is described in detail in Ref. 4. Applications of this feature of the plate include automatic toll billing, automatic monitoring of public service vehicles, and monitoring highways for stolen vehicles.

The electronic license plate also provides an electronic communications link for sending messages to and from the vehicle. Messages sent to the vehicle must be encoded on the fundamental frequency f_0. Examples of messages that could be sent are warnings that the vehicle is moving too fast for road conditions, or that the vehicle is proceeding the wrong way into a one-way street. Messages coded on the second harmonic diode of the license plate can be read by roadside or vehicle-mounted interrogators. Distress calls are likely to be the most important type of message that would be sent from vehicles.

The electronic license plate meets, of course, all of the requirements for a second-harmonic reflector for the harmonic radar system. Thus, if an electronic license plate were to be put into nationwide use, it would become practical to equip highway vehicles with harmonic radars.

Dual-mode radar

In 1975, G.S. Kaplan and the present author proposed a dual-mode version (cooperative and non-cooperative) of the harmonic radar.[6] The cooperative mode of the radar is based on tagging cooperating vehicles and other potential highway hazards with modulated fundamental frequency reflectors, rather than with harmonic reflectors. When operating with tagged targets, the dual-mode radar retains the advantage of immunity to clutter and blinding of the harmonic radar, yet it operates at only one carrier frequency rather than two, and requires much less transmitter power than the harmonic radar. Furthermore, modulated fundamental frequency reflectors make simpler electronic license plates than harmonic reflectors. When looking at tagged targets, the range of the dual-mode radar is the same as that of the harmonic radar—approximately 100 m.

The dual-mode radar also recognizes targets that do not carry tags. However, in order to minimize the "false target" problem, the range of the non-cooperating mode of the radar is

restricted to much shorter distances than the range for cooperating targets.

The modulated fundamental frequency reflector used as a tag in the dual mode radar consists of a printed-circuit antenna, a biphase modulator, and a tone generator of frequency f_T.[7] The tone generator periodically drives the phase modulator between two states: when the modulator is in the first state, an rf signal incident on the antenna is reflected with a phase shift θ_0; when the modulator is in the second state, an rf signal incident on the antenna is reflected with phase shift $\theta_0 + 180°$. The waveforms of the modulation and of the incident and reflected signals are shown in Fig. 4.

In the processor of the dual-mode radar, returns from tagged and untagged targets are separated by suitable bandpass filters. This separation can be accomplished because the beat frequencies generated in the fm radar by returns from the modulated reflectors are modulated at frequency f_T, while the beat frequencies generated by targets without reflectors are not modulated. Returns from tagged targets are accepted to a range of 100 meters, while returns from untagged targets are accepted only to a range of 20 to 30 meters.

Radar for the Minicars Research Safety Vehicle

In the middle of 1975, RCA Laboratories received a contract to develop a radar and an electronic dashboard display for the Minicars Research Safety Vehicle (RSV)*. (See Fig. 5 for a photograph.) This development is being carried out by a team headed by Dr. E.F. Belohoubek. The members of the team include J. Rosen, J.J. Risko, J.M. Cusack, R.E. Marx and E.C. McDermott, Jr.

The radar for the RSV is a fundamental-frequency cw-fm radar powered by a 25-mW varactor-tuned transferred electron oscillator operating at 10.525 GHz. The rf components used in the RSV radar are similar in design to the rf components that were used in the harmonic radar, and most of them are built in hybrid integrated form. The processing of the radar returns in the RSV radar is carried out in a microcomputer, rather than in a hardwired processor as in the harmonic radar. The CPU of the microcomputer is the RCA COSMAC microprocessor. COSMAC is powerful enough to handle the algorithms for deciding whether a target in front of the RSV is dangerous or not, and at the same time can carry out the logic functions required to control the electronic dashboard display. COSMAC is currently programmed to accept radar from all targets within a range of 30 meters. If the RSV approaches one of these targets at an unsafe closing rate, COSMAC triggers an alarm to warn the driver, except that no alarm is sounded when the speed of the RSV is less than 20 mi/h. (Details of the operation of the RSV microcomputer will appear in a forthcoming special issue of the *RCA Engineer* devoted to microprocessor applications.)

The performance of the radar in initial road tests has been most encouraging. While a considerably further amount of engineering will be required before we arrive at a truly cost-effective radar configuration, the basic design of the radar appears to be sound. One of our major tasks for the future will be to interface the radar with a cruise-control system to automatically maintain a safe headway distance between the radar-equipped vehicle and the vehicle in front of it.

*Minicars, Inc. of Goleta, California, is developing the RSV under contract to the National Highway Safety Traffic Administration, an agency of the U.S. Department of Transportation. The goal of the Minicars RSV program is to develop a 2000-lb. automobile that protects occupants in 50-mi/h frontal crashes and in 30-mi/h side crashes.

Fig. 5 — Latest version of Research Safety Vehicle. Radar will be fitted under rectangle on right side of hood.

Conclusions

The latest Department of Transportaion statistics show that motor vehicle accidents in the United States are currently occurring at an annual rate of 36,000,000. The annual death toll resulting from these accidents is about 46,000. Automotive radars have the potential of reducing the number and the severity of motor vehicle accidents. The advent of low-cost microprocessors suitable for use in motor vehicles, together with the availability of low-cost microwave solid-state sources and hybrid integrated circuits, makes it likely that cost-effective versions of automobile radars will become available in the not-too-distant future.

References

1. Shefer, J. and Klensch, R.J.: "Harmonic radar helps autos avoid collisions," *IEEE Spectrum*, Vol. 10 (May 1973) p. 38.
2. Shefer, J. et. al., "A new kind of radar for collision avoidance," SAE Automotive Engineering Congress and Exposition, Detroit, Mich. (Feb 26, 1974).
3. Wilkinson, W.C; "A class of printed circuit antennas," IEEE 1974 Antennas & Propagation Symp., Session AP-S10, p. 270-273.
4. Sterzer, F.; "An electronic license plate for motor vehicles," *RCA Review*, Vol. 35 (June 1974) pp. 167-175.
5. Klensch, R.J. et al.; "A microwave automatic vehicle identification system," *RCA Review*, Vol. 34, No. 4 (Dec 1973).
6. Kaplan, G.S. and Sterzer, F.; "Dual-mode automobile collision avaoidance radar," SAE Automotive Engineering Congress and Exposition, Detroit, Mich., (Feb 24-28, 1975).
7. Kaplan, G.S., and Ritzie, A.D.; "An x-band system for automatic location and tracking of vehicles using semi-passive signpost reflectors," 26th Annual Conf. of the IEEE Group on Vehicular Technology, Washington, DC (Mar 24-26, 1976).

Automatic vehicle tracking using microwave signpost reflectors

G.S. Kaplan|A.D. Ritzie

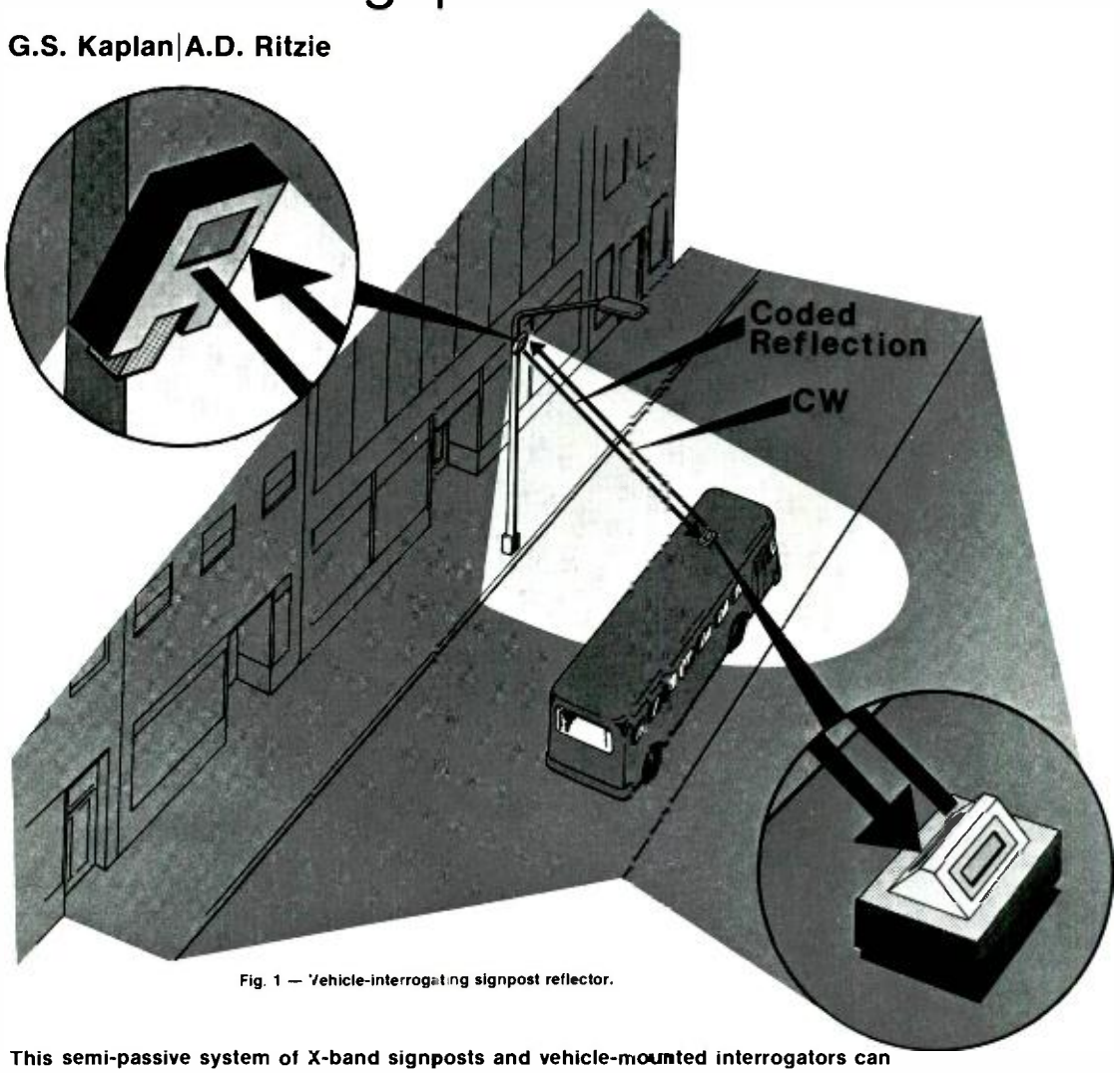

Fig. 1 — Vehicle-interrogating signpost reflector.

This semi-passive system of X-band signposts and vehicle-mounted interrogators can track and locate vehicles in urban and suburban areas. The system has immediate applications on urban buses and has undergone successful tests in Philadelphia.

AN AUTOMATIC vehicle-monitoring system (AVM) can provide its users with valuable information concerning the location and status of the vehicles in their truck and bus fleets. More efficient utilization of existing vehicles and/or the provision of additional services are possible benefits of proper AVM system implementation.

Perhaps the most immediate applications occur in transportation and law enforcement, but the benefits of an AVM system are applicable to many other users as well. By using AVM, properly integrated into their overall command and control systems, police departments could speed up their response to reported incidents. Improved schedule adherence for buses should result from AVM use by using a

Reprint RE-22-2-11
This paper appeared in similar form in the *Proceedings* of the 26th Annual Conf. of the IEEE Group on Vehicle Technology, held in Washington, D.C., March 24-26, 1976.

This work was performed when the authors were at RCA Laboratories, Princeton, N.J.

mobile radio link to notify drivers to take appropriate action, including adaptive rerouting, to traffic conditions. The trucking industry could use AVM to control hijacking—deviation from a predetermined route (in time and/or space) would cause an alarm. It is clear that a plethora of applications exist for AVM systems; we will now examine possible approaches to implement such systems.

Alternative approaches to AVM systems

An AVM system can use many different methods to obtain the basic location information. These include phase-ranging, pulse-ranging, dead reckoning, and signpost (proximity). There are, of course, many ways of implementing each of these systems. The choice of a particular type of system depends on a number of factors, and the economically preferred system can depend greatly on the number of vehicles in the system. Some users may require accuracies of better than 500 ft, while other applications may be satisfied by accuracies of one-half mile or more.

The proximity AVM system

For a number of reasons, we decided to use a proximitv-type system as the AVM's basic position-determining element. These reasons include the large bandwidth required to accommodate the narrow pulses for a pulse-ranging system, thereby aggravating the spectrum-congestion problem in metropolitan areas, and the added expense for high-power wideband pulse transmitters in each vehicle. While phase-ranging equipment should be implementable at a more modest cost, the system accuracy may not be adequate for many applications when severe multipath exists in a built-up urban area (such as Wall Street in New York).

A signpost system is almost certainly the simplest and least expensive alternative for fixed-route systems (such as with buses). Electronic signposts, when coupled with odometer readings between signposts, offer an extremely accurate and cost-effective system. Since accuracy is a function of signpost spacing, signposts can be deployed with different spacings to obtain variable accuracy in

Andy Ritzie received his electronics training while in the Air Force, where he served as a Master Instructor. He also took courses from Denver University and the Air University. He was employed by RCA from 1967 to 1975, spending the latter 5 years at the RCA Laboratories in Princeton, N.J. There, he worked on the design, fabrication and test phases of several electronic vehicle tracking and identification systems. He has patent applications in the fields of digital logic, optical systems, radar and automatic electronic identification systems. Andy left RCA in 1975 to accept a position as Project Development Manager with Langberg Associates, Inc., working on bio-medical and industrial instrumentation and control systems.

Gerald S. Kaplan, RCA American Communications, received the BSEE from the City College of New York in 1962, and the MSEE from Princeton University in 1964. In June 1964 Mr. Kaplan joined the technical staff of RCA Laboratories in Princeton, N.J. where he investigated various problems involving electromagnetics and communications. He was a major contributor to the design of the electronic Automatic Vehicle Monitoring (AVM) system for locating and tracking motor vehicles in urban areas. His work in the areas of semi-passive and passive electronic labels resulted in new techniques applicable to automatic vehicle location, container identification, the electronic license plate, and automotive radars. Mr. Kaplan joined the staff at RCA American Communications in 1975, where his areas of responsibility include advanced system planning for satellite-serviced communication systems. He has patents issued or pending in the areas of vehicle location, automotive radar, electronic labels, and medical electronics.

Andy Ritzie (left) and Jerry Kaplan, here examining another automotive microwave project, the "electronic license plate."

different parts of the city. In some sections of the city, signposts may be installed on each block, while in other sections an accuracy of five to ten blocks may be adequate. Furthermore, it is possible to change the accuracy in a given area, if desired, by installing additional signposts. Although the initial capital investment for a signpost system may be high, relatively low additional costs are incurred as the number of vehicles in the system increases.

Signpost location technique

This proximity system uses an array of signposts placed throughout the city for vehicle location. There are two basic approaches to a signpost system. In one approach the signposts serve as receivers, picking up vehicle-identification signals as the vehicles pass the signpost, which then adds its own location identification and transmits these two signals to a control center. In a second approach, the signpost imparts its location information to all properly-equipped vehicles that pass the signpost. These vehicles, when interrogated via a two-way mobile radio, then relay the vehicle's location information to a control center.

The first approach requires all the (receiver) signposts to be connected to the control center by telephone lines or radio links, either of which would involve a substantial cost. In addition, if a parked or slowly-moving vehicle continuously injects its message into the same signpost receiver, a large amount of redundancy results. This redundancy can put a great burden on the central processor or require pre-processing equipment at the signpost receivers. For these and other reasons, the adopted system imparts the signpost location information to the passing vehicles.

Semi-passive signpost system

As shown in Fig. 1, the signposts are mounted on streetlight poles so that all properly-equipped vehicles driving along the street can receive a message from the signpost. The signpost (acting as a coded reflector) operates by modulating and reflecting an X-band interrogation (cw) signal emanating from passing vehicles. There are a number of reasons that point to signpost operation at X-band. Since X-band signals decay rapidly over non-line-of-sight paths, they cannot readily propagate around corners into adjacent streets to interfere with other signpost signals. And, since the wavelength at X-band is small, it is possible to achieve gain in the radiating antennas with physically small components. The use of antenna gain at the signpost (which is not practical at lower frequencies) is an additional factor in confining the reflected energy to the immediate vicinity of the signpost. This prevents interference between signposts and also may be used to define a narrow "ribbon-like" beam across the street. This can allow precise determination of a vehicle's position and is especially useful for bus-checkpoint applications.

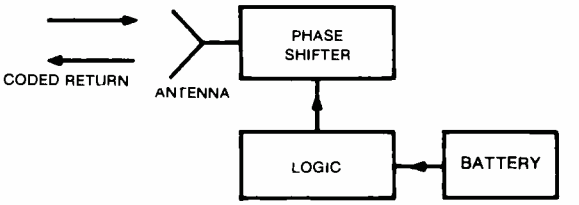

Fig. 2 — Signpost.

As described above, the uniquely coded reflection from the signpost is detected and the signpost identity (location) is decoded and stored at the vehicle. A digital command from the central station via mobile radio has the location of the vehicle, its identification, and its status relayed to the central processor.

Fig. 2 is a block diagram of the transmitter. In it, an interrogation signal is received, phase-modulated under logic control, and reflected back with its unique coding. The COS/MOS logic circuit is similar to electronic watch circuits (consuming microwatts of power). As shown in Fig. 3, the information is sent by phase-modulating the reflection carrier at a rate that is either one of two tones. In other words, the tone is encoded by the rate of change of the phase of the reflected signal (PM/FSK).

The phase-modulation is detected at the vehicle by comparing the reflected signal with a sample of the transmitted signal (Fig. 4). The coherent demodulation used at the vehicle allows the processor to filter out all extraneous reflections (such as from buildings and other vehicles) and ensures a clutter-free signal for decision purposes.

Conquering fade and noise

As with all homodyne systems, the exact rf phase is of importance and, if not properly accounted for, could cause difficulty. Changes in relative rf phase

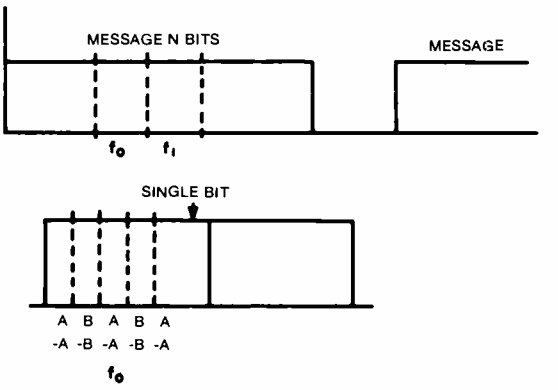

Fig. 3 — Message format—each bit is subdivided into intervals, with alternate intervals on different rf phases.

caused by motion of the vehicle effectively superimpose a fading (at the doppler rate) on the received signal at the output of the mixer (Fig. 4). This slow fading can cause signal dropouts that could result in unreliable message reception. This could also happen if the vehicle stops at a location where the reflected signal and the local oscillator are in phase quadrature. This problem is eliminated by a signaling format using phase diversity.

As shown in Fig. 5, phase diversity consists of switching in and out additional phase shifts of approximately 90° at a rate that is fast compared with the data. This additional phase shift ensures that the local oscillator and the reflected signal will not remain in phase quadrature for any significant length of time. Basically, diversity has the effect of introducing fast (compared with the data and doppler rates) fading, which dominates the slow fading caused by doppler effects and results in the reliable reception of otherwise unreceivable messages.

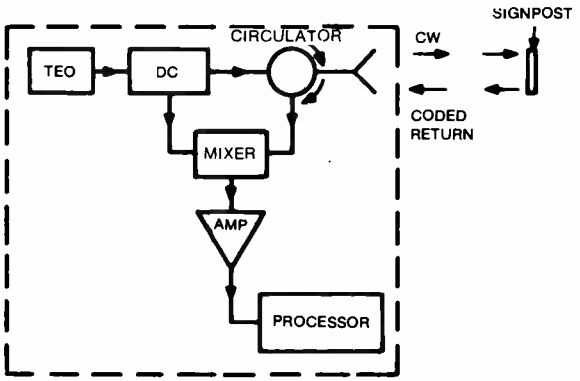

Fig. 4 — Interrogator.

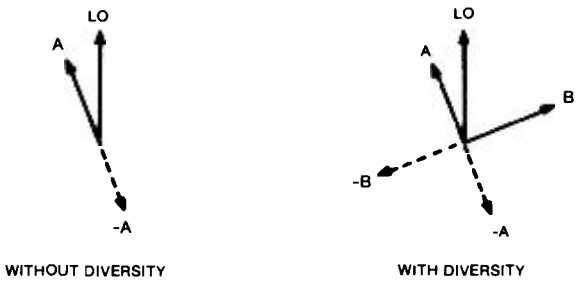

Fig. 5 — Phase diversity adds an additional phase shift to make sure that the local oscillator and reflected signal do not remain in phase quadrature for any significant length of time.

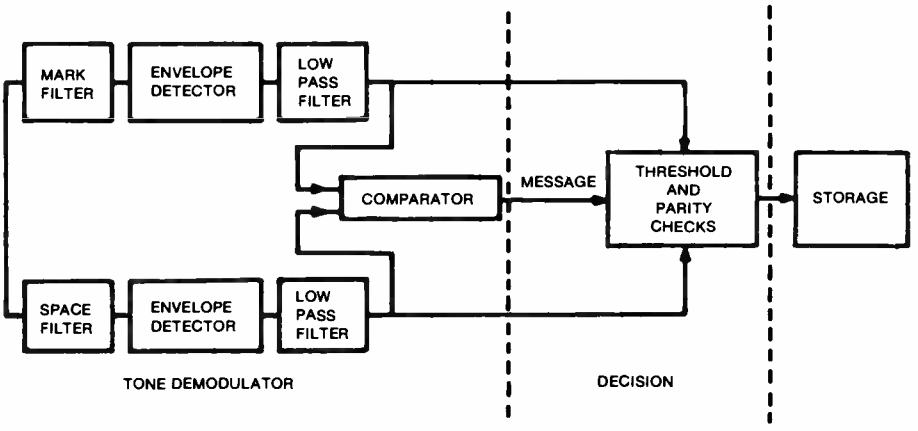

Fig. 6 — Processor.

Each message consists of N bits, each conveyed by a phase-modulated signal at a tone rate f_0 or f_1. In addition, to prevent slow fading, phase diversity is introduced by subdividing each bit into intervals and sending each interval in phase quadrature with the adjacent interval. When used with the coherent detection process of the receiver shown in Fig. 4, this signaling format is not subject to slow fades and allows proper reception of messages.

The output of the receiver amplifier (Fig. 4) is an FSK-type signal, i.e., one of two tones. These tones are detected in the processor (Fig. 6), which consists of a conventional bandpass filter, envelope detector, and comparator chain. The received signal is also subject to both signal-strength and parity checks. Messages that fail either the parity or signal strength checks are rejected in the receiver. This ensures that weak signals (or noise alone) will be ignored and only reliable messages based on strong signals will be received and accepted for storage.

An analysis of the system indicates that excellent system performance can be obtained for threshold-to-noise values of 10 to 12 dB and signal-to-noise values of 14 to 16 dB when the vehicle is within the reception range.

The interrogator (Fig. 4) consists of a TEO (transferred electron oscillator) that produces a cw X-band carrier of approximately 100mW. This carrier is transmitted to the antenna by way of the directional coupler and circulator. The signpost receives the cw carrier, phase-modulates the reflected return signal with an FSK-encoded signal (including diversity) and sends this coded return back towards the interrogator. The phase modulation is removed by the mixer, which is used as a phase detector (the local oscillator for the mixer is a sample of the transmitted signal). The resulting FSK signal is amplified and processed as described previously.

The signpost (Figs. 7 and 8) consists of a printed-circuit antenna, a phase shifter that uses a GaAs varactor diode as a voltage-variable capacitance to produce the desired phase shifts, and low-power COS/MOS logic powered by a lithium battery. It is expected that the signpost will operate for several years between battery changes. The signpost antenna (Fig. 9) consists of a flat printed-circuit 1 × 4 array. The interrogator (Figs. 10 and

11) uses two of these arrays, properly phased, to produce its pattern. All microwave components have been fabricated in integrated-circuit form. Fig. 12 shows the printed-circuit microwave module containing the mixer, directional coupler, and circulator used in the interrogator.

The signpost link has undergone extensive testing, both in the laboratory and under actual field (urban and suburban) conditions. The range obtained is more than sufficient to cover a 10-lane roadway under all resonable speed conditions and driving patterns. Reflections from buildings, adjacent traffic, etc., have had no deleterious effects on system performance. The field test also verified the use of phase diversity to eliminate signal fades caused by doppler effects.

Fig. 7 — Signpost exterior.

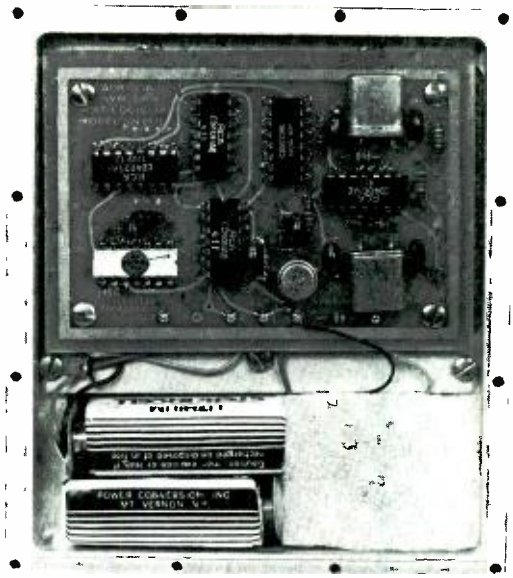

Fig. 8 — Signpost interior.

Conclusions

The new X-band signpost system is capable of providing accurate indications of a vehicle's location. Spacing of the signposts can be close without danger of mutual interference, since antenna gains and signal propagation characteristics have been chosen to limit reception range. The signpost, which does not have to be coupled to utility power lines, can be powered for several years by small batteries, as the power drain is in the microwatt range. This allows for relatively inexpensive installation.

Although this paper has been concerned with a signpost vehicle-location system, it should be recognized that the signposts are really "electronic labels" and that many other uses may be found for them, such as automatic toll collection or container identification.

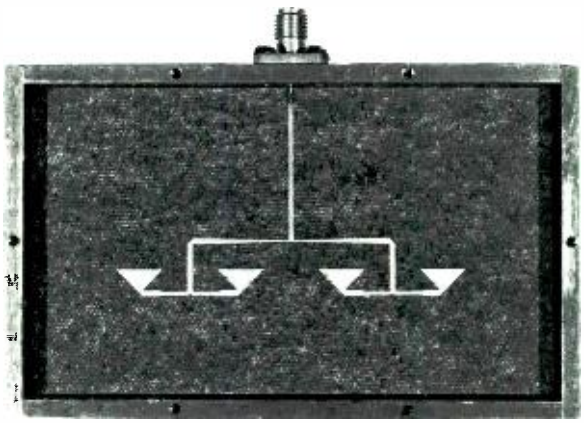

Fig. 9 — Printed-circuit antenna.

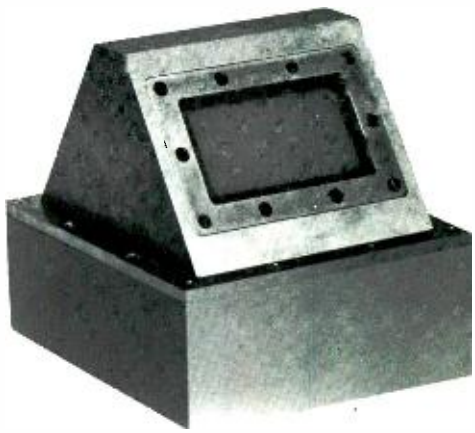

Fig. 10 — Interrogator exterior.

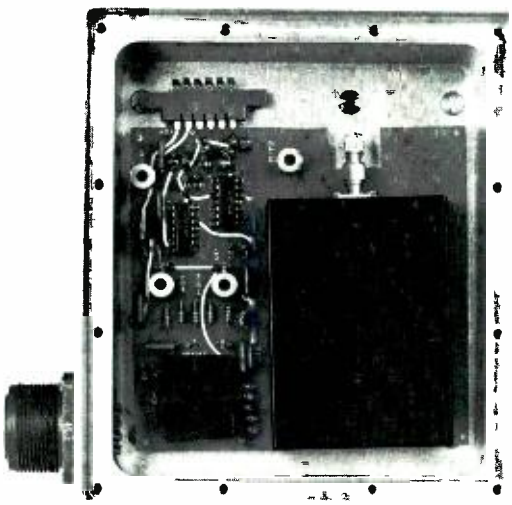

Fig. 11 — Interrogator interior.

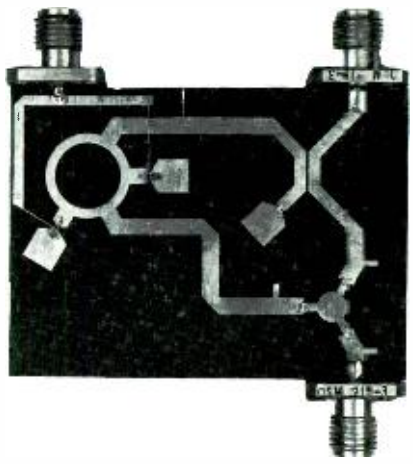

Fig. 12 — Microwave module for interrogator.

Acknowledgments

Acknowledgments are extended to J. Rosen, who designed the printed-circuit antennas and varactor phase-shifter, and R. Marx, E. McDermott, H. Johnson, and R. Paglione, who all contributed to the integration of the microwave portion of the interrogator. Discussions were held with F. Sterzer concerning various applications of the electronic label to other dystems; a special thank you to Peter Korda for many helpful discussions and encouragement.

Speed sensors for locomotives

H.C. Johnson

Microwave speedometers are simple, accurate, and self-calibrating. The one described here, originally developed as part of an automatic braking system for automobiles, may soon replace mechanical speedometers in the rugged railroad environment.

MANY STATES now require speedometers on locomotives used for passenger and freight service. Speedometers are needed in areas where there are track speed restrictions, and are increasingly used to drive on-board speed recorders. In addition, alarms tied in to speedometers are often used to alert operators of excessive speed.

In the railroad environment, where maintenance is costly and conditions are extreme in terms of shock level and exposure to the elements, great attention is paid to the reliability of all instruments. Fifteen-year lifetimes, with 100,000 miles or more of service per year, are a standard industry goal. Existing speedometer designs, all of which measure wheel rotation to determine locomotive speed, have had difficulties in this regard. The mechanically-driven sensors wear quickly, and magnetic axle-mounted sensors on electric speedometers are subjected to severe shock levels, resulting in high failure rates for both types. Recalibration owing to wheel wear and relatively complicated replacement procedures also add to speedometer operating costs.

Thus an electronic system operating independently of the wheels appears to be a natural candidate for replacing the conventional unit. A radar speedometer that accurately determines true ground speed without connections to the wheels or the ground has been developed at the RCA Laboratories for locomotive use. In addition to being inherently more reliable than the standard speedometer, the radar unit can be easily replaced by changing a few bolts, in contrast to the time-consuming partial disassembly of the locomotive axle required for replacing the conventional speedometer. Also, the radar speedometer is unaffected by both wheel slip and wheel wear, and its built-in calibration feature easily checks system performance and accuracy.

Henry C. Johnson, Member, Microwave Technology Center, RCA Laboratories, Princeton, N.J. attended Johns Hopkins University and received the BS from Drexel University. He joined the RCA Electron Tube Division in Harrison, N.J., in 1956, working on pencil tube design. In 1959, he transferred to the Microwave Technology Center at the RCA Laboratories, where he has made significant contributions in the field of optical communications and microwave transistor and bulk-device circuitry. He has successfully completed programs involved with the development of radiosonde transmitters, high-power fm microwave sources and wideband local oscillators. More recent responsibilities include the design, construction and preproduction development of collision-avoidance and ground-speed radar systems and frequency-synthesizer systems. Mr. Johnson holds patents in these fields, and has contributed more than 30 papers and presentations to technical journals and conferences.

Reprint RE-22-2-12 Final manuscript received May 4, 1976.

Author Johnson holding microwave speed sensor.

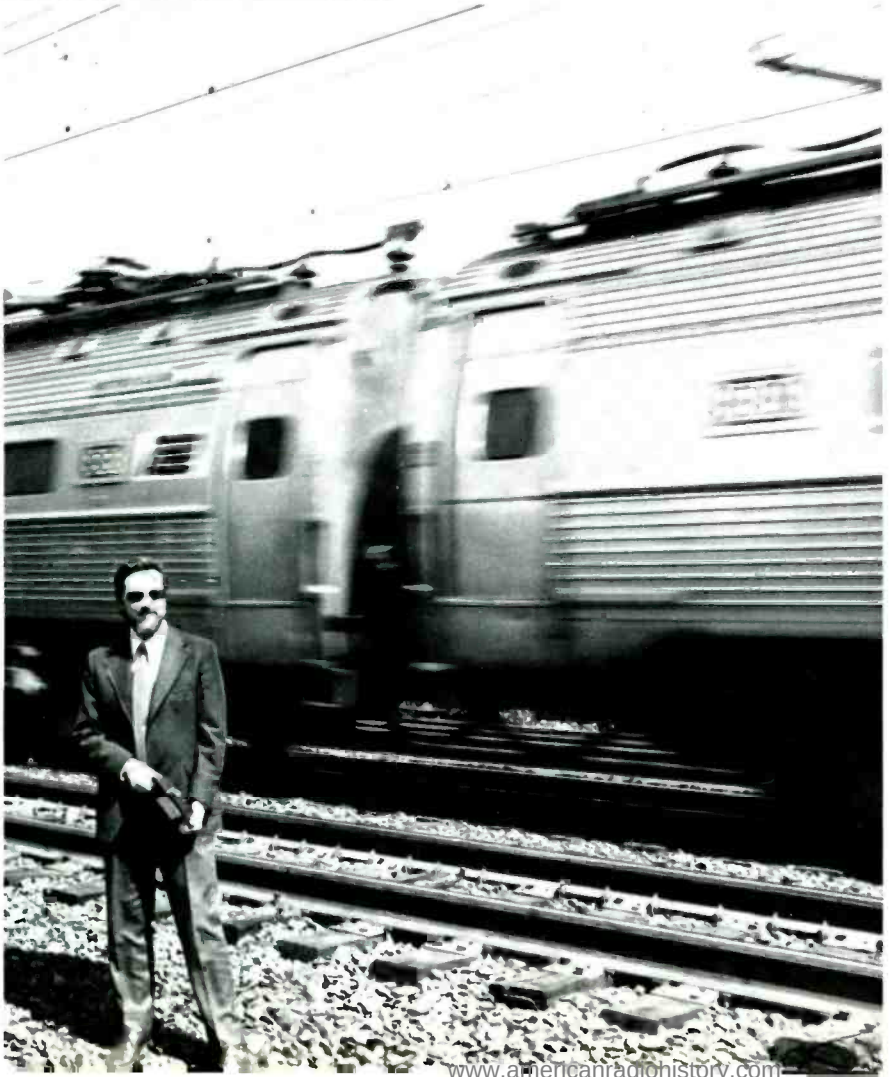

Speedometer circuit

The speedometer is a microwave doppler radar that measures ground speed by determining the frequency shift between the signal transmitted from the moving locomotive and its reflection from the ground.

Numerous doppler radar configurations have been considered for use as on-board ground-speed sensors,[1] weighing the trade-offs of sensitivity, ruggedness, stability and, of course, cost. The single-antenna, circulator-coupled mixer configuration using a bulk transferred elec-

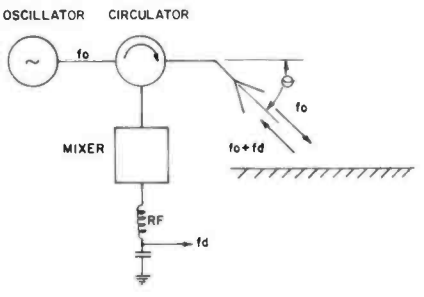

Fig. 1 — Radar's rf circuit.

tron oscillator (TEO), shown in Fig. 1, was eventually chosen as the most suitable. This homodyne circuit mixes the frequency-shifted signal that is back-scattered from the ground with the transmitter frequency to obtain the difference, or doppler-shift frequency. The choice of an approximately 10-GHz transmitting frequency was based on factors such as the back-scatter properties of various surfaces, minimum antenna aperture, FCC frequency allocations, and device and circuit considerations. The back-scatter amplitude from all surfaces increases with increasing fequencies,[2] while the antenna size for the desired gain decreases. However, oscillator and mixing devices for the higher frequencies become less efficient and more costly.

The radar transmits less than 20 mW of power, and most of this energy is absorbed or diffusely scattered by the ground. Under these circumstances, it may be possible under an FCC regulation to operate the speed sensor after certification without a station license. There are a number of frequency bands in the 10-to-12-GHz range that may be used for doppler speed measurement, and although the initial radar quantities operate at 10.525 GHz, the final operating frequency will be determined at the conclusion of this investigation.

The radar's rf section uses a rugged coaxial oscillator for the rf source, followed by a microstrip circulator, mixer, and antenna. The coaxial oscillator's performance is easily reproducible and, owing to the high Q, provides better temperature, VSWR pulling and supply-voltage pushing stabilities than a microstrip oscillator. The oscillator is both tuned and temperature-stabilized by a polycrystalline rutile rod. Temperature stability at 10.525 GHz is better than 50 kHz/°C over the −50 to + 65°C range.

The circulator consists of a metallized ferrite disk mounted through a hole in the microstrip circuit board. The necessary magnetic field is provided by a Sm-Co permanent magnet mounted below the ferrite disk. The circulator exhibits an isolation greater than 25 dB and an insertion loss of approximately 0.5 dB.

The single-ended microstrip mixer uses a Schottky barrier diode that is rf-matched to the 50-ohm line after assembly with the oscillator and circulator. A small mismatch is introduced in the microstrip line that feeds the antenna (see Fig. 2). This mismatch provides the local-oscillator signal by reflecting a small portion of the oscillator power back into the mixer. An optimum signal-to-noise ratio is obtained for an 0.5-mW local-oscillator power level.

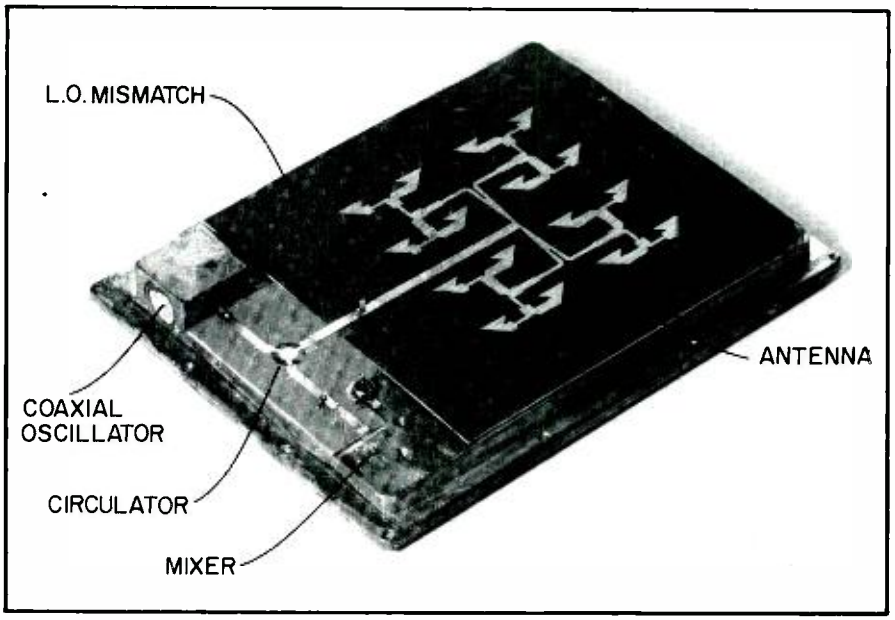

Fig. 2 — RF circuit.

Antenna

The choice of antenna performance is directly related to the operating frequency and desired beamwidth. A large antenna beamwidth results in excessive doppler-frequency spread and the need for a correspondingly long data-smoothing time. A narrow beam requires a large antenna aperture. A design compromise was reached, using a modification of a printed antenna initially developed at the RCA Missile and Surface Radar Division.[3] The antenna has an aperture of 3-1/2 × 3-3/4 in, a 3-dB beamwidth of 20°, and sidelobes greater than 17 dB at 10.5 GHz. The antenna consists of 16 fan-shaped dipoles in a tapered array configuration printed on both sides of a 1/32-in polyethylene sheet. The dipoles are phased into a 50-ohm input line through successive quarter-wave balanced transmission lines. The 50-ohm line is fed from the 1/32-in microstrip circulator board, thereby eliminating the need for connectors. The antenna is protected by a window constructed of high-impact polystyrene.

Signal processing

The doppler frequency shift f_d for radial velocities v is given by $f_d = f[1 - (c-v)/(c+v)] \approx 2(v/c)f$, where f is the transmitted frequency and c is the velocity of light.

For a ground-speed sensor with a narrow beam that lies in a common vertical plane with the locomotive's velocity vector and illuminates the ground at an incident angle θ, the doppler shift is given by $f_d = 2v_g \cos\theta/\lambda$, where v_g is the vehicle speed over the ground and λ is the wavelength of the transmitted signal.

For the ideal case of a transmitted frequency of 10.5 GHz and an incident angle of 45°, the doppler frequency is approximately 31 Hz/mph. However, this assumes a narrow, parallel antenna beam and therefore constant θ. This is not the actual case. The antenna beamwidth is determined by the antenna aperture and frequency. The beam spread produces a doppler-frequency smearing that is proportional to the antenna aperture, so that the doppler signal is therefore a distribution of frequencies. Another factor, referred to as ground bias shift, further influences the frequency distribution. This effect is caused by increasing back-scatter amplitude with increasing incident angle.[2]

In the locomotive application, this spectrum is further modified by the low-

frequency signals induced by extraneous vehicle motion such as rolling, side-to-side sway, and engine and track vibrations. The effects of rough and smooth track are shown in Fig. 3. The actual frequency distribution for a given antenna aperture including all of these effects is shown in Fig. 4. The left-hand trace shows the time-based doppler frequency from a locomotive-mounted radar. The doppler signal is amplified through a flat wide-band amplifier to eliminate frequency distortion. The right-hand trace shows the frequency spectrum of a 200-ms sampling of this signal. The problem is to extract a valid doppler frequency from the signal that will remain proportional to ground speed.

Since the amplitude distribution is a function of the extraneous vehicle movements, a simple average frequency count would not be acceptable. Although an amplifier having monotonically increasing gain versus frequency will accentuate the desired frequency, this is not sufficient, since the required gain slope would cause the circuit to be dominated by noise at low speeds. A tracking low-pass filter that limits the shaped amplifier's bandwidth to include the desired frequency circumvents this noise problem. Although the tracking filter effectively reduces the doppler frequency spread, it does not eliminate all of the frequency jitter. An overdamped phase-locked oscillator produces a spectrally clean output and an additional high-frequency tracking filter function. The latter feature is a result of a phase-lock loop oscillator's inherent ability to lock onto a higher frequency faster than it will lock to an equally-spaced lower frequency. Since the number of phase-locked loop oscillator cycles required to lock onto a frequency spaced an equal distance above or below the oscillator's frequency is fixed, it will take a shorter time to lock onto the higher frequency.

Fig. 5 is a block diagram of the complete signal-processing circuit. The voltage-tunable filter is driven from an essentially flat-gain amplifier, followed by a frequency-to-voltage converter. The filter transfer characteristics are conservatively chosen so as not to interfere with the desired signal frequency. Both pulse and analog outputs are provided through a buffer amplifier and frequency-to-voltage converter, respectively. The analog output can drive one to three standard locomotive speed indicators. The pulse output, which has a 50% duty cycle and a rate of 24 Hz/mph, is useful for driving a speed recorder or triggering an overspeed alarm.

The signal-processing circuitry is constructed on a single board that also includes the voltage regulator and calibrator circuits. The calibrator circuit consists of a two-frequency oscillator that drives a varactor diode mounted on the antenna surface. When activated, the varying diode capacitance phase-modulates a portion of the transmitted microwave signal and reflects it back through the antenna and circulator into the mixer. This simulated doppler signal is processed as a normal velocity signal. The calibrator serves two purposes: it provides an operating check for the complete radar system including all of the circuits; and, since the two varactor modulating frequencies are known, it can verify the radar's speed readout calibration.

Radar construction

The doppler radar is mounted beneath the locomotive and is subjected to an especially hostile environment including vibration, dirt, grease, temperature ex-

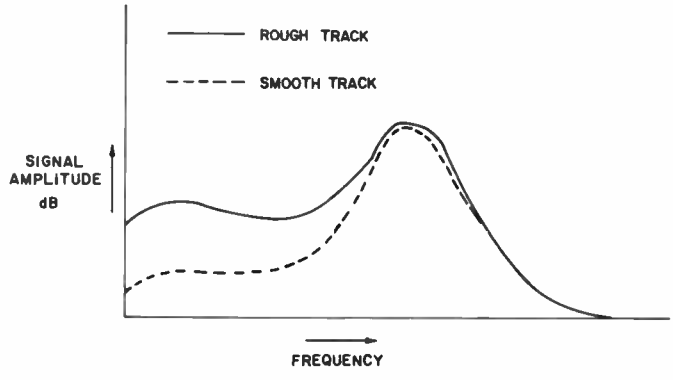

Fig. 3 — Idealized doppler frequency distribution.

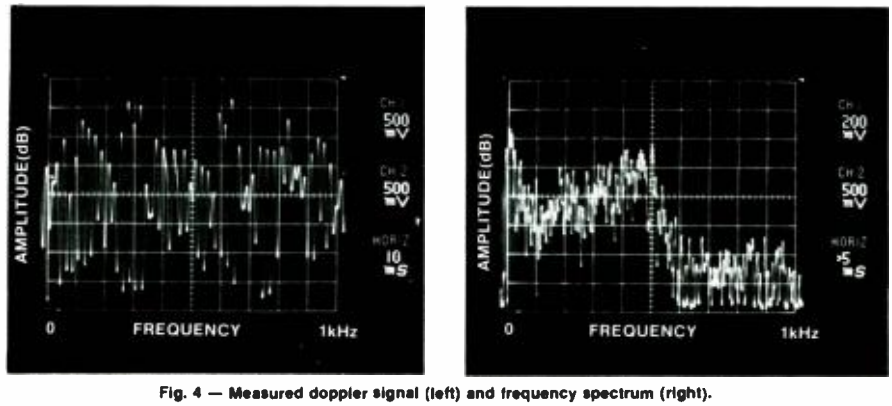

Fig. 4 — Measured doppler signal (left) and frequency spectrum (right).

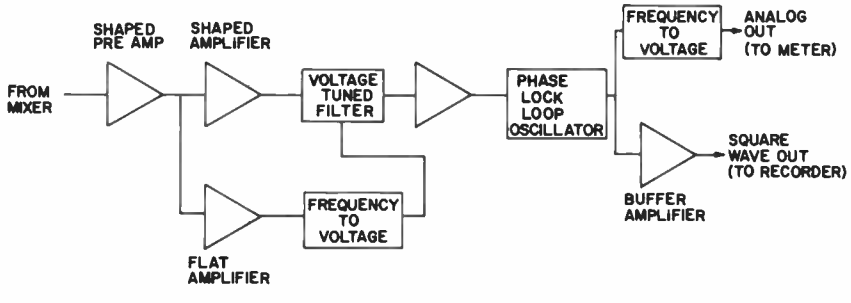

Fig. 5 — Signal processing block diagram.

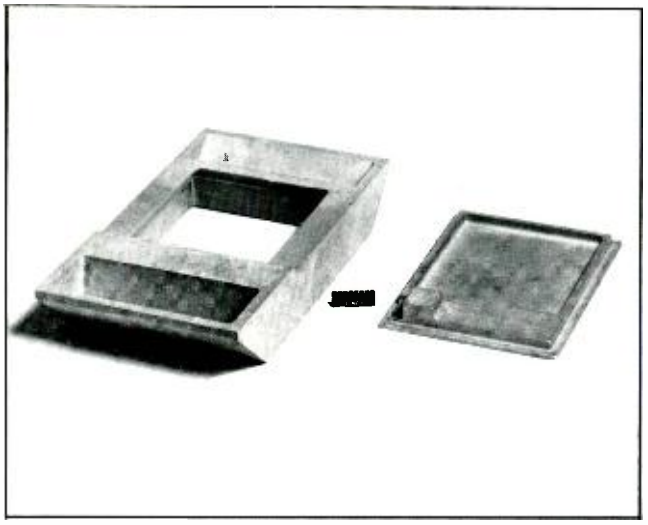

Fig. 6 — Cast radar parts.

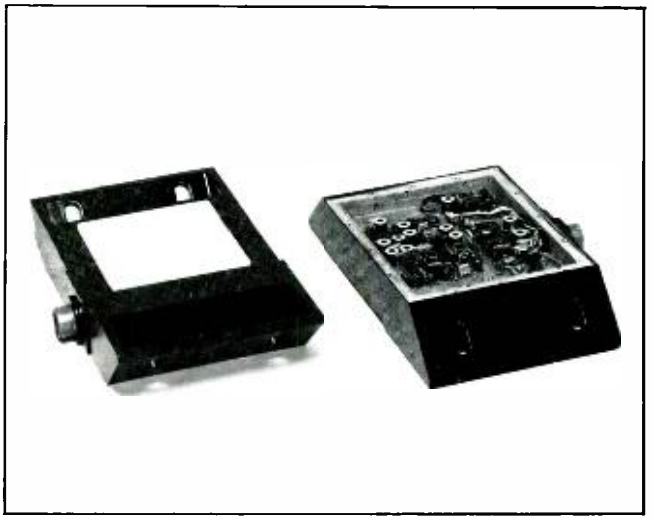

Fig. 7 — Completed radar with back cover removed.

tremes, and caustic cleaners. The radar construction therefore must be both rugged and chemically inert. The main radar structure consists of two aluminum parts, the tray and the housing (Fig. 6), cast in precision plaster molds. The housing includes two integral mounting brackets designed to mount on either a horizontal or vertical surface. After machining, the housing is epoxy-painted and baked, resulting in a surface resistant to corrosive cleaners, abrasives and salt spray. The radar's rf portion is assembled and tested on the tray, which is then mounted within the housing. The signal-processing board is tested and mounted on the back of the rf tray assembly. The polystyrene window and back cover are sealed to the housing with an elastic non-hardening gasket material.

Operating characteristics

Although the speed range of interest is typically from 2 to 90 mi/h, the measurement capability of the radar extends through 120 mi/h. To minimize the effects of $1/f$ noise, the radar processing circuit is designed to be unresponsive to frequencies below 35 Hz, which corresponds to approximately 1.5 mi/h. The doppler radar has already logged many thousands of track miles over snow, sand, open-tie bridges, road crossings, and normal track bed. Reported velocity errors when the locomotive travels over these surfaces are a maximum of ± 0.2 mi/h at 2 mi/h to ± 0.5 mi/h at 50mi/h. These accuracies are maintained even with 1/4-to-3/8-in. accumulations of dirt and grease on the antenna window.

The radar can be powered from a grounded dc supply of from 10 to 17V, and consumes approximately 6 watts. A separately packaged power conditioner converts the locomotive's floating 74-V source to a grounded 15-V supply. As mentioned previously, all of the radar's electronics are mounted on the cast tray. This configuration provides the possibility for dc isolation of the tray from the housing—with this optional circuit geometry the radar housing can be bolted to the locomotive underbody without grounding the electronics.

Radar speed sensors using a previous generation of the signal-processing circuitry have successfully completed tests through various environments from desert to snow-covered mountain regions. Laboratory temperature tests on the latest design show signal sensitivity variations of approximately 2 dB over the -50 to +65°C range. The sensitivity margin for accurate speed measurement has been shown to be greater than 10 dB.

Conclusions

The microwave radar speedometer developed for locomotive use appears to represent a useful advance in railroad instrumentation systems. Rugged, simple, accurate, self-calibrating, and easy to replace, the RCA unit has a good chance of becoming the prototype of an inherently new speedometer for all types of vehicles—an instrument that measures true ground speed directly, with accuracies acceptable for modern transportation systems.

The ability to measure ground speed independently, without reference to wheel rotation, may lead to applications other than replacements for conventional speedometers. Some of the applications already being studied are: accurate distance measurements for farm equipment and vehicle monitoring systems; obstacle detection and anti-collision systems; and anti-skid and anti-hydroplaning systems. In addition, this type of speed sensor may be useful on vehicles that have no wheels at all, such as speedboats, snowmobiles, and tank-like and air-cushion vehicles.

The RCA radar speedometer is presently undergoing extensive field testing. The first pre-production quantity of units has been fabricated, and plans are being formulated for a pilot run involving the manufacture of a moderate quantity of units.

Acknowledgments

Grateful acknowledgment is given to J. Rosen for his antenna design work, to F. Vaccaro and J. Paczkowski for their able help in the housing and tray designs, and to L. Zappulla, E. Mykietyn, and J. Brown for their skillful layout and assembly work.

References

1. Johnson, H.C.; and Presser, A., "Automotive doppler radar speed sensor," *RCA Engineer*, Vol. 18 No. 6 (Apr-May 1973) p. 62-65.

2. Skolnik, M.I.: "Radar Handbook," McGraw-Hill (1970).

3. Wilkinson, W.C.; "A class of printed circuit antennas," 1974 IEEE Antennas & Propagation Symp., Session AP-S10 pp. 270-273.

A microcomputer-controlled spark advance system

A. D. Robbi | J. W. Tuska

A microcomputer can calculate and control the exact time of spark firing as a function of speed and load to give better engine timing accuracy and dynamic response than a mechanical advance-retard system. Microcomputer control also allows the engineer to build in additional features, such as automatic misfire protection, and has noticeably improved "driveability" in road tests.

DURING the 1950's solid-state devices capable of switching the primary current of an automobile ignition coil became available. Ignition systems using these transistors, normally with a specially designed ignition coil, were built by enthusiasts and offered on the aftermarket in either kit or finished form by many suppliers. These systems retained the conventional mechanical breaker points, but the breaker points switched transistor base current rather than coil current. Well-designed "transistor ignition systems" increased the amount of energy delivered to the spark plugs and extended the mileage that the vehicle could be operated without significant performance deterioration.

Breakerless electronic ignition systems became available as a factory option during the 1960's,[1] and by late 1973 a significant percentage of the new automobiles produced in North America were assembled with breakerless solid-state ignition systems as standard equipment. It was at this time that we decided to investigate and implement a fully electronic spark timing system. The authors, and their colleagues, are not automotive engineers; and we do not profess to know all the answers to the problem of controlling a modern internal combustion engine so that it provides excellent driveability and performance, certifiably low emissions, and improved fuel economy. We believed that a system in which the exact times of spark firings were calculated and controlled electronically, as a function of engine speed and load, would offer improved timing accuracy and faster response than conventional advance-retard systems with centrifugal weights and mechanically moved sensors in the distributor.

We further believed:

1) that a digital system based on a microprocessor would give us the capability to provide the required spark timing and the flexibility to easily modify the spark timing based on additional sensor inputs or vehicle information;
2) that a microprocessor-controlled spark advance system would allow the automotive engineer new freedom to employ sophisticated control algorithms in a cost-effective way, via software, for ideal ignition timing over a greater range of conditions, both environmental and operational, than is possible with mechanically constrained systems; and,
3) that a true test of the suitability of a CMOS microprocessor, the RCA COSMAC, for engine control, was to build such a system and operate it in the hostile environment of an automobile.

The system was designed to match the ignition specifications for the 302-cubic-inch displacement, 8-cylinder engine of our instrumented station wagon, and installed on that vehicle. A year of vehicle operation over a variety of driving conditions, specific tests, and demonstrations has confirmed our beliefs.

In the subsequent sections we describe the spark timing problem and its mechanical solution, the approach we have taken, and the performance of our system.

Spark timing

Spark timing is a critical parameter for the modern internal-combustion gasoline-fueled engine because the spark initiates the combustion process. The combustion of the gas-air mixture in the cylinder of an engine should cause the maximum pressure to occur very near the time when the piston has completed the compression stroke and is about to begin the expansion stroke. The relative timing of the spark must be variable because the speed of combustion of the mixture is not the same under all engine operating conditions, and engine operating speeds vary by a factor of approximately 10 from idle to maximum speed. Thus, at a 500-rpm idle speed, 3° of relative spark timing corresponds to 1 millisecond of time; while at 5000 rpm, 1 millisecond of time is equivalent to 30° of relative spark timing.

Factors influencing the combustion process include the air/fuel ratio, the engine load, the throttle opening; and on recent engines, the amount of exhaust gas recirculation (EGR) added.

Spark timing is normally referred to as the angle in degrees of crankshaft rotation between the angular position of the crankshaft when spark occurs and its position when the piston passes from the compression stroke to the power stroke (top dead center, or TDC). Spark occurring on the compression stroke is referred to as "advanced" as it occurs before top dead center (BTDC); while a "retarded" spark occurs on the power stroke and is after top dead center (ATDC). Fig. 1 illustrates these relative piston-crankshaft positions.

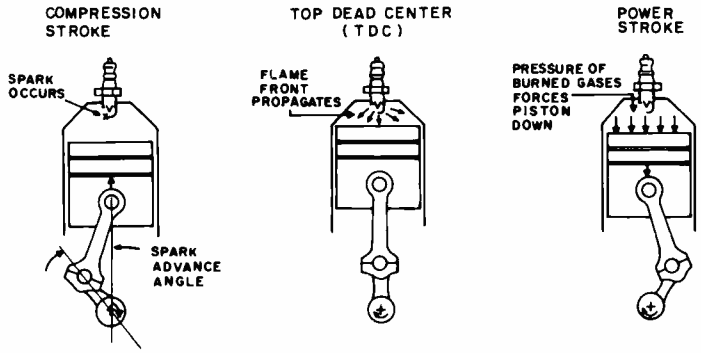

Fig. 1 — Crankshaft vs. piston positions. Spark shown for advanced spark timing (before top dead center).

Nearly all automotive ignition systems, whether conventional breaker-point/coil or variable-reluctance-triggered solid-state types, change the spark advance angle by mechanical means. Changes that are proportional to engine speed (or depart from that relationship as needed) are usually obtained by a centrifugal device that rotates the reluctor (or breaker-point cam) with respect to the distributor shaft in the direction of shaft rotation. This relative rotation increases with speed and generates a trigger (or opens the points) sooner than otherwise, resulting in an earlier (advanced) spark firing.

Changes to the spark advance angle to adjust for torque load or throttle angle are generally accomplished by sensing one or more pressures, (e.g., the intake manifold or carburetor venturi pressure). The differential between the sensed pressures, or sensed pressure and atmospheric pressure, is applied via a flexible diaphragm and rod to control the partial rotation of the nominally stationary plate in the distributor that supports the trigger coil (or breaker points). Rotating this plate opposite to the shaft rotation increases the spark advance angle, and since the sensed pressure is less than atmospheric for normal engines, this component of spark timing is frequently referred to as "vacuum spark advance."

The "vacuum spark advance" and "centrifugal" (or rpm) advance components are combined in the distributor to produce the desired spark timing. Since these components are mechanically generated, their operation is subject to wear, friction, and fatigue of the restoring springs.

Thus far we have defined advanced spark, retarded spark, TDC, and have identified the rpm and vacuum components of specific spark timing. These and two additional terms—timed maximum advance (TMA), and REF, the minimum spark advance—are shown in Fig. 2. REF is the position of spark firing when no rpm or vacuum advance components of spark timing are considered; an engine is usually timed for this spark to occur at the designated crankshaft position by rotating the distributor housing relative to the engine block. TMA represents the most advanced time of spark firing and is the sum of the maximum values of rpm and vacuum advance.

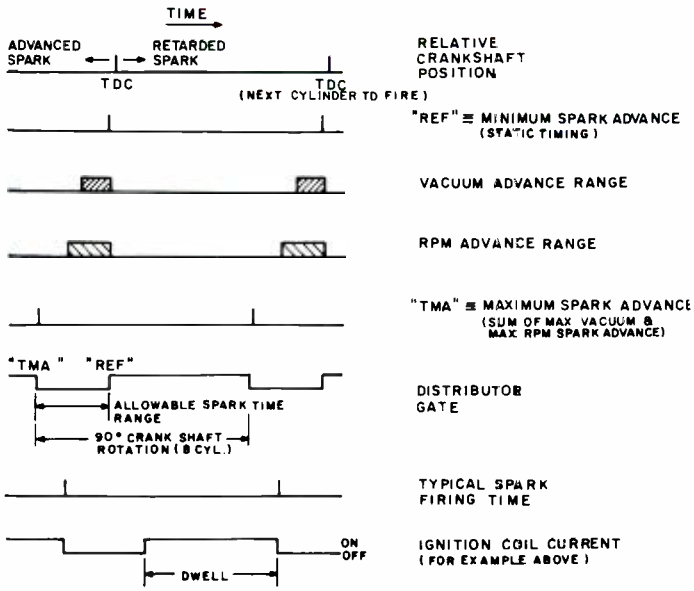

Fig. 2 — Spark timing.

James W. Tuska, LSI Systems Design, RCA Laboratories, Princeton, N. J., received the BS in Electrical Engineering from the University of Pennsylvania in 1956. In 1959 he joined RCA Laboratories, where he has been engaged in memory switching circuit research, permalloy magnetic sheet and plated magnetic wire memory developments, the integration of MOS devices for use with monolithic ferrite memories, and the development of fast, high-voltage switching circuits for computer terminal alphanumeric color displays. In 1967 he was awarded an RCA Laboratories Achievement Award for his work on high-speed laminated-ferrite memory systems. More recently, his research involved the application of the MNOS memory transistor as the storage element in an integrated non-volatile electrically alterable random-access read-only memory. He is presently engaged in the application of integrated circuit technology and digital information processing to automotive electronics systems. Mr. Tuska holds two U.S. patents and has co-authored several papers.

Anthony D. Robbi, Sr. Member, Technical Staff, LSI Systems Design, SSTC, Somerville, received the Ph.D. from Carnegie Institute of Technology in 1961. He has also received much on-the-job education in computers since joining RCA in 1961. Since 1971 Dr. Robbi has worked in microprocessor research, and has participated in CEE-55, a video-tape training course on microprocessors. During his career with RCA he has received three RCA Laboratories Outstanding Achievement Awards, has published many technical papers, and has submitted numerous patent disclosures. Dr. Robbi is active in IEEE, especially in the social implications of working as an engineer. Away from work he serves as a school board member and enjoys the outdoors.

Reprint RE-22-2-8
Final manuscript received January 9, 1976.

Jim Tuska (left) and Toni Robbi check the timing on their 'electronic car.'

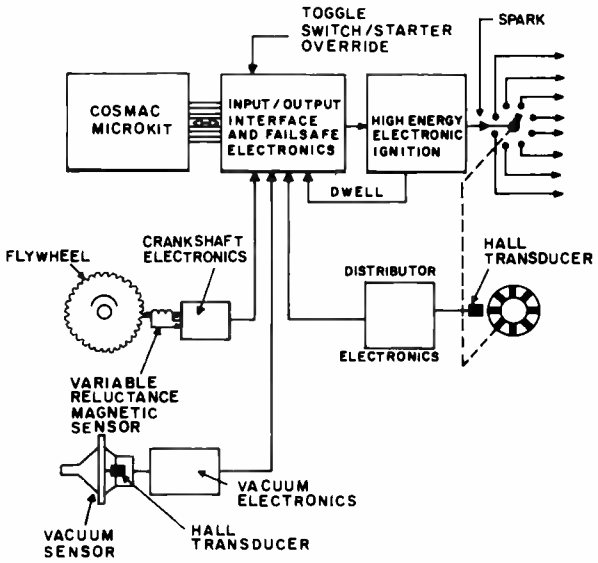

Fig. 3 — COSMAC-controlled ignition electronics.

Up to now we have defined our spark timing in terms of crankshaft degrees. The term *dwell* is generally referred to in ignition system discussions as an angular measure of the time during which current flows in the primary winding of the ignition coil. This term, however, is measured in degrees of *distributor* shaft rotation, which is half the crankshaft speed in a 4-cycle engine. The formula below indicates that for a typical 8-cylinder dwell of 30°, current flows in the ignition coil primary for 2/3 of the available time.

$$\text{Duty cycle} = \frac{\text{indicated dwell}}{\text{available time per cylinder}} = \frac{\text{indicated dwell}}{360^\circ \div \text{no. of cylinders}}$$

System overview

The hardware constituents of the experimental spark control system are shown in Fig. 3. The digital system output is a trigger signal to a commercial high-energy electronic ignition.[2] The ignition electronics determine the spark duration and initiate dwell, and this information is fed back to the digital system. Following the manufacturer's specifications,[3] the spark advance is computed as the sum of two components, vacuum advance and rpm advance. Vacuum is determined by measuring a Hall-effect voltage, which is a function of diaphragm position. Rpm is determined by measuring the duration of a synchronizing signal derived from the distributor. This signal also serves as a reference point for counting degrees to the desired firing angle and as a timer for default firing.

The flywheel, with 164 teeth on its circumference, is an excellent source of crankshaft angular rotation and position, as it is rigidly attached to the crankshaft. The crankshaft electronics converts the tooth count to a 328-cycle-per-crank-revolution wave. Each pulse may be considered to correspond to a "tooth degree", which is thus 360/328 actual crank degrees. To fire an advanced spark the computational system performs two primary tasks: computing the advance (rpm + vacuum) in tooth degrees, and counting tooth degrees from a reference point, TMA, to the desired firing point. The computation is rapid enough to allow a fresh computation for each spark. This, and the fact that spark is synchronized with the crankshaft, which may accelerate as much as 20% per spark firing (1/4 revolution), gives rise to an excellent dynamic response.

The possibilities of misfiring (too early or too late) or an omitted firing are reduced by a failsafe strategy employed in the interface. Computer-initiated sparks are gated by the TMA-REF signal, thus preventing misfiring. If a computer-initiated spark does not occur in the interval, the interface initiates spark at REF. This mode is intentionally used when the starter is active or if an override toggle switch located in the passenger compartment is closed.

A flow chart for the main program loop accomplishing the spark computation and control is shown in Fig. 4.

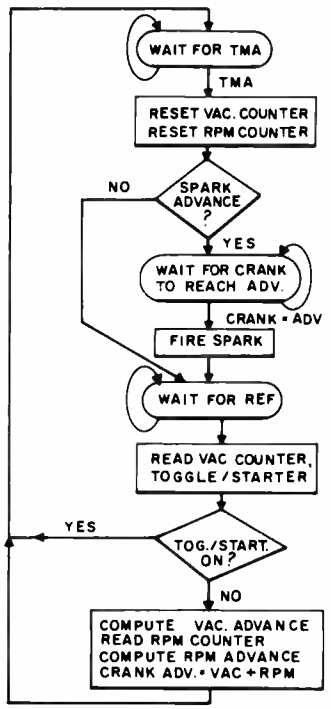

Fig. 4 — Ignition program flow.

Peripheral circuits and sensors

Two of the peripheral sensors shown in Fig. 3, the distributor and the vacuum sensor, are experimental devices fabricated by members of the Laboratories Automotive Systems Group based in Somerville.* While more conventional sensors, representative of the state of the art of the most recent automotive production sensors, could have been used in our system, these experimental types were chosen as part of an ongoing program to investigate and develop effective solid-state sensors fitting the anticipated needs of the automotive industry.

The distributor for this experimental system is greatly simplified when compared to the distributor of a conventional ignition system. The experimental dis-

*J. Olmstead, P. Del Priore, and L. Herrod

tributor is illustrated in Fig. 5. There is no movable baseplate for vacuum advance changes, and no centrifugal advance mechanism with weights, pivots, and springs. A standard distributor housing was used to facilitate installation and to accommodate a cap and rotor designed for high-energy ignition service. The distributor shaft, conventionally gear-driven from the engine, directly drives an inverted segmented cupped ferrous disc. The eight equally-spaced segments rotate between the magnet structure and the Hall-effect detector of the variable-reluctance sensor attached to the distributor baseplate. The distributor shaft extends above the disc to drive the rotor, which directs the high-energy ignition to the proper spark plug as in conventional systems.

The geometry of the rotating segments is chosen such that the sensor output, after amplification and standardization by the distributor electronics, yields the "distributor gate" waveform shown on Fig. 2. The output from the distributor electronics is digital, with state transitions of high to low at TMA, and low to high at REF. The amplitude ("high" = +5V, "low" = 0V) is independent of speed. This output is capable of driving the high-energy electronic ignition module directly without the input/output interface or failsafe electronics. A firewall toggle switch is included in our installation should the need for the direct connection arise, and as a convenience for moving the vehicle when the COSMAC-controlled system is removed for bench testing or modifications. (Spark firing occurs at REF at all times when the direct connection is used.)

The vacuum sensor connects to the normal "vacuum advance port" on the engine. Pressure (less than atmospheric—hence vacuum) variations cause a flexible diaphragm in the sensor to change position. A Hall transducer converts the diaphragm position to a voltage. This analog voltage controls the pulse width of a triggered monostable, providing two outputs that are a function of vacuum—the continuous analog voltage and the width of the monostable pulse.

Crankshaft rotation is measured by a variable-reluctance magnetic sensor in close proximity to the gear teeth on the outer circumference of the flywheel. The output from the sensor is approximately sinusoidal in shape, and as there are 164 teeth on the test vehicle's flywheel, the frequency is 164 cycles per crankshaft revolution. The sensor output is converted by the crankshaft electronics to a 328-cycle/crankshaft-revolution square wave of constant amplitude (5V). These electronics consist of a full-wave diode bridge, voltage clamping, amplification, and wave-shaping circuits. The frequency is doubled to enable its direct use in the spark calculation to a resolution of approximately 1 degree.

The ignition coil used is a standard high-energy coil, controlled by a high-energy electronic ignition module intended for operation with a breakerless distributor. Our only modification to the ignition module was the addition of an intermediate-stage dwell output. (Dwell is initiated by the ignition module electronics and this information is an input to the digital system.)

COSMAC interface

The experimental system was developed on the COSMAC Microkit, a hardware/software development system based on the RCA CDP1801 microprocessor.[4] The interface circuitry unique to the ignition system resides on a 4- by 6-in breadboard that fits into one of the empty slots in the Microkit backplane. A block diagram of this module is shown in Fig. 6. The Microkit provides facilities not required for a final product; the next step in a product design would be to create a minimum-cost system that performs in a functionally identical manner. The interface described here uses the following Microkit facilities: microprocessor, RAM memory, PROM memory, address latch, I/O decode, and a byte I/O input port (interface to RAM memory).

The Microkit operates at the standard V_{DD} = 5V and clock frequency of 1.95 MHz. This gives a machine cycle time, and TPA (CPU timing pulse) period, of a little over 4 μs, and an instruction fetch/execute time of a little over 8 μs. TPA, appropriately gated, drives both the VAC and RPM counters. The contents of the VAC counter (and the toggle/start switch position) are read into memory by issuing an I/O instruction (IOD) just after REF. The contents of the RPM counter are read into memory by DMA input cycles caused by crank square-wave transitions (82 per firing cycle). Since DMA cycles automatically increment COSMAC register R0, its position serves as a "tooth degree indicator." R0 is reset by program at each occurrence of TMA. The program in-

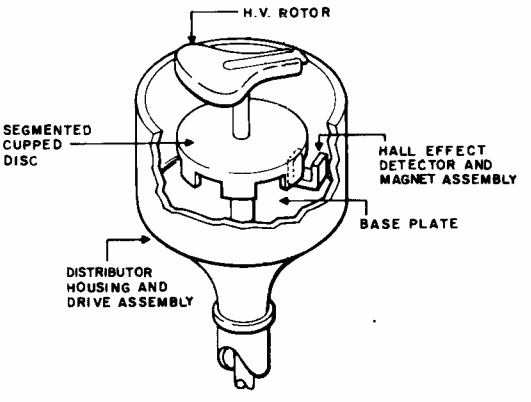

Fig. 5 — Experimental distributor.

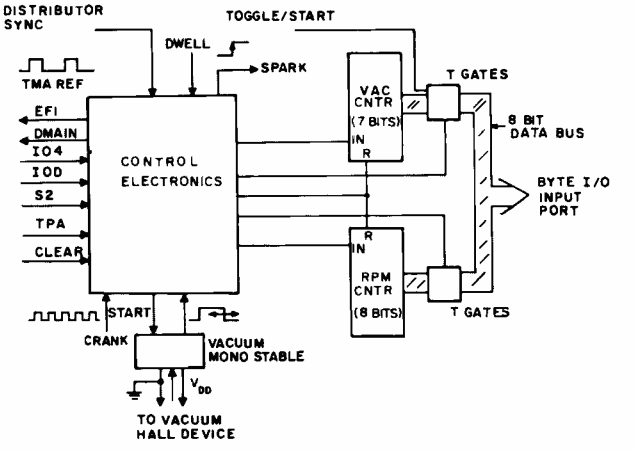

Fig. 6 — Ignition-control electronics module.

itiates spark issuing an I/O instruction (IO4) when the address in R0 matches a pre-calculated value, which is a function of the advance.

Program description

As can be seen in the functional flow chart of Fig. 4, the program operation is synchronized by the distributor waveform, which the program senses by testing an external flag (EF1). At REF, by which time spark has initiated, the VAC and RPM counts are read and the spark advance is computed, in tooth degrees. The program translates this to a count relative to TMA and waits for TMA. At TMA the two counters are reset and the vacuum monostable is started. When the address in R0 reaches the appropriate tooth degree count, spark is initiated and the program execution waits for REF to start the next cycle.

Both the vacuum and rpm advance computations use a table look-up and interpolation subroutine, as both advance components are nonlinear functions of VAC and RPM. The smooth advance curves shown in Fig. 7 are drawn through limit values specified by the manufacturer.[3] Obviously, mechanically-caused advance is not expected to be very precise. The discrete points within the curves correspond to look-up table values stored in the program. Each of the tables actually has 16 entries, but since the abscissas are counts that are not scaled to fit the bounds exactly, some points spill beyond the limits shown (and are never actually used). The table look-up routine linearly interpolates values between the points shown to an accuracy of one part in eight. On average, about 60 instruction executions are required to return an interpolated advance value, given a vacuum or rpm value. Thus the computational portion of program, from TDC to REF, requires roughly 1 ms of processing time. Even at 4000 rpm, roughly 2.5 ms are available in this interval, so the computing load on the microprocessor is light.

The program itself occupies 192 bytes of memory storage, broken down as follows:

	Bytes	*%*
Main loop	71	37
Look-up subroutine	64	33
Initialization and start-up	25	13
Look-up table data	32	17
	192	100

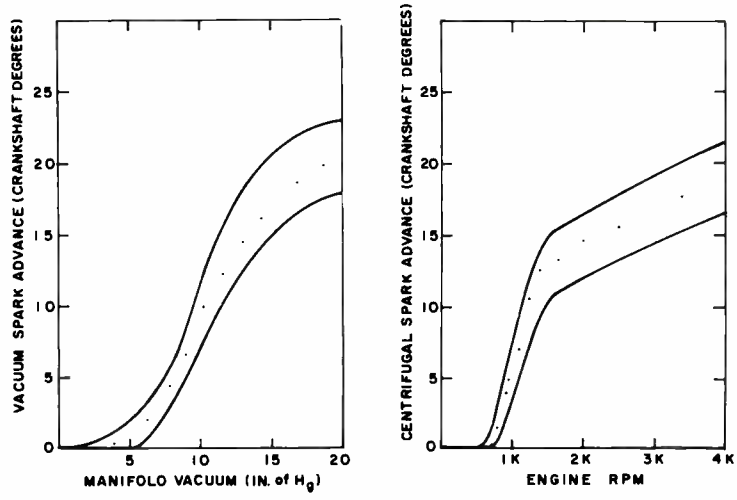

Fig. 7 — Manufacturer's specifications for mechanical control of ignition. Dots indicate stored-program data.

It uses more RAM than it needs to, because it is provided in the Microkit. Since only 7 of the 16 available COSMAC scratch-pad registers (2 bytes each) are used, only a single byte of RAM for arithmetic and input/output would be required.

System performance

When this microcomputer-controlled spark advance system was first installed on our test vehicle we adjusted the distributor position such that default firing, or spark firing without vacuum or RPM advance, would occur at the desired time. We used a high-voltage stroboscopic timing light that we had used on this and other engines many times. This time the timing marks on the rotating damper, illuminated by the timing light, were much sharper and more clearly defined than we had seen before on this or other vehicles. We had expected increased accuracy and improved transient response from our system, and this visible demonstration of more accurate repeatability was the first of many on-the-car confirmations of our expectations. The vacuum and rpm components of spark advance have been measured individually, and in combination, on the operating engine. (The timing light was clamped in position for accuracy, and the standard timing scale (2° graduations) replaced with a temporary scale with accurately marked 1° graduations. The measured advance components were within ±1° of the data points in Fig. 7, with the exception that approximately 2° of spark advance results from manifold vacuums between 3 and 4 inches of Hg.

Our station wagon, with its microcomputer-controlled spark advance system, has been driven in dense traffic and on open interstate roads, and in temperatures varying from summer to winter in New Jersey. The system has been subjected to a variety of intra- and extra-vehicular electrical noise, including the repeated cycling of the vehicle's air-conditioner clutch, normal vehicle controls (e.g., blower, turn signals, etc.), a 550-W inverter, and the car's CB transceiver. The vehicle has been driven in the vicinity of rural electric fences and rf transmission sites, and has been subjected to the radiated noise from SCR-controlled power tools. During all of this testing we have not experienced a failure or detected any irregularities.

The "driveability" of a vehicle is a difficult term to define and impossible to measure in an engineering sense. However, the change in driveability of the test car with the experimental spark advance system, as compared to the same car with a well-maintained, freshly-timed conventional system, is noticeable, with an apparent improvement in smoothness and response. The vehicle's responsiveness, when the 302-cubic-inch engine is operating under microcomputer-controlled spark, is more readily felt than described.

References

1. Norris, J.C.: "Delcotronic breakerless transistor ignition system," SAE paper 617B (Jan 1963).
2. Carlson, D. W.; and Doelp, W. L.: "A successful electronic ignition system through fundamental problem analysis," SAE paper 740154 (Feb 1974).
3. Ford Shop Manual, 1969, Vol. 2.
4. MPM-103, "COSMAC Microkit Operator's Manual," RCA, SSD, Somerville, N.J.

The B-12 — an automotive microprocessor

S.E. Ozga

Microprocessors in automobiles are far past the idea stage; they can be produced in quantity now. Design automation and simulation made it possible to develop and deliver this microprocessor in only seven months.

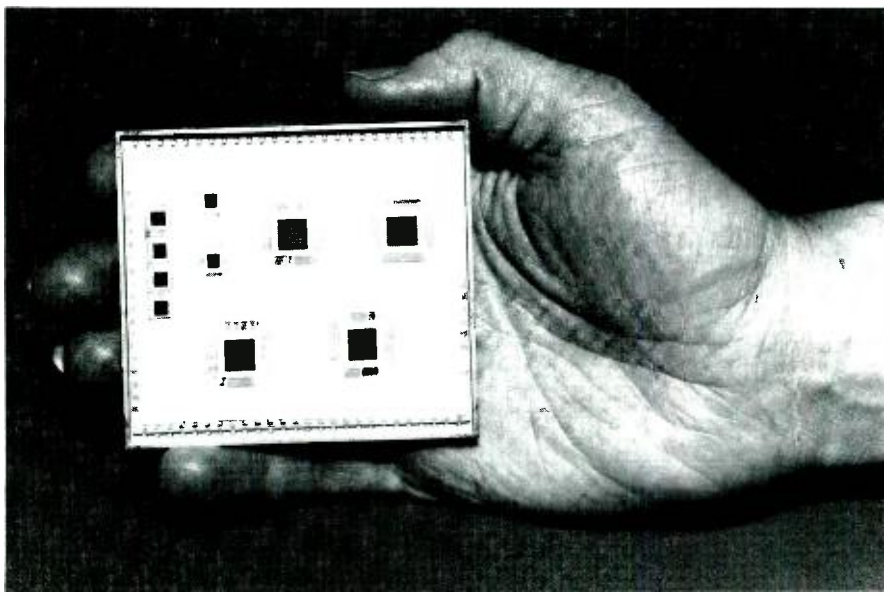

Fig. 1 — Hybrid version of B-12.

S.E. Ozga, Sr. Member, Engineering Staff, Advanced Technology Laboratories, Camden, NJ, received the BE in Electrical Engineering from Villanova University in 1970 and the MS in Systems Engineering from the University of Pennsylvania in 1975. In 1970, he joined RCA's Advanced Technology Laboratories, where he has been a major contributor in the design of several LSI computer systems. His first assignment involved the fabrication of the SUMC/DV computer delivered to NASA, which included architecture design, instruction-set specification and implementation, detailed logic design and system debug. He was the principal engineer in the development of the B-12, and currently is the project engineer of the A²MAC, a CMOS/SOS micro-signal processor, with prime responsibilities in architecture design, detailed logic implementation and system integration.

Reprint RE-22-2-6
Final manuscript received January 23, 1976.

WORKING JOINTLY with one of the major U.S. automakers, the Advanced Technology Laboratories (ATL) has developed a complete microcomputer-based electronic control system for automobiles. The system controls spark timing and exhaust gas recirculation, with future expansion planned for controlling fuel injection and the automatic transmission.

ATL's involvement has primarily been in developing the custom microprocessor that is the brain of the control system. The B-12, developed as a result of the program, was probably the world's first all-CMOS microprocessor. Several versions of the microprocessor have been developed and delivered, with many installed in test vehicles for evaluation; Fig. 1 shows one of the thick-film hybrid units.

The objective of the program was to develop feasibility models at minimum cost and time so that valuable road-test data could be accumulated. These models were designed such that packaging and chip partitioning could be optimized at a later date when firm production commitments were received. With a low large-quantity production cost goal, a single-chip or at most a two-chip microprocessor was necessary, and the B-12 was designed with this configuration in mind for subsequent versions.

This article covers the design choices in architecture, instruction repertoire, and fabrication techniques that were made in the process of producing working chips for this version of an automotive microcomputer. For a different solution to the problem, including the overall design of a spark-advance system and the digital algorithms involved, see Robbi and Tuska's "A microcomputer-controlled spark advance system," in this issue.

CPU architecture and features

The B-12 is a 12-bit, general register-oriented microprocessor with an instruction set and interrupt facilities that approach many minicomputers. It is

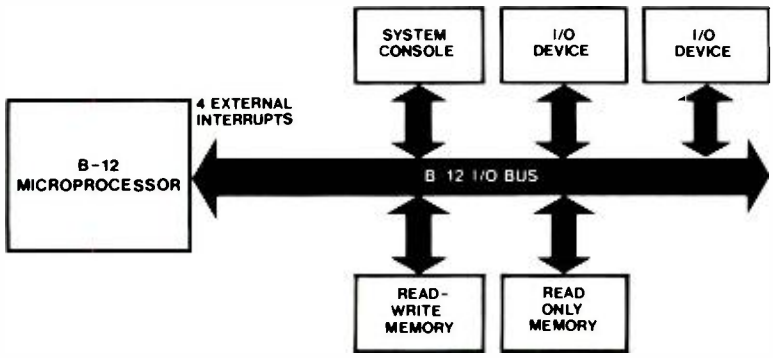

Fig. 2 — Generalized block diagram of B-12.

fabricated in standard aluminum-gate CMOS and operates from a single 10-V power supply. The system is oriented around a single bidirectional address/data bus shared by the B-12, system console (optional), read-write memory, read-only memory, and many input/output devices. Fig. 2 is a simple block diagram of the system.

System and software features

Unlike many of the common 8-bit microprocessors that were available during the program, the B-12's 12-bit word length seemed optimal for the automotive application. Since much of the control algorithm processing involved lengthy calculations on 8-bit data and processing was being performed in real-time, extensive use of double precision calculations was avoided with the significance maintained by the 12-bit word. Also, the longer word length allowed a more flexible set of instruction formats, which offered both single- and double-word instructions with a direct address space to 4096 words.

The instruction repertoire is oriented around eight general registers that share the main memory address space, as shown in Table I. This adds additional flexibility in memory addressing, along with the many advantages of general-register machines over single-address or accumulator-based architectures.

Probably one of the most important features of the B-12 is its powerful addressing capability. Its addressing modes are:

- Single-register
- Register-to-register
- Indirect register-to-register with auto-increments by "1"
- Immediate-to-register
- Indexed-to-register
- Indexed program counter relative to register
- Indirect-indexed to register
- Indirect-indexed program counter relative to register

This flexible addressing capability is important in minimizing the program memory size and execution time, where a conventional microprocessor would require several instructions to calculate the address and fetch the operands before the actual operation.

In addition, the instruction repertoire was carefully chosen to suit the processing requirements of the automotive control algorithms. The critical control loop involved a 40-ms processing frame in which extensive arithmetic processing was performed, including many signed multiplies, divides, and square roots. An instruction complement was formulated that required the microprocessor to have an average execution time of 10 to 20 μs to meet its real-time processing constraints. The repertoire contained 47 generic operations, including the standard arithmetic and logical operations along with a two's-complement multiply and divide, several bit-manipulating instructions, a full complement of conditional branches, and a multiple-option instruction. The inclusion of the multiply and divide in the standard repertoire was crucial to the application, since a software implementation would have required too much processing time. The B-12 executes a 12-bit two's-complement multiply in 38 μs and a divide with full error-checking in 83 μs, thus eliminating the need for an external multiplier and divider. This represents a cost savings for the production version of the control sytem, since less than 10 LSI parts, including memory, were projected for the total system, and any external parts extending the microprocessor's computational power add a very significant recurring cost increase. Table II gives a brief summary of the instruction repertoire.

Another real-time feature of the B-12 is its multiple-level interrupt structure. Facilities are provided to latch four independent interrupts and service them on a priority basis. Also global and individual interrupt-masking is provided. The machine state is preserved and the B-12 performs automatic linkage to specific interrupt-handling routines.

Input output devices are interfaced on the B-12 I/O bus, along with the read-only and read-write memories. Several

Table I — B-12 main memory map.

Location	*Use*
0	GR0 - Program counter
1	GR1 - Program status word
2	GR2
3	GR3
4	GR4
5	GR5
6	GR6
7	GR7
8	Program counter interrupt level 0
9	Program counter interrupt level 1
10	Program counter interrupt level 2
11	Program counter interrupt level 3
12	User-available memory address space
13	
•	
•	
4095	

Table II — Instruction-set summary.

Instructions with 7 optional address modes:

Load	Substract
Swap	Multiply
Logical AND	Divide
Logical OR	Execute
Add	

Instructions with single-register operations or immediate fields:

Branch on true	Set bit
Branch on false	Clear bit
Increment register	Invert bit
Decrement register	Test
Shift left	Test (5 optional
Shift right	operations)

interfacing modes are available for I/O, including:

Interrupt driven I/O
Programmed I/O
Shared memory addressed I/O

A sophisticated set of software tools was developed by ATL's customer to aid in the control algorithm development. The software packages include a Fortran IV cross-assembler, a Fortran IV instruction-level simulator, software debug packages, and several monitor programs. Subsequently, ATL developed a PL/M-like cross-compiler for the B-12.

Hardware features and fabrication techniques

In view of the harsh automotive environment, CMOS was chosen as the ideal technology for the B-12. The system was required to work over the temperature range of −40°C to +125°C, as well as be capable of tolerating voltage fluctuations in its primary supply (car battery) from a high of +16V to a low of +5V during engine starting. Some of the attributes of CMOS in the automotive environment are:

Wide operational temperature range — −55°C to +125°C

Wide operational supply voltage range — +3V to +15V

Single power supply

High noise immunity — 45% of supply voltage

Very low power

Moderate circuit speeds

Its low power and single power supply minimize the cost of the system power supply, which can be quite costly for multiple-voltage and higher-powered technologies.

Table III — B-12 CPU chip statistics.

Chip No.	*System usage*	*Area (mils)*	*No. standard cells*	*No. transistors*	*No. gates*	*Total linear mils*
ATL 054	Arithmetic unit	236 × 239	147	1060	297	999
ATL 055	Mux Reg	246 × 227	222	1642	546	1775
ATL 056	Control A	232 × 244	128	796	204	970
ATL 058	Control B	234 × 244	171	1020	282	1199
		Totals	678	4518	1329	4943

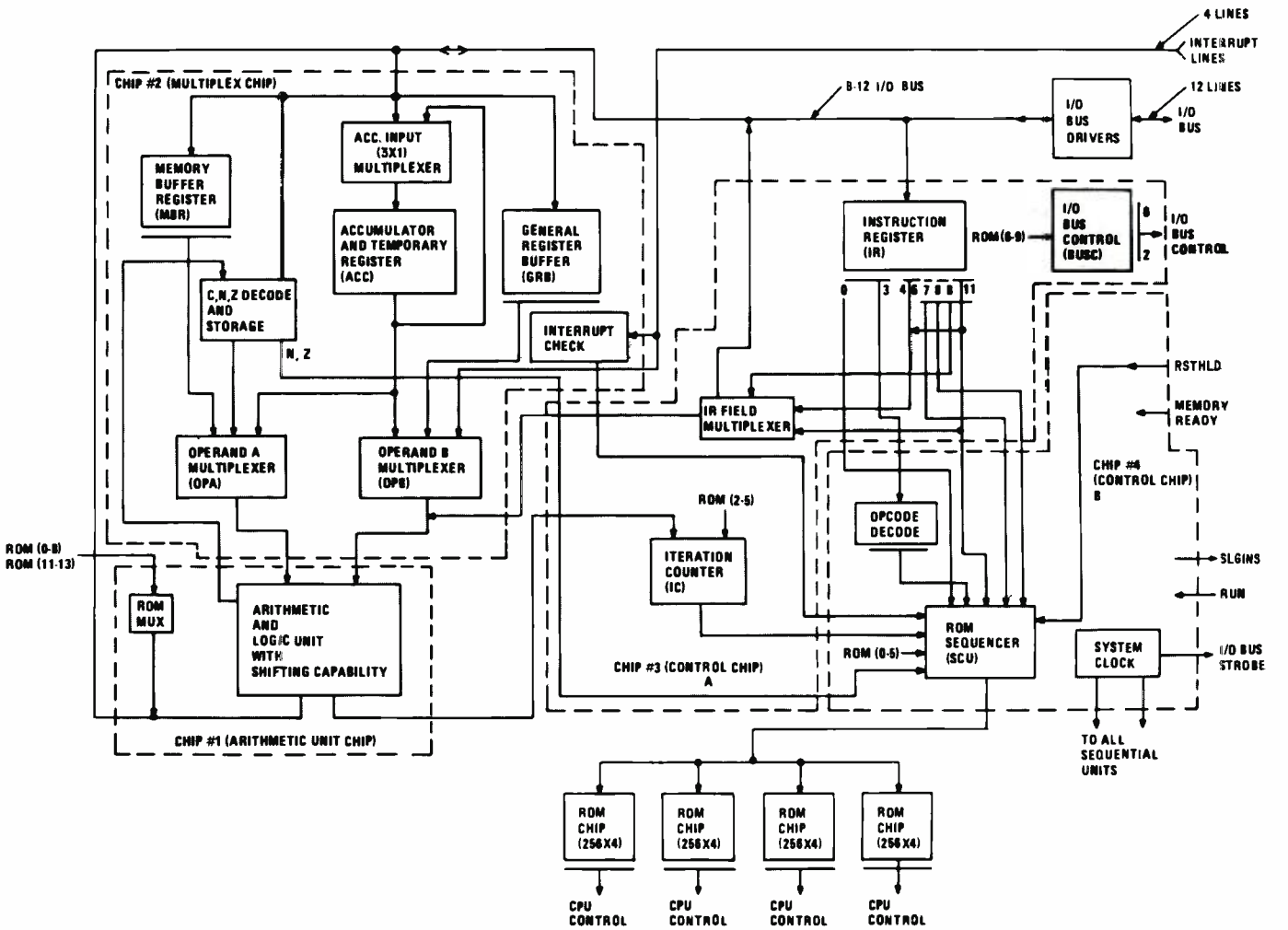

Fig. 3 — System block diagram for Phase III B-12.

All the versions of the B-12 were produced under a very limited development budget and time cycle, which precluded the use of extensive hand-custom layout in the microprocessor. The first integrated version of the B-12 was designed, developed, and delivered in seven months. Extensive use of design automation and simulation made the program possible. The system was fabricated in standard aluminum-gate CMOS, using the design automation system APAR (Automatic Placement and Routing) developed by ATL. The B-12 is partitioned into four LSI arrays plus four CMOS Read-Only Memory chips that can potentially be reduced to one array for the production version. A block diagram of the B-12 architecture appears in Fig. 3, and some of its chip statistics are given in Table III.

The basic data path of the machine resides mainly on chips 1 and 2, as shown in the block diagram, and consists of three 12-bit general-purpose registers, each having sourcing capabilities to the Arithmetic Logic Unit (ALU). The ALU is a full 12-bit parallel unit with output-shifting capability used in the shift, multiply, and divide instructions. The output of the ALU can drive the B-12 I/O bus to transmit data to external devices or to one of its internal registers. The registers can also receive data from memory or I/O devices.

The control of the machine is distributed on chips 3 and 4, where the instruction register, with its field separation and control interface, is located. A microprogram sequencer, iteration counter, and system clock are also contained in these chips.

The B-12 is fabricated using 4500 transistors, not including the microprogram memory. However, some inefficiencies and logic duplications are introduced by the multichip partition of the processor. A single-chip implementation would require approximately 3500 to 3750 transistors.

A microprogrammed control strategy was chosen as the most efficient control scheme for the B-12, because of its sophisticated instruction repertoire. A hardware approach would be much too complicated and too rigid for the customer's changing instruction-set requirements. The B-12 actually emulates the target repertoire by breaking the macroinstructions into a series of micro or elementary operations which are stored in a Microprogram Read-Only Memory (MROM) controlled by the microprocessor. Since the instruction characteristics are controlled by the information in the MROM, new instructions or changes are made by altering the MROM, thus avoiding the need for expensive modifications to the processor.

The B-12 instruction repertoire is implemented in approximately 150 words by 16 bits of control storage. Each control word is organized in a compact, vertical format so that future integration in the microprocessor chip is possible. In a single-chip implementation, the MROM would add approximately 2600 transistors, assuming a single-transistor-per-bit design in the memory elements. However, with ROM layouts being very regular and compact, this approach yields a much more efficient layout than a hardwired control scheme. Extensive chip-size estimates were performed for production planning, and a single-chip B-12 with an integrated microprogram ROM could be fabricated within a reasonable chip size that could be competitively produced in the large quantities required by the automotive industry.

Connections to the B-12 were minimized to improve reliability and reduce costs in the final production version. In a single-chip configuration a minimum allocation of package pins would be:

Address/data bus	12
Interrupts	4
Run	1
I/O control	4
System clock	3
Power and ground	2
	26 pins

Although connections to the microprocessor are few, this scheme is not without disadvantages. The single bidirectional address/data bus degrades system performance, since address and data are sent in a two-phase scheme and not in parallel. Also, it is assumed that memory and I/O have either a single shared address latch or individual selection controls. However, with the severe under-the-hood environment of the car and the potential production of millions of systems per year, the minimum-connection scheme was chosen.

Simulation and design automation

As previously noted, the very small development budget and short time cycle precluded the use of conventional hand-custom layout and breadboard verification of the machine before fabrication. The first version of the B-12 had to be designed, fabricated and delivered to the customer for system integration in less than seven months. Therefore, during this time, less than three man-months were allotted for the layout of the four LSI arrays (from release of firm logic to generation of mask fabrication data), with each containing 250 to 550 gates.

To accomplish this goal, the design process was started with an analysis of the customer-specified instruction repertoire to determine a feasible architecture that could be used to implement it efficiently. From this, a register-level block diagram was derived along with a control strategy. In this case, the only feasible control strategy was one that was microprogrammed, since the instruction repertoire was quite sophisticated and involved too many states for a practical hardwired implementation. Then the customer's instruction repertoire was mapped onto the architecture being developed and was simulated extensively on a register-transfer level using ALSIM, an RCA-developed microprogram simulator.

The simulation process was used to design and verify the proper implementation of the instruction set, as well as optimize the architecture of the microprocessor. The ALSIM simulation model provided an accurate specification of the functional requirements of the machine, and, as an additional benefit, the symbolic microcode representation used in ALSIM was used to generate the final bit pattern used in the microprogram control read-only memory. A sample ALSIM output is shown in Fig. 4.

The logic was designed and partitioned with the library of standard cells used in the APAR design automation system. A partial list of the cells available includes such basic logic building blocks as:

2-, 3-, and 4-input NAND's
2-, 3-, and 4-input NOR's
2-, 3-, and 4-input AND's

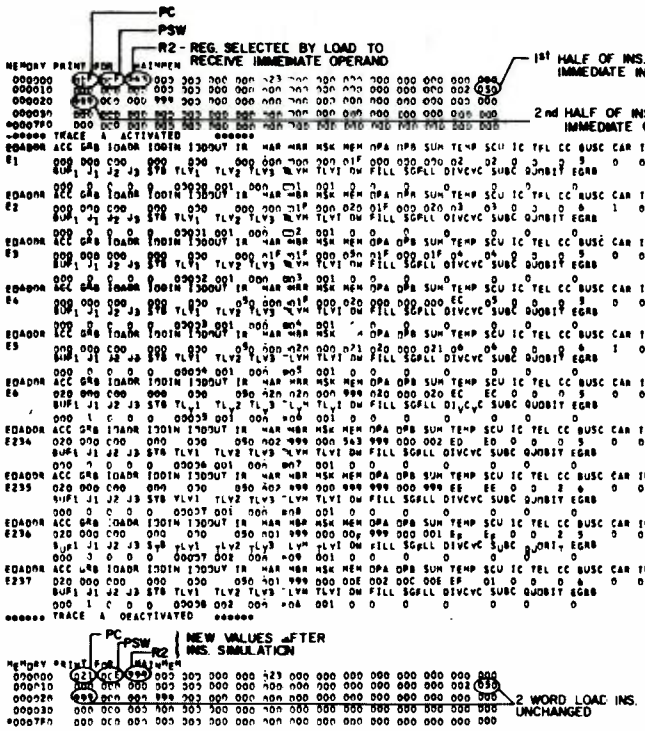

Fig. 4 — ALSIM output of load instruction. Values printed in E1 through E6 are the register and bus values after each micro-cycle for the instruction and operand fetch cycle. E234 through E237 make up the load execution cycle.

2-, 3-, and 4-input OR's

Master slave flip flops

D-type flip-flops

These standard cells were supplied with critical logic-design parameters that were derived by extensive circuit simulation and were very useful in guiding the logic design for optimum performance. Some of the parameters that are included are: input and output capacitive loads, stage delay *vs.* capacitance, and rise and fall times *vs.* capacitance.

Simulation was then performed on the logic-element level. This was accomplished using additional RCA-developed simulation packages such as:

LOGSIM — Functional logic gate level simulation tool. Also provides timing estimates of the logic network.

FETSIM and ARCAP –MOS circuit level simulators used to derive nominal and extreme circuit characteristics as a function of process.

Once the logic network was verified through extensive simulation, the APAR program was run with the networks of standard cells for each of the B-12 chips to generate the chip layout. This program accepts an interconnection list of standard cells as an input and automatically generates the placement of the cells and the routing of the cell-to-cell interconnections. This in turn can by used to generate the final mask-fabrication data of the chips.

Finally, test sequences were generated using the AGAT and TESTGEN programs to provide a full functional test for the LSI array after fabrication. Both combinatorial and sequential logic network tests are generated by the programs to determine whether any nodes of the LSI array are "stuck at zero" or "stuck at one."

Without these simulation and design automation tools, the B-12 microprocessor could not have been built within its time and dollar constraints.

Summary

The B-12 microprocessor, probably the world's first all-CMOS microprocessor, was built for one of the major U.S. automakers for an electronic automotive control system. The computer offers computational and architectural features that approach those of many minicomputers. Its architecture, instruction repertoire, and interfacing capabilities are optimized to provide a cost-effective production solution for its automotive application. Although some existing 8-bit commercial microprocessors could have been used, they presented a potentially costly production problem, since external devices such as multipliers, dividers, system clocks, and interrupt structures would have to be added as external LSI and MSI parts. The CMOS technology is optimal in this application because its extremely-low-power single power supply, high noise immunity, and wide temperature and voltage operating ranges minimize the system's packaging and power supply costs.

Although all the current versions of the B-12 are multichip systems, the design effort is compatible with a single-chip design. The logic implementation of the system was minimized while still meeting the system performance requirements to provide a minimum-recurring-cost solution for the automotive control system. Extensive custom layout estimates of the B-12 performed for production planning show that a single-chip implementation, using current production CMOS design rules, could be competitively produced in large quantities for the automotive industry.

All the current versions of the B-12 were fabricated under tight development dollar and time constraints. The success of the program can be attributed to the extensive reliance on simulation in all levels of design and on fabrication using the APAR design automation system.

Acknowledgment

The author gratefully acknowledges the special efforts of the Solid State Technology Center in providing an excellent technical interface and in expeditiously fabricating and delivering the chips. R. Geshner provided the mask sets for the chips; I. Kalish and A. Dingwall developed a 256-word × 4-bit CMOS read-only-memory used in the B-12 microprogram control storage; A. Rose and R. Zeien developed the thick-film hybrid used in the B-12 Phase II program; and H. Borkan and T. Mayhew processed and packaged the CMOS LSI arrays.

References

1. Clapp, W.A.: "LSI computer design - SUMC/DV," *RCA Engineer*, Vol. 18, No. 2 (Aug Sep 1972) pp. 88-94.

2. Feller, A., "LSI computer fabrication - SUMC/DV," *RCA Engineer*, Vol. 18, No. 2 (Aug Sep 1972) pp. 82-87.

3. Feller, A.: "Design automation techniques for custom LSI arrays," AGARD Lecture Series No. 75 (Apr 1975), pp. 7.1-7.15.

4. Merriam, A.; and Zieper, H.S.: "Simulation: methodology for LSI computer design," *RCA Engineer*, Vol. 18, No. 2, (Aug Sep 1972) pp. 77-81.

The RCA Laboratories' 'electronic car'

microprocessor control for ignition and braking

Read more about the RCA Laboratories' experimental electronic car in "A microcomputer-controlled spark advance system," page 38, by Robbi and Tuska, and "Electronic control of vehicle brakes," page 50, by Lile and Tuska.

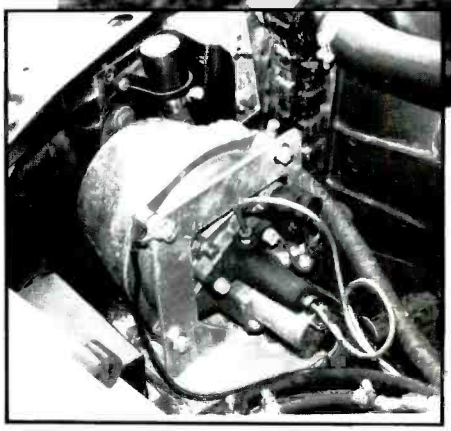

Anti-skid b variety of r on rear a from front

Brake-pressure modulator , commercially available, prevents skids by closing brake line when wheel lock-up is imminent. Solenoid-actuated modulator is computer-controlled.

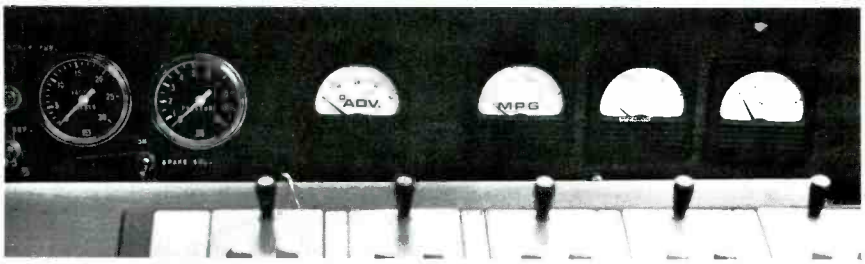

Under-the-hood views show wiring harnesses and interconnections. Large proportion of wiring and sensors is used for monitoring tests only, not for controlling car.

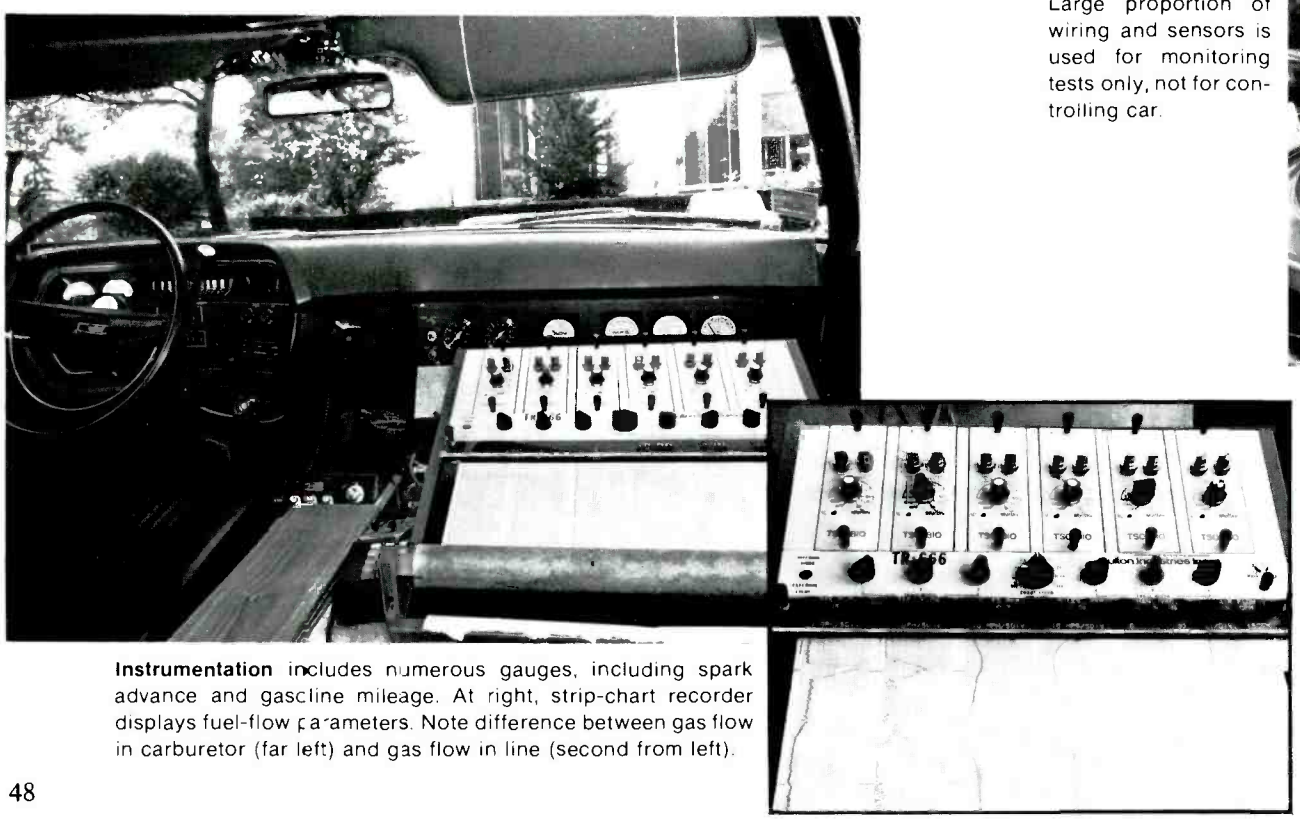

Instrumentation includes numerous gauges, including spark advance and gasoline mileage. At right, strip-chart recorder displays fuel-flow parameters. Note difference between gas flow in carburetor (far left) and gas flow in line (second from left).

aking tests are taking place on a ıad surfaces. System is instal ed ɜ only; skid marks in photo ɜre wheels.

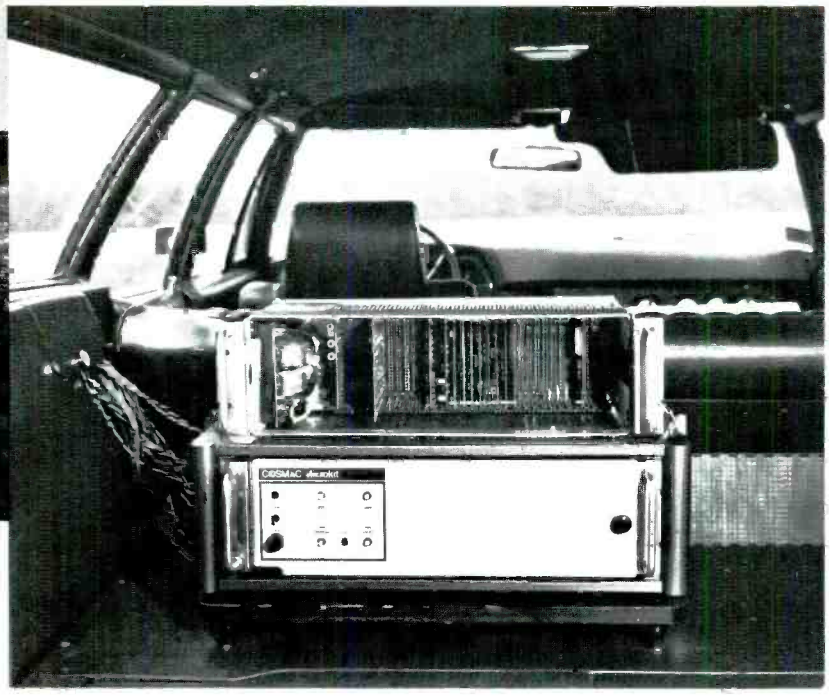

Two COSMAC Microkits control the car's experimental systems; one for braking and one for spark advance. Setup obviously is geared for experimentation, not for production; final product design will involve creating functionally identical system at minimum cost.

Special air-flow straightener on end of air intake is used with air-flow sensor. System is for test-monitoring only.

Engineer Jim Tuska looks over fitting on carburetor modified to accept RCA-developed fuel-flow sensor.

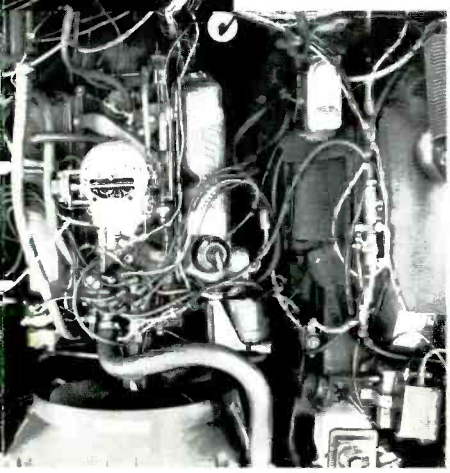

Engine-block temperature sensor is between standard distributor and modified carburetor.

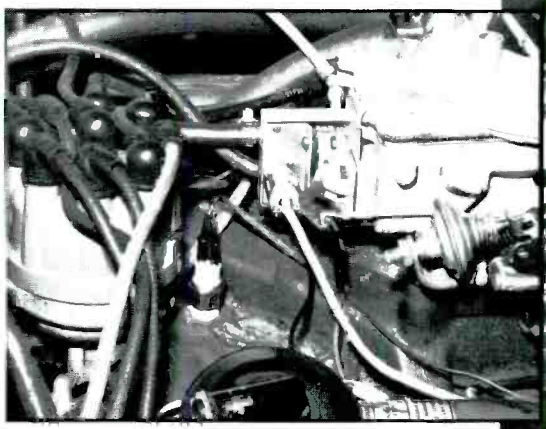

Electronic control of vehicle brakes

W.R. Lile| J. W. Tuska

Anti-lock or anti-skid braking is now used on newly-built trucks to comply with the regulations that limit lateral instabilities when stopping; the Federal Government could possibly extend its braking safety requirements to passenger vehicles. Most of the anti-skid controllers now on the market are analog systems; this article describes a digital system and the advantages that a microprocessor-oriented system can have.

IN THE 1950's the aircraft industry was the first to use electronics to prevent wheel lock-up during hard braking. The need to develop a better brake system became important as pilots had to exercise judicious restraint in braking to minimize tire blow-out, maintain lateral stability, and still stop on the runway.

Several years later, in the 1960's, automobile manufacturers began studies to improve braking systems for road vehicles. They realized—as had the aircraft industry—that a locked wheel causes a loss of lateral stability. Chrysler began to convert their research on anti-skid braking into a production system in 1966;[1] the final product was marketed in 1971. Other manufacturers soon followed suit.

Safety has always been difficult to sell to a "style conscious" public. Why should anyone pay $200 extra for a device to keep his car from skidding? How can it protect the average driver? Is it fail-safe and always advantageous? These questions are still being debated as the public slowly becomes safety conscious.

Federal regulation

We are familiar with the federal government's involvement with automotive design when it imposed pollution standards on the internal combustion engine. There was some give and take, and the standards were postponed and even modified when lawmakers were confronted with realistic engineering problems. The net thrust of the standards remained intact, however; the designers worked and met the challenge, and the price of cars went up.

A similar situation now exists with FMVSS 121 (Federal Motor Vehicle Safety Standard No. 121), which became effective September 1, 1974. In essence, this standard requires all new trucks to remain within a certain width lane while undergoing panic or violent braking. FMVSS 121 does not require anti-lock devices, but its lateral and directional stability requirements imply their use. The object of the government edict was safety, but, again, postponements and modifications have changed FMVSS 121 from its original form and created new deadlines. As yet, no standard exists that requires similar braking restrictions on passenger vehicles. If one is issued, there will be a large market for anti-skid controllers, but cost considerations will otherwise keep the passenger-car market at a minimum.

Skid and slip

All anti-skid controllers anticipate wheel lock-up and momentarily release the brakes, then reapply them when the wheel speed recovers sufficiently. One manufacturer of anti-skid controllers makes a digital system,[2] while all the others use an analog computer with operational amplifiers and discrete components. The use of microprocessors may yield a significant advantage over these existing systems. Let us next examine what is meant by "skid" and exactly what an "anti-skid" system does.

A freely-rolling wheel permits maximum directional control of a vehicle. If the wheel becomes locked and skids, the vehicle loses ability to remain on course.[1] This occurs if the driver vigorously, or, in panic, applies the brakes. When a vehicle is making the transition to a stop, its kinetic energy must be expended somewhere. In a controlled stop, most of the kinetic energy is dissipated in the brake linings and drums as heat. Some is lost in the tire-road interface. However, if the brakes are locked, no energy is lost to the brakes and all the kinetic energy of the vehicle is lost in the tire-road system. Six such stops from 60 mi/h can wear out a new set of tires.[1]

Barely touching the brakes will produce a very slow stop and dissipate almost all the energy in the brake system. Between these extremes lies an optimum combination of short stopping distance and good lateral directional stability.

J. Tuska (left) and W. Lile examining electronic braking data in the RCA Laboratories test vehicle.

William R. Lile, LSI Systems Design, RCA Laboratories, Princeton, N.J., received the BS in Electrical Engineering in 1959 from Mississippi State University. He attended the University of Pennsylvania on the RCA Graduate Study Program and received the MSEE there in 1962. Mr. Lile has also completed additional graduate courses beyond the MSEE requirement and is a licensed Professional Engineer. After joining RCA's Electronic Data Processing Division in Camden, N.J., in 1959, Mr. Lile worked on logic design and worst-case analysis of advanced digital equipment. He was responsible for the electronics and test instrumentation in the superconducting memory effort. He has been a Project Engineer for LSI memory arrays and has published papers in this field. At present he is in the LSI Systems group, engaged in the application of integrated-circuit technology, including microprocessors, to automotive and other vehicle systems. Mr. Lile is a member of Tau Beta Pi and Eta Kappa Nu.

James Tuska's biography appears with his other paper in this issue.

Reprint RE-22-2-9
Final manuscript received April 25, 1976.

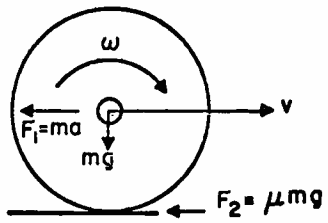

Fig. 1 — Simplified tire-road interface forces.

Fig. 1 illustrates the forces at the tire-road surface interface. The retarding force is $F_1 = ma$ where m is the vehicle mass and a is the deceleration. This is equal to the frictional force $F_2 = \mu mg$, where μ is the dimensionless coefficient of friction and g is the gravitational acceleration constant. The maximum deceleration of the vehicle is 32 ft/s^2, obtained when μ=1.

A free-rolling wheel in the vehicle system indicates the true vehicle speed and deceleration. Best stopping occurs, however, when the braked wheels actually slip. Slip is expressed as $S = (\omega_0 - \omega)/\omega_0$, where ω is the angular velocity of the braked wheel and ω_0 is the angular velocity of its free-rolling counterpart.[4] For example, if a vehicle were going 50 mi/h according to the free-rolling wheel and the braked wheel indicated only 40 mi/h, then 20% slip would exist.

Fig. 2 shows the relationship between the retarding (μ_1) and lateral (μ_2) characteristics as a function of wheel slip.[5] The lateral stability coefficient μ_2 is at a maximum at zero slip and zero at 100% slip. The retarding force characteristic μ_1 is at a maximum at about 20% slip on a normal road surface. Brake controllers then should strive to maintain this optimum slip. However, the problem is not simple, as the coefficient curves change with varying road surfaces. For example, an ice-covered road has its peak retarding force at about 10% slip.

A general indication of wheel lockup occurs at about 1.2 to 1.8 g's wheel deceleration, indicated by an angular velocity sensor on the wheel. This threshold is empirical, but since the vehicle cannot attain this deceleration rate, an indication greater than 1g implies incipient lockup.

Wheel angular velocity sensors

The devices that sense wheel rotation must be rugged, reliable and inexpensive; variable-reluctance sensors are the most common in use today. The pick-up coil assembly is mounted on the axle and a slotted disc or rotor is mounted on the wheel. The output is Hz/mi/h; a change in frequency indicates that an acceleration is taking place. These sensors have a lower speed limit of about 5 mi/h, due to the dependence of voltage output on speed, but are considered to be the most reliable component of the system.[4]

Computer

Wheel angular velocity information is supplied to a computer, which then decides if a lockup is imminent and issues a brake release signal if needed. Once the brake is released, the computer monitors the wheel sensor to determine when to reapply the brakes.

Brake pressure modulator

If the computer determines that the wheel is going to lock up, it issues a signal to a solenoid-actuated modulator, which closes the brake fluid line to that wheel. The modulator also provides an expansion chamber for the fluid on the wheel side of the valve, thereby reducing the pressure and diminishing the braking force.

Stopping the vehicle

Fig. 3 illustrates both the angular velocity of the brake-modulated wheel and the true vehicle speed as a function of time.

The slopes are indicative of both deceleration and acceleration. Fig. 4 depicts an ideal smooth stop, where there is precise control of the braked wheel's speed. Slip is monitored in this case, rather than acceleration or wheel speed. One commercial manufacturer[2] of truck anti-lock systems incorporates a longitudinally-oriented accelerometer as an additional sensor. The accelerometer output signal is integrated from the onset of braking to determine true vehicle speed. Knowing true vehicle speed and the braked wheel's angular velocity, slip can be controlled. In general, though, the cost of independent vehicle-true-speed measuring devices outweigh their advantages, so manufacturers do not incorporate them. Rather, the speed at the onset of lock-up is stored and further wheel angular velocities are compared with it until the next lock-up is recognized.

Looking again at Fig. 3, the slope of the braked wheel's angular velocity is related to the coefficient of friction μ of the tire-road interface. The small the μ, the faster lock-up can occur; the greater the μ, the faster recovery can occur. Also, the greater the μ, the faster the vehicle decelerates. Since μ varies with road conditions, using its instantaneous value rather than an assumed one would help determine brake release and reapplication times more accurately. Existing brake control systems, to the authors' knowledge, do not attempt to measure μ.

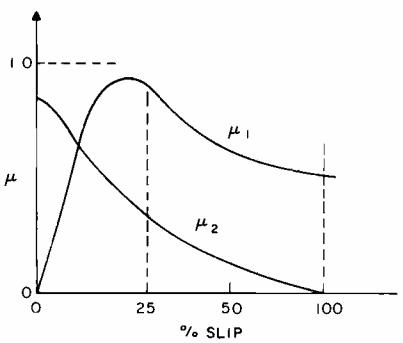

Fig. 2 — Retarding (μ_1) and lateral (μ_2) characteristics vs slip.

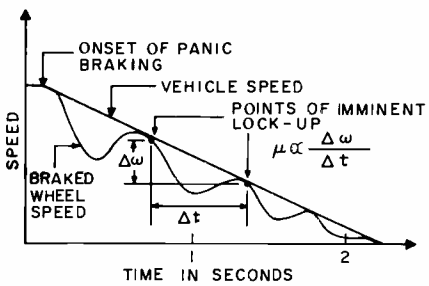

Fig. 3 — Vehicle's braked-wheel speed in a controlled system.

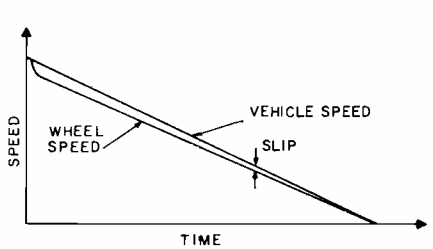

Fig. 4 — Nearly ideal stopping at optimum slip.

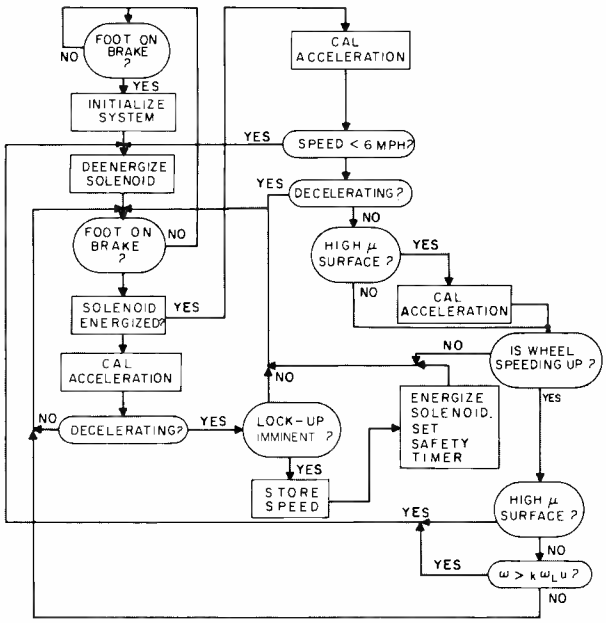

Fig. 5 — Electronic brake control algorithm.

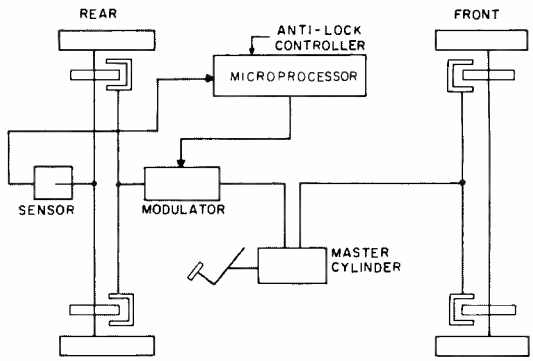

Fig. 6 — Two-wheel, rear-axle control, propellor-shaft sensor system.

Foot-on-the-brake flowchart

The flow diagram of Fig. 5 illustrates a basic algorithm that a digital microcomputer might use for controlling vehicle brakes. This algorithm assumes one sensor and one-wheel control. In practice this sensor could be a pinion (propeller) shaft sensor, and the brake line pressure modulator could be in common with both rear wheels.

An explanation of the flowchart can begin at the "foot on brake?" box. Once the system recognizes that the brakes are being applied, all registers are initialized, and the solenoid that releases brake pressure when activated is de-energized. The acceleration (deceleration) is calculated next ("cal acceleration" box). If it is great enough that there is a likelihood of the wheel's locking up, then the speed is stored as ω_f, the brake modulator relieves the pressure in the brake line by energizing the solenoid, and the safety timer is set. This timer automatically releases the brakes after a predetermined time if the microcomputer should fail.

The program then continues in a loop, calculating acceleration and vehicle speed. If the speed is greater than 6 mi/h, the program determines the point of positive acceleration (the wheel is now speeding up, as the brakes are off). If the road surface has a high μ, the wheel speeds up rapidly. To assure this is actually the case and not just a bounce, a second acceleration calculation is made. If the wheel is still speeding up, and the interface is a high-μ one and the solenoid is de-energized, the brakes are now reapplied. When the speed falls below 6 mi/h, the solenoid is de-energized and there are no further calculations until the next time the brakes are applied.

If the road-tire interface is slippery, the wheel will recover more slowly. If this is the case, the wheel speed must be monitored until it exceeds the release value ω_f. At this time the brakes are reapplied. If this low-μ determination were not made, the positive acceleration criteria (high-μ) might not allow the reapplication of the brakes, since recovery is slow on slippery surfaces.

The cycle is repeated as many times as necessary.

System configurations

Our experimentation has been confined to rear-wheel-only brake control. In our configuration, the average velocity of the wheels is sensed by a pinion shaft sensor, and a single modulator controls the brake pressure to the rear wheels. This is shown schematically in Fig. 6. Other system configurations have been proposed,[3] each with its own advantages, disadvantages and cost/benefit ratio.

Conclusions

Discrete-component analog controllers dominate the anti-skid brake market now, but the advantages of stored-program controllers are becoming evident. Their processing capabilities can handle multiple axles and sensors simultaneously, as well as take instantaneous variations in tire-road conditions into account. As tests proceed, we expect to further modify and enhance our basic algorithm, investigate effects of multi-wheel, multi-mu surfaces and demonstrate how a microprocessor can be used to better advantage in this application.

References

1. Douglas, J.W. and Schafer, F.C.; "The Chrysler 'Sure-Brake' — the first production four-wheel anti-skid system," SAE Paper 710248.
2. "FMVSS 121 — air brake systems: what it means to the truck builder," *Automotive Engineering* (Aug 1973) based on SAE Paper 730698.
3. "Anti-lock brake system configurations," *Automotive Engineering*, (Feb 1976) based on SAE Paper 760348.
4. Frait, J.S.; "Practical aspects of anti-lock braking," Kelsey-Hayes Research and Development Center, Ann Arbor, Mich.
5. "A review of anti-skid braking," *Automotive Engineering* (July 1975) based on SAE Papers 690213, 710248, 741083.

An electronic timing reference with improved accuracy

R. L. Pryor

A signal-to-noise ratio of 1:10 poses heavy problems for any system, but this analog/digital circuit conquers them and produces a timing reference that is the starting point for microcomputer-controlled spark advance.

THE LARGEST and most complex portions of the new automotive electronics are digital, but other portions, such as the timing subsystem described here, must begin with an analog front end. Early in the design process, it became clear that a single monolithic technology which could handle both analog and digital applications was needed, since the entire system must be packaged compactly and fabricated inexpensively. Moreover, the high packing density required, the high-noise environment, and the need to keep power supply regulation to an absolute minimum to reduce cost and complexity, made CMOS the prime digital technology to be considered. The next problem was how to solve the analog problems in a compatible way.

Analog subsystem

The subsystem described here is a signal processor for a mechanical timing reference with improved accuracy. This subsystem was designed to work in the same system with the B-12 computer.[1] Since the B-12 has a 12-bit computation accuracy, and all of the analog sensors in the system have at least 8-bit accuracy, it was desirable to have a mechanical timing reference with an accuracy of at least one part in 256. Conventional automotive ignition systems take their timing reference from the distributor head, which is chain-driven from the engine, but this chain is a potential source of backlash and inaccuracy. Improving the accuracy necessitates replacing the distributor-based reference with a magnetic pickup that senses slots on a flange rigidly attached to a wheel (the damper wheel, or fan-belt pulley) on the main engine shaft.

For an eight-cylinder engine, four of these timing reference slots are required. In such a timing system, a permanent bar magnet wound with a coil is used as a pickup. The slotted flange of the damper wheel is made of cast iron, which is both conductive and ferromagnetic. The resultant raw pickup signal is a bipolar voltage. Wiring and magnetic polarity are arranged such that the positive portion of the waveform precedes the negative.

The valuable property of the signal from the magnetic sensor is that its zero crossing, as the signal inverts from positive to negative voltage, coincides very accurately with the center of the mechanical slot, yet is independent of engine speed.

However, taking this raw signal and processing it inexpensively and reliably for all conditions of engine speed (from sluggish cranking speeds while starting in cold weather to maximum r/min) into digital reference pulses of fixed time duration presents a unique challenge in the field of analog signal processing. The digital reference pulse thus generated is used in a computer-controlled spark advance system.

New approach

Stated as simply as possible, the problem has difficult aspects because of the extreme variation of sensor voltage output – 200mV to 30V — throughout the wide engine-speed range over which the timing system must perform. This problem is as old as the use of magnetic sensors to determine the position of rotating mechanical parts. The voltage developed across the coil is variable because it is proportional to $d\phi/dt$, where $d\phi$ is the change in the magnetic flux encircling the coil wires. The approach of the gap in the wheel changes the shape of the magnetic lines of flux, weakening the magnetic field. The actual flux looping the wires of the coil is a function of the angular position of the slot with respect to the pole piece, and is independent of the wheel velocity. The voltage developed across the coil, however, is directly proportional to the velocity of the wheel, since the voltage is the time derivative of the flux. The result is the great difference in voltage output as the engine speed varies from start to maximum.

High-noise environment

It happens that there is a coherent noise source built into the system. Surface irregularities, imperfections in the material of the damper wheel, play in the bearing, etc., superimpose variations in flux upon those caused by the slot. These

Reprint RE-22-2-7
Final manuscript received April 12, 1976.

R. L. Pryor, Member, Engineering Staff, Advanced Technology Laboratories, Camden, N.J., received the BS in Physics from the Missouri School of Mines and Metallurgy in 1955. He joined RCA in 1955 and is presently working on design of computer subsystems (such as SOS read-only memory layouts) and new cell families for CMOS computer-aided large-scale-array technology (such as programmed logic array cells and analog amplifier cells), as well as radiation hardening techniques for SOS standard cell families. His experience at RCA has included design of analog computer circuits, industrial electronics (including adaptation of minicomputers to industrial applications), experimental memory systems, and production test equipment for LSI chips and hybrid subsystems. Mr. Pryor holds nine patents and is co-author of three papers.

flux variations are also differentiated to produce a voltage that has the same velocity dependence as the desired signal. The system specifications state that the noise at any given engine speed should be less than 7 per cent of the signal. If the speed were constant, or if the output voltage were independent of speed, this would be a very good signal-to-noise ratio indeed. However, since the signal varies from 200mV to 30V over the speed range through which the system must function, this means that the noise varies from 14mV to 2100mV. Therefore, the noise at high speed is more than 10 times the signal at low speed, a signal-to-noise ratio of less than 1:10.

Earlier attempts to solve this problem revolved around automatic gain control servo loops, but these servomechanisms inherently possess limited response speeds. This disadvantage is especially noticeable when the engine is being cranked by the starter, since an enormous acceleration takes place when the first cylinder fires. Moreover, the magnitude of the acceleration due to this first firing is random and unpredictable. Since the acceleration is caused by an explosion, the velocity of the engine can be represented as a step function, where the height of the first step can vary randomly from zero to a very large velocity increment. At this critical time there is no way that an AGC servo loop can react quickly enough to prevent noise from coming through to cause false triggering. What would literally be demanded of the servo loop is some kind of precognition that a cylinder was about to fire. An AGC can react only after the next bipolar signal comes in, and is found to be too high in amplitude, but the attendant high noise can frequently cause one or more false signals first. It is true that this defect does not affect engine performance once the engine is running smoothly, but it does affect how easily the engine can start on cold days.

Integrating out the voltage variation

Since the voltage from the magnetic sensor varies because the flux, which is a speed-independent representation of the surface of the wheel, has been differentiated, integrating the raw bipolar analog voltage will then remove the voltage variation. The noise, being coherent with the signal, is also restored to speed independence by this processing. Thus, an instantaneous increase in engine speed has no effect at all on either signal or noise amplitude. The signal-to-noise ratio remains a constant 14:1 over the entire speed range.

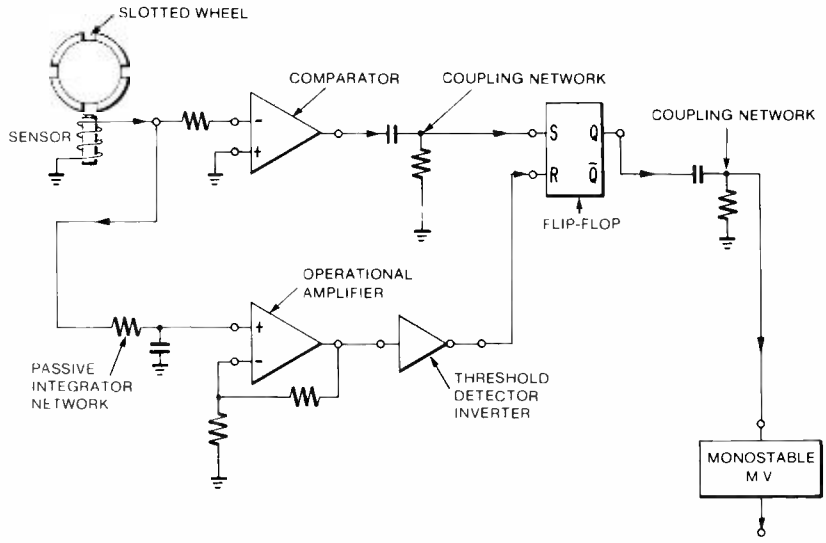

Fig. 1 — Zero-crossover detector system.

Since the reference point to be detected is at the zero crossing of the raw (speed-dependent) voltage waveform directly from the sensor, this signal can be fed into a comparator that is operated open-loop. However, there is a problem in removing the noise from this comparator channel. The signal is greater than the noise at all times when the slot is near the pole piece, but at other times the noise predominates and will cause sporadic reversals of the comparator output. A separate integrator channel can be used to detect the proximity of the pole piece, and the noise can be gated out by means of this channel. The output of the integrator channel repeats the same voltage sequence for every cycle of the wheel. The slot appears as a positive "mesa" voltage well above the noise level. In the output of this channel, both the slot "mesa" voltage and the noise voltage are independent of the velocity of the engine. A voltage analog of the magnetic flux has been restored by integration.

System operation

Fig. 1 shows the system that uses these principles to eliminate the noise, and Fig. 2 gives its operating waveforms. The comparator channel runs wide-open and sets a flip-flop on the positive-to-negative zero-crossing of the bipolar signal. The reset input to the flip-flop is controlled by the integrator channel output, after passing it through a threshold detector set to discriminate between the slot and the noise. Then it is inverted. This flip-flop has the characteristic that a high reset input overrides the set input. Since the reset input remains high during all of the time that the comparator channel is prone to noise, the flip-flop can never be set by anything other than a legitimate zero-crossing. It is then reset again at the end of the "mesa" from the integrator channel. The flip-flop output is subsequently standardized in width by allowing its leading edge to trigger a one-shot.

Hardware implementations

The two operational amplifiers shown in Fig. 1 can be identical. The open-loop gain needed is 2000 to 3000 or greater, with a bandwidth of about 100 kHz at maximum gain. The comparator is the only channel where bandwidth becomes critical, and then only at high engine speed, when there is a lot of overdrive at the input due to the velocity dependence of the bipolr signal. An all-CMOS differential operational amplifier was first tried in the application. It was found to be adequate for the application, although there was some question about input drift over the lifetime of the device. (To keep the offset drift from adversely affecting the signal-to-noise ratio, it is

necessary to keep the offset at the input less than 5mV.)

The CA3129 differential bipolar amplifier was tried as a direct replacement in the same breadboard and performed equally well in both the integrator and comparator channels. Here offset drift was less of a problem. Both amplifiers were able to perform over the required supply voltage range, 11V to 5V.

It was desirable to keep the input impedance to the comparator channel high, to avoid loading the sensor. As a matter of fact, a 150-kilohm resistor was put in series with it to prevent distortion at high speeds when the amplifier is overdriven. This impedance level did not prove to be a problem either for the bipolar amplifier or the MOS amplifier.

Because of the offset voltage problem at the input to the integrator channel, and because the integrator itself is a passive network, the breakpoint of the integrator had to be set rather carefully. Setting it too high in frequency would attenuate the input to the operational amplifier to the point where offset drift could seriously cut into the signal-to-noise ratio. On the other hand, setting the breakpoint at too low a frequency would mean imperfect integration at frequencies of interest for the low engine speed range, tending to reintroduce the undesired frequency dependence in the output of the integrator channel. The actual breakpoint was set at about 7 Hz, whereas the lowest signal frequency of interest was about 10 Hz.

Specification sidelight

The history of how the proper integrator breakpoint and consequent gain for the integrator channel were determined provides an interesting sidelight. While the problem was being tackled in the laboratory at RCA, we were relying on the specifications furnished by the sensor manufacturer for the duration of the bipolar signal. These specifications related the positive and negative voltage peaks to angular degrees of the wheel carrying the slots. After the entire spark reference system was designed in the laboratory on the basis of these specifications and shipped to Detroit, we were informed that the system was not performing properly when installed on an automobile. This difficulty necessitated a trip to Detroit, where it was discovered that the sensor manufacturer's specifications were off by a factor of three to one in relating angular degrees of the wheel to positive and negative voltage peaks. The actual peaks were spread over an angle three times larger than specified, resulting in an integrated pulse width three times greater than expected. This meant that both the breakpoint of the passive integrator network and the gain of that channel's operational amplifier had to be radically altered. After these changes had been made (and the reasons for them understood) it was very gratifying to see the strip plotter producing perfect spark reference records as the automobile engine was being started.

One interesting thing about this gross inaccuracy in the specification is that it had no effect at all on the performance of the earlier systems, which had relied on AGC, rather than signal integration, to gate out the noise. The portions of the sensor specifications dealing with signal amplitude and amplitude-speed dependence had been accurate, and these were the only parameters affecting the earlier systems. This, of course, does not mean that a system sensitive to the angular relationship of the slot and the sensor is less reliable or adds to the expense of the sensor needed; it merely illustrates how changing the approach to an engineering problem may upgrade the importance of certain component specifications previously neglected as unimportant.

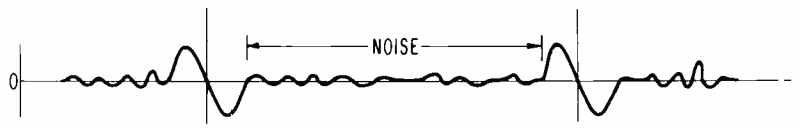

Fig. 2a — Raw signal from magnetic pickup.

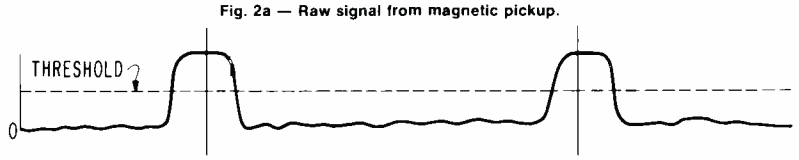

Fig. 2b — Constant-amplitude integrated signal.

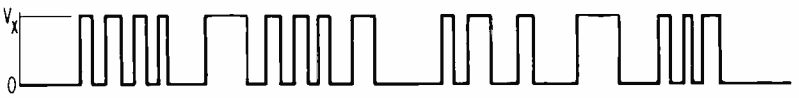

Fig. 2c — Comparator output.

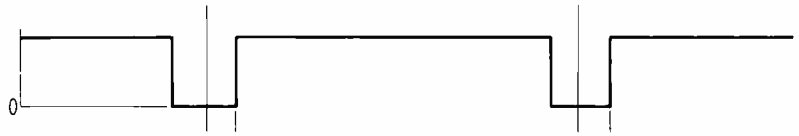

Fig. 2d — Inverted and saturated integrator output.

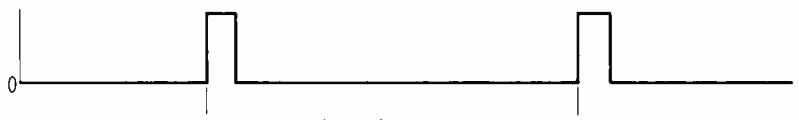

Fig. 2e — Flip-flop output.

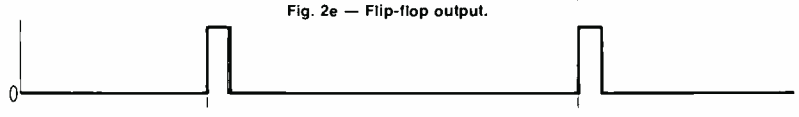

Fig. 2f — One-shot output.

Conclusions

Although there were some secondary problems caused by waveform distortions from the sensor when the engine reached higher speeds, integrating the raw signal to gate out the noise definitely seemed to improve performance right at the instant of engine start, relieve the sensor pole piece's gap-adjustment tolerance, and relieve the amplifier performance specifications to the point where a monolithic analog and digital solution became feasible.

The final decision regarding the CMOS operational amplifier versus the bipolar operational amplifier will be greatly affected by the economics of mass production, where the volume permits a completely new custom design.

References

1. Ozga, S.: "The B-12—an automotive microcomputer," this issue.

Short course in DIGITAL ELECTRONICS—

Concepts and sampling theory

Dr. L. Shapiro

This is the first in a series of tutorial articles on digital signal processing— a subject that is currently of major importance to designers of electronic equipment and systems. The entire series will focus on design and applications so that, insofar as practicable, these articles may have value as a reference source for the practicing engineer. This introductory article explores the conversion of analog signals to digital and examines bandwidth considerations pertinent to the successful transmission of digital signals. Succeeding articles will probe more deeply into bandwidth and power expenditures from the standpoint of information theory and deal in some depth with digital filters, spectral analysis, and complete digital systems.

WE ARE witnessing a revolution in the handling of information which is as fundamental and sweeping as the conversion from vacuum tubes to solid-state components. There is reason to believe that the trend toward processing information in digital form will soon extend into most major areas of electronic-signal processing.

Why digital signal processing?

A question that naturally arises is—Why do we need digital signal processing? Why should there be such a major transition from the analog to the digital field, particularly at this time? If we wished to be brief we could say that by placing information in digital form we act to preserve its accuracy, increase its immunity to noise, and make it much more independent of circuit tolerances and instabilities. However, it may be of interest to take a closer look.

Freedom from time constraints

Delay and storage of information in digital form represent no problem. The transmission or reproduction of information can be speeded up or slowed down, stored and retrieved at different speeds, played backwards if desired, and converted back and forth from digital to analog form at will. As compared to information in analog form, these advantages represent a major breakthrough.

Accuracy

In its usual quantized form, in which the pulse amplitudes are limited to one of a prescribed number of discrete amplitudes, the signal information is preserved as long as incoming noise does not cause the signal to enter another amplitude level. Hence we can sense the signal at various points along its transmission path and regenerate a clean noise-free signal as often as required. In this manner we can insure ultimate reception of an essentially accurate, noise-free signal.

Reliability

Information in digital form is basically much more immune to component and circuit instabilities. This is particularly the case with binary signals where only the presence or absence of a pulse needs to be determined. This type of "yes/no" circuitry can operate reliably under conditions that would substantially deteriorate an analog signal, such as power supply fluctuations, thermal effects, component aging, etc.

Compatibility with digital computer

Digital information, by its nature, is in a form suitable for processing by digital computer. This brings into play the immense precision and resourcefulness of digital computation. In effect, we have replaced analog hardware with computer software. Such software can be modified at will, instantly, if necessary, even during the processing operation itself.

New vistas in computation

Presently available software for digital computation has now made it convenient (utilizing Fourier methods*) to convert information back and forth between time and frequency domains. We have the choice of processing material in either domain since, in either case, we simply have a series of numbers. Insofar as the digital computer is concerned, it perceives

*See Appendix

Reprint RE-22-2-20
Final manuscript received May 11, 1976.

Reviewer's comment: After reading this article, I feel that some additional introduction is needed to underscore the importance of this subject. To my recollection, public attention was first focused on digital processing when the Jet Propulsion Laboratories used computer enhancement on pictures of the moon's surface taken by the unmanned probes. The enhanced pictures, broadcast on network television, showed a dramatic improvement over the originals. Of course, behind the scenes and not receiving much public notice were the years of work which had gone into the digital computer, the algorithms, and the programs to achieve this.

Research work had started earlier towards the implementation of digital filters for seismology and geophysical work which can be done in non-real time. However, implementing the real-time hardware needed for sonar, radar, and speech signal processing was limited by speed, size, and cost. The breakthrough was a combination of a new Fourier transform algorithm, known as the Fast Fourier Transform; large scale integration (high speed); and imaginative systems and hardware designers. Real-time signal processing was born and its effects were almost immediately felt in almost all disciplines—including biomedical engineering, seismology, nuclear science, data communications, radar, and sonar.

I hope this series of articles on digital signal processing will aid those not familiar with the field in obtaining a basic understanding of the processes, its present applications, and its future potential in their own work.

Dudley M. Cottler, Staff Technical Advisor,
Government and Commercial Systems, Moorestown, N.J.

no difference and performs equally well with signal information in either domain.

Methods to facilitate the above transformations have been refined, particularly the z transform.** Theoretical understanding of these manipulations has advanced on a broad front. As an additional consideration, ingenious coding systems have been developed in which errors may be sensed and automatically corrected.

With the tremendous capabilities of the digital computer at our command, it becomes possible and convenient to extract desired signal components from complex signals so that particular objectives, such as pattern recognition, may be achieved.

Hardware and software availability

Digital-signal-processing hardware and software are now available for highly complex requirements. Their development has been greatly facilitated by the fact that basic building blocks (e.g., the multivibrator and its principal variations) are similar throughout these applications. Hence, there has been an enhanced freedom on the part of imaginative individuals (engineers) to create fanciful configurations as the need for them has arisen.

The development of these circuits has gone hand-in-hand with the continued size and cost reduction of high-speed circuitry, particularly where IC's have been involved.

New approaches to old problems

The advancing art of digital signal processing has now made it possible, for example, to obtain practically any desired frequency from a single highly stabilized master oscillator. Such capabilities are important in applications ranging from sophisticated military systems to home television receivers.

Another important application has been the development of simulation methods to explore the behavior of equipments still in the design stage. In this way it has become feasible and convenient to predict the performance of complex systems before an investment in hardware and fabrication has been made. Computational techniques, for example, have

**To be treated in a subsequent article.

Dr. Louis Shapiro, Engineering Education, Corporate Engineering, Cherry Hill, N.J., received the BS in physics-math from the City College of New York, the MS in physics-math from Washington University, St. Louis, the PhD in physics from Temple University, and has completed coursework in circuit-theory, feedback, servomechanisms, and solid-state electronics at the Moore School of Electrical Engineering. His 14 years of direct engineering experience include employment as a microwave engineer with the Polytechnic Research and Development Company, Brooklyn, and eight years with RCA as project engineer in color correction and as senior design engineer with the RCA electron microscope activity. Dr. Shapiro holds 18 patents of which nine are assigned to RCA. Ten years of full-time faculty experience include employment at the University of Missouri, St Joseph's College, Philadelphia, and the William Paterson College of New Jersey where he served as department head of Physics and Earth Sciences. Dr. Shapiro is presently on the graduate faculty of the Center of Engineering of Widener College, Chester, Pa. He has been associated with the RCA Engineering Education activity both as staff member and consultant since 1966 and has videotaped many of their courses. He is a member of the American Institute of Physics, IEEE, AAAS, Phi Beta Kappa, N.J. Academy of Sciences, and the American Society for Engineering Education.

Glossary

Aliasing: A phenomenon arising as a result of the sampling process in which high frequency components of the original analog signal (whether information or noise) appear as lower frequencies in the sampled signal. Aliasing occurs when the sampling rate is less than twice the highest frequency existing in the original analog signal.

Analog/digital converter: A circuit which samples an analog signal at specified periods of time to produce a discrete signal which is then quantized.

Analog signal: A signal that is continuous in both time and amplitude.

Binary signal: A digital signal with only two available amplitudes or levels, variously called on/off, one/zero, or high/low. A binary signal may be "positive" in the sense that the "one" level may be a positive voltage, or it may be "negative" in the sense that the "one" level may be a negative voltage. In either case the "zero" level is ground. A binary signal may also be "bipolar", in which case the "one" is usually a positive voltage while the "zero" is a negative voltage of the same amplitude.

Continuous amplitude signal: A signal that is able to assume any amplitude value, usually between certain prescribed limits.

Continuous time signal: A signal that is defined for all values of time, usually between certain prescribed limits.

Digital signal: A discrete signal in which the available amplitude values constitute a discrete series, each member of which can be represented by a number having a finite number of digits. The terms digital and discrete are sometimes loosely used interchangeably.

Delta function (*Dirac delta function*): A function defined by the following relationships:

$$\delta(t) = \begin{cases} 0 & , \text{ for } t \neq 0 \\ \text{arbitrarily large}, & \text{for } t = 0 \end{cases}$$

$$\int_{-\infty}^{\infty} \delta(t)\, dt = 1.0$$

As a consequence,

$$\int_{-\infty}^{\infty} f(t)\, \delta(t)\, dt = f(0)$$

The delta function is also called the impulse function.

Digital/analog converter: A circuit which transforms a digital signal into an analog signal, usually by some type of filtering action.

Discrete signal: A signal defined only at a particular set of time values. Between these values the amplitude may be zero or have an amplitude of no additional information value.

Fourier methods: See Appendix

Frequency domain: A graphical way of representing signals in which the horizontal axis is calibrated in units of frequency. Alternatively it may be applied to a mathematical representation of signals in which the variable is in units of frequency.

Impulse function: See delta function.

Linear system: One in which the behavior of the system is not dependent upon the amplitude of the input signal, or upon the simultaneous presence of other signals.

Quantization: The process of constraining the values of a signal, whether continuous or discrete, to assume one or another of a discrete set of values. By quantizing a discrete signal we obtain a digital signal.

Time domain: A graphical way of representing signals in which the horizontal axis is calibrated in units of time; alternatively, it may be applied to a mathematical representation of signals in which the variable is in units of time.

Z-transform: A modification of the Fourier transform for use with digital signals in which the Laplace variable s is replaced by $z = e^{sT}$. The meaning and utilization of this transform will be developed in a future article of this series.

allowed designs to be optimized, variously, for performance, cost, noise immunity, size, number of components, etc. In fact, optimization can be performed for almost any relevant design parameter.

The use of digital techniques has found important applications in key areas such as communications. The overriding requirement for maintenance of accuracy of information over both long and short hauls has, in a number of instances, resulted in the conversion of audio and video information to digital form. Thus, NBC recently converted its video programs to digital form in the local routing of these programs (at the New York studio) for switching purposes.*

It is interesting to note that much work is presently being done in applying digital control techniques to the functioning of passenger automobiles so that ignition, carburetion, and other operating functions may be continuously optimized.

Additional applications of digital-signal-processing techniques occur in such diverse fields as speech research, biomedical engineering, and seismology.

Development and transmission of digital signals

In this section we will examine the generation of a digital signal from its original analog form. This will involve sampling of the signal at given discrete moments separated by a (usually constant) sampling interval. We will then investigate the effect of transmitting these samples through a channel of given bandwidth. The objective will be to determine the minimum bandwidth needed to preserve the accuracy of this digital information.

Sampling theory

It is critically important at the outset to define and delimit the bandwidth occupied by the input analog signal. This follows from the fact that the sampling process introduces additional frequencies which, after demodulation, may find their way back into the spectral region occupied by the original information. This phenomenon is called "aliasing." We therefore speak about a "band-limited" analog signal as being the proper input to a digital system. In practice, it is customary to insure the band-limited condition by the insertion of a filter into the analog path before digital processing commences.

Theoretical investigation of the sampling rate required to reproduce, with complete accuracy, all of the information present in a bandlimited analog signal has resulted in the requirement that the sampling frequency f_s must be at least twice the analog bandwith B:

$$f_s \geq 2B. \qquad (1)$$

Although the usual mathematical developments treat the above relationship as an equality, it is worthy of note that, in actual practice, the inequality sign is normally operative. The reasons for this are twofold: namely, the equality sign would require the use of an ideal filter for demodulation (ideal filters are physically unrealizable and, hence, represent a procurement problem) and, in addition, in certain applications there seems to be a real advantage in noise reduction with an increased sampling rate. For our present purposes, we will remain uncommitted to the equality of Eq. 1.

The sampling process is normally accomplished by means of an analog/digital converter. In its simplest form, we may imagine that we take a quick, almost instantaneous, look at the signal at certain prescribed moments separated by a given sampling interval T. The situation is as shown in Fig. 1, where the analog signal is identified as $f(t)$ and the sampled signal as $f^*(t)$.

It is convenient to make use of the delta function $\delta(t)$ as a sampling operator. The delta function may be defined by the following two properties:

1) it has a nonzero value only when its argument is zero, at which time its amplitude becomes arbitrarily large;
2) its integral over all of time is unity, e.g.:

$$\int_{-\infty}^{\infty} \delta(t)\, dt = 1.0$$

Thus, if we write:

$$f^*(t) = f(t) \sum_{n=0}^{\infty} \delta(t - nT) \qquad (2)$$

where we are considering positive time only, we note that $\delta(t - nT)$ operates to allow a quick look at the value of the analog function $f(t)$ whenever the argument $(t - nT)$ becomes zero. This occurs when t assumes integer multiple values of T. Between these moments, the value of $\delta(t - nT)$ is zero causing the right-hand side of Eq. 2 to vanish. Hence, the final result of the operation indicated by Eq. 2, is the series of samples shown in Fig. 1b. In the use of $\delta(t)$, as in Eq. 2, it is assumed that, at the sampling instants, we are multiplying $f(t)$ by the "strength" of the delta function, which is taken to be unity.

For analytical purposes, we sometimes use the delta pulse, itself, as the input to a system. In such a case we call the input an "impulse" and refer to subsequent system events as the "impulse response." This "impulse response" is an extremely useful way of describing the operation of a system.

Attainment of our "instant look" samples is, of course, physically impossible since (voltage or current) samples must necessarily have finite widths. The normal output from the A/D converter is therefore a series of flat-topped samples of width τ as shown in Fig. 2.

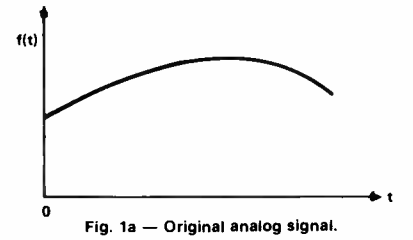

Fig. 1a — Original analog signal.

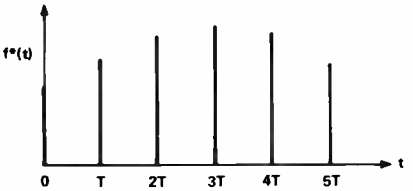

Fig. 1b — Sampled analog signal.

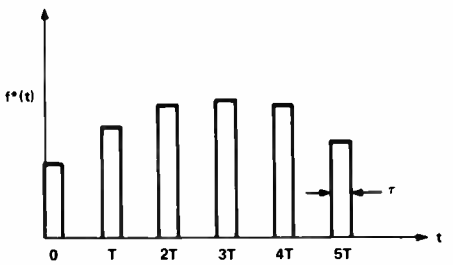

Fig. 2 — Series of flat-topped sample pulses.

For various purposes it is convenient, and even necessary, for these pulses to be quite narrow, at least as compared to the sampling interval T. However, for the

*See *RCA Engineer*, Vol. 21 (Apr - May 1976).

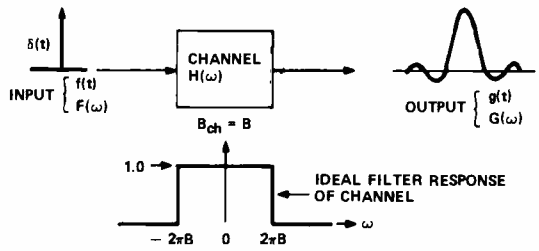

Fig. 3 — Example of digital transmission system.

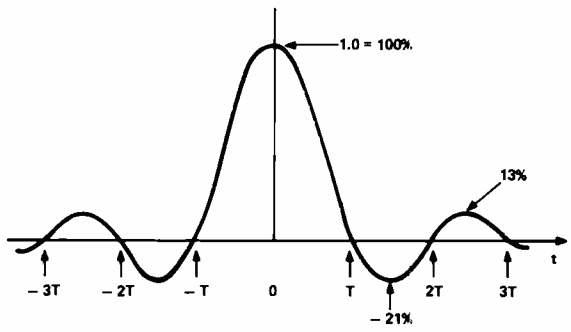

Fig. 4 — Output waveshape from ideal filter with impulse input.

demodulation process, there is a bit of a problem since these narrow samples necessarily carry very little power. It then becomes desirable to increase their power content by "holding circuits," which stretch the pulsewidth τ to the full sampling interval T.

The transmission of sampled data

We may visualize our system as shown in Fig. 3 where we have shown a $\delta(t)$ impulse input. For the present we will assume that our transmission channel has a bandwidth $B_{ch} = B$ (the bandwidth of the original input information) and a frequency response corresponding to that of the ideal filter also shown in Fig. 3. The output of the transmission channel is $g(t)$.

In order to obtain the frequency content of $g(t)$ it is necessary to obtain its Fourier transform. This transform is defined in the usual way as:

$$G(\omega) = \int_{-\infty}^{\infty} g(t)e^{-j\omega t}\,dt$$

where $G(\omega)$ is now a function specifying the frequency distribution of $g(t)$. If Fourier transforms are taken of input and output signals, we obtain the simple relationship:

$$G(\omega) = H(\omega)F(\omega)$$

where $H(\omega)$ represents an operation (transfer function) performed by the transmission channel on the input signal to produce the output signal.

With an input signal $f(t) = \delta(t)$, the Fourier transform of the input, $F(\omega)$, becomes

$$F(\omega) = \int_{-\infty}^{\infty} \delta(t)e^{-j\omega t}dt$$

Since the integrand is non-vanishing only at $t = 0$, the exponential factor becomes unity and we can write

$$F(\omega) = \int_{-\infty}^{\infty} \delta(t)dt = 1.0$$

where we have used the defining property of the delta function to obtain our final result. It then follows that

$$G(\omega) = H(\omega)F(\omega) = H(\omega)$$

We obtain the shape of our output pulse by taking the inverse transform of $G(\omega)$, which is defined as:

$$g(t) = (1/2\pi) \int_{-\infty}^{\infty} G(\omega)e^{j\omega t}d\omega$$

From the shape of our ideal filter of Fig. 3 we can write

$$g(t) = (1/2\pi) \int_{-2\pi B}^{2\pi B} (1.0)\, e^{j\omega t}d\omega$$

which evaluates to

$$g(t) = 2B\,\frac{\sin 2\pi Bt}{2\pi Bt}$$

The last result is obtained by expanding the exponential factor and discarding the sine term since it is an odd function being evaluated between equal positive and negative limits.

The shape of our final pulse is shown in Fig. 4. It is evident that the amplitude passes through zero at neighboring sampling points, but that significant under- and overshoots exist between these sampling points. A small time displacement would therefore result in substantial spurious amplitudes at these sampling moments. However, under favorable conditions, we may obtain an output pulse that is usable, that goes through zero at adjacent sampling intervals, and hence does avoid interference between adjacent samples.

If we deal with real-life input samples having finite width, however, we find that our output samples also increase in width and intersymbol interference does occur. The details of the moderately involved mathematics will not be reproduced here, but the final shape of our output pulse is:*

$$g(t) = (AV/\pi)\,\{\mathrm{Si}\,[2\pi B_{ch}(t - t_o + \tau/2)] - \mathrm{Si}[2\pi B_{ch}(t - t_o - \tau/2)]\}$$

where A and V correspond to the low-frequency bandpass gain and pulse height, respectively, and t_o corresponds to the pulse delay due to the phase characteristic of the transmission channel. It can be shown that if we make use of the relationship $2B = f_s = 1/T$ we obtain, at the adjacent sampling intervals $t = \pm T$, a value of $g(t)$ that vanishes only when the pulsewidth τ goes to zero.

Things are really not quite so bad, however, and a fairly modest decrease in pulsewidth can put us back into business. Relative percentages of the amplitude of our sample pulse $g(0)$ appearing at the adjacent sampling points $g(\pm T)$ are shown in Table I for various pulsewidths. It is noted that a pulsewidth of $\tau = 0.3T$, for example, produces a spurious amplitude of only 0.29%.

Table I — Relative percentages of sample pulse at adjacent sampling points for various pulsewidths.

τ	% of $g(0)$ present at $t = \pm T$
1 × T	9.3
0.5 × T	1.2
0.3 × T	0.29
0.2 × T	0.073

The raised-cosine channel response

There are certain remaining serious problems with our communications system of Fig. 4, however. For one thing, real transmission channels do not have the response of the ideal filter shown in this figure. In fact, the ideal filter response is unattainable with filters having a finite number of components. In addition, as

*This formula makes use of the so-called "sine integral," which is defined as

$$\mathrm{Si}(x) = \int_0^x (\sin t/t)\,dt;$$

see *Handbook of Mathematical Functions*, Nat. Bur. Standards (1964) for tables.

indicated above, the shape of the output pulse is such that an appreciable time shift will result in spurious sampling information. Some time shift (or jitter) is always present and must be allowed for in design margins. More serious, perhaps, is the requirement that synchronization of sample pulses with the original sampling instants, especially at the demodulation stage, precludes the use of modulation methods in which the timing of the sample pulse varies, such as in pulse position and pulse duration modulation. A final factor to be considered is that the substantial undershoots and overshoots of the sin x/x type of pulse may somehow add to adjacent sample pulses and produce amplitudes that might exceed channel linearity limits.

As a result of the above problems, it was found desirable to develop a model in which the frequency characteristics of the channel would more nearly resemble those of the real world and also which would produce an output $g(t)$ with reduced undershoots and overshoots—while yet passing through zero at adjacent sampling points. A solution acceptable in most cases was found in the so-called "raised-cosine" response of Fig. 5. The

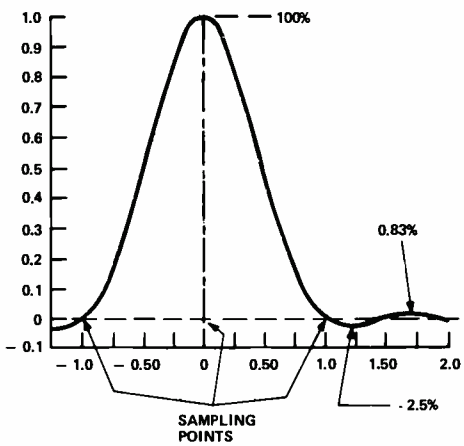

Fig. 5a — Characteristics of channel with raised-cosine impulse response.

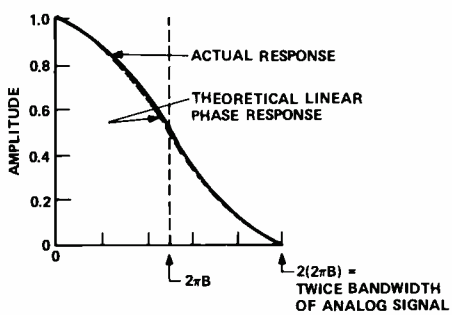

Fig. 5b — Characteristics of channel with raised-cosine frequency response.

frequency response required of the transmission channel is now double that of the original analog signal ($B_{ch} = 2B$), but the undershoots and overshoots have been drastically reduced in amplitude. Also, the movement of the pulse amplitude through adjacent sampling points is much gentler. The raised-cosine response closely approaches the actual response of many transmission channels and, very fortunately, also has a very nearly linear phase response. This latter characteristic is essential for the preservation of waveshapes in their passage through the transmission channel. The impulse response and frequency-domain formulas for the raised-cosine transfer function are:

$$g(t) = 2B \frac{\sin 4\pi Bt}{4\pi Bt[1 - (4BT)^2]}$$

$$G(\omega) = \cos^2(\omega/8B).$$

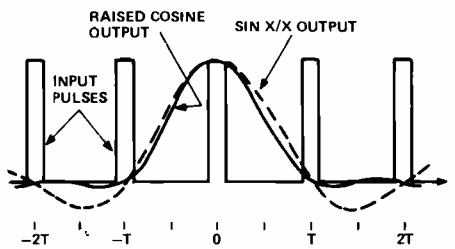

Fig. 6 — Comparison of output of a channel with an ideal filter characteristic with that of a channel with a raised-cosine characteristic.

A comparison of the output of a raised-cosine-type transmission channel with that of an ideal filter-type response is shown in Fig. 6 where the input consists of a series of flat-topped pulses. As before, adjacent samples are located at points where the waveshape passes through zero. However, there is now more room for time displacement and, certainly, much less undershoot and overshoot.

From a theoretical standpoint, the raised-cosine response gives the minimum possible spurious ripple while maintaining zero amplitude at adjacent sampling points for impulse-type inputs. In practice this response can also be used for systems without exactly prescribed pulse positions, such as in pulse position modulation (PPM) and pulse duration modulation (PDM). In some instances it can also be used for detection without exact synchronization.

Types of modulation

The principal types of pulse modulation are shown in Fig. 7. Pulse amplitude

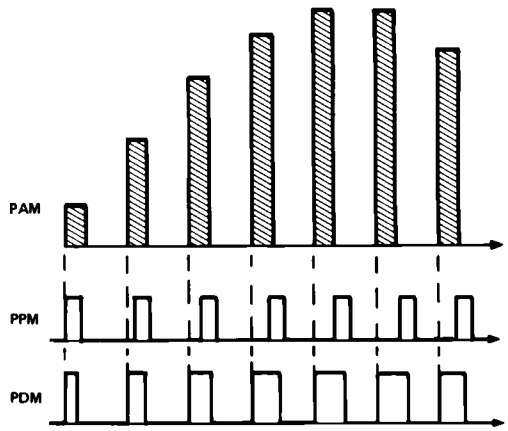

Fig. 7 — Principal types of pulse modulation.

modulation (PAM) corresponds to the initial sampled form of an amplitude-modulated signal. PPM utilizes the position of the pulse (in relation to a fixed point of reference) to represent the information, while PDM utilizes the width of the pulse to represent the information. Each of these types is widely used but does not, however, represent the more favored type of modulation, which is PCM (pulse code modulation).

Before proceeding to PCM, it is necessary to quantize the signal. By this we mean requiring that the various sample amplitudes be constrained to a specific set of values, usually, but not always, equally spaced.* This is shown in Fig. 8 where the

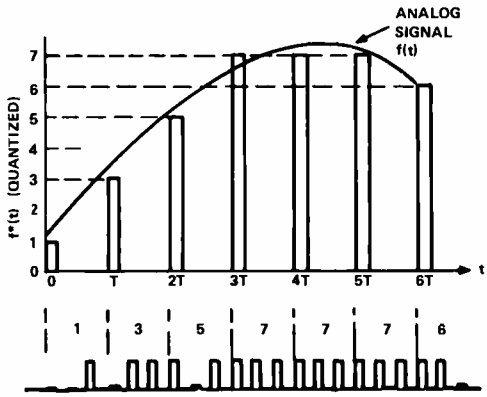

Fig. 8 — Quantized samples and their representation in a pulse-code-modulation scheme.

available sample amplitudes do not exactly correspond to the actual amplitude of the original analog signal at sampling moments. Rather, the sample amplitudes are required to assume the value of the nearest available level. Our samples may

*It is often advantageous to resort to nonlinear signal compression prior to quantization followed by a corresponding signal expansion after reception in order to equalize signal-noise ratios for low and high signal levels. The process is called "companding," and will be treated in a subsequent article.

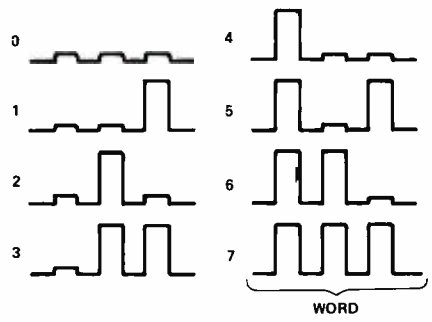

Fig. 9 — Binary counting scheme.

now be represented by a series of numbers, each being an integer as shown in Fig. 8. Fig. 8 also shows a possible binary counting scheme for representation of these numbers. The method is tabulated in Fig. 9 where each group of three pulses (or combination of pulses and nonpulses) is called a "word."

The advantages of binary pulse code modulation are quite important. For one thing, in accordance with the scheme of Fig. 9, only the presence or absence of a pulse is needed to establish the value of the number involved. Thus, once the presence or absence of the pulse has been established (by suitable circuitry), the signal may be regenerated for a fresh start against noise. The circuitry involved is entirely digital with corresponding advantages in simplicity and commercial availability. As a final note, PCM lends itself to coding schemes, which include error detection and correction.

Use of the switching function

The sampling process may advantageously be represented by a switching function $S(t)$, e.g.:

$$f^*(t) = f(t)\ S(t). \qquad (3)$$

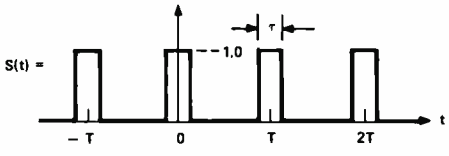

Fig. 10 — Switching function.

The switching function is shown in Fig. 10. The operation is very much like that of our previous delta function of Eq. 2. $S(t)$ multiplies our original analog function $f(t)$ by unity during the actual sampling moments and then returns to zero between such moments. The sampling pulses now, however, have a finite width of value τ. The switching function may usefully be expanded in the following Fourier series:

$$S(t) = (\tau/T) + \frac{2\tau}{T} \sum_{\substack{n=-\infty \\ (n\neq 0)}}^{\infty} \frac{\sin \omega_n \tau/2}{\omega_n \tau/2} \cos \omega_n t$$

where:

$$\omega_n = 2\pi n f_s = 2\pi n/T.$$

Upon taking the Fourier transform of Eq. 3, above, we obtain, with some manipulation:

$$F^*(\omega) = (\tau/T)\ F(\omega) + \frac{\tau}{T} \sum_{\substack{n=-\infty \\ (n\neq 0)}}^{\infty} \frac{\sin n\pi\tau/T}{n\pi\tau/T} F(\omega - n\omega_s) \qquad (4)$$

where $\omega_s = 2\pi f_s$ = radial sampling frequency.

This equation represents the complete spectrum of the sampled signal. Examination of Eq. 4 shows that the first term is simply the Fourier transform of our original unsampled analog signal. This corresponds to the spectral distribution centered at $\omega = 0$ appearing in Fig. 11. The additional terms (under the summation sign) represent the remaining spectral distributions, which appear on either side of the origin.

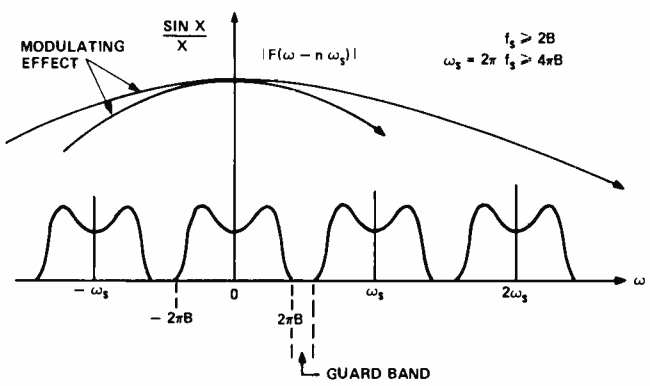

Fig. 11 — Spectrum of sampled signal showing origin of aperture effect and guard band.

The spectral distributions under the summation sign are multiplied by a factor of the form $\sin x/x$. (The first term is also multiplied by such a coefficient. Note that when $\omega = 0$, $\sin x/x$ becomes unity.) The situation is illustrated in Fig. 11 in which two possible forms of the $\sin x/x$ multiplying coefficient appear as curved lines above the spectral distributions. In either case, the effect is to favor the lower frequencies in the various spectral distributions at the expense of the higher frequencies. The final result is to distort the waveshape of the pulse in the time domain. This phenomenon is known as the aperture effect. The effect disappears as the pulsewidth τ goes to zero. This procedure, however, would defeat our objective of obtaining samples, since τ, itself, is a multiplying factor for the spectral distributions. Thus, we seek a compromise between a small value of pulsewidth τ and a value of energy in the signal samples sufficient for our signal processing.

The aliasing problem

The phenomenon of aliasing, previously mentioned, appears when our original analog signal is not properly band-limited. This condition is shown in Fig. 12, where spectral distributions overlap and there is a considerable contribution into the spectral distribution centered at

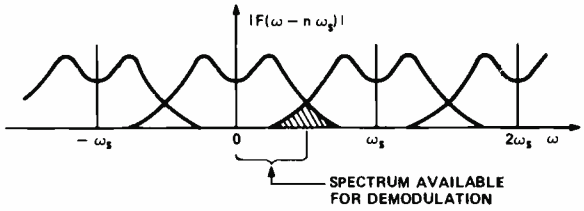

Fig. 12 — Origin of the aliasing problem.

$\omega = 0$ from spectral distributions on either side. Effectively, the spurious high frequencies in the original analog signal appear as low frequencies in the detected output.

It is interesting to note that in the case of telephone communications, band-limiting usually occurs at 3.3 kHz while the sampling frequency is usually at 8 kHz. This leaves a safety margin, or "guard band," of 1.4 kHz between the spectral distribution centered at zero and that centered at the first harmonic, 8 kHz.

Demodulation of sampled signals

Referring to Eq. 4, it would seem that separation of the desired signal from its high-frequency sampling-generated components is easily accomplished by a low-pass filter. This is essentially true but some points need to be made. For one thing, the existence of a guard band between spectral distributions is extremely advantageous—in fact, essential, for use with realizable filters. This is shown in Fig. 13 where a possible filter characteristic taking advantage of such a guard band is shown. A more important consideration is the question as to whether our series of signal samples will actually combine to reproduce the original analog signal. This is in fact an important question. The details of the mathematics proving that this is really the case will not be given here. However, we will survey a few of the important relationships, which show that the original analog signal can, in fact, be reconstructed from such samples. Thus, using the case of the sin x/x type signal as an example, it can be shown rigorously

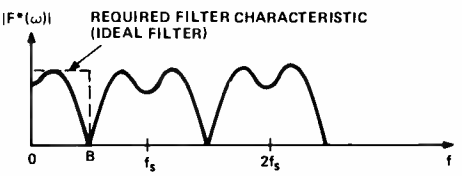

Fig. 13a — Absence of guard band requires use of unrealizable ideal filter.

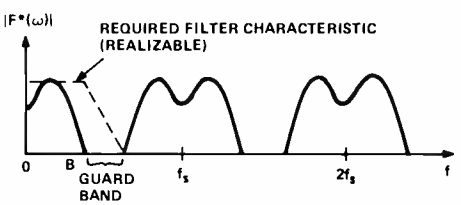

Fig. 13b — Presence of guard band allows use of realizable filter.

that our original analog signal can be represented by the following expression:

$$f(t) = \left\{ \sum_{n=-\infty}^{\infty} f(-n/2B) \cdot \frac{\sin 2\pi B(t + n/2B)}{2\pi B(t + n/2B)} \right\} \quad (5)$$

where we recognize that we have a summation of sin x/x type pulses, each assigned an amplitude corresponding to

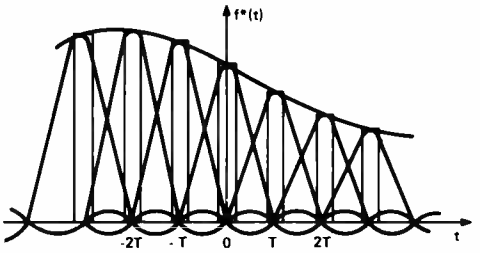

Fig. 14 — Reconstruction of original analog signal from summation of sin x/x pulses resulting from impulse response (or narrow flat-topped pulse response) of transmission channel with ideal filter characteristic.

the actual amplitude of the analog function at the sampling point involved. From a physical standpoint this means that these pulses will actually add to reproduce the original analog signal, which is shown as the envelope in Fig. 14. Skeptics may verify this by actually calculating amplitudes at any point along the time axis. It can similarly be shown that a summation of raised-cosine pulses will also add up to the original analog signal. These considerations need to be modified, of course, in the case of quantized signals where some of the original analog information has been lost. The question of resultant quantization noise, as well as bandwidth and power considerations, will be treated in a subsequent article in which use will be made of the fundamentals of information theory.

Final note

Of the various types of pulse modulation treated in this article, the most advantageous has been found to be pulse code modulation (PCM). The following points may be made:

1) PCM is normally operated near noise threshold since the only requirement for information recognition is the determination of signal amplitude. Once we are above noise there is no further advantage in increasing signal power. From this standpoint, PCM is more economical of power than other types of pulse modulation.
2) PCM has a small but definite advantage over (analog) frequency modulation at the lower signal/noise ratios.
3) Systems designed to handle PCM, being themselves digital, lend themselves naturally to transmission of other types of digital data, e.g., digital computer information signals.
4) PCM naturally lends itself to periodic signal regeneration over long-haul transmission channels.

In the next article we will consider time-division multiplexing systems and explore the bandwidth and power requirements for the pulse modulation approach. In doing so we will introduce and make extensive use of information theory. Future articles will deal with digital filters and spectral analysis. In the meantime, interested readers are urged to avail themselves of one of the basic references given below and dig into the subject of digital systems.

References

It should first be noted that the information contained in this article is covered in much greater detail in the Corporate Engineering Education Course E11, Communications Theory II. This is the second of a three-course series dealing with basic communication theory. Recommended textual references are:

1. Schwartz, M.; *Information, Transmission, Modulation, and Noise*, 2nd ed., McGraw-Hill (1970).
2. Carlson, A.B.; *Communication Systems: An Introduction to Signals and Noise in Electrical Communication*, McGraw-Hill (1968).
3. Bennet, W.R., and Davey, J.R.; *Data Transmission*, McGraw-Hill (1965).
4. Telephone communications are well covered in: Martin, J.; *Telecommunications and the Computer*, Prentice-Hall (1969).
5. A text with much out-of-the-way information: Hamsher, D.H. Ed; *Communication System Engineering Handbook*, McGraw-Hill (1967).

It is difficult to find a suitable extended treatment of the Fourier transform in the current literature. However, there is a good introduction, with many applications, in the study guide material accompanying Session 1 of CEE course M52 (Fourier Analysis and the Laplace and Z-Transforms). The following texts may also be consulted:

6. Skilling, H.H.; *Electrical Engineering Circuits*, 2nd ed., Wiley (1965).
7. Schwartz, M.; *Information Transmission, Modulation, and Noise*, 2nd ed., McGraw-Hill (1970).
8. Cheng, D.K.; *Analysis of Linear Systems*, Addison-Wesley, (1959).

Appendix A — The Fourier transform

In its broadest terms, the Fourier transform maps a function from one domain into another domain where certain otherwise hidden properties of the function are prominently displayed and certain desired processing operations are much simplified. In electronics the two domains involved are normally the time and frequency domains. For example, suppose that we have the waveshape shown in Fig. A1 (in the time domain).

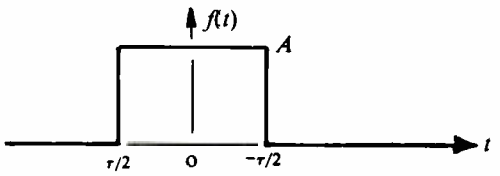

Fig. A1 — Rectangular pulse.

Although this waveshape clearly outlines the time-dependent shape of the pulse, the important frequency content is not shown. It often becomes desirable (even essential) to obtain a plot of the relative intensity of the frequencies contained in this pulse. We easily obtain this information using the Fourier transform:

$$F(\omega) = \int_{-\infty}^{\infty} f(t)e^{-j\omega t}\,dt$$

$$= \int_{-\tau/2}^{\tau/2} A\,[\cos \omega t - j \sin \omega t]\,dt.$$

The sine term in the last integral above (including the constant A coefficient) is an odd function and vanishes when integrated between equal positive and negative limits. The remaining term may be written as:

$$F(\omega) = 2A \int_{0}^{\tau/2} \cos \omega t\,dt$$

$$= 2A \left.\frac{(\sin \omega\tau/2}{\omega}\right|_{0}^{\tau/2}$$

and evaluated

$$F(\omega) = 2A\,\frac{\sin \omega\tau/2}{\omega}$$

$$= A\tau\,\frac{\sin \omega\tau/2}{\omega\tau/2}$$

The result is shown in Fig. 4 in the body of the article.

Where we already possess the frequency function $F(\omega)$ and wish to retrieve the time function, or waveshape, we make use of the inverse Fourier transform, e.g.:

$$f(t) = (1/2\pi) \int_{-\infty}^{\infty} F(\omega)e^{j\omega t}\,d\omega$$

where the evaluation follows along similar lines. The plus and minus infinity limits of the integral do not usually cause difficulty since realizable transmission channels have finite cutoff values, which replace these limits. The result is normally a well-defined waveshape for $f(t)$.

This review question uses the material you just learned to set the stage for the next article of the series.

We are planning to transmit a musical program which has a frequency range of 20 to 20,000 Hz and a dynamic range of 100 dB. We also assume that the human ear can distinguish between intensity levels differing by 0.5 dB. Compute the bandwidths required for transmission under each of the following conditions.

1) We transmit the electrical signals in their original analog form.
2) We sample the signals (see figures at right) and then transmit the program in PAM form via a transmission channel having a raised-cosine type of response.
3) We reduce our signal to a binary PCM code (see quantized samples at right) and transmit the result through a transmission channel having a raised-cosine type of response.
4) We reduce our signals to a ternary PCM code (each pulse can have three levels) and again transmit our signal through a transmission channel having a raised-cosine type of response.

As a final consideration, we assume a (positive or negative) peak noise level excursion of 1V and a peak available signal excursion of 4V. Which of the above systems would be most practicable from the standpoint of preserving accuracy of information for minimum bandwidth expenditure?

Ed. note: The answers to these questions will be given in the next issue. If you can't answer them yourself and don't want to wait, write to Dr. L. Shapiro, Continuing Engineering Education, RCA Bldg. 204-2, Camden, N.J. 08101 for the solutions.

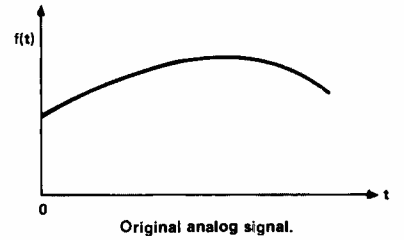

Original analog signal.

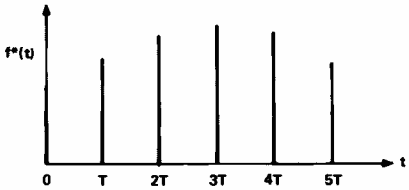

Sampled analog signal.

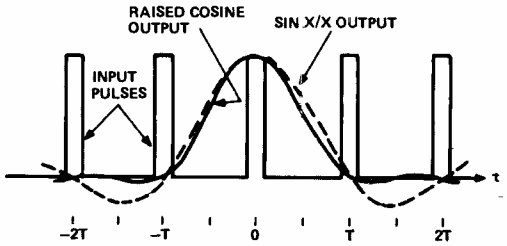

Quantized samples and their representation in a pulse-code-modulation scheme.

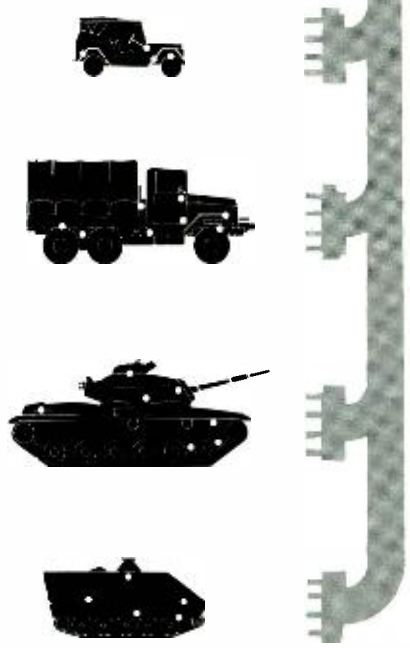

Engine test at the Automated Systems Division

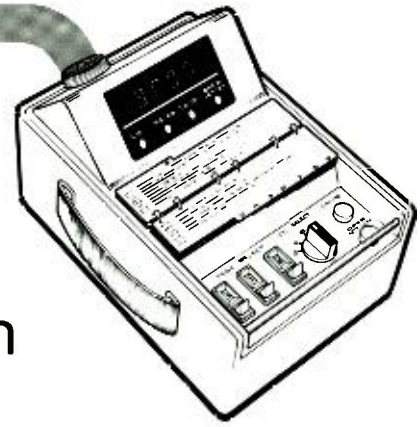

R. T. Cowley

Military vehicle maintenance, when done in "diagnose by replacement" style, is costly and produces a valuable scrap barrel. Advanced test and diagnostic techniques are being produced to remedy this situation.

R.T. Cowley, Mgr., Government Communications and Automated Systems Division, Burlington, Mass., received the BSME from Iowa State University in 1950. Mr. Cowley joined RCA in 1961. From that time to the present, he has worked in ATE Engineering in a supervisory capacity. He was responsible for the design and development of various Apollo prelaunch test systems in addition to various ATE technique studies and contracts. Currently, Mr. Cowley is manager of non-electronic test engineering, which includes RCA's investment programs and contracts relative to the application of the ATE technology to the test and process control of mechanical systems. He has spearheaded the drive to make RCA a leading firm in the areas of turbine and internal combustion engine test and diagnosis.

Reprint RE-22-2-16
Final manuscript received June 25, 1976.

AS ENGINES have become more complex and costly, the ability of mechanics to effectively diagnose malfunctions has declined. Fault isolation is primarily a function of the varying skill and judgement of the individual mechanic. The prevailing attitude towards vehicle repair is to adopt the easiest and quickest method. If it is more difficult or time-consuming to test and identify the faulty component or assembly than it is is to change it, the suspected item will be changed without testing. Similarly, if it takes longer to adjust or repair an item than to replace it, it will be changed. Different configurations of test equipment, which are difficult to relate to the vehicle manuals, test diagrams, and instructions, are an additional source of confusion.

A majority of mechanics, therefore, become frustrated and finally discard the test equipment and rely upon the time-honored substitution method, diagnosis by replacement. In the instance where the mechanic does not have the proper test equipment, he has no option other than to diagnose by replacement. Good parts and assemblies that are unnecessarily replaced are seldom reinstalled after the trial-and-error approach. The result is a costly maintenance program and a valuable scrap barrel.

During the 1960's, the U.S. Army's Tank Automotive Command conducted studies to determine the value of the good components that were being discarded. With these results as a base, we conducted further studies to identify the test capabilities needed to prevent or reduce the incidence of faulty maintenance diagnosis. Our goal was to determine if it was technically feasible to reduce the value of the scrap barrel and save wasted time.

The Army's early studies had shown that over 40% of the discarded assemblies and components were not faulty. Our studies on two high-population vehicles showed that the engine or components from the engine-related subsystems, i.e., fuel, air, ignition, starting, and charging, made up 89% of the good discarded components. With these conclusions as a guide, we emphasized research and development to conceive test and diagnostic concepts which would solve the Tank Automotive Command's problem where it first occurs, at the organizational level. To be useful, the test equipment must be rugged and either built-in or one-man portable. It must also be configured to encourage the mechanic to test and diagnose, thus enabling him to determine the correct maintenance action prior to exchanging parts.

Our studies at the Automated Systems Division were paralleled by customer-funded hardware feasibility programs and advanced test and diagnostic techniques developed under RCA's Independent Research & Development program. At this time, under contract to the Tank Automotive Command, we are redesigning for production the STE/ICE (Simplified Test Equipment for Internal

Combustion Engines), which is an organizational-mechanic's test set. Low-rate initial production is scheduled to start in 1977. Production quantities of 5000, at a rate of 300 per month, are planned. STE/ICE testing of other military commodities such as motor-generators, earth-movers, etc., is a strong probability. Although the test technologies developed by ASD are applicable to commercial engines, our products, which implement these techniques, are designed specifically for our military customer. ASD's resources, personnel and facilities will continue to be needed to support our customer in fielding STE/ICE and meeting their engine maintenance problems of the future.

Equipment classifications

The Tank Automotive Command classifies new vehicle test and diagnostic equipment into three generations, as follows:

First generation—
external instrumentation

All test equipment is external to the vehicle to be tested, and the engine is instrumented specifically for test. The mechanic implements the test procedures with off-board equipment that receives and processes signals from transducers and direct electrical test points. Test results are displayed either as a measurement or directed maintenance action, and at the conclusion of test, the instrumentation is removed for further use on other vehicles.

Second generation—
built-in instrumentation

Here, the instrumentation and direct electrical interfaces are built into the vehicle and terminated for convenient interfacing with portable measurements and diagnostic equipment. This eliminates the time-consuming, and sometimes impossible, task of instrumenting the vehicle. When you consider the mechanic's role in bad weather, or the inaccessibility of the engines in armored vehicles, you can readily visualize that built-in-transducers are a big step forward in inducing the mechanic to test before replacement. The key requirement for this implementation is the availability of low-cost, reliable transducers to measure pressure, temperature, position, etc.

Third generation—
continuous monitoring

This is the ultimate. It consists of permanently built-in transducers and test equipment designed and configured to meet the peculiar measurement and diagnostic requirements of a vehicle and its engine. It continuously monitors performance and can immediately alert the driver to the presence of a malfunction. In addition, transient malfunctions or significant performance data can be obtained under actual operating conditions and stored for deeper off-road diagnosis or trending.

Implementations and evaluations

At ASD, we have designed, fabricated and delivered examples of each of the above generations for customer evaluation, in additon to a hybrid system, STE/ICE, which is an important example of both the first and second generation. The earliest systems fabricated by RCA were second-generation. All of the electrical test points and signals from selected transducers were terminated at a convenient point in the vehicle. These systems were directed solely at solving the accessibility problems associated with the Army's current inventory of test equipment. Evaluations were performed on a spark-ignition-powered 1/4-ton truck (Jeep) and a diesel-powered 2-1/2-ton truck. The results showed this system reduced the time required to perform existing test procedures in a dry garage on a clean vehicle by a minimum of one-eighth. The reduced test time under adverse environmental conditions, i.e., mud, snow, sleet, etc., was not determined; however, you can well imagine that it would have been more dramatic. In general, it was concluded that the second-generation system, implemented with current test equipment, was an effective answer to many current maintenance problems. However, it was not a total solution, nor does it solve the problem with the existing fleet.

The next systems delivered were examples of third-generation built-in test equipment. These systems were designed to determine vehicle readiness, detect faults during normal vehicle operation, and assist the operator or mechanic in locating and correcting the fault conditions. In this program we expanded the test equipment's role to include new measurement techniques and diagnostic algorithms which were not possible with the Army's standard-issue test equipment. Two models of this system were fabricated and installed; one on a spark-ignition-powered 1/4-ton truck (Jeep); the other on a diesel-powered 2-1/2-ton truck. Approximately forty interfaces with the vehicle and its power plant were terminated in a box of electronics mounted under the dash. The electronics were designed to continuously measure, compare and store performance data while the vehicle was being operated. Those events significant to a mechanic for diagnosis were stored for later readout with a portable mechanic's display. The system performed well under actual operating conditions and solved many of the maintenance problems. However, the projected per-vehicle retrofit cost was prohibitive for all except the higher-cost vehicles. Fig. 1 gives the configuration of these systems.

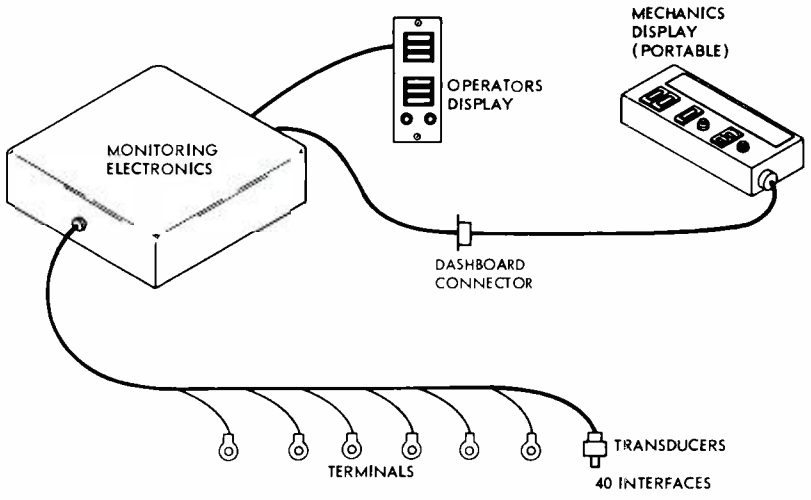

Fig. 1 — Go/no-go system configuration.

Cost-effective solutions

At this point, we concentrated on evolving cost-effective concepts to solve the maintenance problem on both the existing fleet and new vehicles. The next system terminated its electrical test points and transducer signals at a diagnostic connector on the vehicle dash. Three different portable test equipments were designed to interface with the diagnostic connector (Fig. 2). The simplest was the Test Point Unit, which provided a junction between the diagnostic test connector and the standard-issue test equipment used for performing tests on the electrical subsystems. The Vehicle Test Meter eliminated the need for the standard test equipment. A digital display was used to display all measurements in engineering units. A "go/no-go" section at the top of the meter provided a quick indication of service requirements. The Vehicle Readiness Unit combined the features of third-generation electronics, operator display and mechanic's display into one portable unit that could interface with the vehicle at the diagnostic connector to perform dynamic operational tests and display overall system faults. It was envisioned that this equipment would be employed when the driver had a complaint which could only be diagnosed during vehicle operation.

We now had three alternatives for a second-generation system implementation. The Vehicle Test Meter (VTM) was the strong preference of experienced personnel. It was easy for the novice mechanic to use and provided in-depth measurements for the skilled diagnostician. More importantly, the VTM could be produced at an acceptable cost to interface with many different vehicles and power plants. Encouraged by the results of this program, the Tank Automotive Command contracted for the development of a system they named Simplified Test System for Internal Combustion Engines (STE/ICE). The goal was to provide the organizational mechanic with a one-man portable measurement system that would enable him to test and diagnose transport and tactical vehicles, present and future. STE/ICE prototype diagnostic connector assemblies (DCA) were designed and fabricated for initial application to a Jeep, 2-1/2-ton truck, armored personnel carrier, and a tank. All of these vehicles are diesel-powered with the exception of the Jeep. The STE/ICE system also included a complement of transducers to enable a mechanic to test vehicles which lacked a built-in diagnostic harness.

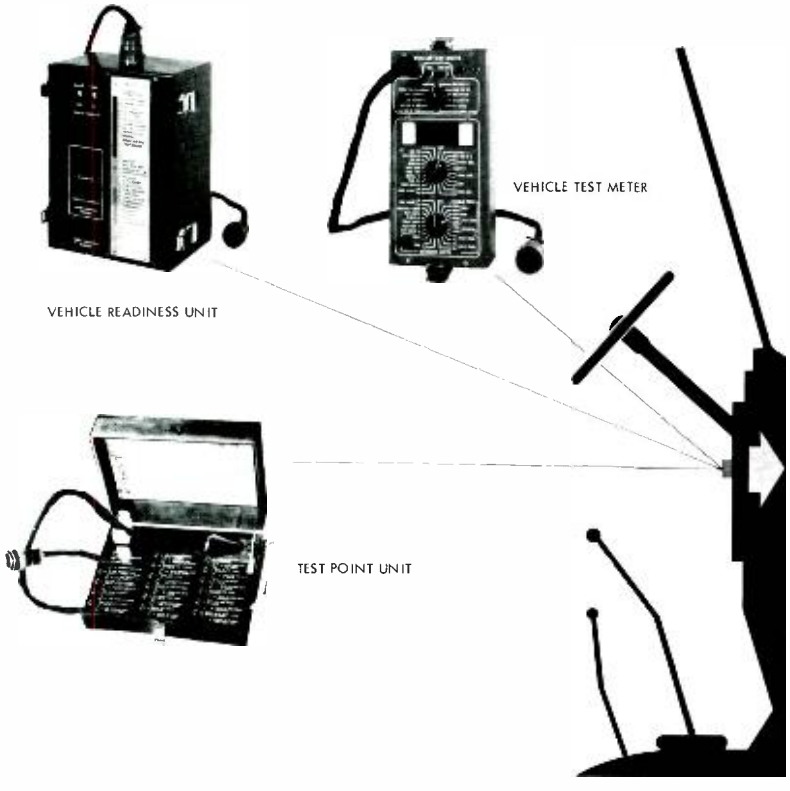

Fig. 2 — Diagnostic test equipment.

Prototype and production

The prototype STE/ICE Vehicle Test Meter (VTM) is shown in Fig. 3. It contains all the electronics required by the mechanic to make measuremnts or perform special test algorithms developed by RCA. It is controlled by a microprocessor and can be used in either the diagnostic-connector or transducer-kit mode. A significant new test function includes the ability to perform power tests on both spark- and compression-ignition engines without a load dynamometer or road test. An equally important feature is its ability to survive and perform in the vehicle's field environment, including repeated drops from vehicle fenders to concrete floors.

Six prototype STE/ICE systems were subjected to design and operational tests by the U.S. Army, and the program was successfully completed in 1975. It demonstrated the STE/ICE system was an accepted mechanic's tool, combining the most cost-effective features of the first-, second-, and third-generation hardware.

The present contract activity, Engineering Development/Producibility Engineering Planning (ED/PEP), is to design the STE/ICE set (VTM and TK) to a production cost target. The maximum acceptable unit cost for a production run of 5000 is $4,360. The minimum cost, at which RCA will receive the maximum incentive fee for the ED/PEP program, is $3,240. Obviously, there are other constraints and incentives to insure we do not sacrifice performance and reliability for production cost. The ED portion of the program involves design and development, which will enable us to propose desirable enhancements in the STE/ICE performance.

Interactive system

The evolution of STE/ICE was closely paralleled by a program which demonstrated the feasibility of using a more powerful computer and more complex algorithms to automate the in-depth diagnosis required at a repair depot. In it, hardware called Automatic Test Equip-

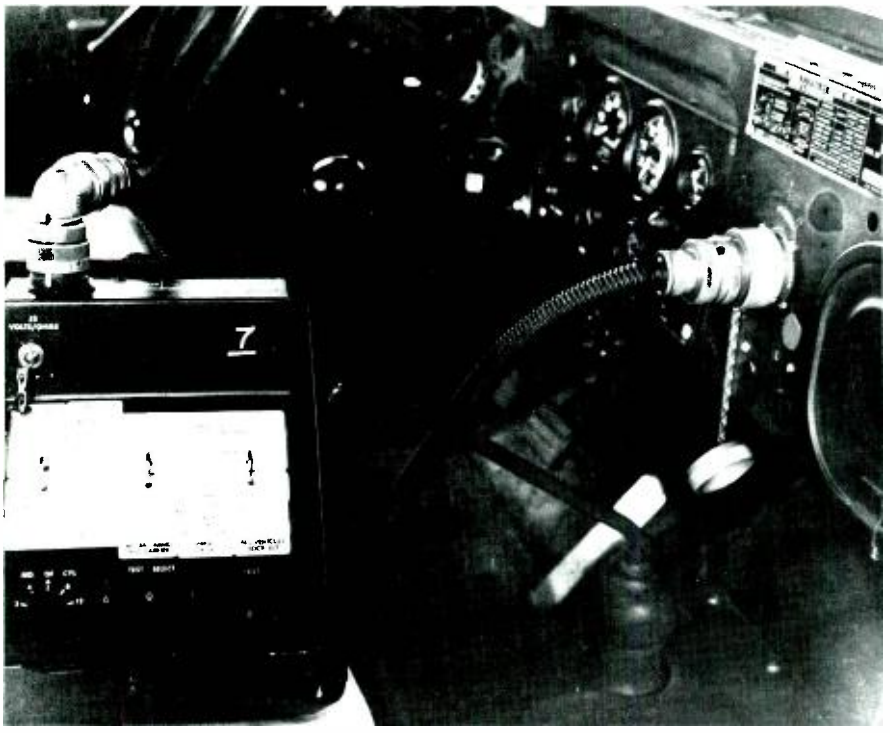

Fig. 3 — Vehicle Test Meter connected to diagnostic connector.

ment for Internal Combustion Engines (ATE/ICE) was interfaced with a vehicle and its power plant, using either a transducer kit or diagnostic connector. A unique feature of this system was an interactive, conversational interface with the mechanic, used to lead the mechanic through progressive instrumentation of the vehicle and automatically display the correct repair action. The success of this program did much to enhance RCA's image in the field of engine test.

New technologies

The hardware developments that evolved into the STE/ICE and ATE/ICE systems owe a significant measure of their success to some important test and diagnostic technologies first conceived and reduced to practice under IR&D programs at ASD. The most interesting ones are engine power tests without a dynamometer and using starter-current waveform analysis to determine the health of the combustion chamber. ATE/ICE used these, coupled with dynamic waveform analysis of electrical, pressure, and speed signals, to fault-isolate individual-cylinder, fuel-system and ignition-system failures. Our current IR&D effort is concentrated towards simplifying the test-equipment interface with diesel engines, with the goal of performing all testing and diagnosis without installing or mounting a transducer to the engine. We refer to this as our "non-contact" technology. To date, we have reduced to practice the measurements of speed and horsepower on a normally-aspirated diesel engine. In addition, we have demonstrated the ability to detect, identify, and differentiate minor faults in the combustion chamber and fuel-injection system. All of the above have been implemented via a hand-held transducer. Details of this technology are contained in "Non-contact instrumentation for engine testing and monitoring," by Hadden, Hulls, and Sutphin, in this issue.

Computer modeling

Our technical position has also been enhanced by our computerized engine models and data-reduction capability. The diesel model permits an engineer to evaluate the effects of various types of malfunctions on many different engine parameters, thus eliminating the time-consuming, and often impractical, procedure of introducing real faults into actual engines. This model can be used to simulate almost any diesel engine, two- or four-cycle, with or without faults, in various operating modes. The vehicle data-reduction system makes use of ASD's Software Development Center, which has a Data General NOVA computer and the normal complement of peripherals found in a programming facility. Added to this is a seven-channel portable instrumentation tape recorder, a programmable A-to-D converter, pulse-data timing devices, and a plotter, which allow fast, comprehensive reduction of data recorded on actual engines. The system is presently in use reducing field data as part of a test-requirement analysis for ten new vehicles to be tested by STE/ICE. It will also be used for test-algorithm validation of diagnostics to be programmed for the production STE/ICE system and thereby minimize microcomputer assembly-language integration problems.

Conclusions

Let me leave you with a look into the near future. The role of electronics in assisting the mechanic in the test and diagnosis of internal-combustion engines will expand as the engines become more complex and costly. The need for periodic evaluation of engines for peak performance, even when a fault is not apparent, will increase as the cost of fuels increase and our clean-air laws are strengthened. STE/ICE, based upon the need it fulfills, will become the U.S. Army's organizational test set for all of its transport and tactical vehicles. I expect to see it applied to other equipments for the military. Typical candidates are motor-generators, earth movers, small boats, landing craft, etc. This more powerful tool in the hands of the field mechanic will create a need for equipments similar to ATE/ICE to perform expanded in-depth diagnosis at depots and overhaul facilities. The "non-contact test" technologies we are developing are essential for the success of such a system. As you can see, I anticipate an active continuing relationship between RCA and the military user of internal-combustion engines.

References

1. Hadden, S.C.; Hulls, L.R.; and Sutphin, E.M.: "Non-contact diagnosis of internal combustion engine faults through remote sensing," SAE Automotive Engineering Congress and Exposition. Detroit, Mich. (Feb 1976)
2. Fischer, H.L.; and Hanson, R.E.; "New techniques for automated engine diagnostics," *RCA Engineer*, Vol. 21, No. 6 (Apr/May 1976) pp. 74-79.
3. Fineman, H.E.; Fitzpatrick, T.E.; and Fortin, A.H.; "Simplifying automotive test equipment through the use of advanced electronics" IEEE NEREM '74, Boston, Mass., (Nov 1974).

Application of automatic test equipment to bus maintenance

R.F. Barry| J.M. Laskey

Built-in instrumentation can improve effectiveness and efficiency in maintaining a fleet of buses. The connections, sensors, and transducers required for testing are permanently installed on each bus and terminate at a single 'diagnostic' connector. Testing is then done by connecting analytic instrumentation to this connector.

THERE IS a growing need in vehicle maintenance for new approaches aimed at reducing vehicle downtime and curbing the upward repair cost spiral. Increases in vehicle complexity and the shortage and rising cost of skilled mechanics create serious problems in the timely inspection and accurate diagnosis of vehicle malfunctions. The energy shortage further compounds the situation and, in particular, will impact long distance, high-speed, intercity bus fleets. Increased demand for passenger service combined with the imposition of lower

J.M. Laskey, Mgr., Air Force Affairs Marketing Department, Burlington, Mass., received a BSEE from Carnegie-Mellon University in 1955 and an MS in engineering management from Northeastern University in 1968. In 1955, he joined RCA, Camden, N.J., where he was responsible for the design and development of a variety of electronic test systems utilized for depot and field test of U.S. Air Force radar systems. During this time period the automatic test equipment technology matured and he was part of the team that established RCA's present ATE Product Line. In 1962 this organization was transferred to Burlington, Mass. where he served as Project Engineer for the USAMICOM Automatic Missile Test System until 1965. From 1965 to 1972 Mr. Laskey played a major role in management of the LCSS project and was responsible for the initial production program, and establishment and operation of a worldwide field support team for these systems. Currently, Mr. Laskey is responsible for managing the marketing development of ATE systems involving extension of the ATSJEA and EQUATE system technology.

R. F. Barry received the BSEE with high honors from Michigan State University in June 1959. He then participated in the RCA Graduate Study Program, receiving the MS in engineering from the University of Pennsylvania in 1964. His responsibilities include the error analysis of a statistical technique for isolating faulty components in electronic equipment and the analysis of significance tests for hypotheses appropriate to this technique; the development and study of statistical models appropriate to maintainability testing of electronic equipment; and the technical analysis and development on the Test Point Algorithm Contract. This program developed techniques for automatic testing and test point placement in electronic circuits. He was responsible for all ATE programs with NAVAIR, and was Project Engineer on the project developing noise testing techniques and assumed engineering responsibility for its technical development. Mr. Barry is a member of Tau Beta Pi, Eta Kappa Nu, and the AAAS, and is a Registered Professional Engineer. Mr. Barry is no longer with RCA.

highway speeds has created a bus shortage. Industry spokesmen have noted that since buses typically have only four-speed transmissions, operation at 50 or 55 mi/h will increase fuel consumption and the likelihood of engine and transmission maintenance problems.[1] These elements provide added incentive to improve maintenance efficiency. U.S. Army programs have made considerable progress in solving maintenance problems in their large fleet of motorized vehicles.[2] Army interest in maintenance is not solely restricted to militarized, combat-type vehicles. Recently completed studies[3] conducted by the Army recommend increasing the commercial unit population from 20 to 45% of the wheeled vehicle inventory. This paper describes the suitability of applying military technology to commercial fleet maintenance problems, using bus maintenance as a specific example.

Objectives of automatic test

The fundamental objectives of maintenance are to prevent, detect, and correct failures (or impending failures) at the most economical stage and by the most economical repair or replacement action. For automatic test equipment (ATE), as applied to vehicle tests/diagnostics, the tests are structured around scheduled maintenance operations.

Preventive maintenance is a combination of tests, checks, visual inspection, and lubrication operations aimed at preventing excessive wear and on-road failures, and detecting existing problem conditions before they become more serious or more costly to repair. Obviously, test automation of all preventive maintenance operations is impractical. There are a large number of inspections and checks that rely entirely on visual inspection and judgment by the mechanic looking for signs of wear, cracks, degradation, etc. However, preventive maintenance also entails a considerable amount of testing (described later in the paper) that could be automated. Such tests could be performed rapidly, with consistency, and with documented printouts of results. This would permit the mechanic to concentrate on those functions that he alone can perform. The result is a more effective and less time-consuming service operation.

Development status

Development of the U.S. Army vehicle automatic test equipment has concentrated around the concept of permanently mounted vehicle instrumentation, connections, and wiring harness, including the diagnostic connector. All pertinent electrical points in the vehicle, as well as special transducers, sensors, and fluid level detectors are connected via the wiring harness to a diagnostic connector, which serves as a single interface point for connection of test instruments. The objective is to enable comprehensive measurement of vehicle parameters without requiring the mechanic to climb around, under, or in the vehicle engine compartment to make a series of individual connections or attach an assortment of mechanical or electrical test devices or adapters. This approach not only saves time and frustration, but also eliminates errors caused by improper hookup.

Three types of test instrumentation have been developed to interface with the diagnostic connector. Each of the designs is intended to satisfy different test objectives and varying degrees of test automation (particularly in the area of diagnostic test sequencing). In addition, the designs will provide several different approaches to mechanic skill re-

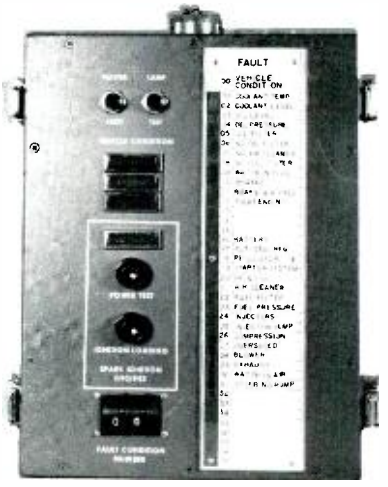

Fig. 1 — Vehicle readiness unit.

Fig. 2 — Venicle test meter.

Table I — Typical list of tests performed by the VTM.

Spark ignition (SI) power tests	*Compression ignition (CI) power tests*
Compression balance test	Fuel supply pressure
Fuel return pressure	Fuel filter pressure drop
Air cleaner pressure drop (single or right)	Air cleaner pressure drop (left)
Turbocharger outlet pressure (single or right)	Turbocharger outlet pressure (left)
Airbox pressure	Intake manifold vacuum
Intake manifold vacuum variation	Oil pressure
Oil temperature	Coolant temperature
Engine r/min (SI engines)	Engine r/min (CI engines)
Coil primary volts	Coil primary resistance
Points voltage	Dwell angle
Dwell angle variation	"Crank-no-start" due to ignition failure
Total starter amperes	Starter amperes, initial peak
Starter motor volts	Starter and circuit cable drop
Starter-circuit cable drop	Battery volts
Battery amperes	Battery electrolyte level
Alternator/generator output volts	Alternator/generator output amperes
Alternator/generator sense volts	Alternator/generator field volts
Alternator/generator field amperes	Alternator/generator and cable drop

Reprint RE-22-2-13
Final manuscript received September 15, 1975.

quirements, test result display, and the mechanic's interface to the test instrument. It is beyond the scope of this paper to delve into detailed descriptions of these devices; such information has been previously published and is referenced.[4] Functional descriptions of these devices are provided.

Vehicle readiness unit (VRU)

An experimental VRU (Fig. 1) has been built and successfully demonstrated. Its purpose is to provide for complete on-board checkout and retention of the vehicle condition during road test or sample duty cycles. It provides for the continuous, parallel monitoring of significant vehicle operation parameters, latching into memory any parameters that fall outside pre-set limits. At the completion of a road test, the mechanic can quickly read a display of more than 25 specific tests of vehicle operating conditions. Further, the device uses a special technique[5] to measure the overall operating condition of spark ignition engines operating under simulated full-load conditions without an external loading device or dynamometer.

Vehicle test meter (VTM)

This second device, shown in Fig. 2, has the capability of performing a large number of vehicle- and engine-related tests. It is designed to accomplish effective and efficient tests and diagnoses when operated by mechanics with low skill levels. A typical list of tests is shown in Table I. The technique measuring overall engine performance under simulated full-load conditions is also included in the VTM device. A similar testing procedure[5] for compression ignition (diesel) engines has been developed, and it too is part of the VTM capability. A transducer kit compatible with the VTM is used to test vehicles not equipped with a diagnostic connector.

Located on the front of the VTM is a set of plasticized printed flip cards, which cue the mechanic for the proper test sequence for the vehicle under test. For each test parameter, the flip cards identify a test number and test information. When a mechanic enters the proper test number on the VTM, the test results are displayed in numerical form on the display window.

Fig. 3 — Programmable diagnostic unit in M151A2 truck.

The primary advantage of this system (whether it is used with a diagnostic connector or attachable transducers) over the existing commercially available test equipment is that it greatly simplifies and speeds up the testing procedure. A speed advantage of 20:1 is estimated at the present time. Further, this system tends to minimize problems associated with test omissions.

Programmable diagnostic unit (PDU)

The third device, shown in Fig. 3 and currently under development, is a portable compact testing unit, which utilizes a stored program for internal combustion engine diagnostics. This unit is a part of the automatic test equipment/internal combustion engine (ATE/ICE) and consists of a transducer kit, a data processor with readout and hard-copy capability, and an operator entry device. The system, originally conceived under the direction of Frankford Arsenal, Pa., is now under formal development by a TRW/RCA team. It permits a dynamic interchange of information between the operator and the PDU, a feature which distinguishes it from other present-day systems. A magnetic tape cassette is used for programming calibration data, test sequencing, and parameter limits into the internal computer.

It is significant to mention that this system is designed to minimize the number of transducers or attachments required. Normal engine testing requires only four: battery voltage, ignitor probe, firing probe, and temperature. If, during the course of a test sequence, "the computer decides that additional information is required," it will instruct the mechanic to attach an additional transducer. There are three available: a clamp-on current probe and two pressure transducers. One of these senses intake manifold vacuum and the other blow-by pressure.

Bus maintenance characteristics

The character of bus maintenance differs markedly from that of military vehicles. A bus represents a large capital investment, and must be in service to yield a return. Consequently, the maintenance program must be structured to prevent major breakdowns and defer rebuild work in a high-mileage, scheduled operation environment. Intercity buses typically log about 250,000 mi/yr. Time/usage items such as lubricating oil and filters

Table II — Bus maintenenace program.

Mileage Interval	*Purpose*
Every 4000	Check and top up all fluid levels, adjust brakes, check tires, tighten wheel lugs, check lights, etc.
Every 8000	Above plus inspect body, glass, and all DOT items
Every 16,000	Above plus change oil, filters, minor inspection; engine, electrical, and air conditioning/heating
Every 100,000	Major coach cleaning and fumigation
Every 200,000	Major rebuild
Every 400,000	Major body rework
Once a year	Major electrical inspection
Once a year	Major air-conditioning/heating inspection

dictate the wisdom of established periodic inspections as well as the desirability of inspecting the condition of the various systems comprising the bus before they have had a chance to deteriorate to a breakdown. Preventive maintenance, of course, will vary from major rebuild to checking fluid levels and adjusting brakes. A well-structured maintenance program might be quite similar to that outlined in Table II.

Obviously, such a maintenance program encompasses a wide spectrum of skills and effort, ranging from simple servicing to major engine tear-down and rebuild. The 16,000-mi inspection, for example, would typically require about 15 to 20 items of test equipment in addition to the normal mechanic's toolbox.

Upon closer examination, this 16,000-mi inspection shows up as a key maintenance action in that it requires skilled mechanics, occurs frequently (about every 25 days), ties up the bus (about a full day), and is the keystone inspection to detect the mechanical condition of the bus.

In its useful life a bus might undergo 200 such inspections, representing about 1600 man-hours of work. The thoroughness and detail demanded in such an inspection appear to be self-evident—the number of road breakdowns and out-of-service buses are primarily determined by the effectiveness of this inspection. Unfortunately, the press of schedules and other operational difficulties work counter to the required thoroughness; thorough procedures tend to be lengthy and easily forgotten (or skipped), some procedures require locating another mechanic for assistance, good skilled mechanics (especially diesel) are scarce, and often the required instruments must be shared. Not infrequently, a bus will be needed for passenger service before its inspection can be thoroughly completed, and so sections of the procedures will be abbreviated or skipped, or the inspection terminated. More experienced mechanics will often adjust their inspections to the time allotted, inspecting only the driver complaints or obvious major trouble items. All of this, of course, deteriorates the maintenance program and results in a higher than necessary number of breakdowns and out-of-service units. This, in turn, decreases the number of operational buses and thereby increases their utilization factor—resulting in even less time per bus for inspections. This aspect is particularly critical now because of the increasing use of public transportation and lower speed limits (at 55 mi/h an intercity bus fleet of 5000 buses will need about 200 more buses in service to meet its schedules).

Test system requirements

From the foregoing, it is apparent that bus maintenance (and operation) could be substantially improved by the use of automated testing aids at the 16,000-mi inspection that would reduce inspection time, and ensure a thorough and complete inspection.

Such automated aids should have the following minimum characteristics:

1) Testing sensors, wiring, and inspection connector built into each bus.

2) A garage testing unit, which mates with the inspection connector and automatically sequences through the necessary tests. Instructions for manual inspections of bus

Table III — Fuel/air/exhaust subystem.

Measurement	*Purpose*
Air intake	Dirty/restricted air inlet
Airbox pressure	Blower condition/dirty inlet screen
Exhaust back pressure	Restriction
Fuel pressure	Fuel pump low/blocked restrictor
Fuel filter ΔP	Filter clogged/dirty
R/min	
Idle	Idle and governor settings
Fast idle	
Governor	
Smoke test	Overfueling/combustion efficiency

Table V — Cooling subsystem.

Measurement	*Purpose*
Coolant pressure	Air leaks/relief valve/radiator cap
Coolant level	Level/leaks
Radiator ΔT*	Clogging/scale/low airflow/stuck thermostat
Coolant temperature radiator engine	Stuck thermostat
Hot-engine light buzzer	Alarm circuit

*Temperature drop across radiator.

Table IV — Lubrication subsystem.

Measurement	*Purpose*
Oil pressure	Oil pump/clogging
Oil temperature	Oil cooler/use with cooling system tests/use for engine operation temperature
Oil cooler ΔP	Clogged cooler/bypass stuck open
Low-oil light	Alarm circuit
Oil fuel-dilution level	Injector dribble

Table VI — Engine subsystem.

Measurement	*Purpose*
Crankcase pressure	Crankcase ventilation/blow-by
Compression balance	Valve/ring condition
Acceleration test	Engine power

Table VII — Starting/charging.

Measurement	*Purpose*
Cables/connectors	
Positive circuit	Cable resistance/corroded terminals
Negative circuit	
Starter motor	Burned-out motor/shorted windings/bad brushes/ corroded commutator
Starter solenoid	Excessive current/no pull-in
Reverse solenoid	Excessive current/no pull-in
Engine emergency stop	Excessive current/no pull-in
Battery	
Discharge	Capacity
Charge	Chargeability
Temperature	Correct above calculations
Level	Detect low level
Alternator	Low output/open diode or stator
Regulator	Correct current output
	Regulator condition/setting
	Correct voltage-current

Table VIII — Air conditioning/heating.

Measurement	*Purpose*
Blower	
Condenser	Correct r/min (airflow conditions)
	Proper adjustment/condition-amperes
Evaporator	Correct r/min (airflow conditions)
	Proper adjustment/condition-amperes
Oil pressure	Compressor lube (with P_s)
Suction pressure	Unloading/enthalpy Δ for evaporator (with P_H)
Head pressure	Condenser temperature and enthalpy Δ (with P_s outside air temperature, and assumed airflow)
Bulb temperature	Superheat (with T_s)
Outside air temperature	Condenser pressure (with P_H and airflow)
Evaporator airflow	Air leaks/restrictions
Return air	
Temperature	Enthalpy change and refrigerant airflow
Humidity	
Evaporator air temperature	

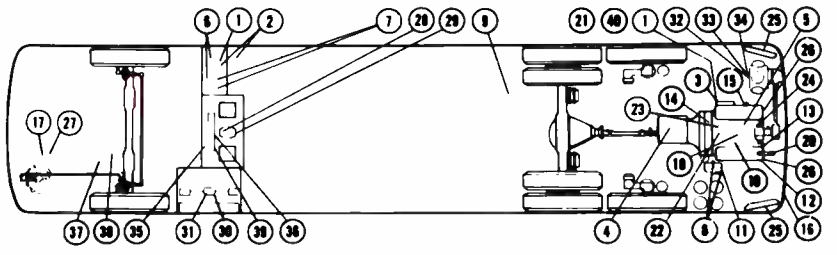

- ENGINE ELECTRICAL
  1. CABLES/CONNECTORS - POS. CRT.
  2. CABLES/CONNECTORS - NEG. CRT
  3. STARTER MOTOR/SOLENOID/BATTERY DISCHG
  4. REVERSE SOLENOID
  5. ENG. EMERG. STOP SOLENOID
  6. BATTERY TEMPERATURE
  7. BATTERY LEVEL
  8. ALTERNATOR
  9. REGULATOR
- AIR/FUEL/EXHAUST
  10. AIR INTAKE
  11. AIR BOX PRESSURE
  12. EXHAUST BACKPRESSURE
  13. RPM
  14. FUEL PRESSURE
  15. FUEL FILTER ΔP
  16. SMOKE TEST
- ENGINE LUBE
  17. OIL PRESSURE/LO OIL LITE
  18. OIL TEMPERATURE
  19. OIL LEVEL
  20. OIL COOLER ΔP
  21. OIL FUEL DILUTION
- ENGINE
  22. CRANKCASE PRESSURE
  23. COOLANT PRESSURE
  24. COOLANT LEVEL
  25. COOLANT TEMPERATURE - RADIATOR
  26. COOLANT TEMPERATURE - ENGINE
  27. HOT ENGINE
  3. COMPRESSION BAL.
  13. POWER TEST
- AIR CONDITIONING/HEATING
  28. BLOWER - EVAP. - RPM
  29. BLOWER - EVAP. - AMPS
  30. BLOWER - COND.- RPM
  31. BLOWER - COND.- AMPS
  32. OIL PRESSURE
  33. SUCTION PRESSURE
  34. HEAD PRESSURE
  35. BULB TEMPERATURE
  36. EVAP/HEATER AIRFLOW
  37. RETURN AIR - TEMPERATURE
  38. RETURN AIR - HUMIDITY
  39. EVAP. AIR TEMPERATURE
  40 OUTSIDE AIR TEMP

Fig. 4 — Bus instrumentation.

operation would be communicated to the mechanic and would require a response from him, and all test results would be printed out on hard copy for record keeping.

Three major bus components that lend themselves to a significant amount of automated testing are the engine, the starting/charging system, and the air-conditioning/heating system. The engine can be further subdivided into the fuel/air/exhaust subsystem, the lubrication subsystem, the cooling subsystem, and the power subsystem.

Engine test

Engine inspection procedures are characterized by a number of pressure and temperature measurements designed to assess the amount of mechanical wear or clogging internal to the engine. Measurements that might be automated in a good inspection program are set forth in Tables III - VI.

The starting/charging system tests are normally voltage and current measurements designed to assess the electrochemical/mechanical condition of the components and the electrical condition of cables and connectors. Tests for this system are listed in Table VII.

Table IX — Bus instrumentation summary.

Engine electrical
- 4 current shunts
- 1 temperature sensor
- 2 level switches
- 8 electrical connections

Engine lubrication
- 1 temperature sensor
- 1 switch
- 2 electrical connections

Fuel/air exhaust
- 1 tachometer
- 5 pressure switches

Air conditioning
- 2 current shunts
- 2 tachometers
- 3 pressure transducers
- 4 temperature sensors
- 1 airflow sensor

Engine
- 1 pressure transducer
- 1 liquid level switch
- 3 temperature sensors
- 3 electrical connections

Air-conditioning/heating system tests

Air-conditioning/heating system inspection tests encompass pressure, temperature, and airflow measurements to determine first the state of the refrigerant/heating subsystem and then the airflow/heat-transfer subsystem. For long-distance buses, it is necessary to inspect the system under one set of ambient conditions and deduce if it will work under a different set. For example, inspection of an air-conditioning system performed in a cool northern state must ascertain if that same system will perform when the bus reaches a hot, humid southern state. The converse is true with respect to tests on the heating system. Tests determined for this system are shown in Table VIII.

Bus instrumentation

The location of sensors for these inspection tests are shown in Fig. 4. Some tests involve alarms, which would be observed at the driver's seat. Switch closures to activate these alarms are located in the engine compartment. The types of instrumentation required are summarized in Table IX.

Summary and conclusions

In the evaluation study on which this paper is based, the authors concluded that the 16,000-mi preventive maintenance inspection was a key bus maintenance operation, which would benefit from test automation. The ATE developments previously described were assessed with regard to satisfying the measurement and operational requirements for this inspection.

Vehicle test meter

The VTM fully met the measurement requirements that were established for bus inspection. This device had the capability to interface with buses that were prewired with an instrumentation system (harness, sensors, and inspection connector), and also with buses that were not specially instrumented (through the use of an attachable transducer kit). The front panel flip cards could be structured to interleaf the mechanic manual actions and the automatic tests in the proper sequence for the entire inspection routine. Each test would be under the direct control of the mechanic, who would be required to enter the proper test number, read the test results displayed in digital form in the display window, and compare the test results with the limits printed on the flip cards. The purpose of this device is to provide quick, unambiguous test parameter information to the mechanic who, in turn, is required to make the diagnostic decisions. In some applications, there might be a strong desire for a permanent hard-copy printout of all test results. Overall, the VTM was found to be well suited to the defined maintenance inspection requirements.

Vehicle readiness unit

Since the design of the VRU is intended for on-board mounting applications, it was outside our immediate area of interest, which was 16,000-mi inspection.

Programmable diagnostic unit

The PDU also fully met the measurement requirements that were established for bus inspection. This device includes a computer-controlled, tape-programmed capability and a mechanic/operator handheld set communicator, which contains both a display and a keyboard and has several advantages over the VTM design. This device can automatically sequence through the entire inspection procedure, performing both automatic tests and conveying instructions to the mechanic for all required manual actions and inspections. In addition, since this device contains a memory unit, it has extensive diagnostic capability. This interpretive diagnostic power can be used to minimize instrumentation requirements of sensors, transducers, and electrical pick-offs. The present design provides for an interface with the hard-copy printout. However, the PDU hardware is not as advanced in its development phase as the VTM, and it obviously would be a more expensive device in production.

Cost-benefit analysis

The evaluation study included postulating a bus inspection system based on the VTM design and instrumenting the bus fleet with on-board sensors, wiring, and connectors. The following conclusions were established:

1) The investment in ATE and the bus instrumentation would realize a payback in less than two years of operation.
2) Mechanic man-hours for inspection would be reduced by 65%.
3) Road failures could be reduced by 22%. (Obviously, this area is restricted to those failures that could be prevented by better preventive maintenance and does not include such failures as flat tires, broken springs, or mechanical damage, etc.)
4) On-road engine failures requiring rebuild would be reduced by 60%.

Justification of investment

In past years, labor represented a small contribution to the overall cost of operation and maintenance of commercial vehicles. Investments in the development of systems and equipment aimed at minimizing the labor portion of maintenance cost simply were not cost-justifiable. However, during the past 20 years the investment represented in a commercial vehicle has more than doubled, and so has the cost of labor per hour. The improvements in the national highway system and the corresponding developments of complex and higher horsepower vehicle components have put pressures on keeping the vehicles productive and minimizing vehicle downtime for maintenance and service actions.[6] Further, there is a mechanic shortage now, which will grow more acute in the future. This is particularly true in the area of diesel mechanics, where high investments in training time to make a mechanic productive are required. Because of the growing complexity in the general automotive sector, the mechanic shortage will tend to grow, not diminish, with time. It appears that automatic test holds some of the answers to commercial vehicle maintenance, and that all that may be required is a hard look at the economics and cost benefits of such an application.

References

1. Editorial: "The special problem of buses," *Fleet Owner Magazine* (Jan. 1974) p. 59.
2. Studies, supporting most of this work performed on Contracts DAAE07-71-C-0235, DAAE07-72-C-0089, DAAE07-72-C-0340, DAAE07-73-C-0035, and DAAE07-73-C-0314.
3. Project "Wheels" Study, Hearings before the Committe on Armed Services, U.S. Senate, 93rd Congress, 1st Session on S. 1263 (May/June 1973) p. 1335.
4. Teixeira, N.A. and Pradko, F.; "Test equipment for automotive vehicles," presented at Automatic Testing 1973 Conf., Electronics Engineering Assoc., Brighton, England.
5. RCA developed techniques: U.S. Patents 3757570, 3757571.
6. Mannix, T.; "Diagnostic levels required for heavy-duty vehicles," presented at SAE Combined Commercial Vehicle Engineering and Operations and Powerplant Meetings, Chicago (June 1973) Paper 730659.

Non-contact instrumentation for engine testing and monitoring

S.C. Hadden | L.R. Hulls | E.M. Sutphin

A single transducer, held in a diesel engine's exhaust and coupled to special-purpose circuitry, can identify minor compression losses or fuel injection faults in less than one minute of testing. With additional signal processing, the system can also rapidly determine the engine's power output.

THE ROLE OF diagnostic systems for internal-combustion engines in improving the effectiveness of the maintenance process is now well established.[1,2,3,4,5] Early programs involving diagnostic inspection lanes showed that the time required for a complete diagnostic inspection posed a serious obstacle to the commercial viability of the approach. Unfortunately, the more detailed and more reliable diagnostic procedures require more extensive instrumentation and longer testing. In the military field the penalty for more extensive instrumentation can be even greater because protective armor may make the engine virtually inaccessible.

This problem is so critical for the military that they have already undertaken programs involving built-in test equipment,[6] where the use of transducers already installed on the engine reduces instrumentation time to the time it takes to plug in to a diagnostic connector located at some readily-accessible point on the vehicle. This approach is particularly attractive for tanks and other high-cost vehicles where the cost of the built-in equipment is in a favorable proportion to the cost of the vehicle.

This paper discusses another method for minimizing instrumentation time and thereby enhancing the viability of diagnostic test systems for both military and commercial use. In this approach, the diagnostic system uses signals that can be remotely sensed and, therefore, do not require transducers to be mounted on the engine under test. The signals that can be remotely sensed include exhaust-pressure pulsations, intake-pressure pulsations, acoustic noise, and pulsations in crankcase pressure. Of these, the first two are available to the outside world regardless of the inaccessibility of the engine. To limit the scope of this paper, only the exhaust pressure is discussed in detail, but the signal-processing techniques are applicable to other non-contact signals. The technique described here measures the power output of a diesel engine from a remote sensor receiving a signal from the

Reprint RE-22-2-14
This paper was presented in similar form at the SAE Automotive Engineering Congress and Exposition, Detroit, Mich., February 23-27, 1976.

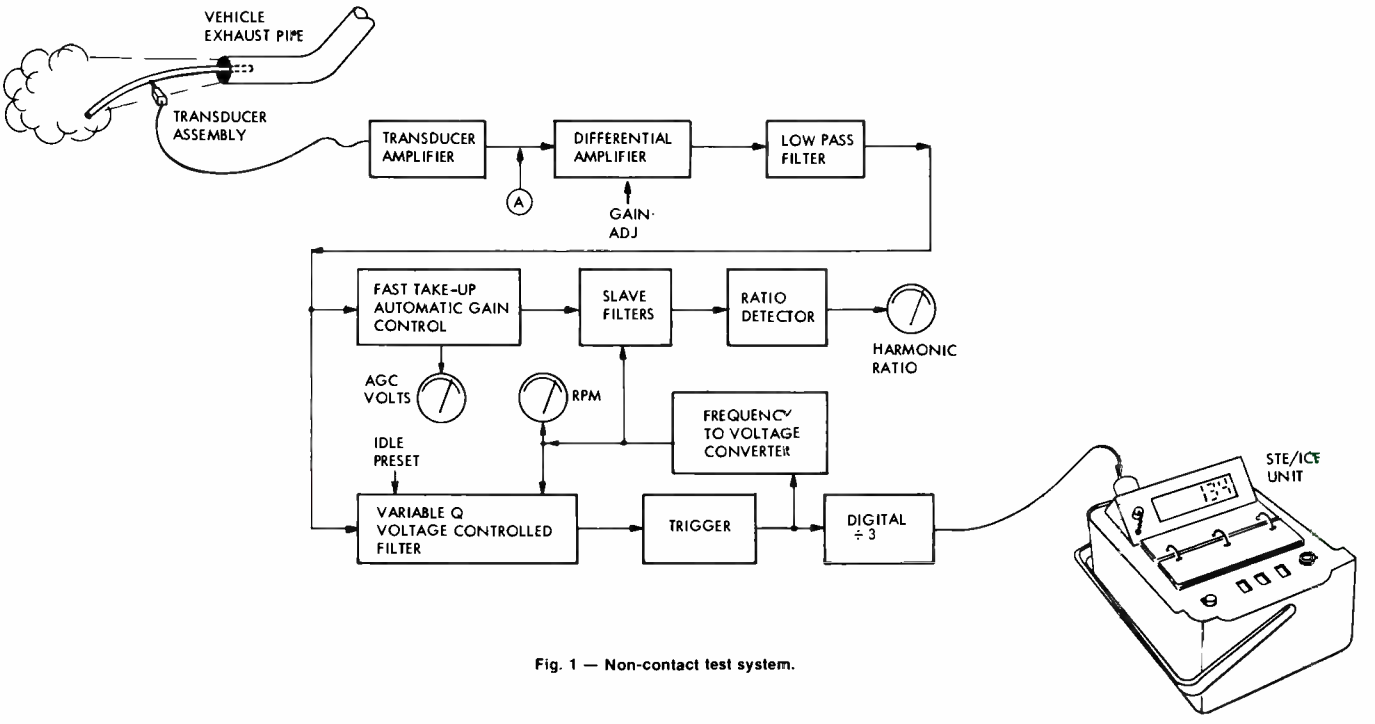

Fig. 1 — Non-contact test system.

Stephen C. Hadden, Non-electronic Test Group, Automated Systems Division, Burlington, Mass., graduated from Cornell University's co-op program in 1970 with a B.S. in Engineering Physics. During 1971 and early 1972, he was employed by a commercial diagnosis and maintenance firm which serviced private passenger cars. After joining the Non-Electronic Test Group at RCA in 1972, Mr. Hadden performed a study on the feasibility of built-in exhaust-emission monitors for motor vehicles, which included a survery of the state-of-the-art in exhaust-emission detection and measurement, and a series of dynamometer tests of diesel and gasoline engines to evaluate gas sensors. Since July 1973, he has been working on the development of automatable test and diagnosis methods of internal-combusion engines. This work has included detailed study and experimentation in the dynamic-pressure, flow, and optical properties of exhaust gases, and the development of specialized transducers for recording new diagnostic engine parameters. Mr. Hadden is a member of Sigma Xi and the SAE; he holds one patent and has four applications pending.

L.R. Hulls, Government Communications and Automated Systems Division, Burlington, Mass., received the BS in Physics and Electrical Engineering from Manchester University, England, in 1944 and has done considerable postgraduate work in England and the U.S. During his tenure as Section Chief in English Electric Company's Industrial Electronics Department, he was responsible for a variety of instrumentation and control projects, including the development of electronic ignition analyzers for internal-combustion engines. At Philco-Ford Corporation, he was section manager for vehicle engine diagnostic and checkout activity. Mr. Hulls acted as consultant to the Ford Motor Company for the special dynamometer in their new Service Reserach Center at Dearborn. Since joining RCA in 1968, Mr. Hulls' projects have included the demonstration of automatic engine ignition analysis using the Army's LCSS equipment, the testing of diesel engines and high-speed gear trains using an RCA-developed accelerometer, and a pattern-recognition analysis for inspection and life prediction of turbine engine bearings. He also performed the major instrumentation systems design on an automatic test system for J-79 jet engine fuel controls.

Eldon M. Sutphin, Engineering Scientist, Automated Systems Division, Burlington, Mass., received his BSEE from Pennsylvania State in 1965, and has studied on the graduate level at Northeastern University and Lowell Technological Institute. Since joining RCA in 1965, Mr. Sutphin has concentrated heavily in the area of analog and digital design for automated test systems. His design projects include work on the LCSS Waveform Conversion subsystem; redesign of the DIMATE Time Interval/Frequency Conversion subsystem; design of the NASA Data Bus Interface Encoding and Decoding subsystem; and analog, digital designs and system integration on the EQUATE program. More recently, he has been working in the area of non-electronic automated test systems, with the primary emphasis on automotive test equipment. His areas of responsibility include analog, digital, and tape-transport interface designs on ATE/ICE, STE/ICE, and the IR&D non-contact automotive test technology.

vehicle exhaust pipe. As well as being able to make this power measurement, which establishes the overall health of the engine, the technique can provide diagnostic information on malfunctioning engines.

The original work was done on a six-cylinder, four-cycle, normally-aspirated, military LD-465 diesel engine manufactured by Teledyne/Continental. Fig. 1 shows the equipment used to measure engine horsepower remotely. The input signal is obtained from a transducer assembly, which is hand-held at the exhaust pipe while the engine is put through an acceleration/deceleration cycle. The raw signal is processed by the electronic equipment to produce a pulse train whose frequency is proportional to engine speed. This pulse train is then fed to the STE/ICE (Simplified Test Equipment for Internal Combustion Engines) unit.[7] This particular unit, developed for the U.S. Army, has the capability of analyzing engine speed-change profiles. Combining this with a predetermined knowledge of the inertia of the rotating parts of an engine, a built-in microprocessor computes a factor linearly related to the horsepower generated during a full-throttle acceleration.

An essential element of the non-contact system is its variable-Q frequency-tracking filter, which extracts the speed information from the exhaust-pressure signal. To perform the power measurement, it passes the speed information as a variable-frequency pulse train to the STE/ICE unit.

Fig. 1 also illustrates a slave filter and ratio detector, which continuously indicate the amplitude ratio of selected harmonics present in the exhaust-pressure signal. As explained later in this paper, the harmonic-ratio signal provides a powerful indication of the existence of engine malfunctions.

Signal information

The investigation into remotely sensing engine parameters began with the assumption that the CFF (cylinder firing frequency) of the engine would be detectable in signals emitted by the engine. For the six-cylinder diesel under investigation, this frequency ranged from 35 Hz at low idle to 140 Hz at full speed. (E.g., 700 rev/min ÷ 60 sec/min × 3 firings/rev = 35 Hz at low idle.) Typical engine firing frequencies stay within the 10-to-500-Hz range. Recording and analysis of remotely-sensed engine signals showed that the CFF is indeed discernible. For example, the exhaust-pressure signal is a variable-amplitude non-sinusoidal signal that has a frequency component corresponding to engine CFF. In general, the amplitude is low during idle at either high or low engine speeds, or during engine deceleration with the fuel shut off. During acceleration, when the engine is working hard to provide the torque required to accelerate its own inertia, the amplitude is high. It was noted that when the amplitude is high, the signal approximates a sinusoid at engine cylinder firing frequency, whereas at low amplitude the harmonic content increases and the signal becomes very non-sinusoidal. This characteristic of the signal suggested the use of a variable-Q filter, which would vary its Q or damping ratio according to signal amplitude in a way which would enhance its ability to extract the CFF.

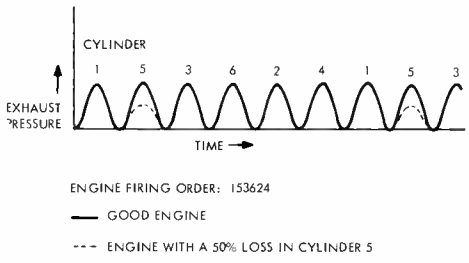

Fig. 2 — Computer-modeled exhaust pressure.

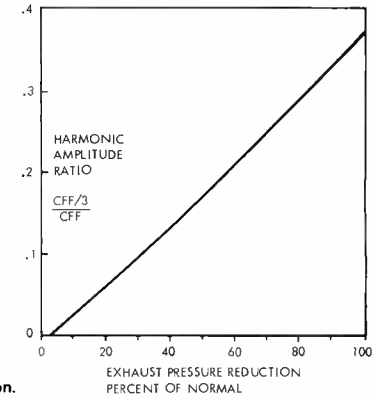

Fig. 3 — Harmonic ratio as a malfunction indication.

Malfunction indicators

The presence of a strong CFF signal component results from the fact that each cylinder-firing causes an equal-magnitude perturbation in the exhaust pressure. If one or more cylinders malfunction, then the uniformity will be destroyed and frequencies that are lower than the nominal CFF will be produced. The presence of these lower frequencies provides an immediate indication of the presence of a malfunction.

In order to investigate the formation of these low-frequency components, a simple model of the exhaust pressure was programmed on a digital computer. This model assumed a sinusoidal exhaust-pressure waveform, and the presence of a malfunction was considered to reduce the pressure amplitude for a particular cylinder by a certain percentage between two successive minima in the waveform. (See Fig. 2.) As well as demonstrating the rise in frequency content below CFF for single-cylinder faults, the model provides a useful insight into the sensitivities of frequencies to the occurrence of multiple-cylinder faults. Fig. 3 shows the increase in the amplitude ratio of the CFF/3 to the CFF calculated by the model as a function of exhaust pressure reduction for one cylinder.

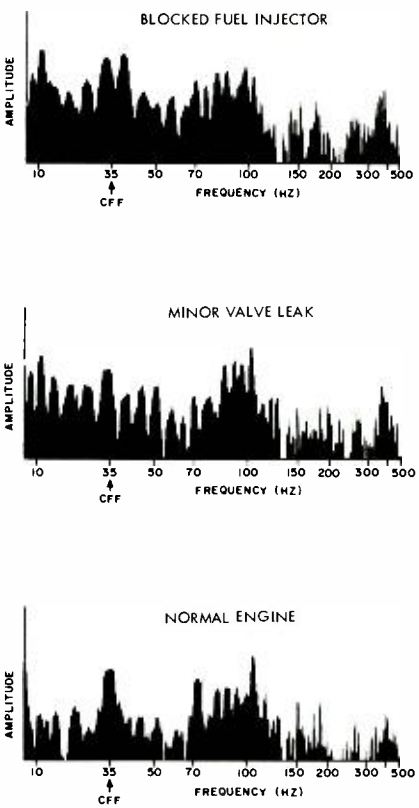

Fig. 4 — Exhaust pressure spectral content.

Spectral analyses of exhaust-pressure signals obtained on an actual engine are shown in Fig. 4 for a normal engine and an engine with two types of cylinder faults. These signals were recorded using a transducer assembly inserted a short way (one to five inches) into the tailpipe while the engine was operating at its low-speed idle of about 700 rpm. Note that for the normal engine the 35-Hz firing frequency is clearly a dominant signal component, matched in amplitude only by its higher harmonics at 70 and 105 Hz. Fig. 4 also shows the approximate spectral content of the transducer output when the six-cylinder diesel under test had one fully-blocked fuel injector, and the same analysis for an engine with a minor exhaust-valve leak. For this test the valve leak caused a 25% loss of compression in one cylinder. From this figure it can be seen that the amplitude ratio of a lower harmonic frequency to the CFF will be a sensitive fault indicator. Note that measuring the amplitude ratio also provides a convenient technique for normalizing the signal for variations in amplitude that may result from variation in the location of the transducer.

Power testing technique

Because the lower harmonics arise from the differences between the contributions to the signal by individual cylinders, they will not appear in the case of an engine which has uniformly deteriorated in all cylinders. However, such deterioration is detectable by the resulting loss in power output.

An evaluation of a diesel engine's full power output can be accomplished by evaluating dynamic speed measurements during a full-rack acceleration, letting the engine's own internal inertia act as the load. As the spectral analyses show, the engine speed information can be obtained by the exhaust-pressure transducer without contacting the engine.

The acceleration-burst test is performed as follows. The engine is accelerated to full speed from low-speed idle by abruptly moving the fuel control (accelerator pedal) to the full-power position. The speed is recorded as the engine accelerates and is held at full speed by the governor. Then the fuel shutoff is activated, cutting the fuel-feed sharply to zero. The engine is decelerated to a standstill by its frictional load, pumping losses, accessory load, etc. The speed recording then gives two important quantities: the full-power acceleration rate and the zero-power deceleration rate.

If we define

α_a = full-power acceleration rate
α_d = zero-power deceleration rate
T_B = brake torque output of engine
T_F = sum of the torques contributing to deceleration
T_I = indicated torque = $T_B + T_F$
I = effective moment of inertia of the rotating system system, including internal engine parts, flywheel, fan, alternator rotor, etc.

then at any given engine speed it can be said that

$$T_I = T_B + T_F = I\alpha_a + I\,\alpha_d$$

I is a constant which can be caluclated or measured empirically, and α_a and α_d can be determined at the speed of interest from the slopes of the engine-speed curve obtained during an acceleration-burst test. Of course, the power can then be obtained directly from the torque and speed. The full power output can thus be quickly determined without a dynamometer.

Test system hardware

The exhaust-pressure transducer assembly is constructed of a copper tube and a commercially-available variable-reluctance pressure transducer. The copper tube is half-inch inside diameter, cut to a length short enough so that the natural frequency of the tube is above the range of interest. It is curved for convenience when holding it in the exhaust stream. The transducer is mounted in the center of the length of the tube.

The signal from the exhaust-pressure transducer does not lend itself directly to easy processing and measurement because it has gross variations in harmonic content and amplitude. The block diagram in Fig. 1 gives a general overview of the processing required to present normal measurement devices with useable inputs. There are two distinct areas of processing: a tracking filter that locks onto the waveform and extracts the CFF; and hardware that provides spectral data on the pressure waveform. A more detailed description of these two areas follows.

Our original goal was to track the CFF during all engine operating conditions, including acceleration burst. It was demonstrated that with phase-locked-loop techniques, the classical problem of narrow bandwith versus tracking speed was present, as a result of the "noise" content of the exhaust-pressure waveform and the abrupt change in frequency during acceleration-burst testing. To overcome this, a frequency-tracking filter was designed, using a voltage-controlled filter and a frequency-to-voltage converter in a loop configuration. The nearly sinuosidal output of the filter was "clean" enough to shape and count directly. The shaped signal was then fed to a frequency-to-voltage converter to determine the center freqeuncy of the filter, thus enabling the filter to track the changing-frequency input signal. This concept was successfully realized in hardware.

Frequency tracking

The voltage-controlled filter was constructed using a minimum of hardware by synthesizing a basic bandpass filter and adding multipliers to make it controllable by a dc voltage. These multipliers were

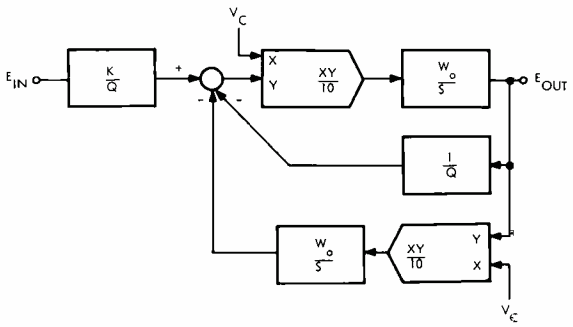

Fig. 5 — Voltage-controlled filter.

added to vary the center frequency of the filter; they have the effect of changing the constant of integration for the integrators used to synthesize the transfer function. Fig. 5 shows the filter in block-diagram form. In it s = the laplace operator, ω_o = natural frequency, Q = center frequency/bandwidth, and K = gain at center frequency.

To make a tracking filter using the voltage-controlled filter, a discrimator (frequency-to-voltage converter) must included within the loop. In this case, desirable qualities for the discriminator are a fast response without output decay or ripple. Since an ordinary one-shot/filter arrangement introduces extra lag into the loop as well as pulse-to-pulse ripple at the filter, a more sophisticated analog/digital approach was used. Fig. 6 is a block diagram of the discriminator used in the non-contact system. The circuit measures the period of each and every input cycle and converts it to a dc voltage proportional to frequency. The counter continuously counts a high-frequency clock while, at every positive transition of the input, the contents of the counter are strobed into a storage register and the counter is reset. This storage register programs a digital-to-analog converter, the dc output of which is proportional to the period of the input. An analog divider takes the reciprocal of this value and provides a dc voltage proportional to the input frequency. This produces an instantaneous output based on the last measured period without output decay or ripple.

A tracking bandpass filter's ability to follow a rapid frequency change is inversely proportional to the Q of the filter. The spectral content of the exhaust-pressure waveform (Fig. 4) requires a high Q to extract the CFF at idle; however, during the acceleration burst, when the CFF changes most rapidly, the waveform is "cleaner," and requires a lower Q. Thus, to improve the tracking ability of the filter, the Q was made a dynamic variable. Since the amplitude of the exhaust-pressure signal increases during the cleaner and most rapidly-changing frequency portion of the waveform, the Q of the filter was made a function of the filtered signal's amplitude. As may be seen from Fig. 5, one of the feedback paths is $1/Q$. Fig. 7 illustrates the variable-Q filter, in which the fixed $1/Q$ path is replaced by a multiplier to vary the Q. In it, the output of the filter is examined by the peak detector and amplified by α, and a voltage reference is subtracted from it to provide an offset in the transfer function. This difference signal is then fed into a multiplier, which functions as a variable-gain element in the $1/Q$ feedback path.

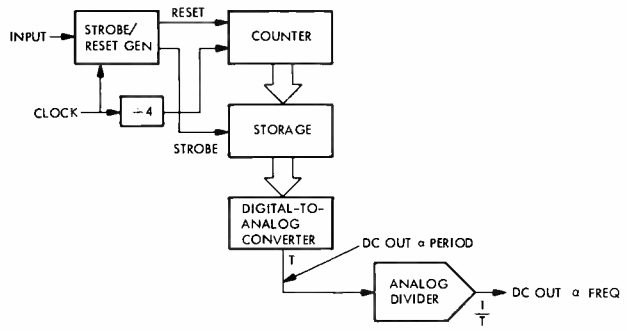

Fig. 6 — Frequency discriminator.

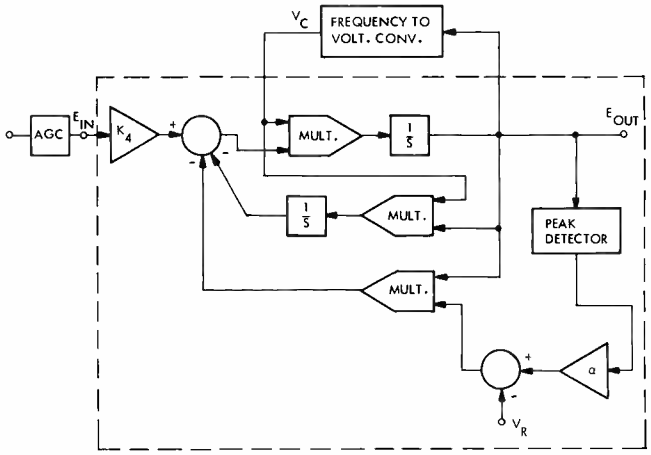

Fig. 7 — Tracking filter with automatic Q control.

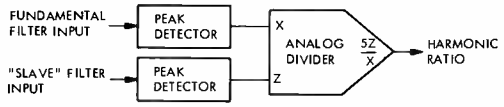

Fig. 8 — Harmonic ratio detector.

In addition to the voltage-controlled filter used in the tracking filter, similar "slave" filters with fixed Q, tuned by the same discriminator, are used to extract the fundamental and subharmonics from the input signal. The outputs of these filters are routed to a ratio detector to provide meaningful spectral information about the input signal. Fig. 8 illustrates the ratio detector in block form. An AGC (Automatic Gain Control) circuit prior to the "slave" filters and ratio detector normalizes the signal prior to spectral analysis.

Experimental results

An electronic engine-test system developed by RCA for the U.S. Army was used as a standard to evaluate the performance of the non-contact test system. Known as the STE/ICE system, it employs a magnetic-pulse tachometer on the engine camshaft to digitally measure and display engine speed. The error of this measurement is less than 0.5%. Using this speed measurement capability, the STE/ICE system can determine the full-power acceleration rate and zero-power deceleration rate of the engine during an acceleration-burst test. As described above, the sum of these rates is proportional to the indicated torque developed by the engine.

The non-contact system's speed-measuring ability was tested by direct comparison with the speed measured by the STE/ICE system. Early models of the

Table I — Harmonic ratio x5 for LD-465 diesels.

	Engine condition		
Engine A	*Normal*	*Bypassed injector*	*Minor valve leak*
Low idle	0.5	7	7
Full speed	2	10	3
During deceleration	1	1	3
Engine B			
Low idle	1.2		
Full speed	2.5	Not tested	Not tested
During deceleration	1		

non-contact system agreed well with the STE/ICE measurement only when the engine was in good condition. The introduction of malfunctions, which made the engine run roughly, caused the tracking filter to lose lock on the signal and output an incorrect speed value. Improvements in the signal processing have resulted in tracking capability that allows the circuit to track the engine speed even when the engine operation is erratic. For example, when one fuel injector on the six-cylinder test engine is bypassed, simulating a fully-blocked injector, the non-contact speed measurement agrees with the STE/ICE measurement within ±1% over the entire speed range.

As a test of the non-contact system's dynamic tracking ability, it was used as a speed-signal source to the STE/ICE system for measuring the indicated torque output of the LD-465 engine by the acceleration-burst method. Then the test was repeated using the magnetic pickup as the speed-signal source.

This was done with the engine in three different conditions: nominally good condition (i.e., no known faults); one fuel injector bypassed; and one exhaust valve leaking slightly. The exhaust-valve leak was induced by overtightening the valve adjustment until the compression pressure (engine hot and running) dropped to 75% of its original value. This resulted in approximately a 3% loss in peak torque output. In all three cases the agreement between the torque measurement with the non-contact signal source and that with the hard-coupled mag-pickup source was excellent.

The repeatability of the tracking-circuit performance was checked using magnetic tape recordings because the test engine itself may vary in torque output as much as five percent from one test to another.

Recordings were made of the transducer assembly output (point A in Fig. 1) during acceleration-burst tests with the engine in each of three above described conditions. By testing the circuitry with the tape instead of the live engine, variations in the engine itself were eliminated. In these tests the engine torque output measurement was repeatable within one per cent for each of the three engine conditions.

As discussed earlier, it was believed that the harmonic ratio is a sensitive indicator of engine condition. For the six-cylinder test engine, the ratio is defined as the amplitude of the exhaust-pressure signal component occurring at the CFF divided into the amplitude of the component occurring at one-third of the CFF. The circuit built to extract this ratio actually gave the ratio times five, for convenience of gains in the circuit. Tests were made using two LD-465 engines in normal condition and one engine with the two previously-described faults singly induced. The tests were performed by simply inserting the pressure transducer assembly a short way into the exhaust pipe and running acceleration-burst tests while recording the ratio. The results are tabulated in Table 1.

For normal engines, the ratio has a value less than 1.5 during idle and decleration, and less than 3 at full speed. The bypassed injector raises the ratio to 7 at idle and 10 at full speed. Because the injector fault has no effect when the fuel is shut off, the ratio is unaffected by it during the deceleration. The valve fault, in spite of being very minor, also lifts the ratio to about 7 at idle. But at higher speed, where compression losses have less time to affect engine operation, the ratio is only mildly increased over the normal value. During deceleration, the valve fault still shows up as an increase to a ratio of 3.

If this non-contact system were to be used as a diagnostic tool in its present form, performing an acceleration-burst test would allow evaluation of engine torque output and, by comparison of the harmonic ratio to normal values during low idle, full speed, and deceleration, identification of malfunctions in the fuel-injection or compression system.

Conclusions

An experimental system which can make useful diagnostic measurements on a diesel engine without physical connections to the engine has been assembled. The input to the system can be exhaust pressure, intake pressure, or crankcase pressure, obtained by simply holding a pressure transducer assembly in the exhaust, air inlet, or oil filter, respectively; or the input can be engine or exhaust noise. Specially-developed circuitry permits the system to determine engine speed and the amplitude ratios of selected spectral components in the signal that have been found to be very sensitive to the presence of some engine malfunctions. The precision of the system's dynamic speed determination allows it to be used for non-contact acceleration burst testing, which permits calculation of the power produced by the engine.

Harmonic-amplitude ratio measurements and an acceleration-burst test can easily be performed in half a minute. Thus, the non-contact system has potential for evaluating engine condition extremely rapidly by power output measurement and fault detection.

References

1. Fineman, H.E.; Fitzpatrick, T.E.; and Fortin, A.H.; "Simplifying automotive test equipment through use of advanced electronics," presented at IEEE NEREM 1974, Boston, Nov 1974.
2. Barry, R.F; and Laskey, J.M.; "Application of automatic test equipment to bus maintenance," paper 740532, presented at SAE Fleet Week 1974, Chicago, June 1974.
3. Bokros, P.; and Teixeira, N.A.; "Current status and activities in automotive ATE," presented at IEEE INTERCON, 1974, New York, Mar 1974.
4. Pradko, F.; and Teixeira, N.A.; "Test equipment for automotive vehicles," presented at the Electronic Engineering Association's Conf.—Automatic Testing 1973, Brighton, England, Nov 1973.
5. Garland, P.; Pradkoo, F.; Sarna, D.; and Teixeira, N.A.; "Diagnostic instrumentation for military vehicles," paper 730658, presented at SAE Fleet Week 1973, Chicago, June 1973.
6. H.F. Fineman, "Go/No-go indicator system for vehicle readiness testing," presented at IEEE Automotive Systems Support Conf., Philadelphia, Nov 1972.
7. This STE/ICE equipment was developed by RCA for the U.S. Army Tank-Automotive Command under contract number DAAE07-73-C-0314.

Portable test equipment for army vehicles

G. Grube | D.J. Morand

This simplified and automated system uses sensor inputs and logic circuitry to diagnose engine faults in army vehicles. The design concepts and trade-offs, human engineering, and environmental considerations discussed here have resulted in a proven system now slated for initial production.

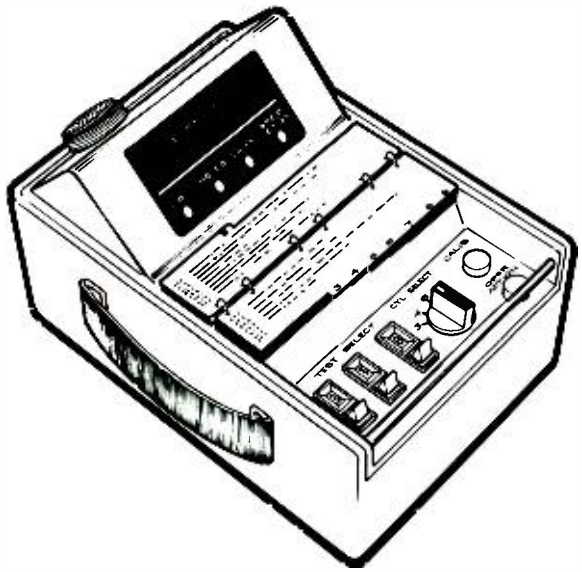

Fig. 1 — Design concept of Vehicle Test Meter (VTM).

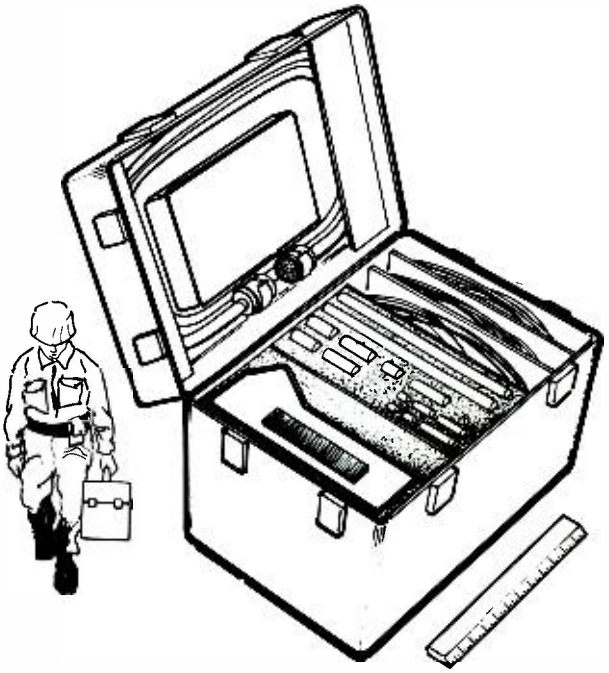

Fig. 2 — VTM and Transducer Kit (TK) design concept.

THE SIMPLIFIED TEST equipment for internal combustion engines (STE/ICE) was developed for the U.S. Army. The objective of this development was to improve the cost, simplicity, accuracy, reliability, and efficiency of making repairs to automotive mechanical and electrical components. The hardware for the STE/ICE was to include sensors, harnesses, diagnostic connectors and a Vehicle Test Meter (VTM) for both gasoline and diesel powered wheeled and tracked vehicles.

The VTM was to be used on vehicles both with and without built-in diagnostic systems. The contract called for RCA to build in diagnostic systems into four different types of vehicles. The vehicles selected by the Army were a jeep (M151A2), a 2-1/2 ton truck (M35A2), an armored personnel carrier (M113A1), and a tank (M48A3). The VTM was to be used in conjunction with a Transducer Kit (TK) to test those vehicles that were not equipped with diagnostic harnesses. The VTM and TK were to be made as a portable package transportable by one man.

Reprint RE-22-2-15
Final manuscript received March 19, 1975.

Trade-offs

To arrive at the original design concept a number of trade-offs were evaluated. Some of the most important considerations pertained to such areas as the on-vehicle diagnostic connector (DC), VTM-to-DC interface, and VTM-to-TK interface.

The criteria applied to the selection of the diagnostic connector included such factors as cost, availability, ruggedness, ease of connecting, contact type, size and number, and environmental resistance. All known military and commercial connectors were considered. The selected connector is a recently developed version of the MIL-C-5015-type standard circular connector. The diagnostic connector has 54 crimp-type contacts, a quick-connect bayonet coupling device and accepts AWG 16 size wire.

The DC-to-VTM interface constituted a critical link from both the machine and human standpoint. Several means of connection such as direct coupling, use of coiled cord, pigtail-type cable, and separate jumper cable were evaluated. After considering the differences in vehicle configurations, available space, ease of handling, and maintenance, the jumper cable solution was chosen.

Initial design called for simultaneous use of up to four transducers when checking out vehicles which do not have the built-

in diagnostic harnesses. The cable length had to satisfy the requirements of the largest vehicle — the tank. This made the cables 20 feet long. To avoid the "spaghetti effect" on the smaller vehicles such as jeeps and trucks, the unused portions of the cables had to be stored. Self-retracting reels were considered the most suitable devices for this purpose. Since each of the cables contained about a dozen wires, the reels made the equipment very bulky. This approach, besides making the VTM and TK package large and heavy, tied the equipment storage case into the test link-up. Such an arrangement was undesirable because it made the use of test equipment less convenient. By reducing the simultaneous transducer application to two, the interconnection problem was solved by a three-legged, branched cable. The latter consisted of a 20-foot power branch and two very short transducer connecting branches. These branches accepted extension cables for use, as needed, with either one or two transducers.

Various concepts were explored to arrive at the most desirable configuration for the VTM and TK. Such industrial design and human factors as packaging, handling, environmental protection, practicability, esthetics, and control/display implementation were carefully considered and a number of conceptual sketches prepared. Figs. 1 and 2 show the preferred version of the original design concept. This concept was accepted by the STE/ICE program personnel and the customer. The final hardware design retained, with some minor variations, the originally established design features. The VTM (Fig. 1) was conceived as a small, rugged, sealed (against rain) unit, with inclined display, attached test cards, and protected, easy-to-operate controls. A foam cushioned transit case (Fig. 2) was to store the VTM, transducers, and associated cables.

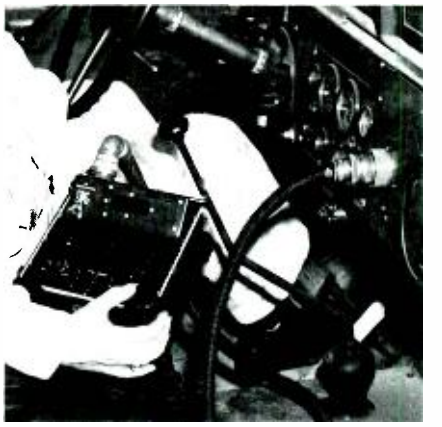

Fig. 3 — VTM used with built-in harness.

Design concept

The STE/ICE system consists of three functional elements: diagnostic harnesses, vehicle test meter, and transducer kit. The diagnostic harnesses interconnect the transducers and sensors with the 54-pin diagnostic connector on the vehicle instrument panel (dashboard). Fig. 3 shows the VTM (breadboard model, less the test cards) connected to the built-in harness for diagnosing faults in an Army 2-1/2 ton truck. Fig. 4 shows the hardware of the portable portion (less the built-in vehicle harnesses) of the STE/ICE system. This equipment is known as the VTM and Transducer Kit. The cables and the current and temperature probes are common to both modes of the VTM usage—with and without the built-in vehicle diagnostic harnesses. The other items such as pipe fittings, adapters, and transducers are used to instrument vehicles at the time of fault isolation.

The entire VTM and TK package weighs 47 pounds. Of this amount the VTM constitutes 12.0 pounds, the transit case 15.0 pounds, the storage tray assembly 10.00 pounds, and the rest is cable weight. With the case closed the assembly measures 12.0 × 18.0 × 13.8 inches in size. The VTM, storage tray, and transit case are finished in the Army olive drab color.

G. Grube, Sr. Project Member, Technical Staff, Automated Systems, Burlington, Mass., received the BME from Auburn University in 1952. After service in the Army as a mechanical engineer, he joined RCA in 1955. Mr. Grube has had responsibilities for a variety of ground, airborne, and space hardware. Of the ground type, he designed the signal simulation, depot, and antenna test range equipment for the MA-10 and a maintenance facility for the ASTRA fire control system. He participated in the development of mechanical standards and hardware for the Dyna-Soar program and the design of the Atlas launch control consoles. He led cost reduction and engineering documentation work on the HAWK checkout equipment and was involved in the development of the multi-purpose test equipment for other Army missiles. Mr. Grube designed airborne equipment, supported production, and performed environmental testing on the E-4, E-6 and MA-7 fire control systems and ARC-142 transceiver. In the space equipment area, he has played significant roles from technical proposals through design and verification of the LM Communications Subsystem, Lunar Communications Relay Unit, and CSAR lunar sounder. More recently he has been involved in the development of automotive diagnostic equipment, and AEGIS test and monitor central.

D.J. Morand, Sr. Project Member, Technical Staff, Automated Systems, Burlington, Mass., received the AE in Mechanical Engineering from Worcester J.S. in 1955 and a BS in Mechanical Engineering from Tri-State College in 1957. Upon joining RCA in 1958, Mr. Morand worked on the Astra Data Link Coupler for the CF-105 aircraft, the Converter Signal Data Unit, and the Radio System Analyzer Unit, checkout equipments. He was responsible for harness layout and wire routing for the AN/DRR-1 Coupler Units used in the Bomarc missile, and also for a production redesign of the servomechanisms in these units. Mr. Morand also worked in close liaison with the Perkin-Elmer Company on the AN/FSR-2 telescope magnetic shielding and interface problems such as cables. He was responsible for the thermal design of the ATCA and Rendezvous Radar Power Supplies on the LM Programs. On Project "N" he was responsible for thermal design of a temperature controlled narrow bandpass optical filter He was a co-author on a technical paper on this filter design. Following Project "N" he was responsible for the thermal design of a laser altimeter to be used on the Apollo 16 mission. He was selected as engineer of the month (April 1971) for his work on the Laser Altimeter program.

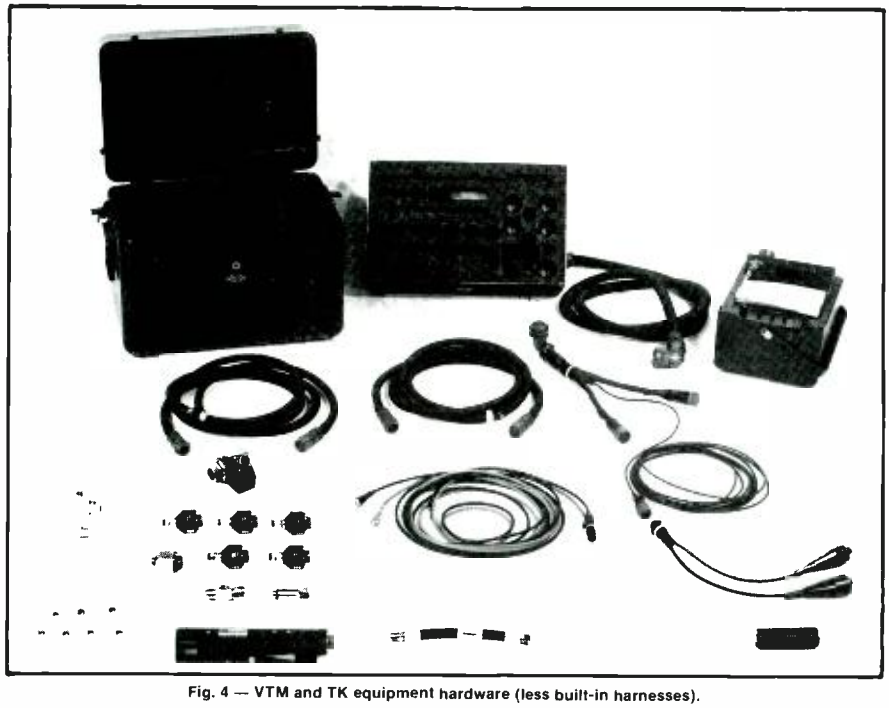

Fig. 4 — VTM and TK equipment hardware (less built-in harnesses).

Fig. 5 — Vehicle test meter.

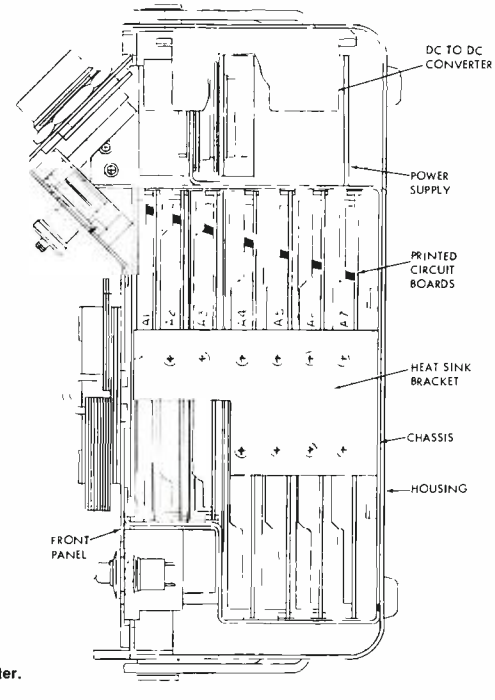

Fig. 6 — Cross section of the vehicle test meter.

Vehicle test meter

The portable VTM is the main element of the STE/ICE system. It contains the input-output devices and the necessary measurement and logic circuits. The VTM is able to measure all the signal outputs from the built-in diagnostic harnesses and transducers of the TK. The VTM combines in a single instrument the capability of a low-voltage circuit tester, multimeter, tach dwell meter, and compression and vacuum testers.

In designing the VTM, solutions were needed in such areas as human factors, physical characteristics, moisture sealing, heat transfer, maintainability, and ruggedness. The resultant design is depicted in Figs. 5 and 6. These figures show the front view and a longitudinal section of the VTM. The unit breaks down into two subassemblies — the panel/chassis and the housing. Of these, the front panel, chassis, printed-circuit boards, housing, power supply, and dc-to-dc converter are the major components. The front panel besides serving as the closure and structural element for the top surface also mounts all the input and output devices of the VTM. The upper portion of the panel is raised to afford better visibility for the display which provides readouts of the measurements and messages.

All types of readout devices were considered, but only the incandescent filament type was bright enough for use in direct sunlight. The selected display is made up of flatpack style, plug-in devices which are mounted on a printed-circuit board behind a protective window. The latter also doubles as a neutral density light filter that enhances readout sharpness and reduces glare and background clutter. Of the two connectors—also located in the raised panel area—the larger one serves to interface the VTM with the diagnostic connector or TK. The other one attaches the test prod cable for voltage and resistance measurements. The test cards list the tests together with their limits and three-digit test numbers. The mechanic uses the test numbers to set up the test on the three lever-actuated digital switches in the lower portion of the panel. Then, upon pushing the test switch in the right corner, the display reads out the measurement. The switch in the lower left corner selects the number of cylinders of a test vehicle. It is used only with the TK as the built-in harnesses already contain the vehicle data.

The panel, chassis, and plug-in boards form a removable assembly which, once the panel and chassis screws are removed, can be lifted out of the housing assembly. The chassis contains seven multilayer printed circuit boards with edge-type connectors. The seven mating board connectors form a wire wrap back plane. With the panel/chassis and housing assemblies separated all electronic circuits are accessible for servicing.

The power supply and dc-to-dc converter make up the larger subassemblies, and

they dissipate significant amounts of heat. Therefore, these two subassemblies are mounted directly to the inside walls of the VTM housing. The latter is made up of a commercially available deep-drawn aluminum box (8.38 × 11.50 × 4.50 × 0.060 in) and flange extrusion. Four rubber feet on bottom and a pivoting plastic covered handle that locks in the carrying position round out the housing assembly.

When assembled the panel fits inside the flange of the housing to form a rugged assembly. Further, corner bumps on the housing protect the panel controls against damage during falls on flat surfaces. In addition to being able to take accidental falls on floors and vehicle metal bodies, the VTM is also protected against entry of dirt, dust, and rain water. All panel components are of the sealed type, and all joints and penetrations of the VTM enclosure, including the outside screws, incorporate appropriate seals.

Thermal design

The VTM thermal problem consisted of finding a solution to several difficult design requirements:

1) To dissipate a large amount of heat in a small, portable box.
2) To assure reliable operating temperatures for high heat generating components on printed circuit boards.
3) To provide safe handling concitions for the operator when the VTM is exposed to high ambient temperatures and solar radiation.

The VTM has to dissipate 30 watts. Of this amount, approximately one half is dissipated by one major component — a purchased dc-to-dc converter. The remaining heat was created by the power supply and the printed circuit boards. On the boards, the main heat generators were the programmable memory chips. Each integrated circuit dissipated as much as a watt; one board contained eight IC's.

Further, human engineering design guides indicate that a temperature of 130°F is uncomfortable to the touch and 140°F can cause burns. Yet the VTM design guide called for operation in an ambient of 125°F with solar radiation. This can effectively raise the equipment temperature—a well-known fact which may be verified by noting how hot the hood of a car gets in a parking lot on a sunny summer afternoon.

In an effort to fulfill these requirements certain thermal guidelines were established during the initial mechanical layout phase of the VTM design. These thermal guidelines included the following:

1) Establishing the dissipation level of each component.
2) Providing minimum thermal resistance paths to the VTM case.
3) Minimizing hot spots by spreading out the higher dissipators to the extent allowed by electrical design parameters.
4) Screening the thermal characteristics of the various candidate components.
5) Reducing heat dissipation by switching of power.
6) Minimizing thermal resistance losses at the various interfaces in the assemby.
7) Selection of finishes with the best emissivity and absorptivity characteristics for radiational cooling.
8) Optimizing the configuration of the chassis for maximum efficiency for free convective cooling of the VTM.

A preliminary thermal analytical model was developed for the VTM following completion of the initial layout. Computer results for this model indicated that some problem areas existed in the printed wiring board areas.

The printed-wiring board designs were modified by extending portions of the aluminum stiffeners on the boards down over the surface area of the boards. The higher dissipating components were mounted directly upon these aluminum extensions and bonded down with thermally conductive adhesive. The top of each stiffener was bolted to an aluminum L-shaped plate which, in turn, was bolted to the VTM case. The thermal model was updated to reflect this design change and an additional computer run was completed. The results indicated that the printed wiring board design was now satisfactory.

A series of design variations and computer analyses were then completed to evaluate such other problem areas as the dc-to-dc converter mounting and the VTM external interface by:

1) Adding a finned heat sink to the VTM wall where the dc-to-dc converter was mounted.
2) Mounting the dc-to-dc converter directly to a finned heat sink exposed to the ambient and thermally decoupling the heat sink from the VTM.
3) Varying the finish of the exterior surfaces of the VTM exposed to sunlight.

Of these, approach 3) indicated the most significant thermal gains. The VTM, painted with a standard olive drab paint having a solar absorptivity coefficient of 0.94, had peak solar loads in excess of 50 watts or almost twice as much as the dissipated load. A white paint with a solar absorptivity coefficient of 0.22 would reduce the solar load to approximately 12 watts, but a white VTM resting on an olive drab vehicle in a combat area is inappropraite. Also, the white finish would not stay white in a garage environment. The results, however, did indicate that a significant reduction in the solar load was required.

Further investigation into solar heat reflecting coatings disclosed that the U.S. Army Coating and Chemical Laboratory had formulated an olive drab paint which, in the infrared region of the solar spectrum, reflects 50 to 60% of the solar energy compared to 6% for standard olive drab paint. This is significant since 52% of the 360 Btu/h-ft^2 of solar energy impinging on a surface is in the infrared region of the spectrum. The specially formulated solar reflecting paint reduces the solar load to between 250 to 160 Btu/h-ft^2, and it was selected for the VTM. The model was adjusted to reflect the final inputs. Subsequent computer runs indicated that an acceptable VTM thermal design had been achieved.

The thermal model was developed in the following manner. Nineteen locations were selected in the VTM assembly in areas where computed temperatures were desired. Each preselected location was then assigned an identification "T" number called a node. A nodal network was then developed which showed the heat transfer couplings from node to node. These couplings represented heat transfer by free convection, radiation, and conduction. A portion of the network is shown in Fig. 7. The magnitude of each conductive path was hand calculated as a thermal conductance value. All of the parameters necessary for calculating the free convective film coefficients and radiational couplings were also included as inputs in the transient analysis thermal program. The free convective couplings and radiational couplings change in magnitude as a function of temperature and the properties of the air film. The computer program continuously

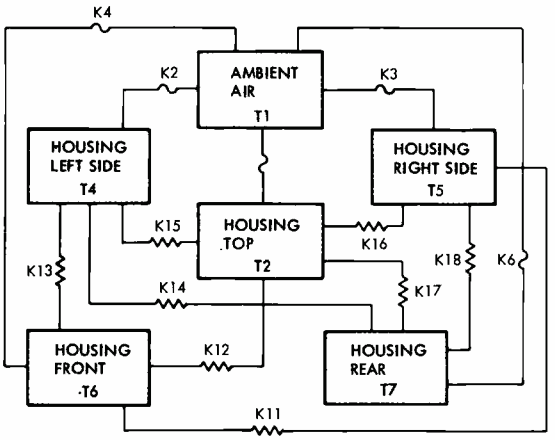

Fig. 7 — Vehicle test meter nodal network (partial segment).

recalculates these couplings as the temperatures change.

The computer program written for the model was a Tel-Comp time-sharing program. Heat balance equations were written for each node in the model as shown by the following example for node T2 of Fig. 7.

$$I_2 = K_1(T_1 - T_2) + K_{16}(T_5 - T_2) - K_{17}(T_7 - T_2)$$

$$I_2 = I_2 + K_{15}(T_4 - T_2) + Q_2 \text{ solar}$$

where:

I_2 = net heat balance for node T2 at any given time in Btu/h

K = thermal conductance value between the various nodes in Btu/h - °F

T = temperature of various nodes in degrees F.

It should be noted that at time of power turn-on all temperatures are equal to the ambient temperature. Therefore, at time zero, $I = Q$, where Q = the dissipated or solar heat at a given node. The program, starting at time zero, calculates the net heat balance at each node for a given elapsed time period.

After calculating these values for I_2, I_3, I_4, etc., the program calculates the temperature rise at each node by the following equation:

$$T_2 = T_{2P} + I_2 \times dt/mc_{p2}$$

where:

T_2 = new temperature for node T2

T_{2P} = previous temperature for node T2

I_2 = heat balance for node T2 in Btu/h

dt = time increment in hours

mc_{p2} = thermal capacitance for node T2

m = mass of node T2 in lb

c_{p2} = specific heat for material of node T2 (Btu/lb-°F).

After calculating the new temperatures for all nodes, the loop is repeated until steady state temperatures are obtained. A big advantage of this program is its versatility. The equations can be quickly changed to reflect design changes by adding or deleting couplings.

Engineering design tests

The STE/ICE engineering design tests consisted of performance and environmental tests. These tests had the following objectives:

1) To determine if the STE/ICE system meets the established performance and environmental limits.
2) To identify any areas that need further engineering work.
3) To establish any testing limitations which should be observed by the Army during the development test/operational test.
4) To evaluate adaptability of the TK to each of the four vehicle types.

During the performance tests the accuracy of the VTM measurements was verified. This was done in conjunction with the built-in diagnostic harnesses and the transducer kits. The VTM thermal performance during these tests was slightly better than predicted indicating the value of the heat transfer design.

The environmental tests were performed on the unpackaged VTM. MIL-STD-810B test procedures were used, modified where necessary to agree with the VTM mission and design requirements. The tests included:

1) High temperature — MIL-STD-810B, Method 501, Procedure 1.
2) Low temperature — MIL-STD-810B, Method 502, Procedure 1.
3) Temperature-humidity — MIL-STD-810B, Method 507, Procedure 2.
4) Vibration — MIL-STD-810B, Method 514, Procedure 8.
5) Dust — MIL-STD-810B, Method 510, Procedure 1.
6) Shock — MIL-STD-810B, Method 516, Procedure 2.
7) Electromagnetic interference — susceptibility to EMI generated by vehicle ignition system and arc welder.

The VTM operational test was performed before, during, and after the environmental exposures, as called for by the test profiles. The operational test consisted of six test numbers which exercised 90% of the VTM measurement hardware and control logic and included all the circuits considered to be the most sensitive to the environmental conditions.

The VTM passed the high temperature (160° F non-operating, 125° F operating), low temperature, dust, and EMI tests without encountering any problems. There were no signs of penetration of the condensate. After minor problems were eliminated the vibration tests were also passed successfully. Nine 48-inch drops (on wooden planks backed by concrete floor) on all sides and two corners constituted the shock test. Minor dents sustained by the housing under the recorded shocks of 170 to 260 g did not affect the performance of the VTM.

Conclusion

All STE/ICE systems successfully passed the established requirements for the performance and environmental tests and they were accepted by the customer — the U.S. Army Tank Automotive Command.

Acknowledgment

Mr. R.N. Gillis of Government Plans and Systems Development contributed to the success of the STE/ICE program by preparing the industrial design sketches and assisting in the human factors engineering evaluation of the Vehicle Test Meter and Transducer Kit designs.

on the job/off the job
The ideal combo—a microprocessor and a music synthesizer

R.L. Libbey

A hobby is pursued for the fun it provides, but having fun does not exclude the educational benefits and intellectual stimulation that a hobby can offer. In this paper, a hobbyist describes the marriage of a music-making machine and its controller—the RCA COSMAC Microtutor.

Robert L. Libbey, Broadcast Synchronizer and Time Base Corrector Group, Commercial Communications Systems Division, Camden, N.J. received the BSEE in 1950 and the MA in Dramatic Arts in 1952 from the University of Wyoming. Before joining RCA in 1952, Mr. Libbey had a diversified background in radio broadcasting and sound recording. Also, he has taught at Drexel University and the University of Wyoming. At RCA, he first did advanced development work in acoustics and magnetic recording in the Home Instruments Division. From 1958 to 1969, he was with the RCA Electron Microscope group. There, he specialized in high-voltage regulation, and was project engineer for the design and installation of the first one-million-volt electron microscope in the western hemisphere (developed for the U.S. Steel Corporation Laboratories in Monroeville, Pennsylvania). After joining the Television Terminal Group in 1969, he designed video switching and effects systems and is now involved in the design of digital television products. Mr. Libbey's hobbies include music, multi-channel sound recording, and now microprocessors.

Author with his Combo. At left is the RCA COSMAC Microtutor; at center (front to rear) are the keyboard, interface, and attenuator; synthesizer at far right.

Ed. Note: Last fall, Bob Libbey of Commercial Communications Systems Division in Camden took the CEE course, "Microprocessors for Logic Design—C55." After the formal learning period, Bob considered ways of increasing his understanding of the RCA Microtutor used in the course. Because of his background and interest in music, Bob decided that mating a microprocessor and a music synthesizer would be a logical step for furthering his understanding of the Microtutor and its programming. Although Bob says it was "a first, crude attempt at programming," the system worked and delighted Bob and his music-loving family. Bob's next project is to build and program a system to play complete chords.

The programming portion of this paper, of necessity, assumes some familiarity with the RCA COSMAC Microtutor and its software techniques. References are also made to the COSMAC User's Manual and COSMAC Microtutor Manual, which are produced by the Solid State Division and are included in the course material of "Microprocessors for Logic Design."

If you are interested and want more detail on Bob's project, write to him at Bldg. 10-2, Camden, N.J.

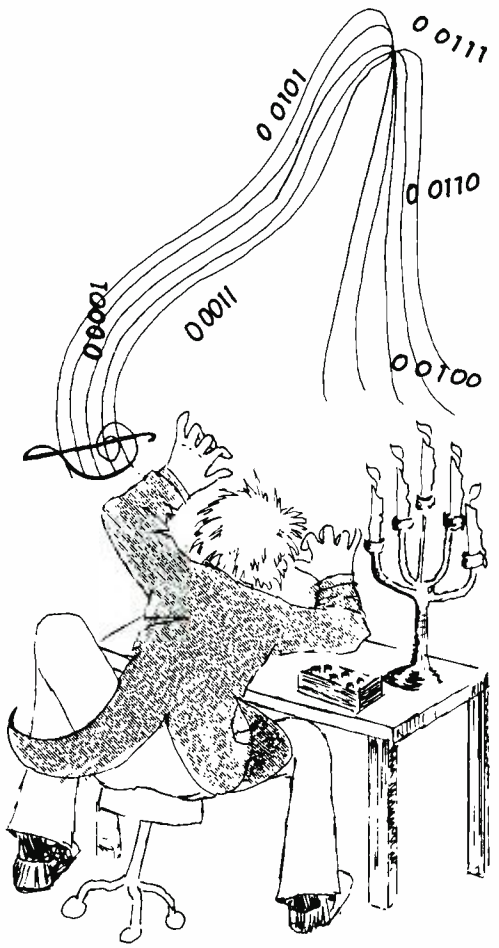

THE COMBINATION of a microprocessor and a music synthesizer creates an instrument with outstanding artistic and educational potential. By using a microprocessor to control a sophisticated synthesizer, sounds, tempos, modulations, etc., can be produced that could only be dreamed a few years ago. Even a modest synthesizer makes an exemplary output device for learning programming and multiple input/output techniques. If the synthesizer used is somewhere between the simplest and the most complicated, rudimentary software and hardware skills can be expanded to include analog-to-digital-to-analog (we still listen for analog signals) techniques and, as one advances further, the Combo can be used to produce more complex musical sounds and harmonies, using (and learning about) digital filters.[1]

Combo system

Our first-attempt Combo consisted of the RCA COSMAC Microtutor and a PAIA Electronics "Gnome" micro-synthesizer.[2] It was decided that even this first attempt at processor-controlled music should have the ability to control the character of the tone (note), as well as its pitch and duration.[3] The Gnome synthesizer had previously been adapted to a surplus organ keyboard and could be tuned to play music using the familiar western world even-tempered scale.[4] A switch made it possible to control the synthesizer with either the keyboard or the microprocessor. Fig. 1 shows the system block diagram. The Microtutor and its interface create coded signals that choose notes in a manner similar to striking a key on the keyboard. In addition, the output

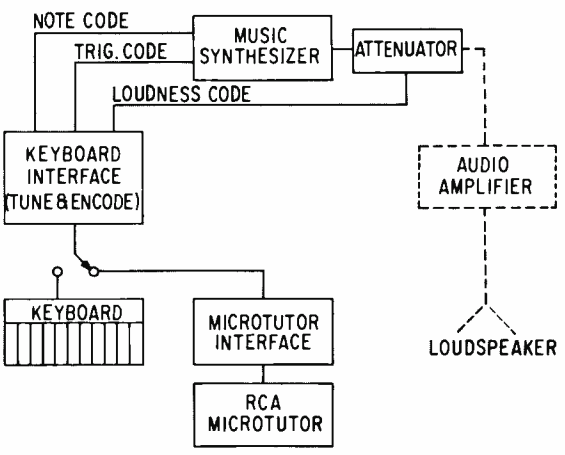

Fig. 1 — Combo system block diagram.

Reprint RE-22-2-21
Final manuscript received August 6, 1976.

codes can control the characteristic sound and loudness of each note. The loudness attenuator is a resistor-diode network (a simple digital-to-analog converter) that changes its attenuation when different parts of the network are grounded with a logic "LO". The amplifier and loudspeaker were part of a home hi-fi system.

The program software had a goal of performing five major functions. First, it should select the proper pitch and duration of the note (including "no note"—a rest). Similarly, it should change the character of the note by triggering the voltage-controlled amplifier and voltage-controlled filters in the synthesizer. Also, there should be a provision to select one of four loudness values. Finally, it would be desirable to change the key in which the music is played. This "key change" feature would be especially useful to the music student using the microprocessor-synthesizer Combo in composition studies.

The program included memory tables for pitch and duration. The duration tables included a time: T1, T2, T4, T8 and T16 for one-sixteenth, one-eighth, etc., through whole notes; and T1.5, T3, - T24 for "dotted" notes.[5] The duration value for each note depends upon the type of note, the tempo of the work being played, the programming technique, and the clock and instruction speed of the microprocessor. The Microtutor Manual and the COSMAC User's Manual describe the time calculations. The Microtutor has an adjustment on its clock frequency which provides for a convenient way to change the tempo.

The pitch code can be any system of binary outputs that will translate into the desired musical note. As an example, middle-C might be code "0 0001", C-sharp "0 0010", and D would be "0 0011", etc. Moreover, appropriate codes can be used for loudness values, key signatures, and for triggering the synthesizer.

Using the music sheet, each note could be given a separate code for pitch, duration, loudness, key and character (wave-shape—attack and delay).

Hardware

The interface hardware for this first-attempt combo proved extremely interesting. The first paper design required *seventeen* interface chips as compared with thirteen chips for the complete Microtutor. The final design required ten CMOS interface ICs. Fig. 2 shows the interface hardware. This first-attempt system used a simplistic hardware design. Integrated circuit U2 inverted the sense of the output data to make it compatible with the decode/latch IC's U3 and U4. U3 will decode only the lower four data bits DB0 through DB3. A "1" on DB4 will inhibit U3 but, with the help of U1B, will enable U4. If all data bit lines are "0," all outputs of U3 will be "0" (high) and likewise U1A will cause all data output lines of U4 to be "0" (high).

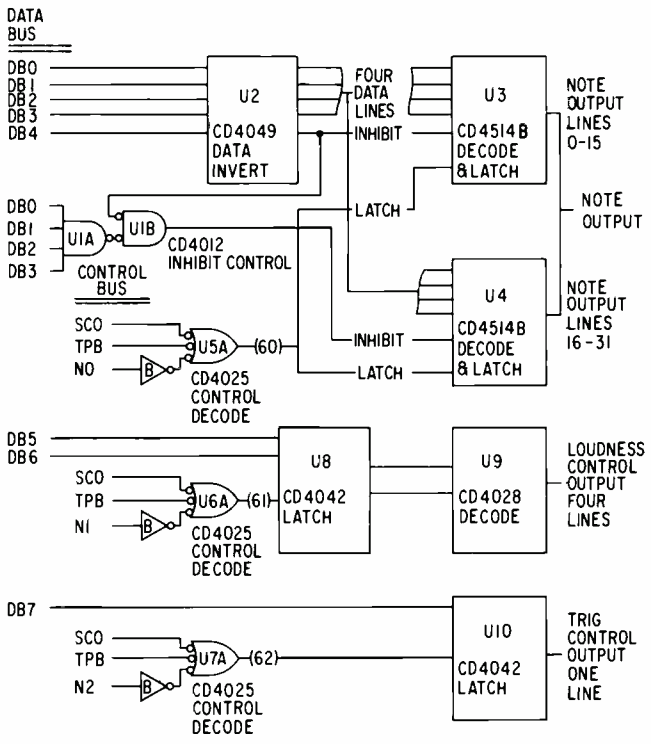

Fig. 2 — Interface circuits.

The control lines SC0, TPB, and N0, acting with U5, will cause data to be latched in U3 and U4, and only in U3 and U4, when a "60" output instruction is executed. In a similar manner, the data on lines DB5 and DB6 only is latched in U8 and decoded in U9 when control lines SC0, TPB, and N1 enable U6 with a "61" instruction. Likewise, U7 and U10 use DB7, SC0, TPB, N2, and the "62" Microtutor instruction.

Software

The program was patterned after the "Table Driven Sequence" in the Microtutor Manual. Fig. 3 shows the software program flow chart. The COSMAC (Microtutor) microprocessor contains sixteen very powerful and convenient registers that, in this program, are used to count and point—in consecutive order—to different blocks of memory. The block (table) containing the addresses for the 32 note codes starts in memory location 223 and is pointed to by the register termed note pointer or "NP." The table for the loudness values starts at memory location 190 and uses pointer register "LP," etc. The counter register used in several parts of the program is "CR"; and "PC" is the program counter. The steps in the first column of the flowchart are preparatory steps—they input data, set up the tables, etc.; the steps in the second column make up the working program—they play the music.

Thus, for each note a pitch value was chosen, outputted, and latched. If loudness and triggering information was required, it was immediately chosen and sent out. The program would then go through an appropriate delay loop to hold the selected note the proper time. At the end of the delay, the next note and loudness and trigger values are selected. Because of memory limitations, the key-

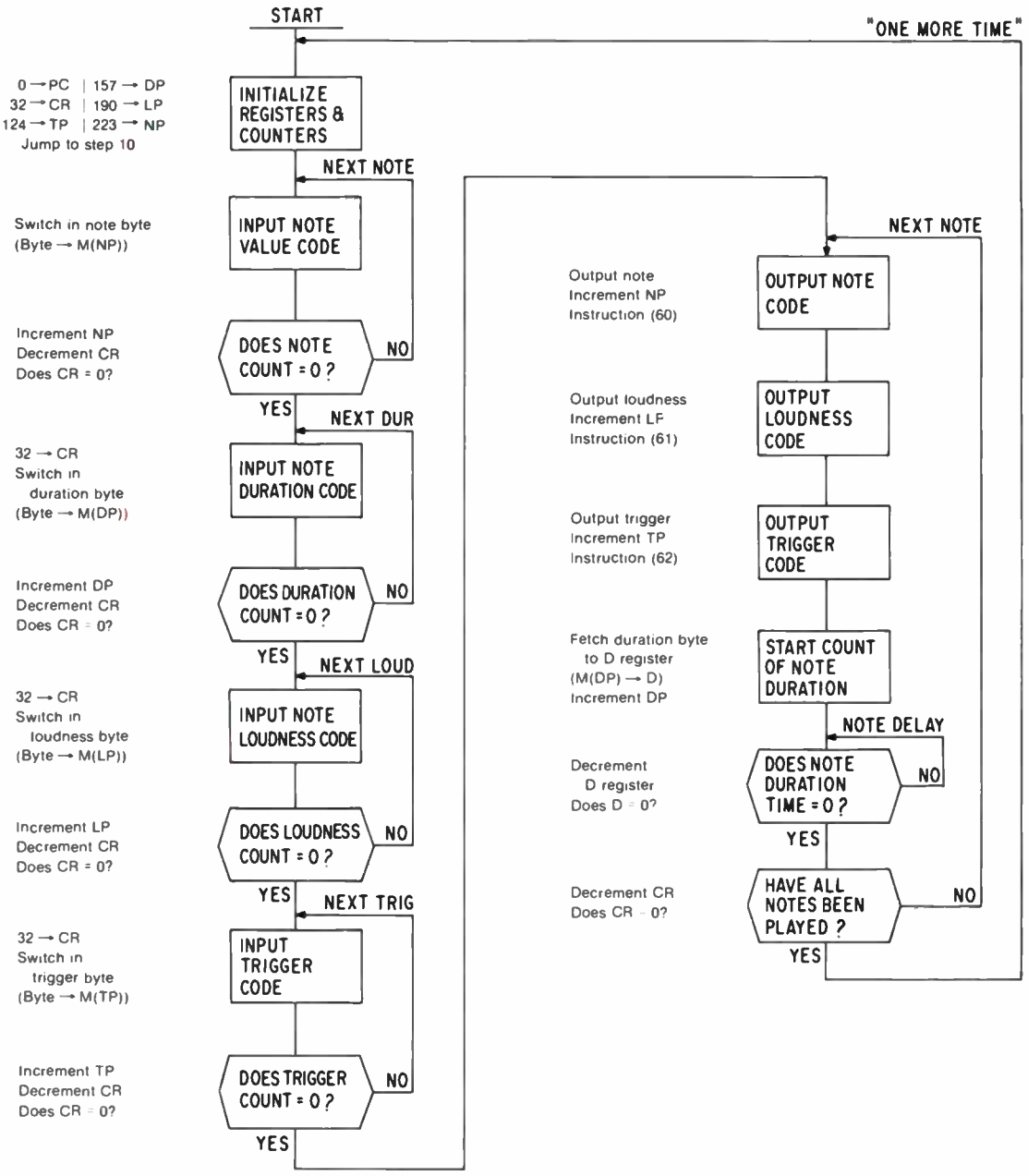

Fig. 3 — Combo flow chart.

change feature was not implemented in this first-attempt combo.

Conclusions

In keeping with the Bicentennial, my son—who was taking a high school course in fundamentals of music—transcribed the Revolutionary War marching song "Chester" for our microprocessor-synthesizer experiment. The program and sixteen measures of the music took all 256 bytes of memory.

References

1. Alles, H.G. (Bell Telephone Laboratories): "A Hardware Digital Music Synthesizer" *Proc. IASCON* '75," pp. 217-A to 217-L.
2. Simonton, J.S. Jr., "Build a Portable Synthesizer", *Radio-Electronics* (Nov 1975) pp. 37-101.
3. L. Bazin and D. Schneider of Broadcast Camera Engineering used the Microtutor to control a "Music Maker" with programmed pitch and rhythm generators, based upon "A Rhythm Section You Can Build," *Electronics Illustrated* (Nov 1968) pp. 57-66.
4. This was accomplished even though the Gnome manufacturer states that this can not be done. If the scale was not so tuned, programming the pitch would be much more difficult. In fact, tuning and keeping them in tune is a problem in many music synthesizers. Also, see Carl Helmer's "Add a Kluge Harp to Your Computer," *BYTE* (Oct 1975) pp. 14-18.
5. A dotted note is held 1.5 times as long as the note would be held without the dot.

Hobbyists...share your hobby interests with *RCA Engineer* readers! The "on-the-job/off-the-job" column offers you the opportunity to report on your experiences. The information should be related to technology and be of general interest to engineers. If you wish to contribute, contact Frank Strobl, Bldg. 204-2, Cherry Hill, N.J., ext. PY-4220.

Pen and Podium

Recent RCA technical papers and presentations

To obtain copies of papers, check your library or contact the author or his divisional Technical Publications Administrator (listed on back cover) for a reprint. For additional assistance in locating RCA technical literature, contact RCA Technical Communications, Bldg. 204-2, Cherry Hill, N.J., extension PY-4256.

Government and Commercial Systems Div.

J. Knoll
Prosthetic heart valve, *RCA Technical Note,* (5/24/76).

G. Mackiw| G.V. Wild
Microwave frequency synthesis for satellite communications ground terminals, Thirtieth Annual Frequency Control Symposium, Atlantic City, NJ (6/2/76).

Advanced Technology Laboratories

D.G. Herzog
Laser battlefield surveillance radar concept, *Proceedings* 7th Classified Conference on Laser Technology, US Military Academy, West Point, NY (6/8-10/76).

A. Feller
Low cost, quick turnaround random logic custom LSI's using automatic layout programs, *Proceedings* 13th Design Automation Conference, San Francisco, CA (6/28-30/76).

Astro-Electronics Div.

G. Brucker (AED)| W. Heagerty (ATL)
Radiation effects in a CMOS/ SOS/Al-gate D/A converter and on-chip diagnostic transistor, IEEE Nuclear and Space Radiation Effects Conf. (7/27-30/76).

G. Brucker| R. Ohanian
Prediction and measurement of radiation damage to CMOS devices on board spacecraft, IEEE Nuclear and Space Radiation Effects Conf. (7/27-30/76).

D. L. Balzer
The monopropellant hydrazine reaction control subsystem for RCA Satcom, AIAA/SAE 12th Propulsion Conf. (also *Journal of Spacecraft and Rockets*), Palo Alto, CA (7/26/76).

G. Brucker| B.R. Parson
Radiation test and simulation of CMOS/SOS/Si-gate ALU and ROM devices, IEEE Nuclear and Space Radiation Effects Conf., San Diego, CA (7/27-30/76).

T.J. Faith| J.W. Jennings
Fluid abrasive trimming of thin-film resistors, *IEEE Trans. on Parts, Hybrids, and Packaging* (6/76).

C.A. Berard
A high-power, boost-mode, switching regulator for high-performance application, *Proceedings,* POWERCOM, Los Angeles, CA (6/24-26/76).

E.W. Schlieben
System aspects of magnetically supported energy wheels, *Proceedings,* 2nd Int'l Workshop on Rare Earth Cobalt Permanent Magnets and Their Applications, Dayton, OH (6/8-11/76).

F.A. Beisel
RCA test program for a commercial communications satellite, Symposium on Reliability Engineering, Univ. of Ottawa, Ottawa, Ont. (6/5/76).

G.T. Tseng| K.J. Phillips
Attitude stability of a flexible dual-spin spacecraft with active nutation damping using products of inertia, 1976 ESA Symp. on Dynamics and Control of Non-Rigid Space Vehicles, Frascati-Rome, Italy (5/24-26/76).

J. Kaleigh
Estimation of direction cosine matrix by velocity measurements and two inertial measurements units through optimal filtering, National Aerospace and Electronics Conf., Dayton, OH (5/19/76).

H.K. Law
Quasi-steady diffusion flame theory with variable specific heats and transport coefficients, *Combustion Science & Technololgy* (Apr/May/Jun 1976).

RCA Laboratories

E.K. Sichel| R.E. Miller
M.S. Abrahams| C.J. Buiocchi
Heat capacity and thermal conductivity of hexagonal pyrolytic boron nitride, *Phys. Review B,* Vol. 13, No. 10, p. 4607 (5/15/76).

B. Dorner| R.E. Ghosh| G. Harbeke
Phonon dispersion in the layered compound PbI_2. *Phys. Stat. Sol. (B),* Vol. 73, p. 655 (1976).

J.P. Wittke| I. Gorog| A.H. Firester
CW semiconductor injection lasers in information handling systems, *Optical Engineering,* Vol. 15, No. 2, p. 128 (Mar/Apr 1976).

H.A. Weakliem| B.F. Williams
Review and analysis of optical recording media, *Optical Engineering,* Vol. 15, No. 2, p. 99-108 (Mar/Apr 1976).

V.S. Ban| E.A.D. White
Mass spectrometric study of processes in the closed-tube vapor growth of CdS and ZnS, *J. Crystal Growth,* Vol. 33, p. 365 (1976).

P.K. Baltzer| J.A. Weisbecker| R.O. Winder
Interpretive programming of small microprocessor-based systems, Electro 76 (5/11-14/76).

T. Takahashi| O. Yamada
Growth of cadmium boracite single crystals by chemical vapor transport, *J. Crystal Growth,* Vol. 33, p. 361 (1976).

W. Kern
Analysis of glass passivation layers on integrated-circuit pellets by precision etching, *RCA Review,* Vol. 37, No. 1, p. 79 (3/76).

G.A. Alphonse
Optical storage in lithium niobate, *Third Conf. on the Laser,* Vol. 267, p. 373.

Y.S. Chiang| E.J. Denlinger| C.P. Wen
Contact resistance of metal-silicon systems at microwave frequencies, *RCA Review,* Vol. 37, No. 1, p. 107 (3/76).

S.M. Perlow
Noise performance factors in television tuners, *RCA Review,* Vol. 37, No. 1, p. 119 (3/76).

S.T. Hsu
COS/MOS linear amplifier stage, *RCA Review,* Vol. 37, No. 1 p. 136, (3/76).

W.E. Ham
Test data reduction, *IEEE Trans. on Manufacturing Technology,* Vol. MFT-5, No. 1, p. 24 (3/76).

H. Kressel| F.Z. Hawrylo
Red-light-emitting laser diodes operating cw at room temperature, *Applied Phys. Lett.,* Vol. 28, No. 10, p. 598 (5/15/76).

R.J. Powell
Vacuum ultraviolet induced space charge in Al_2O_3 films, *Appl. Phys. Lett.,* Vol. 28, No. 11, p. 643 (6/1/76).

D.E. Carlson| C.R. Wronski
Amorphous silicon solar cell, *Appl. Phys. Lett.,* Vol. 28, No. 1, p. 671 (6/1/76).

A.C. Ipri| J.C. Sarace
CMOS/SOS semi-static registers, *J. Solid-State Circuits, p. 337 (4/76).*

B.J. Curtis
Temperature asymmetrics and fluctuations, *J. Electrochemical Soc.,* Vol. 123, No. 3 pp. 438-439 (3/76).

A.W. Fisher| G.L. Schnable
Minimizing process-induced slip in silicon wafers by slow heating and cooling. *J. Electrochemical Soc.,* Vol. 123, No. 3, pp. 434-435 (3/76).

R.B. Comizzoli
Bulk and surface conduction in CVD SiO_2 and PSG passivation, *J. Electrochemical Soc.* Vol. 123, No. 3, (3/76).

H. Schade
Evidence for electron emission stimulated desorption from negative electron affinity GaAs surfaces, *Surface Sciences,* Vol. 55, No. 1, p. 20 (1976).

T.T. Hitch| H.H. Whitaker
E.M. Botnick| B.L. Goydish
Chemical analyses of thick-film gold conductor inks, *IEEE Trans. on Parts, Hybrids, and Packaging,* Vol. PHP-11, No. 4, p. 248 (12/75).

W. Kern| G.L. Schnable| A.W. Fisher
CVD glass films for passivation of silicon devices: Preparation, composition, and stress properties, *RCA Review,* Vol. 37, No. 1, p. 3 (3/76).

W. Kern
Densification of vapor-deposited phosphosilicate glass films, *RCA Review,* Vol. 37, No. 1, p. 55 (3/76).

R.K. Wehner| D. Baeriswyl
Equation of state of a classical anharmonic oscillator, *Physica A,* Vol. 81, p. 129-144 (1975).

W. Rehwald| K. Frick
G.K. Lang| E. Meier
Doping effects upon the ultrasonic attenuation of $Bi_{12}SiO_{20}$, *J. Applied Physics,* Vol. 47, No. 4, p. 1292 (4/76).

R.U. Martinelli| G.H. Olsen
Improved transmission secondary emission from InxGa1-xP/GaAs self-supporting films activated to negative electron affinity, *J. Applied Physics,* Vol. 47, No. 4, p. 1332 (4/76).

M.D. Miller| H. Schade| C.J. Nuese
Lifetime controlling recombination centers in platinum-diffused silicon, *J. Applied Physics,* Vol. 47, No. 6, pp. 2569-78 (6/76).

G. Trachman
A simplified technique for predicting traction in elastohydrodynamic contacts, ASLE/ASME Lubrication Conference, Boston, MA (10/5/76).

C.W. Struck
Model of cathodoluminescence allowing both free carrier and trapped carrier diffusion to glossy surfaces, Electrochemical Society Spring Meeting, Washington, DC (5/2-7/76).

G.E. Skor
High performance 300-gate SOS universal array, IEEE SOS Technology Workshop, Palo Alto, CA (8/11-13/76).

G.H. Olsen| M. Ettenberg
Growth effects in the heteroepitaxy of III-V compounds, chapter for *Crystal Growth—Theory and Techniques,* Vol. 2, edited by C. Goodman (9/76).

J.A. Amick
Copper degradation of silicon and the behavior of copper in silicon, Electrochemical Soc. Meeting, Las Vegas, NV, *Electrochemical Soc. Extended Abstracts* (10/76).

C J. Nuese| G.H. Olsen| M. Ettenberg
Vapor-grown cw room-temperature GaAs/$In_yGa_{1-y}P$ lasers, *Applied Physics Letters,* Vol. 29, No. 1, pp. 54-56 (7/1/76).

D. Vilkomerson| R. Mezrich| K.F. Etzold
A general purpose research instrument for the measurement and visualization of ultrasound, 1st Meeting of the World Federation of Ultrasound in Med. & Biology.

C.W. Struck| W.H. Fonger
Temperature quenching of luminescence for linear and derivative nuclear operators, Electrochemical Society, Spring Meeting, Washington, DC (5/2-7/76).

Automated Systems Div

T.J. Dudziak
A pulse code modulation system for classroom demonstration, *Master's Thesis* for U. of Lowell (EE) (5/25/76).

C.W. Asbrand
Photography in industry, NEPA (N.E. Police Photographers Assoc.) Somerville, MA (5/4/76).

C.W. Asbrand
Photography in industry, State Police Academy, Framingham, MA (5/19/76).

L.R. Hulls
RCA ATE/ICE and STE/ICE projects, Auto. Test Equipment Conf., San Diego, CA (4/13/76).

S.C. Hadden| L.R. Hulls| E.M. Stuphin
Instrumentation for non-contact IC engine test and monitoring, ISA 22nd Intl. Instrumentation Symp., San Diego, CA (5/26/76).

J.G. Bouchard
Automation production of thick film hybrids, American Defense Preparedness Assoc., Eglin AFB (4/776).

C.W. Asbrand
Fire photography; an aid to investigation, State Police Academy, Framingham, MA (6/9 and 6/25/76).

G.E. Maguire
Materials requirements planning, Summer seminar of the Materials Procurement Committee of the Electronic Industries Assoc., Valley Forge, NY (6/9/76).

J.G. Bouchard| J.A. Kelly (ECOM)
Automation of ceramic microcircuit fabrication, ECOM Hybrid Microcircuits Symp., Ft. Monmouth, NJ (6/8/76).

B.T. Joyce
Trade-off considerations in contrasting hybrid applications, ECOM Hybrid Microcircuits Symp., Ft. Monmouth, NJ (6/8/76).

J.H. Woodward
Modular design of the AN/GVS-5(V) hand held laser rangefinder, *Proceedings* Seventh Classified Conf. on Laser Technology, West Point, NY 6/8/76).

O.T. Carver
EQUATE matches today's complex EW equipment testing needs, *Countermeasures* (6/76).

Picture Tube Div.

S.L. Babcock
Process capability studies in mass production, ASSO 3rd Annual Seminar on Quality Control, Univ. of Delaware (5/21/76).

J.C. Turnbull
One piece bimetal cathode cup and sleeve, *RCA Technical Note.*

B.L. Blessinger
Pierce control for laser beam drilling through glass, *RCA Technical Note.*

RCA Service Company

J.S. Hill
0.4 to 10GHz airborne electromagnetic environment survey of USA urban areas, *Record* Intl. Symp. on Electromagnetic Compatibility, Washington, DC (7/14/76).

Dates and Deadlines

Upcoming meetings

Ed. Note: Meetings are listed chronologically. Listed after the meeting title (in bold type) are the sponsor(s), the location, and the person to contact for more information.

SEPT. 12-17, 1976 — **Intersociety Energy Conversion Engrg. Conf.** (IEEE *et al*) Sahara Tahoe, Stateline, Lake Tahoe, NV **Prog Info:** E.J. Cairns, Gen'l Motors Res. Lab., 12 Mile & Mound Rds., Warren MI 48090.

SEPT. 14-17, 1976 — **WESCON** (IEEE, ERA) Los Angeles Conv. Ctr., Los Angeles, CA **Prog Info:** W.C. Weber, Jr., WESCON, 999 N. Sepulveda Blvd., El Segundo, CA 90245.

SEPT. 20-24, 1976 — **Int. Broadcasting Conf.** (EEA, IEE, IEEE UKRI Section) Grosvenor House, Park Lane, London, England **Prog Info:** IEE, Savoy Place, London WCZR OBL, England.

SEPT. 23-24, 1976 — **Broadcast Symp.** (BCCE) Washington Hilton, Washington, DC **Prog. Info:** Victor Nicholson, Cable Television Info. Ctr., 2100 M St., Suite 412, Washington, DC 20037.

SEPT. 26-29, 1976 — **Electronic & Aerospace Sys. Convention (EASCON)** (AES, IEEE) Stouffers Inn, Washington, DC **Prog. Info:** V.P. Healey, Edo Corp., 2001 Jefferson Davis Hwy., Suite 605, Arlington, VA 22202.

SEPT. 27-OCT. 1, 1976 — **Underground Transmission & Distribution** (IEEE) Convention Hall, Atlantic City, NJ **Prog Info:** P.H. Ware, Alcoa Conductor Pdts. Co., 510 One Allegheny Sq., Pittsburgh, PA 15212.

SEPT. 29-OCT. 1976 — **Ultrasonics Symp.** (IEEE) Annapolis Hilton Hotel, Annapolis, MD **Prog Info:** L.R. Whicker, Code 5250, Naval Res. Lab., Washington DC 20375.

OCT. 10-15, 1976 — **Int. IEEE/AP Symp. & USNC/URSI Meeting** (IEEE USNC/URSI) Univ. of Mass., Amherst, MA **Prog Info:** R.E. McIntosh, Dept. of Elec. & Computer Engrg., Univ. of Mass., Amherst, MA 01002.

OCT. 11-14, 1976 — **Industry Applications Society Annual Meeting** (IEEE) Regency Hyatt O'Hare, Chicago, IL **Prog Info:** G.R. Griffith, Atlantic Richfield Co., Harvey Tech. Ctr. 400 E. Sibley Blvd., Harvey, IL 60426.

OCT. 13-15, 1976 — **Display Conf.** (IEEE, SID) Statler Hilton Hotel, New York, NY. **Prog Info:** Frederick Kahn, Hewlett Packard Lab., IU, 1501 Page Mill Rd., Palo Alto, CA 94304.

OCT. 13-15, 1976 — **Software Engineering Conf.** (IEEE ACM, NBS) Jack Tar Hotel, San Francisco, CA **Prog Info:** R.T. Yeh, Dept. of Computer Sci., Physics Bldg. 3.28, Univ. Texas, Austin, TX 78712.

OCT. 21-22, 1976 — **Canadian Communications & Power Conf.** (IEEE) Queen Elizabeth Hotel, Montreal, Quebec, Canada **Prog Info:** Jean Jacques Archambault, CP/PO 958, Succ. "A" Montreal, Quebec H3C, 2W3 Canada.

OCT. 25-26, 1976 — **Joint Engineering Management Conf.** (IEEE, EIC *et al*) Hyatt Regency Hotel, Toronto, Ont., Canada **Prog Info:** K.L. Couplan, Ministry of Colleges & Univ., 60 Sir Williams Lane, Islington, Ont., Canada M9A IV3.

OCT. 25-27, 1976 — **Foundations of Computer Science** (IEEE) Warwick Hotel, Houston, TX **Prog Info:** J.W. Carlyle, 4531 Boetter Hall, UCLA, Los Angeles, CA 90024.

OCT. 5-27, 1976 — **High Speed Computation Symp.** (IEEE) Univ. of Illinois, Urbana, IL **Prog Info:** Duncan Lawrie, Dept. of Computer Sci., Univ. of Illinois, Urbana, IL 61801.

NOV. 1-3, 1976 — **Cybernetics & Society Int'l Conference** (SMC, IEEE) Mayflower Hotel, Washington, DC **Prog Info:** W.H. VonAlven, FCC, 1919 M St., N.W., Washington, DC 10554.

NOV. 1-3, 1976 — **Position Location and Navigation Symposium (PLANS)** (AES, IEEE) Hilton Inn, San Diego, CA **Prog Info:** J.R. Iverson, POB 81127, San Diego, CA 92138.

NOV. 6-10, 1976 — **Engineering in Medicine & Biology Conference** (EMB, AEMB, IEEE) Sheraton Hotel, Boston, MA **Prog Info:** AEMB, Suite 1350, 5454 Wisconsin Ave., Chevy Chase, MD 20015.

NOV. 8-11, 1976 — **Pattern Recognition Jt. Conference** (IEEE *et al*) Del Coronado Hotel, Coronado, CA **Prog Info:** A. Rosenfeld, Univ. of Maryland, Computer Sci. Ctr., College Park, MD 20742.

NOV. 9-11, 1976 — **Pulsed Power International Conference** (IEEE) Hilton Hotel, Lubbock, TX **Prog Info:** T.R. Burkes, Texas Tech. Univ., Dept. of EE, POB 4439, Lubbock, TX 79409.

NOV. 17, 1976 — **Computer Networks—Trends & Applications** (IEEE) NBS, Gaithersburg, MD **Prog Info:** J.H. Tilley, Collins Radio Co., 1200 N. Alma Rd., Richardson, TX 75080.

Calls for papers

Ed. Note: Calls are listed chronologically by meeting date. Listed after the meeting (in bold type) are the sponsor(s), the location, and deadline information for submittals.

FEB 16-18, 1977 — **IEEE International Solid State Circuits Conference** (IEEE, Univ. of Penn.) Sheraton Hotel, Philadelphia, PA **Deadline Info: 10/4/76 to** Lewis Winner, 152 W. 42nd St., New York, NY 10036.

MARCH 28-31, 1977 — **IEEE 1977 Int. Semiconductor Power Converter Conf.** Walt Disney Contemporary Hotel, Orlando, FL **Deadline Info: (ms) 11/5/76 to** R.G. Hoft, Univ. of Missouri, Columbia, MO 65201.

APRIL 25-27, 1977 — **Circuits & Systems International Symposium** (IEEE) Del Webb's Towne House, Phoenix, AZ **Deadline Info: 10/1/76 to** T.N. Trick, Dept. of EE, Univ. of Illinois, Urbana, IL 61801.

MAY 9-11, 1977 — **Acoustics, Speech & Signal Processing Int. Conf.** (ASSP) Sheraton Hartford Hotel, Hartford, CT **Deadline Info: (100 wd abst) 10/15/76 (4-pg. ready paper) 1/14/77 to** Dr. N. Rex Dixon, T.J. Watson Res. Ctr., POB 218, Yorktown Heights, NY 10598.

MAY 24-27, 1977 — **1977 Power Industry Computer Application Conf. (PICA X)** (IEEE) Toronto, Ont., Canada, **Deadline Info: (150-200 wd. abst) 10/8/76 (ms) 1/3/77 to** IEEE Technical Conference Services Office, 345 E. 47th St., New York, NY 10017.

JUNE 20-24, 1977 — **Int. IEEE/AP Symp. & USNC/URSI Meeting,** (IEEE, USNC/URSI) Palo Alto, CA **Deadline Info: (papers) 1/77 to** K.K. Mei, Dept. of EE&CS, Univ. of Calif., Berkeley, CA 94720.

JUNE 21-23, 1977 — **Int. Microwave Symp.** (IEEE) San Diego, CA **Deadline Info: (papers) 1/77 to** G. Schaffner, 6320 Elmcrest Dr., San Diego, CA 92119.

JULY 17-22, 1977 — **Power Engineering Society Summer Meeting** (IEEE) Mexico City, Mexico **Deadline Info: 1/1/77 to** IEEE, 345 E. 47 St., New York, NY 10017.

AUG. 24-25, 1977 — **Product Liability Prevention Conf.** (IEEE *et al*) Newark College of Engrg., Newark, NJ, **Deadline Info: 11/1/76 to** R.M. Jacobs, Newark College of Engrg., 323 High St., Newark, NJ 07102.

SEPT. 18-21, 1977 — **American Ceramic Society Fall Meeting** (IEEE, ACS) Queen Elizabeth Hotel, Montreal PQ, Canada **Deadline Info: (abst.)** 1/77 to Hank O'Brien, Bell Labs, Murray Hill, NJ 07974.

Patents

Automated Systems Div.

R.E. Hanson| W. F. Fordyce
Measuring ignition timing using starter current — 3968425, Jul 6, 1976

E.W. Richter
Variable bandwidth tunable direction filter — 3963998, Jun 15, 1976

R.E. Hanson| T.E. Nolan, Jr.
Engine brake horsepower test without external load — 3964301, Jun 22, 1976

Commercial Communications Systems Div.

L.J. Bazin| G.R. Peterson
Electronic signal mixer — 3970774, Jul 20, 1976

Consumer Electronics

J.B. George
Varactor tuner frequency controller — 3958180, May 18, 1976

H.E. Haslau| W.E. Rigsbee
Coil winding machine — 3957216, May 18, 1976

R.L. Shanley, II
Set-up arrangement for a color television receiver — 3959811, May 25, 1976

J.G. Amery
Defect compensation systems — 3969575, Jul 13, 1976

M.W. Muterspaugh
Freqeuncy selective circuit for automatic frequency control and sound signals — 3970773, Jul 20, 1976

A.J. Suchko
Fault detector and interrupt circuit useful in a television signal processing system — 3970915, Jul 20, 1976

D.H. Willis
Circuit for maintaining operating point stability of an amplifier — 3970895, Jul 20, 1976

M.N. Norman
Automatic beam current limiter — 3971067, Jul 20, 1976

E.M. Milbourn
Video de-peaking circuit in luminance channel in response to AGC signal — 3971064, Jul 20, 1976

L.A. Harwood| E.J. Wittmann
Controller gain signal amplifier — 3970948, Jul 20, 1976

Government Communications Systems Div.

R.G. Stewart
Input transient protection for integrated circuit element — 3967295, Jun 29, 1976

I. Krukaroff| W. Morren
Light shield for a semiconductor device comprising blackened photoresist — 3969751, Jul 13, 1976

Laboratories

G.A. Swartz| R.E. Chamberlain
Method of manufacturing a semiconductor device having a lead bonded to a surface thereof — 3956820, May 18, 1976

P.A. Levine
Charge coupled device systems — 3958210, May 18, 1976

C.L. Upadhyayula| S.Y. Narayan
Planar transferred electron device with integral nonlinear load resistor — 3959807, May 25, 1976

Z. Turski| J.L. Vossen, Jr.
Metallized lithium niobate and method of making — 3959747, May 25, 1976

I. Ladany| D.P. Marinelli
Method for forming an ohmic contact — 3959522, May 22, 1976

G. Mark
Method of forming an overlayer including a blocking contact for cadmium selenide photoconductive imaging bodies — 3964986, Jun 22, 1976

R.J. Himics| S.O. Graham| D.L. Ross
Method of preparing a pattern on a silicon wafer — 3964909, Jun 22, 1976

M. Ettenberg| H. Kressel
Method of making electroluminescent semiconductor device — 3963536, Jun 15, 1976

J.S. Fuhrer
Pickup arm assembly — 3963864, Jun 15, 1976

H.N. Crooks
Disc record groove skipper apparatus — 3963861, Jun 15, 1976

N. Felsdtein
Method of making duplicates of optical or sound recording — 3962498, June 8, 1976.

T.T. Hitch| T.E. McCurdy
Reactively-bonded thick-film ink — 3962143, Jun 8, 1976

G.F. Stockdale
Method for embossing a pattern in glass — 3961929, Jun 8, 1976

W.F. Kosonocky| D.J. Sauer
Charge transfer memory — 3967254, Jun 29, 1976

J.S. Fuhrer
Velocity correction for video disc — 3967311, Jun 29, 1976

H.M Scott
Regulated switched mode multiple output power supply — 3967182, Jun 29, 1976

J.P. Bingham
Single frame color encoding/decoding system —3968515, Jun 6, 1976

G.S. Kaplan
Adaptive parameter processor for continuous wave radar ranging — 3968492, Jun 6, 1976

R.W. Nosker| L.P. Fox
Trapezoidal smooth grooves for video disc — 3968326, Jun 6, 1976

D. Meyerhofer| A. Sussman
Liquid crystal devices of the surface aligned type — 3967883, Jun 6, 1976

R.C. Palmer| J.K. Clemens
Color-picture/multichannel-sound record and recording/playback apparatus and methods therefor — 3969756, Jul 13, 1976

R.S. Mezrich| K.F. Etzold
D.H. Vilkomerson
Visual display of ultrasonic radiation pattern — 3969578 Jul 13, 1976

E.O. Keizer
Apparatus and methods for playback of color picture/sound records — 3972064, Jul 27, 1976

S. Liu
Apparatus for mounting a diode in a microwave circuit — 3972012, Jul 27, 1976

W.F. Kosonocky
Charge coupled device imager — 3971003, Jul 20, 1976

J.A. Weisbecker
Microprocessor architecture — 3970998, Jul 20, 1976

R.S. Englebrecht
Handwriting identification technique — 3962679, Jun 8, 1976

K. Knop
Focused-image hologram system providing increased optical readout efficiency — 3961836, Jun 8, 1976

K. Knop
Diffractive subtractive color filtering technique — 3957354, May 18, 1976

A.G. Dingwall
Memory cells with decoupled supply voltage while writing — 3971004, Jul 20, 1976

Missile and Surface Radar Div.

B.F. Bogner| D.F. Bowman
RF power coupling network employing a parallel plate transmission line — 3958247, May 18, 1976

W.H. Schaedla
Short depth hardened wave guide element — 3942138 assigned to U.S. Govt. Mar 2, 1976

W.A. Harmening
Steerable mount — 3964336, Jun 22, 1976

Picture Tube Div.

J.C. Turnbull
Method for producing a strontium metal film on internal surfaces of a CRT — 3964812, Jun 22, 1976

S.A. Harper
Method for improving adherence of phosphor-photobinder layer during luminescent-screen making — 3966474, Jun 29, 1976

P.R. Liller
Low-voltage aging of cathode-ray tubes — 3966287, Jun 29, 1976

T.W. Branton
Method for preparing a viewing-screen structure for a CRT having temperature-compensated mask-mounting means, including cooling mask during exposure — 3970456, Jul 20, 1976

J.F. Stewart| R.A. Alleman
M.R. Weingarten
Method of installing a mount assembly in a multi-beam cathode ray tube — 3962764, Jun 15, 1976

C.P. Stachel| M.R. Weingarten
Method of installing a mount assembly in a multi-beam cathode ray tube — 3962765, Jun 15, 1976

Solid State Div.

T.G. Athanas
Deep depletion insulated gate field effect transistors — 3958266, May 18, 1976

B.D. Rosenthal
Current mirror amplifiers — 3958135, May 18, 1976

M.A. Polinsky
Method of making an insulated gate field effect transistor — 3959025, May 25, 1976

W.P. Bennett
Apparatus for non-destructively testing the voltage characteristics of a transistor — 3965420, Jun 22, 1976

S.S. Eaton, Jr.
CMOS oscillator — 3965442, Jun 22, 1976

S.S. Eaton, Jr.
Memory cell — 3964031, Jun 15, 1976

O.H. Schade, Jr.
Ground-fault detection system — 3963963, Jun 15, 1976

W.F. Dietz
Side pincushion correction system — 3962602, Jun 8, 1976

B. Zuk
Threshold detector circuitry, as for PCM repeaters — Jun 8, 1976

K.J. Sonneborn
Pattern definition in an organic layer — 3962004, Jun 8, 1976

C.F. Wheatley, Jr.
Amplifier with over-current protection — 3967207, Jun 29, 1976

H.L. Blust| N.L. Lindburg| D.V. Henry
Method of anchoring metallic coated leads to ceramic bodies and lead-ceramic bodies formed thereby — 3970235, Jul 20, 1976

SelectaVision Project

T.W. Burrus
Locked groove detection and correction in video disc playback apparatus — 3963860, Jun 15, 1976

T.W. Burrus
Velocity correction circuit for video discs — 3965482, Jun 22, 1976

T.F. Kirschner
Apparatus for inhibiting a plurality of disc records from being disposed on a turntable and grounding a disc record disposed on the turntable — 3970317, Jul 20, 2976

J.G. Amery
Color image signal processing circuits — 3969757, Jul 13, 1976

Clip out and mail to Editor, *RCA Engineer,* 204-2, Cherry Hill, N.J.

RCA Engineer

Have we your correct address?
If not indicate the change below:

Do you receive TREND?
Yes____ No____

Name _____ Code # _____

Street or Bldg. _____

City and State or Plant _____

*Please indicate the code letter(s) that appear next to your name on the envelope.

Engineering News and Highlights

Kessler

Koppelman

Karoly

RCA Electronics and Diversified Businesses Reorganized

Edgar H. Griffiths, President, RCA Electronics and Diversified Businesses, announced the following executive appointments

Irving K. Kessler is Group Vice President, with responsibility for Commercial Communications Systems Division and Government Systems Division.

Julius Koppelman is Group Vice President, with responsibility for Distributor and Special Products Division, Picture Tube Division, and RCA Service Company.

Julius Koppelman, Group Vice President, appointed **Joseph W. Karoly** President, RCA Service Company.

Irving K. Kessler, Group Vice President, appointed **James Vollmer** Division Vice President and General Manager, Government Systems Division.

Irving K. Kessler, Group Vice President, announced the Government and Commercial Systems organization as follows: **George D. Black,** Division Vice President,

Staff Announcements

Commercial Communications Systems Division

Carl H. Musson, Manager, Transmitting Equipment Engineering and Product Management, Broadcast Systems, appointed **David S. Newborg,** Manager, Radio Station Equipment Product Management.

Solid State Division

Paul R. Thomas, Manager, Marketing Services & International Support, has announced the organization as follows: **Robert E. Brown,** Manager, International Systems & Support; **Antony J. Froio,** Manager, Advertising & Promotion; **Robert T. Jeffery,** Manager, Marketing Services & Control; **John A. Leotti,** Manager, Product Distribution; and **Paul R. Thomas,** Acting, Customer & Order Service.

Astro-Electronics

C.S. Constantino, Division Vice President, RCA Astro-Electronics, appointed **Barbara E. Cohen** Manager, Product and System Safety.

Picture Tube Division

J. Edward Gagan, Manager, Quality, Product Safety and Reliability, Scranton Plant, has announced the organization as follows: **Donald R. Cadman,** Manager, Tube Processing; **John R. Hirschler,** Administrator, Quality Customer Liaison—Domestic; **Lewis R. Malsberger,** Manager, Finished Tube; **Michael Maslak,** Manager, Parts and Materials; and **Milton K. Massey,** Administrator, Quality Customer Liaison—International.

Alan R. Zoss, Manager, Industrial Relations, Scranton Plant has announced the organization as follows: **Richard J. Bednarczyk,** Manager, Employment and Records. **Paula J. Contessa,** Manager, Training, Organization Development and Personnel Services; **Bernard J. Lebojesky,** Administrator, Security; **Raymond A. Orasin,** Manager, Safety and Insurance; **Thomas P. Quinn,** Administrator, Wage and Salary; and **Joseph C. Scagliotti,** Administrator, Labor Relations.

Electronic Industrial Engineering, Inc.

Peter B. Jones, Staff Vice President, Business Planning, has appointed **Henry Duszak** General Manager, Electronic Industrial Engineering, Inc.

Corporate Engineering

Howard Rosenthal, Staff Vice President, Engineering, appointed **John F. Clark** Director, Space Applications and Technology.

Raymond E. Simonds, Director, RCA Frequency Bureau, has appointed **Edward E. Thomas,** Manager, RCA Frequency Bureau—Washington.

Raymond E. Simonds, Director, RCA Fre-

Vollmer

Rittenhouse

Industrial Relations; **Andrew F. Inglis,** Division Vice President and General Manager, Commercial Communications Systems Division; **I.A. Mayson,** Vice President and General Manager, Government and Commercial Systems Division, RCA Limited (Canada); **James Vollmer,** Division Vice President and General Manager, Government Systems Division, and **James H. Walker,** Division Vice President, Finance.

James Vollmer, Division Vice President and General Manager, Government Systems Division, announced the organization as follows: **C.S. Constantino,** Division Vice President, Astro-Electronics; **Max Lehrer,** Division Vice President, Missile and Surface Radar; **George D. Prestwich,** Division Vice President, Government Marketing; **John D. Rittenhouse,** Division Vice President, Government Communications Systems; **David Shore,** Division Vice President, Advanced Programs Development; **Harry J. Woll,** Division Vice President, Automated Systems; and **James Vollmer,** Acting, Government Engineering.

Licensed engineers

When you receive a professional license, send your name, PE number (and state in which registered), RCA division, location, and telephone number to: *RCA Engineer*, Bldg. 204-2, RCA, Cherry Hill, N.J. New listings (and corrections or changes to previous listings) will be published in each issue.

Consumer Electronics

James H. Helm, Indianapolis, Ind.: IN—16250.

Professional Activities

RCA Communications

Martin Gottlieb, senior member, engineering staff, RCA Global Communications, Inc., N.Y., has been elected senior member of the IEEE by the officers and Board of Directors "in recognition of professional standing." He is author of the PEOPLE column in THE PULSE, monthly newsletter of IEEE's Long Island Section, and past vice-chairman of LIPAC.

Degree Granted

Missile and Surface Radar

J.J. O'Brien has been awarded the MS in Systems Engineering, University of Pennsylvania.

---

quency Bureau, has appointed **John D. Bowker** Manager, Technical Projects and Frequency Utilization.

RCA Staff

Herbert T. Brunn, Vice President, Consumer Affairs, appointed **Howard W. Johnson** Staff Vice President, Product Safety.

John V. Regan, Staff Vice President, Patent Operations, has announced the organization as follows: **Harold Christoffersen,** Director, Patents-Solid State and Electronic Systems; **Samuel Cohen,** Managing Patent Attorney; **Joseph D. Lazar,** Managing Patent Attorney; **Allen L. Limberg,** Managing Patent Attorney; **Birgit E. Morris,** Managing Patent Attorney; **Robert P. Williams,** Managing Patent Attorney; **Harry Kihn,** Senior Technical Advisor; **Edward J. Norton,** Director, Patent Planning and Administration; **Eleanor D. Holland,** Manager, Patent Information Systems; **Marie A. McCormack,** Manager, Patent Administrative Services; **Roland L. Morneau,** Resident Patent Agent—Montreal; **T. Ian M. Smith,** Manager, Patents—London Office; **Sharon K. Stepno,** Administrator, Washington Office; **Yoshiyuki Osuga,** Manager, Patents—Tokyo Office; **Albert Russinoff,** Senior Staff Patent Counsel; **Eugene M. Whitacre,** Director, Patents—Consumer Products and Broadcast Equipment; **Glenn H. Bruestle,** Managing Patent Attorney; **Donald S. Cohen,** Managing Patent Attorney; **Murray J. Ellman,** Managing Patent Attorney; **William H. Meagher,** Managing Patent Attorney; **Paul J. Rasmussen,** Managing Patent Attorney; and **Roy M. Christensen,** Technical Advisor.

RCA Laboratories

Emil V. Fitzke, Manager, Technological Services, announced the appointment of **Jack F. Otto** to Manager, Device Technology.

Charles C. Foster, Manager, Scientific Publications, has appointed **Wendy Chu** Librarian.

George C. Hennessy, Director, Marketing and Technical Information Services, has appointed **Albert Pinsky** Manager, Scientific Information Services.

Albert Pinsky has announced the organization of Scientific Information Services as follows: **M. Phyllis Smith,** Administrator, Communications, and **Anthony J. Stranix,** Administrator, Technical Relations.

Charles A. Hurford, Manager, Industrial Relations, has appointed **Paul Brown, Jr.,** Manager, Employment and Records.

Leonard R. Rockett has been named a member of the Scientific Staff, Integrated Circuit Technology, RCA Laboratories.

Dr. Elizabeth S. Lo has been appointed to the scientific staff, Process and Applied Materials Research Laboratory, RCA Laboratories.

Charles A. Hurford, Manager, Industrial Relations, appointed **Elizabeth C. Palmer** Manager, Employee Development and Training.

ENJOYING RECOGNITION are 65 Automated Systems staff members and their wives. The ninth Professional Recognition Dinner, held aboard the SS Peter Stuyvesant in Boston Harbor, honored employees for papers published, patents awarded, professional committee memberships and Engineering Excellence Awards.

Promotions

Missile and Surface Radar

J. Darby from Assoc. Mbr. Engrg. Staff to Mbr. Engrg. Staff (R. Kolc, Hybrid & Envir. Labs.)

T. Guckert from Assoc. Mbr. Engrg. Staff to Mbr. Engrg. Staff (R. Kolc, Hybrid & Envir. Labs.)

P. Horton from Mbr. Engrg. Staff to Sr. Mbr. Engrg. Staff (M. Plofker, Stds. EMX & Safety)

A. Klotzbach from Mbr. Engrg. Staff to Sr. Mbr. Engrg. Staff (J. Friedman. Cont. Reports & Prop.)

J. Schisler from Assoc. Mbr. Engrg. Staff Mbr. Engrg. Staff (W. Rapp, Engrg. Programming)

G. Oakes from Sr. Mbr. Engrg. Staff to Princ. Mbr. Engrg. Staff (W. Sheppard, Signal Processor)

C. Specht from Mbr. Engrg. Staff to Sr. Mbr Engrg. Staff (M. Paglee, Track Processing)

J. DeVecchis from Contract Administrator to Mbr. Engrg. Staff (B. Matulis, Information Processing)

D. Bradley from Princ. Mbr. Engrg. Staff to Ldr., Engrg. Sys. Projects (R.L. Weis, C&D Project)

C. Brown from Ldr. Engrg. Sys. Projects to Mgr., Radar & Supp. Systems (J.T. Threston, Systems Engrg.)

B. Kempf from Ldr. Engrg. Sys. Projects to Mgr., Systems Equipment (E.L. Willey, AEGIS Equipment Proj.)

L. Walker from Ldr., Drftg. Opns. to Mgr. Design Drftg. Opns. (M. Korsen, Equipment Des & Dev.)

R.L. Weis from Ldr., Sys. Engrg. to Mgr. C&D Project (R.W. Howery, Computer Prog. Devel.)

F. Wuebker from Sr. Mbr. Engrg. Staff to Ldr. Engrg. Sys. Projects (R.W. Howery, Computer Prog. Devel.)

W. Banasz from Senior Programmer to Mbr. Engrg. Staff (E.H. Behrens, Data Base Systems)

J. Boswell, Jr. from Senior Programmer to Mbr. Engrg. Staff (E.H. Behrens, Data Base Systems)

K. Kupersmith from Senior Programmer to Mbr Engrg. Staff (E.H. Behrens, Data Base Systems)

R. Tweedie from Senior Programmer to Mbr Engrg. Staff (E.H. Behrens, Data Base Systems)

B. Cunningham from Associate Programmer to Mbr. Engrg. Staff (E.H. Behrens, Data Base Systems)

S. Ronkin from Programmer to Ldr., Engrg. Sys. Projects (E.L. Willey, Cabling-AEGIS Equip.)

Consumer Electronics

L.J. Byers from Mbr., Engrg. Staff to Ldr., Engrg Staff (B.L. Borman, Test Technology)

L.A. Olson from Mbr., Engrg. Staff to Ldr., Engrg. Staff (B.L. Borman, Test Technology)

Errata

In the Anniversary Issue of the *RCA Engineer* (June/July 1976), a typographical error appeared in Mr. Hawkins' inside front cover message on Satellite Communications. In the second paragraph, Mr. Hawkins pointed out that "RCA has developed and provided the first two advanced and most cost-effective domestic satellites, with 24 transponders each, to operate with low-cost earth stations for the Satcom system." However, in the published message, the number of transponders on each satellite was erroneously printed as 4 instead of 24.

Upcoming issues

Your next *RCA Engineer* is going to emphasize **RCA Records,** including

Quadraphonic sound
How records and tapes are made
Polymer science for records
Industrial engineering at RCA Records

and a special article by Executive Vice President and Senior Scientist James Hillier:

History of RCA—Part VI—
The years 1971 - 1976

Further ahead, future issues will cover

Electro-optics
Microprocessors
Advanced communications
Radar
SelectaVision

Obituary

Richard Mendelsohn, Principal Member, Engineering Staff, Avionics Systems, Van Nuys, died August 12. Mr. Mendelsohn received the BSEE from the University of Wisconsin in 1950, did graduate work at the University of Pennsylvania and UCLA, and was a graduate of the Stanford-Sloan Fellowship Program. He joined RCA, Camden, as a Trainee in 1950 and worked at MSRD, Moorestown, from 1951 to 1959, when he transferred to Avionics Systems, Van Nuys. Mr. Mendelsohn worked in design engineering and program management, participating in the TALOS, ATLAS, BMEWS, RANGER, and AEGIS Programs as well as the HPA, RFO, and ULQ-6 Electronic Warfare programs. In his most recent assignment, he was a member of the Standard Projects Engineering Group at Avionics Systems responsible for component selection, component standards, parts management, configuration management and product reliability.

Editorial Representatives

The Editorial Representative in your group is the one you should contact in scheduling technical papers and announcements of your professional activities.

Government and Commercial Systems

Commercial Communications Systems Division

Broadcast Systems
W.S. SEPICH* Broadcast Systems Engineering, Camden, N.J.
K. PRABA Broadcast Systems Antenna Equip. Eng., Gibbsboro, N.J.
A.C. BILLIE Broadcast Engineering, Meadow Lands, Pa.

Mobile Communications Systems
F.A. BARTON* Advanced Development, Meadow Lands, Pa.

Avionics Systems
C.S. METCHETTE* Engineering, Van Nuys, Calif.
J. McDONOUGH Equipment Engineering, Van Nuys, Calif.

Government Systems Division

Astro-Electronics
I.M. SEIDEMAN* Engineering, Princeton, N.J.

Automated Systems
K.E. PALM* Engineering, Burlington, Mass.
A.J. SKAVICUS Engineering , Burlington, Mass.
L.B. SMITH Engineering, Burlington, Mass.

Government Communications Systems
A. LIGUORI* Engineering, Camden, N.J.
H.R. KETCHAM Engineering, Camden, N.J.

Government Engineering
M.G. PIETZ* Advanced Technology Laboratories, Camden, N.J.

Missile and Surface Radar
D.R. HIGGS* Engineering, Moorestown, N.J.

Research and Engineering

Corporate Engineering
H.K. JENNY* Technical Information Programs, Cherry Hill, N.J.

Laboratories
C.W. SALL* Research, Princeton, N.J.

Solid State Division
J.E. SCHOEN* Engineering Publications, Somerville, N.J.
H.R. RONAN Power Devices, Mountaintop, Pa.
S. SILVERSTEIN Power Transistors, Somerville, N.J.
A.J. BIANCULLI Integrated Circuits and Special Devices, Somerville, N.J.
J.D. YOUNG IC Manufacturing, Findlay, Ohio
R.W. ENGSTROM Electro-Optics and Devices, Lancaster, Pa.

Consumer Electronics
C.W. HOYT* Engineering, Indianapolis, Ind.
R.J. BUTH Engineering, Indianapolis, Ind.
P.E. CROOKSHANKS Television Engineering, Indianapolis, Ind.
C.P. HILL Manufacturing Technology, Indianapolis, Ind.

SelectaVision Project
F.R. HOLT SelectaVision VideoDisc Engineering, Indianapolis, Ind.

RCA Service Company
J.E. STEOGER* Consumer Services Engineering, Cherry Hill, N.J.
R. MacWILLIAMS, Marketing Services, Government Services Division, Cherry Hill, N.J.
R.M. DOMBROSKY Technical Support, Cherry Hill, N.J.

Distributor and Special Products Division
C.C. REARICK* Product Development Engineering, Deptford, N.J.
J.N. KOFF Receiving Tube Operations, Harrison, N.J.

Picture Tube Division
E. K. MADENFORD* Engineering, Lancaster, Pa.
N. MEENA Glass Operations, Circleville, Ohio
J.I. NUBANI Television Picture Tube Operations, Scranton, Pa.
C.W. BELL Engineering, Marion, Ind.

RCA Communications
W.S. LEIS* RCA Global Communications, Inc.,New York, N.Y.
P. WEST* RCA Alaska Communications, Inc., Anchorage, Alaska
J. WALSH* RCA American Communications, Kingsbridge Campus, N.J.

NBC, Inc.
W.A. HOWARD* Staff Eng., Technical Development, New York, N.Y.

RCA Records
J.F. WELLS* Record Eng., Indianapolis, Ind.

RCA Ltd
W.A. CHISHOLM* Research & Eng. Montreal, Canada

Patent Operations
J.S. TRIPOLI Patent Plans and Services, Princeton, N.J.

Electronic Industrial Engineering
J. OVNICK* Engineering, N. Hollywood, Calif.

*Technical Publications Administrators (asterisked * above) are responsible for review and approval of papers and presentations

RCA Engineer
A TECHNICAL JOURNAL PUBLISHED BY CORPORATE TECHNICAL COMMUNICATIONS
"BY AND FOR THE RCA ENGINEER"

Printed in U.S.A.

Form No. RE-22-2